

Synthetic approach towards biomass derived pyridinium salts

Subbiah Sowmiah



Dissertation presented to obtain the Ph.D degree in Chemistry
Instituto de Tecnologia Química e Biológica António Xavier | Universidade Nova de Lisboa

Oeiras,
April, 2016



INSTITUTO
DE TECNOLOGIA
QUÍMICA E BIOLÓGICA
ANTÓNIO XAVIER / UNL

Knowledge Creation



Synthetic approach towards biomass derived pyridinium salts

Subbiah Sowmiah

Dissertation presented to obtain the Ph.D degree in Chemistry
Instituto de Tecnologia Química e Biológica António Xavier | Universidade Nova de Lisboa

Oeiras, April, 2016



INSTITUTO
DE TECNOLOGIA
QUÍMICA E BIOLÓGICA
ANTÓNIO XAVIER / UNL

Knowledge Creation



Title:

Synthetic approach towards biomass derived pyridinium salts

Cover Picture:

Designed by Sowmiah

Edition:

April 2016

Author

Subbiah Sowmiah

© Subbiah Sowmiah, All rights reserved

Printed in Portugal.

I declare that the work presented in this thesis, except where otherwise stated, is based on my own research. It was supervised by Professor Luís Paulo N. Rebelo, Professor Carlos Afonso, Dr. José Esperança. The work was mainly performed in Faculdade de Farmácia, Universidade de Lisboa and Molecular Thermodynamics group at Instituto de Tecnologia Química e Biológica (ITQB), Universidade Nova de Lisboa.

Financial support was provided by Fundação para a Ciência e a Tecnologia FCT with the doctoral fellowship SFRH/BD/74088/2010.



Dedicated

To my family

Table of Contents

<i>Contents of the thesis</i>	<i>Pages</i>
Acknowledgements	x
Abstract of the Thesis	xiv
1. General Introduction	
1.1 Chemistry of pyridinium salts	6
1.2 As “ionic liquids”	8
1.3 Synthetic strategies towards pyridinium salts	14
1.4 HMF as renewable feedstock	26
1.5 Goal of the thesis work	29
1.6 References	30
2. Studies on halogenated imidazolium and pyridinium ILs	
2.1 Introduction	45
2.2 Fluidize ionic liquids	48
2.3 Results and discussion	51
2.4 Conclusion	57
2.5 References	58
3. Cannizzaro reaction of HMF to valuable products	
3.1 Introduction	65
3.2 Optimization of reaction conditions	68

<i>Contents of the thesis</i>	<i>Pages</i>
3.3 Scale up and product isolation	73
3.4 Conclusion	79
3.5 References	79
4. Synthesis of <i>N</i>-alkyl pyridinium salts from HMF	
4.1 Introduction	87
4.2 Optimization of reaction conditions	90
4.3 Substrate scope studies	96
4.4 Study on the mechanistic details	103
4.5 Conclusion	104
4.6 References	105
5. Studies on new biomass derived pyridinium salts	
5.1 Chemical reactivity of pyridinium salts	113
5.2 Reactivity of synthesized pyridinium salts	121
5.3 Biological activity of pyridinium salts	129
5.4 Biological studies on new pyridinium salts	132
5.5 Conclusion	139
5.6 References	139
6. Concluding remarks and Future perspectives	145
7. Appendix I – List of Abbreviations	153
8. Appendix II – List of Publications	157
9. Annexure – Supporting details	159

ACKNOWLEDGEMENTS

My sincere thanks to *Prof. Luís Paulo N. Rebelo, Ph.D supervisor, Instituto de Tecnologia Química de Biológica*, for the great opportunity, invaluable guidance provided all these years of my stay. I am very much grateful to *Prof. Carlos Afonso, Ph.D Supervisor at Faculdade de Farmacia* for his inspirational and constructive suggestions which helped me greatly to attain the goal. Your moral support during my stay is greatly appreciated beyond words to sustain myself in the track of my Ph. D progress. Thanks to *Dr. José Esperança, Ph.D supervisor, Instituto de Tecnologia Química de Biológica*, for being both as a source of mentor and companion through his assistance and motivation in the Ph. D pursuit. I feel indebted to all for consistent inputs with your research expertise as well as for the genuine care and unconditional support which made this thesis possible.

I extend my gratitude to the doctoral committee members *Prof. Carlos Romao, Dr. Rita Ventura* from *Instituto de Tecnologia Química de Biológica* for their time and insightful questions. I am also thankful to the members of the Jury for their availability and suggestions. I also thank *Prof. Luis F. Veiros* and *Dr. Raquel Frade* for their collaborative works presented in the thesis. I also would like to thank my teachers and faculty of previous educations who gave me generous advices and for their wishes to my research career.

I am profoundly thankful to *Fundação para a Ciência e a Tecnologia, FCT* and *Prof. Luís Paulo N. Rebelo* for rendering financial support to my research. It is my pleasure to thank my host institutions for the excellent conditions provided to perform this work and extending my

general appreciation to all the persons enrolled in these institutions for providing their kind support.

I thank my colleagues Mohammed Tariq, Sudharshan Reddy, Carlos Monteiro, Luis Gomes, Catarina Rodrigues, Svilen Simeonov, for being my friendly faces to greet me and help with new things especially at my initial days in Portugal. My thanks and wishes for all the former and present members of the lab at institutes, Faculdade de Farmacia and molecular thermodynamics group, ITQB for their tremendous help, encouragement and sharing moments, especially for keeping a brilliant atmosphere. It was great pleasure spending time with you all at different junctures of my research time.

My life in Portugal became enjoyable with my group of Indian friends and families through their concern, availability and party times kept me feel at home. In particular, with years of friendship Narayanan, Sethu, Manikandan had provided me their inevitable support in all possible ways eventually keeping me in optimistic mode no matter what the circumstances are.

I owe a lot to my parents, who encouraged me at every stage of my academic life, and longed to see this achievement come true. Thanks to my father, who is irreplaceable for everything that I am and was the biggest support for my desire to pursue my Ph.D. Never thought would miss him before I could share this joy and success to him. (*"In the middle of difficulty lies opportunity!"*- Albert Einstein). Though I deeply miss his presence, I believe on his eternal blessings for every moment of life and success. Thanks for the wishes and encouragement given by my sister and family.

Thanks to Raja for sensible scientific discussions and for serving as a library of useful information. I personally thank you for being an incredible source of irresistible inspiration and for your unreserved patience to direct me for success and happiness. Also for knowing my mind and for being the symbol of love that carries me through, all these days and in the rest of my life. I am fortunate to have you and still have no words to express how much your presence in my life has meant.

“Gratitude is the memory of the heart.” *Jean Baptiste Massieu* and it is impossible to conclude without my last few words about Portugal:

Não tenho palavras para expressar o quanto eu amo Portugal. Foram anos muito agradáveis e tenho certeza que não teria tanta alegria ou tão boa experiência em outros lugares. Eu sempre me lembrarei da hospitalidade do povo, atmosfera pacífica, as vistas naturais que muitas vezes deixam para trás os meus tempos relutantes. Especialmente a beleza, a vida social que existia dentro e fora do meu laboratório com todos os meus amigos portugueses e vizinhos que são verdadeiramente admiráveis. Eu nunca vou esquecer a minha vida em Lisboa. Agora eu sei que eu vou perder este lugar, mas estou feliz pelas memórias que marcarão a minha vida toda.

*Embora seja bom esta jornada ter um fim,
É a jornada que importa no final.*

Sowmiah

PhD Student, ITQB

Lisbon, Portugal

Abstract of the Thesis

This thesis entitled “**Synthetic approach towards the biomass derived pyridinium salts**” was developed with an aim to develop a sustainable methodology for the synthesis of pyridinium salts that possesses high synthetic value and exhibit potential biological activity along with various industrial applications and were discussed in each chapter wherever necessary.

Chapter I - General Introduction

Chapter I describes the importance of pyridinium salts and biomass 5-hydroxymethyl furfural (HMF) eventually elucidating the goal of this thesis: the need and usefulness of developing sustainable approach towards biomass derived pyridinium salts.

Chapter II - Studies on halogenated imidazolium and pyridinium ILs

Chapter II discusses the efforts towards the study of fluidizing ionic liquids by viscosity measurements with the synthesized new imidazolium and pyridinium ionic liquids.

Chapter III - Cannizzaro reaction of HMF to valuable products

Chapter III describes the synthesis of value added products from HMF obtained *via* Cannizzaro reaction and details the optimization of reaction conditions for scale-up process.

Chapter IV - Synthesis of *N*-alkyl pyridinium salts from HMF

Chapter IV elucidates our synthetic approach towards pyridinium salts from HMF through screening of catalysts, finding optimized conditions, study on substrate scope and relevant mechanistic details.

Chapter V - Studies on new biomass derived pyridinium salts

Chapter V outlines the preliminary efforts to understand these new biomass derived pyridinium salts in terms of reactivity and biological activities.

Chapter VI - Concluding remarks and Future perspectives

This concluding chapter briefly explains the achievements towards the goal of the thesis along with a practical view on the scope of these pyridinium salts.

Finally, it includes the appendices with the list of abbreviations used in the thesis, list of publications and details supporting information in annexure.

CHAPTER I

General Introduction

Chapter 1

This chapter is part of a review on pyridinium salts that will be submitted for publication soon.

This chapter contains essential information for understanding the subsequent chapters enclosed in this thesis.

1. General Introduction

Chapter I - Summary

Chapter I outlines the available literature on the importance of pyridinium salts that exist as privileged scaffolds in many natural and bioactive compounds. This chapter also overviews the role of pyridinium ionic liquids in catalysis and classical to recent approaches towards the synthesis of pyridinium salts. Today's attention on biomass for the production of fuels and bulk chemicals is of great practical benefit as it is an alternative feedstock that enables to reduce the dependence/consumption on fossil resources. Among the possible options, 5-Hydroxymethylfurfural (HMF) is an important bridge molecule linking biomass to fuels and chemicals, as it can be derived from renewable resources like fructose, glucose/cellulose and is very useful for the production of the biofuel dimethylfuran and other important commodities. Thus a new strategy for the sustainable synthesis of pyridinium salts using biomass derived HMF is commenced.

Chapter 1

1. Introduction

Pyridinium salts are privileged scaffolds found in natural and bioactive compounds¹ and employed in wide range of applications such as acylating agents, phase transfer catalysts, biocides like antimicrobial agents, dyes and cationic surfactants or cosmetics.² Pyridinium containing natural products such as Njaoaminiums and Pachychalines (Figure 1.1) are well known for their occurrence widely in marine sponges of the order Haplosclerida.^{3,4}

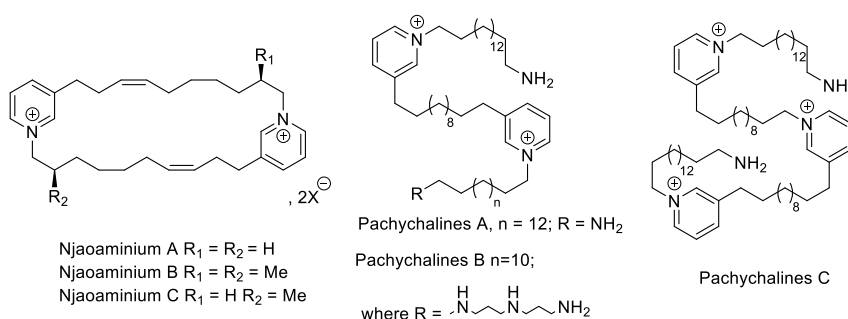


Figure 1.1 Natural products containing pyridinium salts⁵

Being well known for their germicidal properties, they are also efficient in various biological activities such as acetylcholinesterase inhibitors, drug delivery etc. Pyridinium salts are known to inhibit the growth of various microorganisms such as bacteria, viruses, fungi etc. Their effectiveness against microorganisms is employed as antimicrobial agents to our daily life in various ways such as sterilizing surgical instruments, as disinfectant for sanitizer in dairy industry, for the treatment of urological infections, Cetylpyridinium chloride formulated medicines such as griseofluvin for effective skin treatment⁶ and controls supragingival plaque and gingivitis. They also exhibit anti-inflammatory activity by inhibiting several matrix metalloproteinase proteins that causes inflammation. Moreover they become an important ingredient in cosmetic products including skin creams, body lotions, hair conditioner etc.⁷ Cytotoxic agents such as 12-

methacryloyloxydodecylpyridinium bromide (MDPB) and cetylpyridinium chloride (CPC), is used extensively for the treatment of oral infections.⁸

A detailed description of the pyridinium salts in catalysis, its chemical reactivity, synthetic routes together with its material applications and biological activities were explained in a review (*Chem. Soc. Rev.* manuscript to be communicated). This chapter contains only a part of this review that are essential to emphasize the goal of the thesis based on our approach towards biomass derived pyridinium salts.

1.1 Chemistry of pyridinium salts

The classical routes to obtain pyridinium salts involve the reaction of pyridine with organic halides or quaternization of the pyridine nitrogen using chloromethylalkyl ethers or sulphides.⁹⁻¹¹ Moreover, they have high synthetic value as key intermediate for the production of wide range of pharmacologically relevant piperidine, dihydro, tetrahydropyridine frameworks.^{12,13} An intensive research have also been carried out with the use of pyridinium salts as a key substrate for the synthesis of various natural product cores. Figure 1.2 shows some literature examples of the natural products using pyridinium salts.

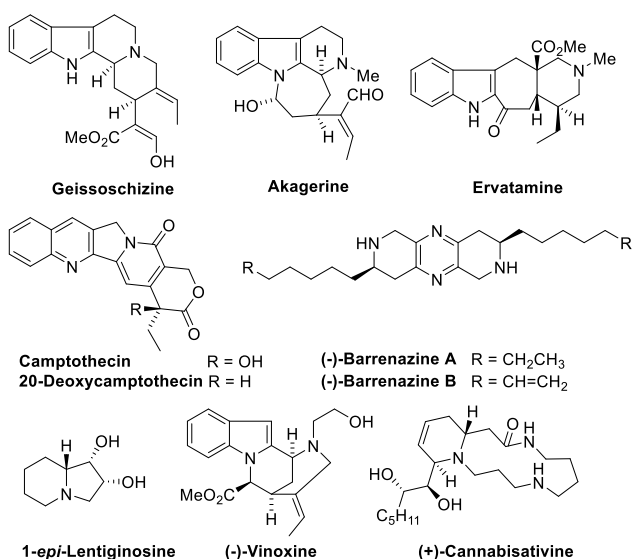
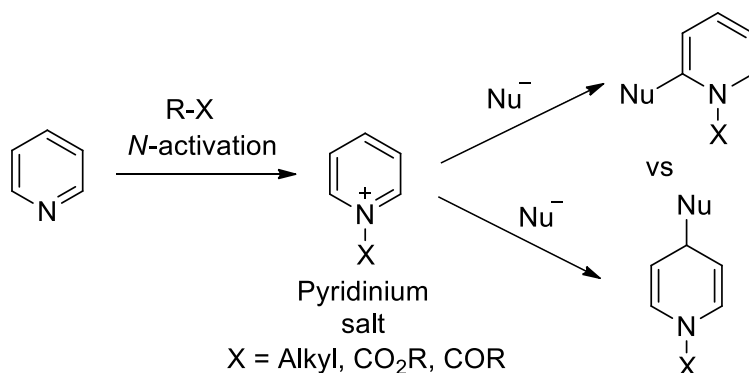


Figure 1.2 Natural products derived from pyridinium salts¹⁴

The addition of a broad variety of nucleophiles to pyridinium salts is, probably, the method of choice for the preparation of functionalized dihydro-, tetrahydropyridines, as well as piperidines. All these heterocycles are important intermediates in the synthesis of piperidine containing biologically active molecules and alkaloids. Due to the aromatic character of the pyridine heterocycle, its basicity and the electron-attracting influence of the nitrogen atom, pyridinium salts are found to be of versatile chemical reactivity. The nucleophilic additions to pyridinium salts for the synthesis of dihydropyridines and 2,3-dihydro-4-pyridones have been studied systematically.^{15,16}

Pyridinium cations can behave as electrophiles and 1,3-dipoles to take part in condensation, Michael addition, 1,3-dipolar addition, nuclear substitution and arrangement reactions, and find vast applications in organic syntheses. A pyridinium salt contains reactive electrophilic sites at the 2, 4 and 6-positions of the heterocyclic ring. Upon addition of nucleophile, mixtures of substituted 1,2- and 1,4-dihydropyridines are frequently obtained (Scheme 1.1).



Scheme 1.1 Functionalization of *N*-activated pyridinium salts

Rich chemical reactivity of pyridinium salts in the synthesis of several heterocyclic cores, also amplified the positive advances of these substrates as biodegradable ionic liquids with extensive applicability as surfactants.

1.2 As “ionic liquids”

Pyridinium salts that are liquid at room temperature, so called “Pyridinium ionic liquids (PyILs)”¹⁷ such as 1-alkylpyridinium salts, are potential solvents in synthesis and catalysis.¹⁸ As the studies towards the understanding of ionic liquid (IL) behaviour increases, the potential applications by controlling the resultant properties keeps growing.

1.2.1 Approaches in the synthesis of PyILs

Tuning the synthesis of ILs upon desired physical, chemical, and biological properties by combining two independent biologically active ions such as anti-microbial pyridinium cations and artificial sweetener anions was studied.¹⁹ Some of the synthesized ILs showed dramatic increase for anti-microbial activity shown in Figure 1.3.

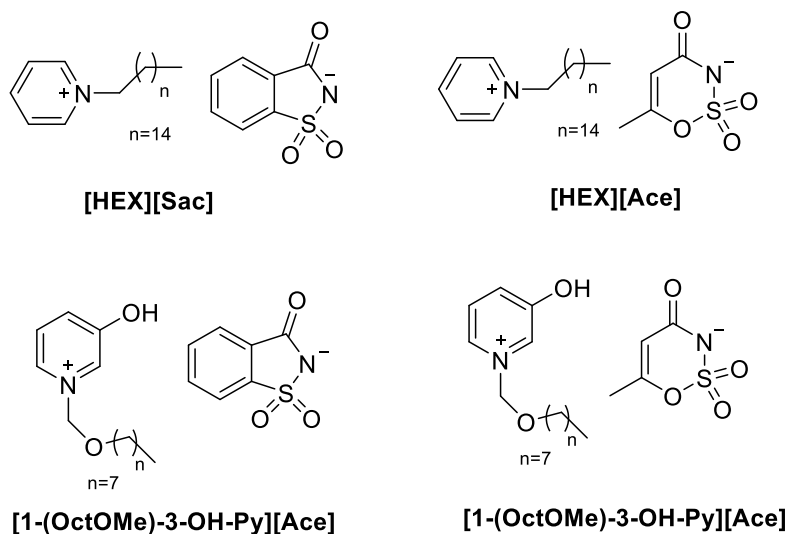
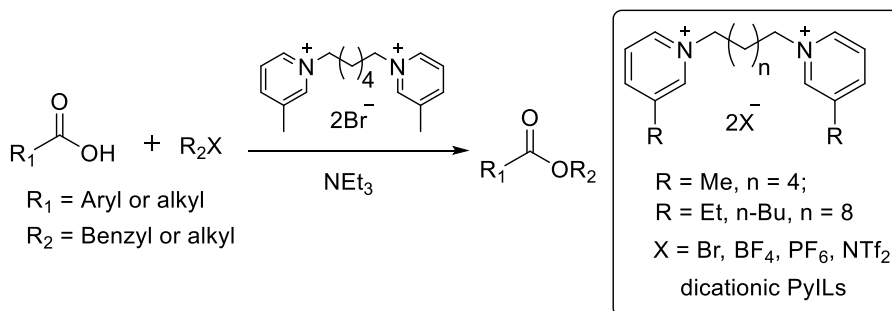


Figure 1.3 Synthesis of anti-microbial pyridinium salts

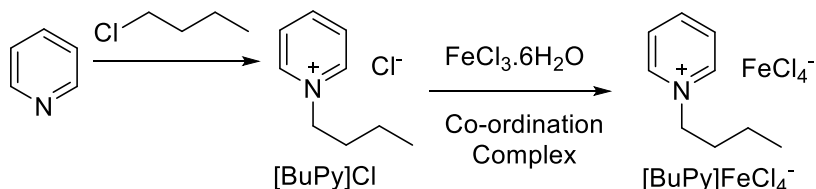
Kim *et al.*²⁰ described a useful strategy for the synthesis of functionalized pyridinium dicationic ILs²¹ which was proved as a benign media for the

esterification of carboxylic acids to react with alkyl or aryl halides in the presence of trimethylamine to give esters in high yields and high selectivity (Scheme 1.2). The utility of such dicationic ionic liquid with reaction conditions that are milder and promoting higher reaction yields, shorter reaction time, and operational simplicity is due to the solubility of the starting materials and products being an adequate reaction media for the catalyst.



Scheme 1.2 Synthesis of functionalized pyridinium dicationic ILs

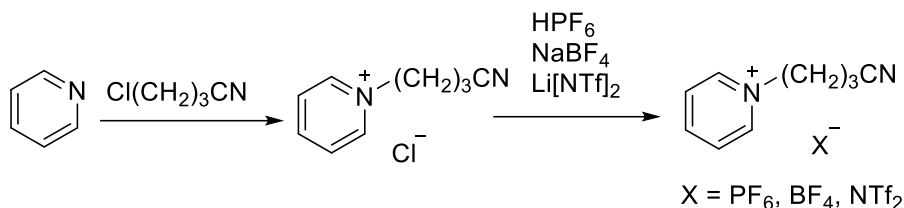
Zhang *et al.* reported the synthesis of Iron-containing magnetic PyILs by reacting pyridine and *n*-Chlorobutane at 80 °C to obtain the intermediate [BuPy]Cl which on mixing with equimolecular of FeCl₃·6H₂O under N₂ atmosphere gave [BuPy]FeCl₄ (Scheme 1.3).²² The magnetic ILs were quantitatively tested by magnetic property measurement system (superconducting quantum interference device), and the results indicated that they had similar magnetic susceptibilities and paramagnetic properties.



Scheme 1.3 Synthesis of iron-containing magnetic PyILs

Dyson *et al.* reported the synthesis of a series of nitrile functionalized PyILs with *N*-butyronitrile pyridinium cation, [C₃CNpy]⁺.²³ The PyILs improve catalyst

retention and their catalytic activity as studied with palladium catalyzed Suzuki and Stille coupling reactions. PyILs with palladium chloride form palladium complexes. If the anion is chloride the complex is $[\text{C}_3\text{CNpy}]_2[\text{PdCl}_4]$, whereas for other anions X (X= PF_6 , BF_4 , NTf_2) the palladium complex formed is $[\text{PdCl}_2(\text{C}_3\text{CNpy})_2][\text{X}]_2$. Among them, $[\text{C}_3\text{CNpy}][\text{NTf}_2]$ is an effective immobilizing solvent for the reactions and also reduces leaching in comparison with non-functionalized PyIL $[\text{C}_4\text{py}][\text{NTf}_2]$ (Scheme 1.4).



Scheme 1.4 Synthesis of nitrile functionalized PyILs

Duan *et al.* synthesized new protic PyILs,²⁴ based on 2-methylpyridinium moiety and studied their performance on the *tert*-butylation of phenol.²⁵ $[\text{2-MPyH}]\text{OTf}$ is superior catalyst to give 2-*tert*-butyl phenol (TBP) compared to $[\text{2-MPyH}][\text{CH}_3\text{SO}_3]$ that favours the formation of 2,4-di-*tert*-butyl phenol (DTBP). Further study on the use of $[\text{2-MPyH}]\text{OTf}$ for the esterification of cyclic olefins with acetic acid also gave good yields. The catalytic activity in reactions is in agreement with the acidity order determined by Hammett method shown in Figure 1.4.

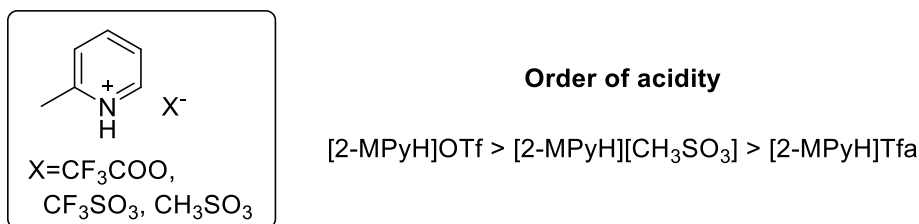
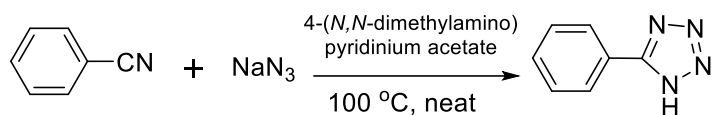


Figure 1.4 Synthesis of protic PyILs and their order of acidity

Nowrouzi *et al.* developed a convenient methodology for the preparation of 5-substituted-1H-tetrazoles using 4-(*N,N*-dimethylamino)pyridinium acetate as a

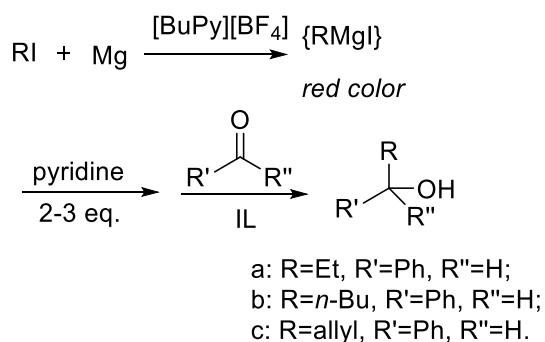
recyclable catalyst (Scheme 1.5).²⁶ 4-(*N,N*-dimethylamino)pyridinium acetate with ionic liquid character is employed as the medium and as the promoter for an effective reaction in shorter time avoiding the use of an excess of sodium azide as previously reported methods. The effect of the catalyst on the [3+2] cycloaddition reaction of structurally diverse nitriles was studied successfully.



Scheme 1.5 Synthesis of 5-substituted-1H-tetrazoles

1.2.2 PyILs in Catalysis

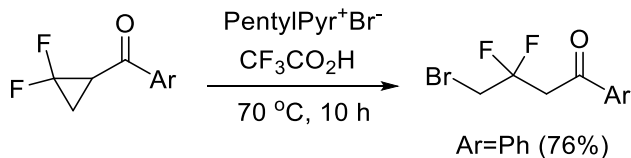
Versatility of pyridinium ionic liquids in catalysis has been proved successfully by various research groups. Based on the stability of preformed phenylmagnesium bromide in ILs,²⁷ an attempt to generate Grignard reagent from magnesium and organic halides in *n*-butylpyridinium tetrafluoroborate, [BuPy][BF₄] was performed (Scheme 1.6).²⁸ The synthesized compound showed a distinctly different reactivity pattern from the ones obtained in organic solvents.



Scheme 1.6 PyILs in Grignard reactions

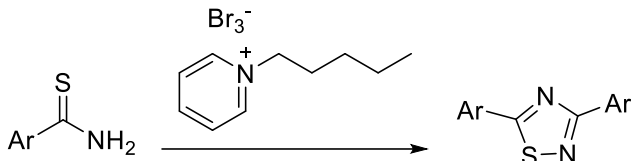
ILs as unique reagents²⁹ for efficient organic transformations was reported. In this case, the use of a PyIL proved to be extremely effective to carry out the ring opening hydrobromination of cyclopropyl ketones to form γ -bromo ketones

(Scheme 1.7).³⁰ *N*-pentyl pyridinium bromide was melted at 70 °C and mixed with 1 equiv of trifluoroacetic acid to form this PyIL hydrobrominating reagent that acts as a potent surrogate hydrobromination reagent.



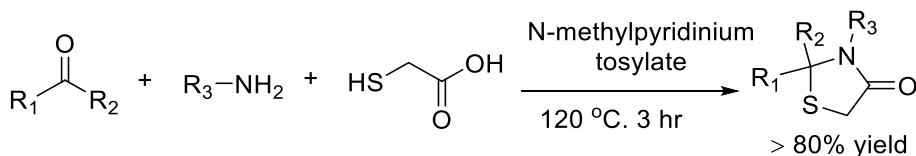
Scheme 1.7 PyILs in hydrobromination of cyclopropyl ketones

A non volatile IL analog of bromine, pentyl pyridinium tribromide³¹ plays dual role as a solvent and reagent for an efficient synthesis of symmetrical 3,5-disubstituted 1,2,4-thiadiazoles by oxidative dimerization of thioamides (Scheme 1.8).³²



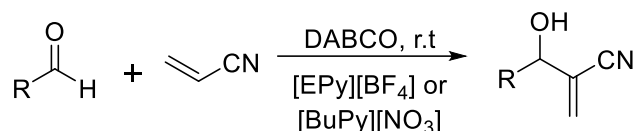
Scheme 1.8 PyILs in oxidative dimerization of thioamides

A convenient one-pot, three-component synthetic protocol for the cyclocondensation of imines (generated *in situ* from aromatic amines) and carbonyls with mercaptoacetic acid mediated by *N*-methylpyridinium tosylate ionic liquid was successfully developed to give 4-thiazolidinones rapidly.³³ Condensation of pyridine and methyl-4-toluenesulfonate at 5 °C provide the fresh *N*-methylpyridinium tosylate IL (Scheme 1.9).³⁴



Scheme 1.9 PyILs in the synthesis of thiazolidinones

Zhao *et al.* reported PyILs as an efficient reaction media for the amine-catalyzed Morita-Baylis-Hilman reaction (Scheme 1.10).³⁵ Following their study with *N*-butylpyridinium tetrafluoroborate ([BuPy][BF₄]) as efficient reaction medium,³⁶ they used other PyILs such as *N*-ethylpyridinium tetrafluoroborate ([EPy][BF₄]) and *N*-butylpyridinium nitrate ([BuPy][NO₃]) to study the efficacy of distinct PyILs on this reaction.



Scheme 1.10 PyILs in the amine-catalyzed Morita-Baylis-Hilman reaction

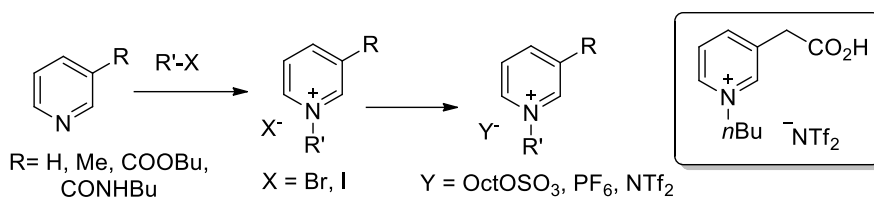
The applicability of DABCO-catalyzed Morita-Baylis-Hilman reaction was investigated for reactions of a variety of aldehydes including electron-deficient or electron-withdrawing aromatic aldehydes and aliphatic aldehydes.

The increased reactivity in PyILs compared to organic solvents is the stabilization of the zwitterionic intermediate obtained as a result of Michael addition of a nucleophilic Lewis base to an activated alkene. The reaction rate is accelerated when the intermediate is trapped at higher concentration in IL facilitating the nucleophilic attack of zwitterionic intermediate to aldehyde yield a Morita-Baylis-Hilman adduct.

1.2.3 Biodegradability of PyILs

Scammells *et al.*³⁷ described the ready biodegradability of pyridinium based ILs derived from pyridine and nicotinic acid, a relatively inexpensive natural product that can be used to incorporate the pyridinium core in the IL moiety. They also performed the biodegradability tests of several pyridinium ionic liquids with allyl, benzyl, *N,N*-diisopropyl, -COOH, -NEt₂ and their susceptibility with these substituents were explained. PyILs with an acid functionality in 3-position of

pyridine ring show high extent of biodegradability whereas the unsaturated substituents allyl, benzyl possessed low biodegradability (Scheme 1.11).³⁸



Scheme 1.11 Pyridinium based biodegradable ILs

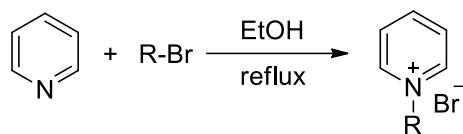
PyILs bearing an ester side chain were classified as ‘readily biodegradable’ whereas PyILs with alkyl side chains exhibits lower level of biodegradability.³⁹ The use of an ester moiety at different positions of the pyridinium ring with octylsulfate and bistriflimide anions were readily biodegradable ILs in comparison with the biodegradable anionic surfactant sodium dodecylsulfate as the reference compound.⁴⁰ The importance of understanding the possible metabolites, their stability during the biodegradable pathways that lead to the rapid decomposition were recently studied by Deng *et al.*⁴¹ The metabolites can be relatively toxic since the substrates may possess different environmental behaviour.

For example, metabolites attained from hydroxylation on the alkyl chain or aromatic ring or hydrolysis of the terminal ester moiety get accumulated in the medium which might have toxic activities resulting on non-biodegradable ILs. Also the introduction of a hydroxyl group in the alkyl chain or the nature of the anions affecting the biodegradability and the possible metabolites were investigated. Pyridinium substrates having biodegradable ester linkages at low pH values show increased efficiency for *in vitro* DNA delivery.⁴²

1.3 Synthetic strategies towards pyridinium salts

A classical method for the synthesis of pyridinium salts is a $\text{S}_{\text{N}}2$ type reaction of pyridine with alkyl halides.⁴³ Quaternary pyridinium salts with alkyl chain length

ranging from C₈ up to C₂₀ were of interest as cationic surface active agents and were easily synthesized under an universal method using ethanol reflux conditions (Scheme 1.12).⁴⁴



chains ranging from C₈ to C₂₀

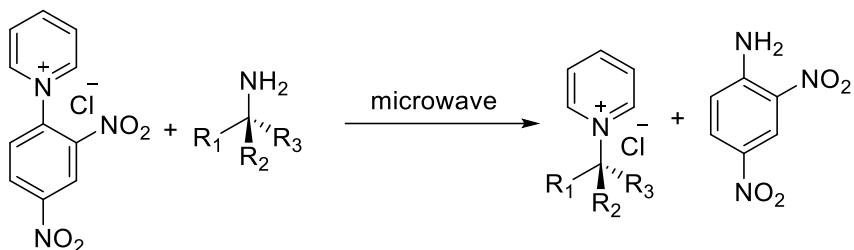
Scheme 1.12 Synthesis of pyridinium salts

Pyridinium salts containing a chiral auxiliary group have been extensively used as starting material in asymmetric synthesis for achieving various simple to complex systems such as dihydropyridines, tetrahydropyridines, piperidines, and nitrogenated complex compounds for example natural alkaloids and synthetic candidates for drugs.⁴⁵ The synthesis of chiral pyridinium salts by the above method may have significant risk of racemization by S_N1 process as well.

1.3.1 Zincke reaction

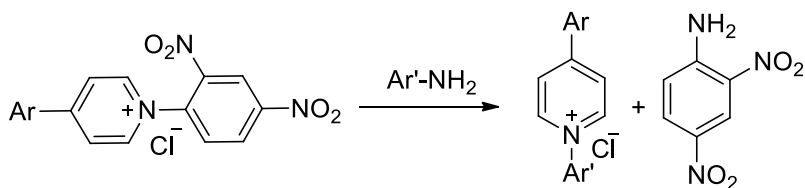
Zincke salt is a highly electrophilic specie that is obtained by reaction between a pyridine derivative and 1-chloro-2,4-dinitrobenzene. The use of the Zincke method involves the attack of a primary amine on the Zincke salt to produce a pyridinium salt. The mechanism of this reaction clearly does not proceed *via* C-N bond cleavage.⁴⁶ The method is used in the preparation of vesamicol analogs, cytotoxic alkaloid Manzamine A and to obtain salts to treat cystic fibrosis.⁴⁷

Viana *et al.* accomplished the synthesis of chiral pyridinium salts *via* zincke reaction under microwave conditions with good yields and less racemization than conventional heating methods (Scheme 1.13).⁴⁸



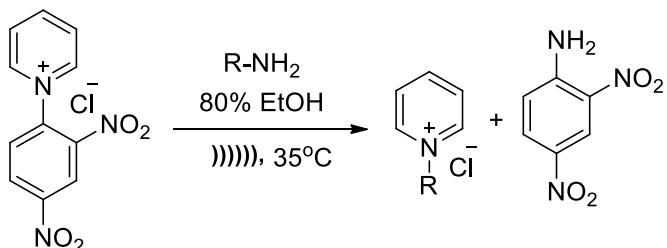
Scheme 1.13 Synthesis of chiral pyridinium salts

Zincke reaction is also versatile method for the synthesis of *N*-arylpyridinium salts reported by Marvel and Ise (Scheme 1.14).⁴⁹ Synthesis of pyridinium salts with different reactive hydroxyl, amine and/or pyridyl groups were also synthesized.⁵⁰ Anion exchange behaviour of the obtained pyridinium salts was studied and revealed that the intramolecular charge transfer occurs when the *N*-phenyl ring of pyridinium salts possess electron-donating groups.



Scheme 1.14 Synthesis of *N*-arylpyridinium salts

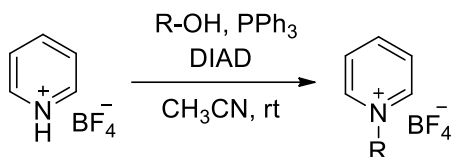
An efficient method using ultrasound irradiation for the synthesis of pyridinium salts based on Zincke reaction with increased yields and lesser reaction time was developed (Scheme 1.15).⁵¹



Scheme 1.15 Synthesis of pyridinium salts by ultrasound irradiation

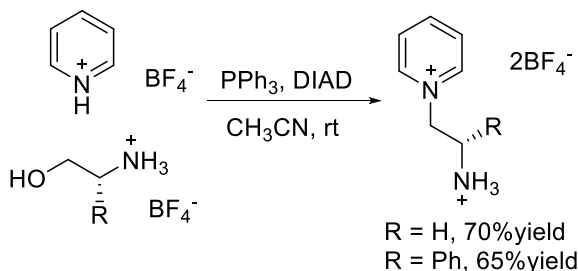
1.3.2 Mitsunobu reaction

Mitsunobu reaction was reported for the preparation of pyridinium salts using pyridines as tertiary nitrogen nucleophiles that undergo alkylation with its ammonium form as the acidic component without presence of nucleophilic counterions. This methodology led to the synthesis of ionic liquids under mild conditions without the use of anion exchange (Scheme 1.16).⁵²



Scheme 1.16 Synthesis of pyridinium salts by Mitsunobu reaction

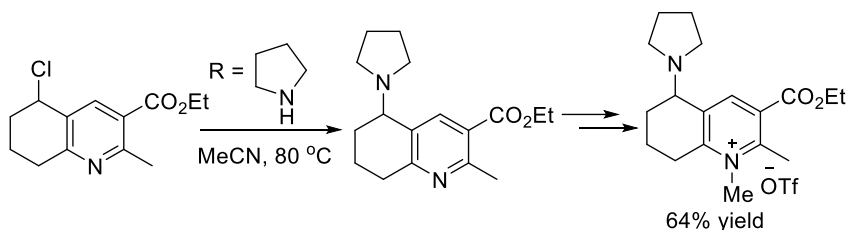
Alkylation of pyridinium tetrafluoroborate by ethanolamine tetrafluoroborate was obtained with an excess of Mitsunobu reagents and alcohol component (Scheme 1.17).



Scheme 1.17 Synthesis of pyridinium salts by Mitsunobu reaction

1.3.3 Simple N- methylation

Several methodologies to functionalize pyridinium salts were of interest overcoming the high electrophilicity of these salts. Pfaltz *et al.* described the synthesis of *N*-methylpyridinium salts bearing tertiary amine group which could act as mediators in hydride transfer reactions (Scheme 1.18). This method uses proton, an effective protecting group as a key step for selective *N*-methylation.⁵³

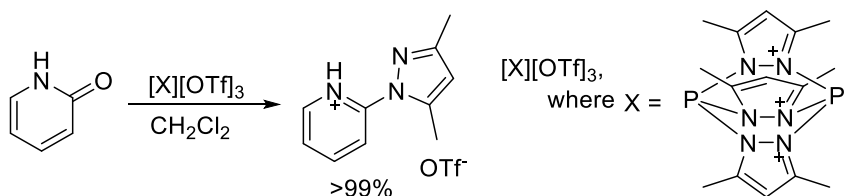


Scheme 1.18 Synthesis of *N*-methylpyridinium salts

The synthesis of tetrasubstituted *N*-methyl pyridinium salts is achieved by the synthesis of benzylic amines from less expensive compounds such as ethyl acetoacetate, ammonium carbamate to form enolate which undergoes condensation with 1,3-cyclohexanedione and ethylorthoformate. To perform selective *N*-methylation of the pyridine ring, one equivalent of acid is used to give the ammonium salts which allow the less basic pyridine N atom to react with the methylating agent to obtain the pyridinium salt after the deprotection using a simple base.

1.3.4 Pyrazolyl-based pyridinium salts

A successful approach for the synthesis of pyrazolyl-substituted pyridinium salts from 2-pyridones, 4-pyridones and urea derivatives were explained by the use of trication such as $(\text{pyr}_3\text{P}_2)^{3+}$, pyr = 3,5-dimethylpyrazolyl) is used as a pyrazolyl-transfer agent (Scheme 1.19). This efficient procedure proceeds *via* exchange of carbonyl oxygen atom from the substrate to the pyrazolyl moiety. 3-hydroxypyridines undergoing different reaction pathways due to the lactam-lactim tautomerism is also explained. This conversion is conveniently obtained in high yields.⁵⁴

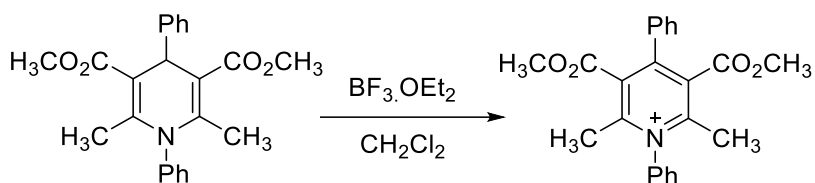


Scheme 1.19 Synthesis of pyrazolyl-substituted pyridinium salts

[X][OTf]₃ also acts as versatile deoxygenation reagent such that the exocyclic oxygen in 2-pyridone is substituted efficiently with pyrazolyl moiety. A wide range of functional groups, for example 2-pyridones with alkyl, nitro, or halogen substituents are tolerated to transform the pyridinium salts.

1.3.5 Pyridinium salts from dihydropyridines

Guaanes *et al.* reported another usual approach for the synthesis of pyridinium salts from *N*-substituted dihydropyridines using BF₃.OEt₂ as promoter. The use of BF₃.OEt₂ as aromatization promoter avoids the need of any oxidizing agents such as quinines, nitrates, peroxides or chromates (Scheme 1.20).⁵⁵

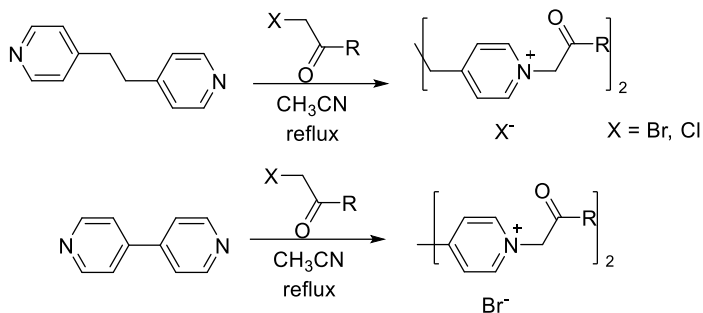


Scheme 1.20 Synthesis of pyridinium salts from dihydropyridines

N-phenyl Hantzsch ester dihydropyridines were transformed into *N*-phenylpyridinium salts using 3 equiv. of BF₃.OEt₂ at 0 °C, in dark conditions in CH₂Cl₂ to give yields up to 80%. These mild conditions and facile work up compared to the oxidizing agents were also applicable to obtain various *N*-substituted dihydropyridines and 1,4-dihydropyridines successfully.

1.3.6 Synthesis of bispyridinium salts

Bispyridinium salts are known for antimicrobial activities and are synthesized by a conventional methodology such as alkylation with halogenated reagents.⁵⁶ Diquaternary bispyridinium salts were synthesized through the alkylation of 4-[2-(pyridin-4-yl)ethyl]pyridine or 4,4-bipyridine with reactive halogenated reagents in anhydrous acetonitrile (Scheme 1.21).⁵⁷



Scheme 1.21 Synthesis of bispyridinium salts

The substituent on the alkylating reagent influences the alkylation reaction and the reactivity of α -halo ketones in nucleophilic substitution in the following order as shown in Figure 1.5.

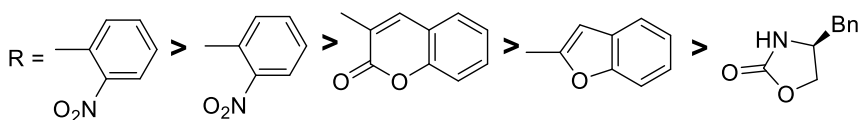
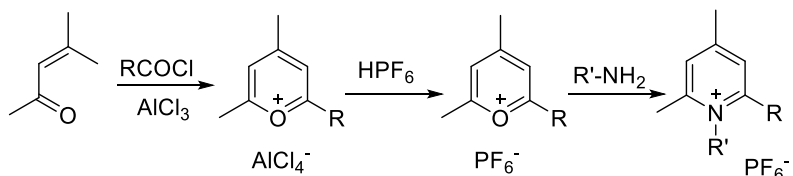


Figure 1.5 Order of reactivity with the alkylating agent

Also, chloro-alkylating reagents showed lower reactivity compared to bromo reagents.

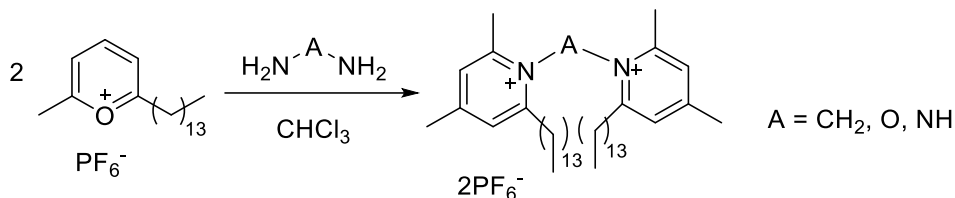
1.3.7 Synthesis from pyrylium salts

High reactivity of pyrylium salts toward primary amines, a simple strategy for the synthesis of new pyridinium salts with alkyl chains directly attached on the aromatic ring, was described.⁵⁸⁻⁶⁰ Pyrylium hexafluorophosphates were reacted with primary linear alkylamines C₁₀ to C₁₈ to generate a library of pyridinium cationic lipids (Scheme 1.22).



Scheme 1.22 Synthesis of pyridinium salts from pyrylium salts

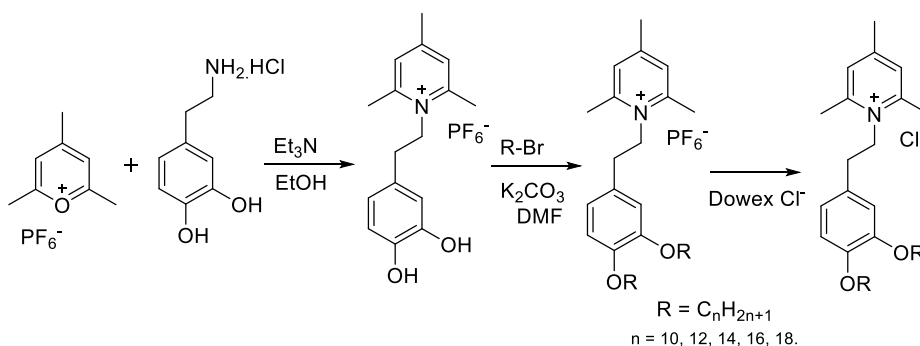
Generation of pyridinium salts with non-polar linkers by reaction of pyrylium salts and *n*-alkyldiamines with various chain lengths from C₂ to C₈ was performed to fine tune the new species on transfection efficiency (Scheme 1.23).⁶¹



Scheme 1.23 Synthesis of pyridinium salts with alkyldiamines

The authors also investigated different constructs using ester and amide polar groups that are biodegradable and can result in pyridinium cations with reduced cytotoxicity.

Similar new biocompatible and low-toxic pyridinium salts based on dopamine backbone with hydrophobic interface with strong self-assembling nature were described (Scheme 1.24). Fine tuning of the counterion, hydrophobic chain length and colipid produced efficient synthetic transfection formulation to transfect neuronal cells.⁶²

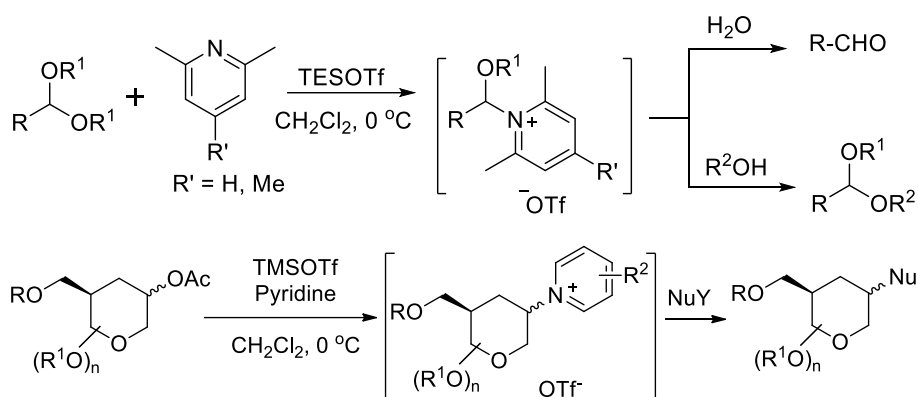


Scheme 1.24 Synthesis of pyridinium salts based on dopamine backbone

1.3.8 Synthesis of THP pyridinium-type salts

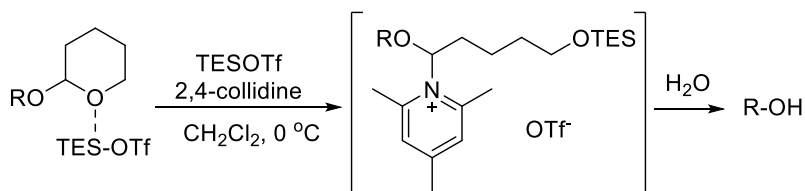
Another method for the synthesis of pyridinium-type salt intermediates is the nucleophilic substitution of tetrahydropyryl (THP) or carbohydrate-derived

esters. By treating 6-substituted-acetoxy tetrahydropyrans with TMSOTf and 2-substituted pyridines,⁶³ such as 2-p-tolylpyridine and 2-methoxypyridine led to the efficient synthesis of *cis*-pyridinium salts which undergo nucleophilic substitution reactions with various heteroatom-containing nucleophiles such as alcohols, azides, thiols reagents. The method is also successfully employed under mild/neutral conditions without affecting acid protecting groups. Nucleophilic reactions with azides and C-nucleophiles provided highly stereoselective 2,6-*trans* products (Scheme 1.25).



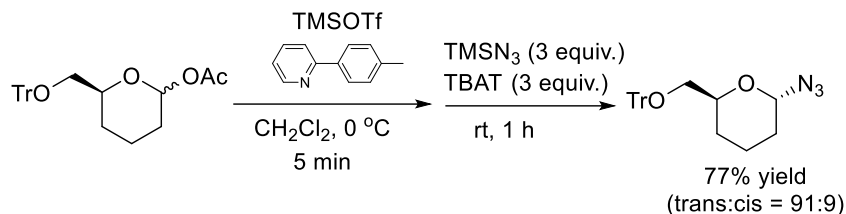
Scheme 1.25 Synthesis of pyridinium type salt intermediates

Synthesis of THP pyridinium-type salts from the reactions of THP ethers with TESOTf and pyridines were also performed (Scheme 1.26). The selective coordination of silyltriflate to the exocyclic oxygen was required to form THP pyridinium-type salts that would participate as intermediates in anomeric-substitution reactions.



Scheme 1.26 Synthesis of pyridinium type salt intermediates

This method was successfully extended to use distinct nucleophiles. For example, the azidation was performed with the THP esters containing trityl group to give the substituted product with good yield and high diastereoselectivity, without the loss of this acid-labile trityl group (Scheme 1.27).

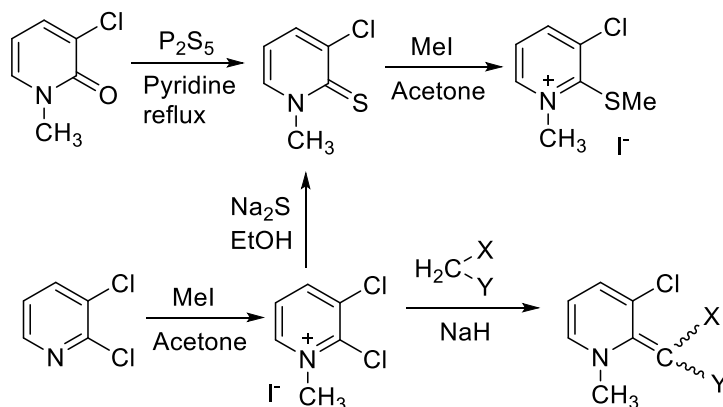


Scheme 1.27 Synthesis of pyridinium-type salt intermediates

The nucleophilic-substitution reaction at the anomeric position of THP and carbohydrate esters employs pre-activation strategy, *via* the initial formation of a pyridinium-type salt intermediate acting as an oxocarbenium-ion equivalent. Alcohols, azides, and C-nucleophiles were introduced onto the anomeric centers of both THP and the carbohydrate substrates.⁶⁴

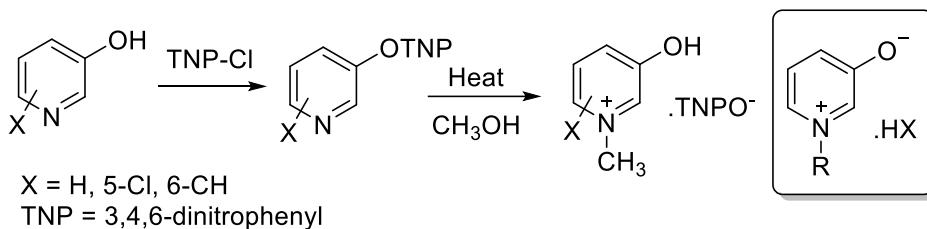
1.3.9 Other approaches

C-C bond forming reactions are highly useful in organic transformations and the reactions of pyridinium salts with active methylene compounds are demonstrated below in Scheme 1.28.⁶⁵



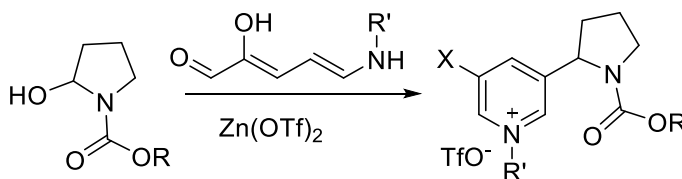
Scheme 1.28 Synthesis of pyridinium salt

Concerning the reactivity of 3-hydroxypyridine and 3-hydroxy-6-methylpyridine with TNP, alkylation of 3-hydroxy pyridines with alkyl halides in acetonitrile solvent provides betaine products. In the case of 3-hydroxy pyridine and 3-hydroxy-6-methylpyridine, the intermediates formed on the attack of the oxygen atom are unstable and even simple heating of its methanolic solutions gives the pyridinium salts (Scheme 1.29).⁶⁶



Scheme 1.29 Synthesis of 3-substituted pyridinium salt

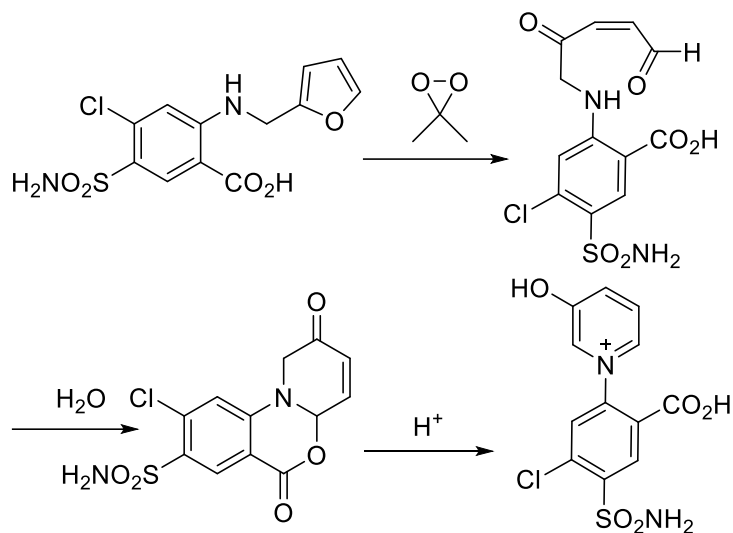
Piperidine/pyrrolidine substituted pyridinium salts are synthesized by the addition of 5-alkylaminopenta-2,4-dienals onto *N*-acyliminium ions, generated *in situ* from α -hydroxycarbamates derived from pyrrolidine or piperidine using zinc triflate followed by dehydrative cyclization (Scheme 1.30).⁶⁷



Scheme 1.30 Synthesis of 3-substituted pyridinium salts

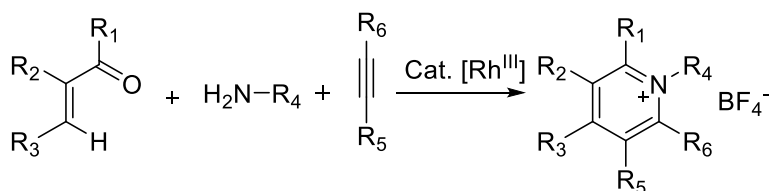
A study based on the oxidative metabolism of furosemide shows the formation of pyridinium salts, also observed in the microsomal incubations of furosemide. Oxidation of furosemide by dimethyldioxirane in acetone underwent Mannich-like reaction to provide ring expanded enone by intramolecular condensation. They also observed the formation of stable pyridinium salt resulting from keto-enol tautomerism and ring opening of the lactone. The toxicity that is usually observed

in furan-type compounds is not seen in this case which might be due to the enonal trapping internal nucleophile (Scheme 1.31).⁶⁸



Scheme 1.31 Synthesis of 3-substituted pyridinium salts

Recently, a direct route for highly substituted pyridinium salts using rhodium catalyst *via* multi-component reaction of vinyl aldehydes/ketones, amines, alkynes was demonstrated.⁶⁹ The catalytic reaction proceeds *via* an *in situ* generated imine assisted Rh(III)-catalyzed vinylic C-H activation (Scheme 1.32). The mechanism involves the co-ordination of α,β -unsaturated imines *in situ* to Rh(III) complex followed by vinylic C-H cleavage, alkyne insertion to Rh complex and then the formation of the pyridinium salt by reductive elimination forming Rh(I) which gets oxidized using $\text{Cu}(\text{OAc})_2$ to turn into active Rh(III) catalyst.



Scheme 1.32 Synthesis of 3-substituted pyridinium salts

Current reports on the synthesis of pyridinium salts by catalytic C-H activation⁷⁰ and the utility of pyridinium salts to originate conjugated dienals, a highly useful synthetic precursor for constructing natural products,⁷¹ reveals the high demand of pyridinium salts in synthetic chemistry.

Various approaches has been developed on the synthesis of pyridinium salts with various target properties such as betaine dyes,⁷² or biomarker, bioactive pyridinium salts for anti-Cholinesterase(AChE) inhibitors (Figure 1.6).⁷³

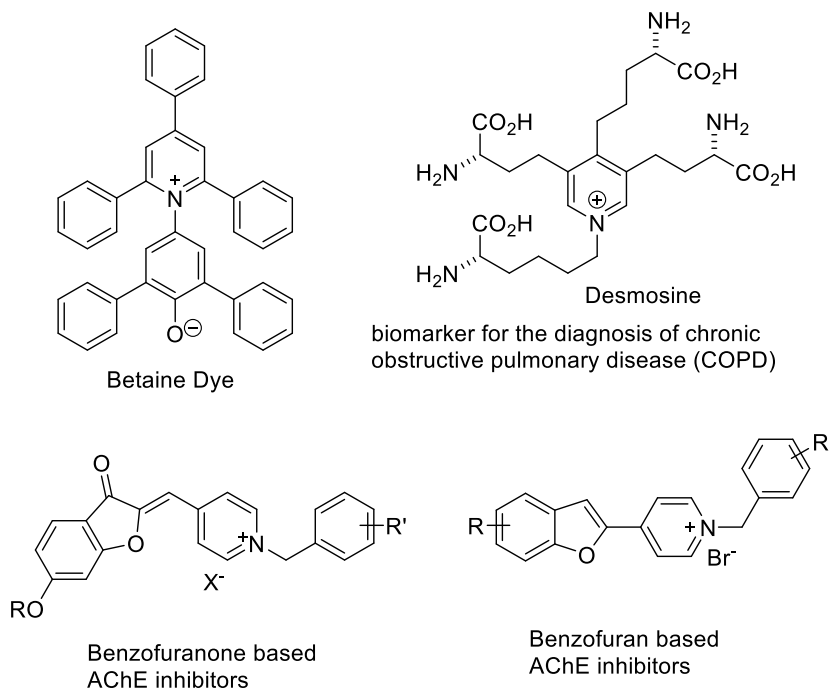


Figure 1.6 Synthesis of pyridinium salts with target properties

1.4 Hydroxymethyl furfural as biorenewable feedstock

Current plans for the implementation of second-generation biofuels are mainly directed towards the conversion of biomass with the effective utilization of carbohydrate feedstock such as cellulose to bioalcohols. Such alternative pathway provides easy access to intermediates and building blocks for chemical products.^{74,75} Great efforts are being made to develop the use of biomass as a raw

material for the production of industrial chemicals.⁷⁶ Herein, it is argued that the optimal use of abundant bioresources could well serve as a renewable feedstock for the chemical industry.⁷⁷ From a chemical perspective, renewable feedstocks, being highly functionalized molecules, are very different from fossil feedstocks which are generally unfunctionalized. Therefore, a huge challenge for chemists today is to provide the chemical industry with a new set of tools to convert renewables into useful chemicals in an economically viable fashion.^{78,79} Here, we illustrate examples of two different approaches or strategies towards potential biomass-derived chemicals. It is proposed that the required cost-competitive and environmentally acceptable (sustainable) industrial chemical processes utilizing renewable starting materials are best achieved by the close integration of biocatalytic and heterogeneous catalytic processes.⁸⁰ Apart from fermentation to bioethanol⁸¹ and reforming to CO/H₂,⁸² the direct conversion of these sugars to useful platform chemicals is highly attractive.⁷⁵ Examples of such chemicals are levulinic acid⁸³ and 5-hydroxymethylfurfural (HMF).⁸⁴ HMF can be prepared in high yield from D-fructose,⁸⁵ although research is underway to convert D-glucose or even cellulose directly into HMF.⁸⁶ It can be converted into a range of derivatives with potential applications as a biofuel (furanics) and as building blocks for the polymer and solvent industry.

Furan derived compounds and intermediates are accessible from furfural, an intermediate that is already produced on industrial scale from pentose sugars. Compounds based on the structural motif of furan have also been discussed as potential biofuel candidates.^{87,88} Given the more versatile and larger availability of C₆ over C₅ sugars in biomass feedstock, it seems attractive to establish an entry into this product and process network by using HMF as the platform chemical. HMF can be obtained through catalytic processes from hexoses or even cellulose.⁸⁹ Recently, a number of examples demonstrated the potential of retaining the furan structure from HMF in the formation of desired biobased target products.⁸⁸ However, processes for the production and further transformation of HMF are

often hampered by its low stability under conventional reaction conditions. In particular, the formation of insoluble polymers, so-called humins, is often observed at elevated reaction temperatures.⁹⁰ The undesired formation of humins strongly limits the yields of the desired products and lowers the carbon efficiency, thus putting severe constraints on the sustainable utilization of HMF as the platform chemical.

One of the useful approaches is the synthesis of caprolactam *via* its derivatives based on HMF. The proposed reaction for the conversion of HMF into caprolactone, *via* 1,6-hexanediol is shown in Figure 1.7.⁹¹

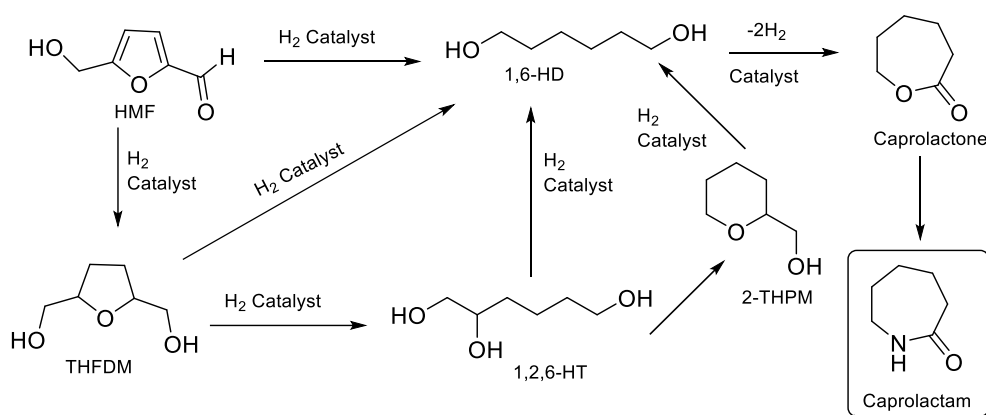


Figure 1.7 Conversion of HMF into caprolactam

On the other hand, with the increasing demand on biorenewable resources as an alternative feedstock for the production of fuels and bulk chemicals,⁹² HMF gained considerable attention as it is derived from renewable resources like fructose, glucose or cellulose. HMF acts as a bridging molecule linking biomass to fuels and chemicals and is also very useful for the production of the biofuel dimethylfuran and other important commodities (Figure 1.8).⁹³

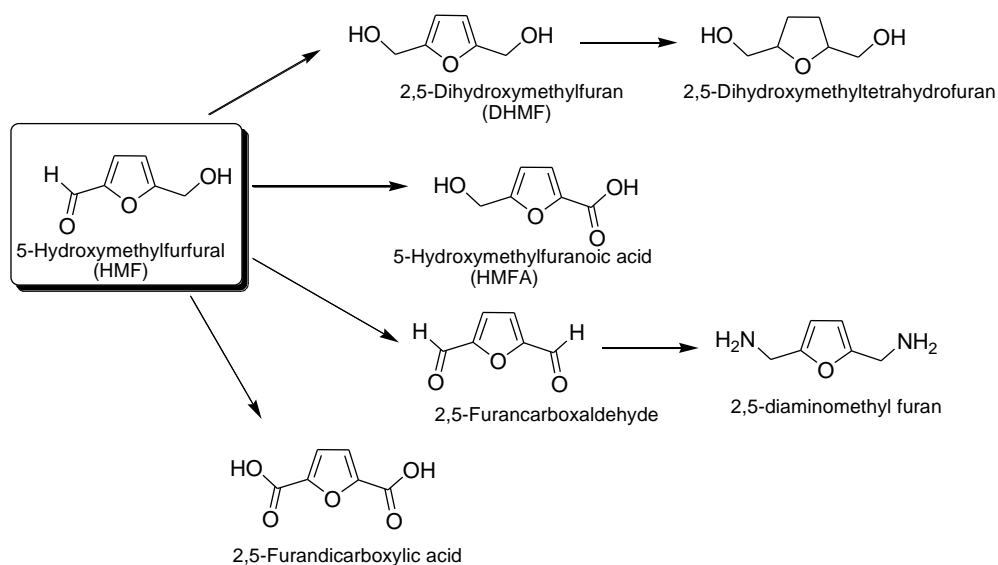


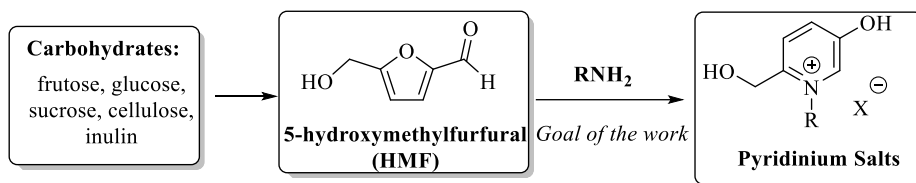
Figure 1.8 Intermediates with great industrial potential from HMF

In summary, nature provides a vast new vista of opportunities for the preparation of new recyclable, biodegradable, chiral and/or functionalized substrates with improved biocompatibility. Thus, we integrate the sustainable synthesis of synthetically valuable pyridinium salts from biomass derived HMF as starting material which can be derived easily from cellulose.

1.5 Goal of the thesis work

1.5.1 Pyridinium salts from hydroxymethyl furfural

Bearing in mind the importance of pyridinium salts as unique heterocycles in natural product synthesis, their rich chemical reactivities, bio-applications and the emerging relevance on developing sustainability, we designed an efficient synthetic and scalable procedure for the synthesis of new Pyridinium salts from bio-renewable resources such as 5-Hydroxymethylfurfural (HMF), which can be derived from glucose, fructose, etc.



After the successful screening to obtain the catalytic conditions, we can further explore the physical, chemical, or biological characteristics of the new biomass derived pyridinium salts. Thus, the thesis work is partitioned into chapters based on the following sectors.

II – Comparative study on the viscosity measurement of halogenated imidazolium and pyridinium salts

III – Reactivity of HMF under basic conditions evolving Cannizzaro reaction

IV – Screening studies for the HMF to pyridinium transformation and their substrate scope study evidencing their mechanistic details

V – Preliminary studies on chemical reactivity and biological activities of biomass derived pyridinium salts

In each chapter, I have explained the literature on different aspects of the work to highlight its importance and novelty along with the results obtained and conclusions & related references. Chapter VI emphasizes the achieved goals and the perspectives detailing the scope of these biomass derived pyridinium salts that could put forward this sustainable approach possible for biocompatible applications.

1.6 References

- (a) Laville, R.; Amade, P.; Thomas, O. P. *Pure Appl. Chem.* **2009**, *81*, 1033;
(b) Temraz, T. A.; Houssen, W. E.; Jaspars, M.; Woolley, D. R.; Wease, K. N.; Davies, S. N.; Scott, R. H. *BMC Pharmacology* **2006**, *6*, 10; (c) Zhang,

- Z. M.; McCormick, D. B. *Proc. Natl. Acad. Sci. U.S.A.* **1991**, *88*, 10407; (d) Dasari, V. R. R. K.; Muthyala, M. K. K.; Nikku, M. Y.; Donthireddy, S. R. *Microbiol. Res.* **2012**, *167*, 346; (e) Mancini, I.; Sicurelli, A.; Guella, G.; Turk, T.; Maček, P.; Sepčí, K. *Org. Biomol. Chem.* **2004**, *2*, 1368; (f) Laville, R.; Genta-Jouve, G.; Urda, C.; Fernández, R.; Thomas, O. P.; Reyes, F.; Amade, P. *Molecules* **2009**, *14*, 4716; (g) Reyes, F.; Fernández, R.; Urda, C.; Francesch, A.; Bueno, S.; de Eguilior, C.; Cuevas, C. *Tetrahedron* **2007**, *63*, 2432.
2. (a) Śliwa, W. *N-Substituted Salts of Pyridine and Related Compounds, Synthesis, Properties, Applications*. Academic Press: Częstochowa, Poland, **1996**; (b) Coe, B. J.; Harris, J. A.; Asselberghs, I.; Wostyn, K.; Clays, K.; Persoons, A.; Brunshwig, B. S.; Coles, S. J.; Gelbrich, T.; Light, M. E.; Hursthouse, M. B.; Nakatani, K. *Adv. Funct. Mater.* **2003**, *13*, 347; (c) Dehmlow, E. V.; Dehmlow, S. S. *Phase Transfer Catalysis*, 2nd ed. Verlag Chemie, Weinheim, Germany, **1983**; (d) Scriven, E. F. V. *Chem. Soc. Rev.* **1983**, *12*, 129; (e) Madaan, P.; Tyagi, V. K. *J. Oleo Sci.* **2008**, *57*, 197.
 3. See review: Sepcik, K. Bioactive alkylpyridinium compounds from marine sponges. *J. Toxicol.* **2000**, *19*, 139.
 4. Andersen, R.J.; van Soest, R.W.; Kong, F. *Alkaloids Chemical and Biological Perspectives*. Pelletier, S.W., Ed.; Elsevier Science: Oxford, UK, **1996**, *10*, 301.
 5. (a) Bennasar, M. L.; Jiménez, J. M.; Vidal, B.; Sufi, B. A.; Bosch, J. *J. Org. Chem.* **1999**, *64*, 9605; (b) Bennasar, M. L.; Zulaica, E.; Alonso, Y.; Vidal, B.; Vázquezb, J. T.; Bosch, J. *Tetrahedron Asymmetry* **2002**, *13*, 95; (c) Focken, T.; Charette, A. B. *Org. Lett* **2006**, *8*, 2985; (d) Azzouz, R.; Fruit, C.; Bischoff, L.; Marsais, F. *J. Org. Chem.* **2008**, *73*, 1154; (e) Kuethe, J. T.; Comins D. L. *J. Org. Chem.* **2004**, *69*, 5219; (f) Bennasar, M. L.; Zulaica, E.; Yuan, C.; Alonso, Y.; Bosch, J. *J. Org. Chem.* **2002**, *67*, 7465; (g) Bennasar, M. L.; Vidal, B.; Bosch, J. *J. Org. Chem.* **1997**, *62*, 3597.
 6. Said, S.; Mahrous, H.; Kassem, A. *Infection* **1976**, *4*, 49-50.

7. (a) Nakamura, K.; Nakamura, K. *U.S. Pat* 66, **2003**, 04, 531 (2003); (b) Gross, P.; Keller, W. *U.S. Pat* 47, **1998**, 19, 930; (c) Bartuska, W.R.; Silverman, P. *U.S. Pat* 41, **1980**, 83, 366.
8. Sreenivasan, P.; Gaffar, A. *J. Clin. Periodontol.* **2002**, 29, 965.
9. Salomaa, P. *Acta Chem. Scand.* **1957**, 11, 468.
10. Pernak, J.; Walerowicz, W. *Polish J. Chem.* **1981**, 55, 1109.
11. Pernak, J. *Polish J. Chem.* **1985**, 59, 439.
12. Lyle, R. E. *In Pyridine and its Derivatives*. Wiley: New York, NY, **1974**, 1, 137.
13. Goldman, S.; Stoltefuss, J. *Angew. Chem., Int. Ed.* **1991**, 30, 1559; (b) Sunkel, C. E.; FaudeCasa, J. M.; Santos, L.; Gomes, M. M.; Villarroya, M.; Gonzalez, M.M. A.; Priego, J. G.; Ortega, M. P. *J. Med. Chem.* **1990**, 33, 3205; (c) Jaing, J. L.; Li, A. H.; Jang, S. Y.; Chang, L.; Melman, N.; Moro, S.; Ji, X.; Lobkovsky, E.; Clardy, J.; Jacobson, K. A. *J. Med. Chem.* **1999**, 42, 3055.
14. (a) Laville, R.; Jouve, G. G.; Urda, C.; Fernández, R.; Thomas, O. P.; Amade, P. *Molecules* **2009**, 14, 4716; (b) Laville, R.; Thomas, O. P.; Berrue, F.; Reyes, F.; Amade, P.; *Eur. J. Org. Chem.* **2008**, 121; (c) Suzuki, R.; Yanuma, H.; Hayashi, T.; Yamada, H.; Usuki, T.; *Tetrahedron* **2015**, 71, 1851.
15. Lavilla, R. J. *J. Chem. Soc., Perkin Trans. 1* **2002**, 1141.
16. Bull, J. A.; Mousseau, J. J.; Pelletier, G.; Charette, A. B. *Chem. Rev.* **2012**, 112, 2642.
17. Welton, T. *Chem. Rev.* **1999**, 99, 2071.
18. Wasserscheid, P.; Welton, T. *Ionic Liquids in Synthesis*, 2nd ed.; Wiley-VCH: Weinheim, Germany, **2008**
19. Hough, T.; Smiglak, W. L.; Griffin, M.; Reichert, S.; Mirska, W. M.; Liebert, J.; Adamska, T.; Nawrot, J.; Stasiewicz, M.; Rogers, R. D.; Pernak, J. *New J Chem* **2009**, 33, 26.
20. Chinnappan, A.; Kim, H. *Chem Eng J.* **2012**, 187, 283.

21. (a) Yu, Q.; Yan, Y. Liang, M. *Tribol. Lett.* **2007**, *25*, 197. (b) Ming, X. W.; Zhou, Z. M.; Li, D.; Yao, F.; Qing, X. *Energy Fuels* **2009**, *3*, 2278. (c) Liu, Q.; Rantwijk, V.F; Sheldon, R. A. *J. Chem. Technol. Biotechnol.* **2006**, *81*, 401. (d) Lee, B. S.; Chi, Y.S.; Lee, S. *J. Am. Chem. Soc.* **2004**, *126*, 480.
22. Wang, J. L.; Yao, H. W.; Nie, Y.; Zhang, X. P.; Li, J. W. *J. Mol. Liq* **2012**, *169*, 152.
23. Zhao, D. B.; Fei, Z. F.; Geldbach, T. J.; Scopelliti, R.; Dyson, P. J. *J. Am. Chem. Soc.* **2004**, *126*, 15876.
24. (a) Arfan, A.; Bazureau, J. P. *Org. Process. Res. Dev.* **2005**, *9*, 743; (b) Xing, H.; Wang, T.; Zhou, Z.; Dai, Y. *Ind. Eng. Chem. Res.* **2005**, *44*, 4147.
25. Duan, Z. Y.; Gu, Y. L.; Zhang, J.; Zhu, L. Y.; Deng, Y. Q. *J Mol Catal a-Chem* **2006**, *250*, 163.
26. Noweouzi, N.; Farahi, S.; Irajzadeh, M.; *Tetrahedron Lett* **2015**, *56*, 739.
27. (a) Gorodetsky, B.; Ramnial, T.; Brandaand, N. R.; Clyburne, J. A. C. *Chem. Commun.*, **2005**, 325; (b) Jurcik, V.; Wilhelm, R. *Green Chem.*, **2005**, *7*, 844.
28. Law, M. C.; Wong, K. Y.; Chan, T. H. *Chem Commun* **2006**, 2457.
29. (a) Chowdhury, S.; Mohan, R. S.; Scott, J. L. *Tetrahedron* **2007**, *63*, 2363; (b) Ren, R. X.; Wu, J. X. *Org. Lett.* **2001**, *3*, 3727; (c) Nguyen, H. P.; Matondo, H.; Baboulene, M. *Green Chem.* **2003**, *5*, 303.
30. Xu, W.; Dolbier, W. R.; Salazar, J. *J Org Chem* **2008**, *73*, 3535.
31. Salazar, P. J.; Dorta, R. *Synlett* **2004**, 7,1318.
32. Zali-Boeini, H.; Shokrolahi, A.; Zali, A.; Ghani, K. *J Sulfur Chem* **2012**, *33*, 165.
33. Lingampalle, D.; Jawale, D.; Waghmare, R.; Mane, R. *Synthetic Commun* **2010**, *40*, 2397.
34. Kroutil, J.; Budesinsky, M. *Carbohydrate Res.* **2007**, *342*, 147.
35. Zhao, S. H.; Zhang, H. R.; Feng, L. H.; Chen, Z. B. *J. Mol. Catal. A-Chem* **2006**, *258*, 251.

36. Zhao, S.H.; Bie, H.Y.; Chen, Z.B. *Org. Prep. Proced. Int.* **2005**, *37*, 231.
37. Harjani, J. R.; Singer, R. D.; Garcias, M. T.; Scammells, P. J. *Green Chem.* **2009**, *11*, 83.
38. Ford, L.; Ylijoki, K. E. O.; Garcia, M. T.; Singer, R. D.; Scammells, P. J. *Aust. J. Chem.* **2015**, *68*, 849.
39. (a) Grabinskasota E.; Kalka, J. *Environ. Int.*, **2003**, *28*, 687; (b) Docherty, K. M.; Dixon, J. K.; Kulpa, C. F. *Biodegradation*, **2007**, *18*, 481; (c) Stolte, S.; Abdulkarim, S.; Arning, J.; Blomeyer, K. N.; Bottin, U. W. Matzke, M.; Ranke, R.; Jastorff B.; Thoeming, J. *Green Chem.*, **2008**, *10*, 214.
40. Harjani, J. R.; Singer, R. D.; Garcia, M. T.; Scammells, P. J. *Green Chem.* **2008**, *10*, 436.
41. Deng, Y.; Beadham, I.; Ghavre, M.; Costa Gomes, M. F.; Gathergood, N.; Husson, P.; Légrret, B.; Quilty, B.; Sancelme, M.; Besse-Hoggan, P. *Green Chem.* **2015**, *17*, 1479.
42. Roosjen, A.; Smisterova, J.; Driessen, C.; Anders, J. T.; Wagenaar, A.; Hoekstra, D.; Hulst, R.; Engberts, J. B. F. N. *Eur. J. Org. Chem.* **2002**, 1271.
43. (a) Lim, C.; Kim, S.-H.; Yoh, S.-D.; Fujio, M.; Tsuno, Y. *Tetrahedron Lett.* **1997**, *38*, 3243; (b) Kondo, Y.; Ogasa, M.; Kusabayashi, S. *J. Chem. Soc., Perkin Trans. 2* **1984**, 2093; (c) Castejon, H.; Wiberg, K. B. *J. Am. Chem. Soc.* **1999**, *121*, 2139; (d) Abramovitch, R. A.; Klingsberg, E. *Pyridine and Its Derivatives: Supplement*; Wiley: New York. **1974**; (e) Pernak, J.; Rogoza, J. *Arkivoc* **2000**, *1*, 889.
44. Marek, J.; Stodulka, P.; Cabal, J.; Soukup, O.; Pohanka, M.; Korabecny, J.; Musilek K.; Kuca, K. *Molecules* **2010**, *15*, 1967.
45. (a) Wong, Y. S.; Marazano, C.; Gnecco, D.; Das, B. C. *Tetrahedron Lett.* **1994**, *35*, 707; (b) Mehmandoust, M.; Marazano, C.; Das, B. C. *J. Chem. Soc., Chem. Commun.* **1989**, 1185; (c) Diez, A.; Vilaseca, L.; Lopez, I.; Rubiralta, M.; Marazano, C.; Grierson, D. S.; Husson, H. P. *Heterocycles* **1991**, *32*, 2139; (d) Comins, D. L.; Joseph, P.; Boehring, R. R. *J. Am. Chem.*

- Soc.* **1994**, *116*, 4719. (e) Palin, R.; Clark, J. K.; Cowley, P.; Muir, A. W.; Pow, E.; Prosser, A. B.; Taylor, R.; Zhang, M. Q. *Bioorg. Med. Chem. Lett.* **2002**, *12*, 2569.
46. (a) Kost, A. N.; Gromov, S. P.; Sagitullin, R. S. *Tetrahedron* **1981**, *37*, 3423; (b) Zincke, T. H.; Heuser, G.; Moller, W. *Ann. Chim.* **1904**, 333, 296; (c) Genisson, Y.; Marazano, C.; Mehmandoust, M.; Gnecco, D.; Das, B. C. *Synlett* **1992**, 431.
47. (a) Eda, M.; Kurth, M. J. *Tetrahedron Lett.* **2001**, *42*, 2063; (b) Urban, D.; Duval, E.; Langlois, Y. *Tetrahedron Lett.* **2000**, *41*, 9251; (c) Eda, M.; Kurth, M. J.; Nantz, M. H. *J. Org. Chem.* **2000**, *65*, 5131.
48. Gustavo H. R. V.; Santos, I. C.; Alves, R. B.; Rossimiriam P.F. G. *Tetrahedron Lett.* **2005**, *46*, 7773.
49. (a) Marvell, E.N.; Caple, G.; Shahidi, I. *J. Am. Chem. Soc.* **1970**, *92*, 5641; (b) Marvell, E.N.; Shahidi, I. *J. Am. Chem. Soc.* **1970**, *92*, 5646; (c) Eda, M.; Kurth, M. J.; Nantz, M. H. *J. Org. Chem.* **2000**, *65*, 5131
50. Yamaguchi, I.; Higashi, H.; Shigesue, S. Shingai, Sato, M. *Tetrahedron Lett.* **2007**, *48*, 7778.
51. Zhao, S. H.; Xu, X. M.; Zheng, L.; Liu, H. *Ultrason Sonochem* **2010**, *17*, 685.
52. Petit, S.; Azzouz, R.; Fruit, C.; Bischoff, L.; Marsais, F. *Tetrahedron Lett* **2008**, *49*, 3663.
53. Auth, J.; Mauleon, P.; Pfaltz, A. *Arkivoc* **2014**, 154.
54. Echterhoff, A. K. C.; Yogendra, S.; Kusters, J.; Fischer, R.; Weigand, J. J. *Eur J Org Chem* **2014**, 7631
55. Guanaes, L. D.; Ducatti, D. R. B.; Duarte, M. E. R.; Barreira, S. M. W.; Nosedá, M. D.; Goncalves, A. G. *Tetrahedron Lett* **2015**, *56*, 2001.
56. (a) Furdui, B.; Dinica, R.M.; Tabacaru, A.; Pettinari, C. *Tetrahedron* **2012**, *68*, 6164; (b) Shi, Z. J.; Neoh, K. G.; Kang, E. T. *Biomaterials* **2005**, *26*, 501; (c) Palin, R.; Clark, J. K.; Cowley, P.; Muir, A. W.; Pow, E.; Prosser, A. B.; Taylor, R.; Zhang, M. Q. *Bioorg. Med. Chem. Lett.* **2002**, *12*, 2569;

- (d) Scriven, E. F. V. *Chem. Soc. Rev.* **1983**, 12,129; (e) Pernak, J.; Rogoza, J. *Arkivoc* **2000**, 1, 889.
57. Furdui, B.; Parfene, G.; Ghinea, I. O.; Dinica, R. M.; Bahrim, G.; Demeunvnc, M.; *Molecules* **2014**, 19, 11572.
58. (a) Ilies, M. A.; Seitz, W. A.; Caproiu, M. T.; Wentz, M.; Garfield, R. E.; Balaban, A. T. *Eur. J. Org. Chem.* **2003**, 2645; (b) Ilies, M. A.; Seitz, W. A.; Ghiviriga, I.; Johnson, B. H.; Miller, A.; Thompson, E. B.; Balaban, A. T. *J. Med. Chem.* **2004**, 47, 3744; (c) Ilies, M. A.; Johnson, B. H.; Makori, F.; Miller, A.; Seitz, W. A.; Thompson, E. B.; Balaban, A. T. *Arch. Biochem. Biophys.* **2005**, 435, 217.
59. (a) Bogatian, M.; Deleanu, C.; Mihai, G.; Balaban, T. S. Z. *Naturforsch.* **1992**, 47b, 1011; (b) Bogatian, M.; Vinatoru, M.; Bogatian, G.; Mihai, G.; Balaban, T. S. *Rev. Roum. Chim.* **2004**, 49, 819.
60. (a) Balaban, T. S.; Balaban, A. T. *Pyrylium Salts. Science of Synthesis. Houben-Weyl Methods of Molecular Transformations*; G. Thieme Verlag: Stuttgart, Germany, **2003**; 11-200. (b) Schroth, W.; Balaban, A. T. *Pyrylium Salts. Methoden der Organischen Chemie (Houben-Weil) (Methods of Organic Chemistry (Houben-Weil))*; G. Thieme Verlag: Stuttgart, Germany, **1992**; 755-963. (c) Balaban, A. T.; Dinculescu, A.; Dorofeenko, G. N.; Fischer, G. W.; Koblik, A. V.; Mezheritskii, V. V.; Schroth, W. *Pyrylium Salts: Syntheses, Reactions and Physical Properties*. In *Advances in Heterocyclic Chemistry*; Academic Press: New York, **1982**; 8-360.
61. Ilies, M. A.; Seitz, W. A.; Johnson, B. H.; Ezell E. L.; Miller A. L.; Thompson E. B.; Balaban A. T. *J. Med. Chem.* **2006**, 49, 3872.
62. Savarala, S.; Brailoiu, E.; Wunder, S. L.; Ilies, M. A. *Biomacromolecules* **2013**, 14, 2750.
63. Fujioka, H.; Okitsu, T.; Sawama, Y.; Murata, N.; Li, R.; Kita, Y. *J. Am. Chem. Soc.* **2006**, 128, 5930.
64. Fujioka, H.; Minamitsuji, Y.; Moriya, T.; Okamoto, K.; Kubo, O.; Matsushita, T.; Murai, K. *Chem-Asian J* **2012**, 7, 1925.

65. Fujita, R.; Hoshino, M.; Nishiuchi, Y.; Tomisawa, H. *Yakugaku Zasshi* **2006**, 126, 109-116.
66. Boga, C.; Bonamartini, A. C.; Forlani, L.; Modarelli, V.; Righi, L.; Sgarabotto, P.; Todesco, P. E. *Eur. J. Org. Chem.* **2001**, 1175.
67. Peixoto, S.; Nguyen, T. M.; Crich, D.; Delpech, B.; Marazano, C. *Org. Lett.*, **2010**, 12, 4760.
68. Chen, L. J.; Burka, L. T. *Chem. Res. Toxicol.* **2007**, 20, 1741.
69. Luo, C. Z.; Jayakumar, J.; Gandeepan, P.; Wu, Y. C.; Cheng, C. H. *Org. Lett.* **2015**, 17, 924.
70. Luo, C. Z.; Jayakumar, J.; Gandeepan, P.; Wu, Y. C.; Cheng, C. H. *Org. Lett.* **2015**, 17, 924.
71. Nolsoe, J. M. J.; Aursnes, M.; Tungen, J. E.; Hansen, T. V. *J. Org. Chem.*, **2015**, 80, 5377.
72. Reichardt, C.; Che, D.; Heckenkemper, G.; Shafer, G. *Eur. J. Org. Chem.* **2001**, 2343-2361.
73. (a) Baharloo, F.; Moslemin, M. H.; Nadri, H.; Asadipour, A.; Mahdavi, M.; Emami, S.; Firoozpour, L.; Mohebat, R.; Shafiee, A.; Foroumadi, A. *Eur. J. Med. Chem* **2015**, 93, 196; (b) Nadri, H.; Pirali-Hamedani, M.; Shekarchi, M.; Abdollahi, M.; Sheibani, V.; Amanlou, M.; Shafiee, A.; Foroumadi, A. *Bioorg. Med. Chem.* **2010**, 18, 6360.
74. (a) Huber, G. W.; Iborra, S.; Corma, A. *Chem. Rev.* **2006**, 106, 4044; (b) Corma, A.; Iborra, S.; Velty, A. *Chem. Rev.* **2007**, 107, 2411.
75. (a) Tolan J. F. in *Biorefineries-Industrial Processes and Products. Status Quo and Future Directions* (Eds.: B. Kamm, P. R. Gruber, M. Kamm), Wiley-VCH, Weinheim, **2006**, 193; (b) Stácker, M. *Angew. Chem. Int. Ed.* **2008**, 120, 9340; (c) Lange, J. P. *Biofuels Bioprod. Biorefin.* **2007**, 1, 39. (d) *Top Value-Added Chemicals from Biomass Vol. I—Results of Screening for Potential Candidates from Sugars and Synthesis* (Eds.: T. Werpy, G. Petersen), U. S. Department of Energy (DOE) by the National Renewable Energy Laboratory a DOE national Laboratory, **2004**.

76. Klass, D. L. *Biomass for Renewable Energy, Fuels, and Chemicals*, Academic Press, California, **1998**, 495.
77. Palsson, B. O; Fathi-Afshar, S.; Rudd, F. F. Lightfoot, E. N. *Science* **1981**, *213*, 513.
78. Kamm, B. *Angew. Chem. Int. Ed.* **2007**, *119*, 5146.
79. Lichtenthaler F. W. in *Biorefineries-Industrial Processes and Products* (Eds.: Kamm, B. Gruber, P. R. Kamm, M), Wiley-VCH, Weinheim, **2006**, 3-51.
80. Christensen, C. H.; Hansen, R. J.; Marsden, C. C.; Taarning, E.; Egeblad, K. *ChemSusChem* **2008**, *1*, 283.
81. Special Issue on Lignocellulosic Bioethanol: Current Status and Perspectives, *Bioresour. Technol.* **2010**, *101*, 4743.
82. Davda, R. R.; Shabaker, J. W.; Huber, G. W.; Dumesic, J. A. *Appl. Catal. B.* **2005**, *56*, 171.
83. Bozell, J. J.; Moens, L.; Elliott, D. C.; Wang, Y.; Neuenschwander, G. H.; Fitzpatrick, S. W; Bilski, R. J.; Jarnefeld, J. L. *Resour. Conserv. Recycl.* **2000**, *28*, 227.
84. a) Kuster, B. F. M. *Starch/Staerke* **1990**, *42*, 314; (b) Lewkowski, J. *Arkivoc* **2001**, 17; (c) van Putten, R. J.; van der Waal, J. C.; de Jong, E.; Heeres, H. J.; de Vries, J. G. *Chem. Rev.* **2013**, *113*, 1499.
85. (a) Gaseet, A. Rigal, L. Paillassa, G. Dsalome, J.-P. Fleche G. FR2551754, **1985**; (b) Seri, K.-I. Inoue, Y. Ishida, H. *Chem. Lett.* **2000**, *22*; (c) Bicker, M. Hirth, J. Vogel, H. *Green Chem.* **2003**, *5*, 280; (d) Moreau, C.; Finiels, A.; Vanoye, L. *J. Mol. Catal. A.* **2006**, *253*, 165; (e) Romn-Leshkov, Y.; Chheda, J. N. Dumesic, J. A. *Science* **2006**, *312*, 1933; (f) Dignan, C.; Sanborn, A. J. (Archer Daniels Midland), WO2009/012445, **2009**.
86. (a) Zhao, H.; Holladay, J. E.; Brown, H.; Zhang, Z. C. *Science* **2007**, *316*, 1597; (b) Hu, S.; Zhang, Z.; Song, J.; Zhou, Y.; Han, B. *Green Chem.* **2009**, *11*, 1746; (c) J. B. Binder, R. T. Raines, *J. Am. Chem. Soc.* **2009**, *131*, 1979.

87. (a) Ullmann's Encyclopedia of Industrial Chemistry, Wiley-VCH, Weinheim, **2001**; (b) Zeitsch, K. J. *The Chemistry and Technology of Furfural and its Many By-Products*, Elsevier, Amsterdam, **2000**; c) Corma, A.; de La Torre, O.; Renz, M.; Villandier, N. *Angew. Chem. Int. Ed.* **2011**, *123*, 2423.
88. (a) Román-Leshkov, Y.; Dumesic, J. A. *Nature* **2007**, *447*, 982; b) Mascal, M.; Nikitin, E. B. *Angew. Chem. Int. Ed.* **2008**, *120*, 8042; (b) Thananathanachon, T.; Rauchfuss, T. B. *Angew. Chem. Int. Ed.* **2010**, *122*, 6766; (c) Chidambaram, M.; Bell, A. T. *Green Chem.* **2010**, *12*, 1253.
89. (a) Román, L.; Chheda, J. N.; Dumesic, J. A. *Science* **2006**, *312*, 1933; b) H. B. Zhao, J. E. Holladay, H. Brown, Z. C. Zhang, *Science*. **2007**, *316*, 1597; c) G. Yong, Y. G. Zhang, J. Y. Ying, *Angew. Chem.* **2008**, *120*, 9485; (d) Vanoye, L.; Fanselow, M.; Holbrey, J. D.; Atkins, M. P. Seddon, R. *Green Chem.* **2009**, *11*, 390;
90. Chambel, P.; Oliveira, M. B.; Andrade, P. B.; Fernandes, J. O.; Seabra, R. M.; Ferreira, M. A. *Food Chem.* **1998**, *63*, 473.
91. Buntara, T.; Noel, S.; Phua, P. H.; Cabrera, I. M.; Heeres, H. J. *Angew. Chem. Int. Ed.* **2011**, *50*, 7083.
92. a) Huang, W. X.; Wu, B.; Gao, X.; Chen, M. W.; Wang, B.; Zhou, Y. G. *Org. Lett.* **2015**, *7*, 1640; (b) Ye, Z. S.; Chen, M. W.; Chen, Q. A.; Shi, L.; Duan, Y.; Zhou, Y. G. *Angew. Chem. Int. Ed.* **2012**, *51*, 10181.
93. Sepcik, K.; Turk, T. *Prog. Mol. Subcell. Biol.* **2006**, *42*, 105.

CHAPTER II

*Studies on halogenated imidazolium
and pyridinium ILs*

I have optimized the reaction conditions, scaled up the synthesis, performed the spectral characterization, and developed the purification methods of all the new ionic liquids presented herein.

2. Studies on halogenated imidazolium and pyridinium ILs

Chapter II - Summary

The flexibility to tailor the size, shape and functionality of the cations and anions of ionic liquids offers great opportunities for tuning their physicochemical properties. Designing less viscous RTILs is of particular interest for their possible industrial application as solvents in reactions and material processing, as extraction media or as working fluids in mechanical applications. On the other hand, the understanding of the intermolecular forces acting between the ions has now become crucial for the development of special ionic liquids with tuneable properties. Correlation studies between the hydrogen bond and the physicochemical properties of RTILs, factors such as charge symmetry, directional H-bonds introduce “defects” into the Coulomb network of ILs and increase the dynamics of the cations and anions, resulting in decreased melting points and reduced viscosities. Thus, fluidizing ionic liquids could be achieved by inducing the increase of the strength of the hydrogen bonds.

Thus, in this chapter we propose an approach to fluidize ILs, where some imidazolium and pyridinium ionic liquids with one or more electron withdrawing groups were synthesized. Viscosity measurements were performed to evaluate the viability of this approach to generate less viscous ILs by increasing the directional H-bond strength.

Chapter II

2.1 Introduction

2.1.1 Ionic liquids (ILs) are organic salts comprised entirely of ions with melting points near room temperature or by convention below 100 °C. They differ from simple inorganic salts such as NaCl that melt at very high temperatures by rendering their routine use as solvents for chemical processing. Past decade has seen the advent of this new class of salts¹ with organic cations opening a window for the liquid state at more moderate temperatures. Though the first report on room temperature molten salt ethylammonium nitrate dates back to 1914,² it was not recognized as solvent. The synthesis of organic chloroaluminates was presented in 1951,³ and was studied in detail only in 1970,⁴ however these salts required inert atmosphere to avoid undergoing rapid hydrolysis. Later, in 1990's, the interesting fact that many ion combinations form air- and water- stable ILs⁵ paved the flexible syntheses of ILs by tailoring the size, shape and functionality of the component cations and anions, that could offer numerous combinations for tuning the physiochemical properties. Knowing their potential use with negligible vapor pressure^{1,2} as new chemical, catalytic and electrochemical reaction media, the design of RTILs is still one of the most fascinating domains of current chemical research. The unique properties of ILs favour applications in diverse fields, such as synthesis, catalysis, biocatalysis, separation technology, electrochemistry, analytical chemistry, and nanotechnology.^{1,6} Optimizing the cations with functionalized, for example, polar, fluorinated, or chiral side chains for given applications developed "task-specific ILs", where one can simply alter the properties of interest makes them being recognized as "designer solvents".⁷ Huge potential within these substitution patterns has already driven them as a promising class of technologically useful and interesting materials.⁷⁻¹² Moreover, the growing interest in a sustainable "green" chemistry has boost the interest on ionic liquids.

Current interests are to experimentally and theoretically correlate the ionic structures of RTILs with the physicochemical properties based on theoretical calculations and simulation. It became evident that tuning the properties of ILs is of great importance for their application in science and technology.

2.1.2 Molecular understanding of ILs and ionic interactions

A molecular-based understanding is of great challenge due to the complex interplay of molecular interactions caused by the charge and the molecular and electronic structure of the ions. It is now understood that rational design of ILs will need a deeper molecular-based understanding of their properties. Though physicochemical properties are now well characterized and available from public data bases, such as “ILThermo” managed by the U.S. National Institute of Standards and Technology, theoretical analyses often have to be based on incomplete or uncertain experimental data.

In general, the molecular interactions between cations and anions result from their geometry and charge distribution. In simple salts the interactions are controlled by long-range Coulomb forces between the net charges of the ions. The molecular ions in ILs with their bulky size and asymmetric charge distribution soften the Coulomb forces and generate highly directional interactions of shorter range. The interaction potential depends on the distance of the ions and a set of angles for their mutual orientation such as electrostatic, inductive, and van der Waals (dispersive/repulsive) interactions.

In order to determine the most stable arrangement, Brobjer and Murrell⁸ represented the molecular multipole moments by distributing point charges within the molecules, evaluating the electrostatic energy at these point charges as a function of angular geometry. In 1986, Buckingham and Fowler,⁹ represented the charge density of any particular monomer, obtained by accurate *ab initio* calculations, by point multipoles-charges that are embedded in hard van der Waals

spheres possessing short-range repulsion. The results of the calculations show that the electrostatic contribution is generally the dominant factor in determining both the strength and the directionality of the complex while the calculated interaction energy is partitioned into electrostatic, exchange, polarization, and charge-transfer contributions.

For example, 1-alkyl-3-methylimidazolium hexafluorophosphates $[C_n\text{mim}][\text{PF}_6]$ contains a cation with a polar head group, where most of the electrostatic charge is concentrated, and a nonpolar alkyl side chain, whereas the PF_6 anion is octahedral, hence almost spherical. Molecular asymmetry built into the ions, usually by cations make the main difference between RTILs and simple molten salts.¹⁰ This asymmetry opposes the strong charge ordering due to the ionic interactions that normally would cause the system to crystallize. The hypothesis is also supported by an extended network of cations and anions connected together by hydrogen bonds (through the aromatic hydrogens or methylene hydrogens of the ring), with each cation surrounded by at least three anions and each anion surrounded by at least three cations. Although the number of anions surrounding cations or vice versa depends the anion size and alkyl substituents of imidazolium ring, this hydrogen bonded network of ions is a common feature of imidazolium crystals 6 that is retained in the liquid phase at molecular level.

Another interesting study by Watanabe *et al.*¹¹ on the dependence of viscosity, diffusion, and ionic conductivity with the alkyl-chain length in $[C_n\text{mim}][(\text{CF}_3\text{SO}_2)_2\text{N}]$ ionic liquids ($n=1, 2, 4, 6, 8$), which showed the increase in viscosity and the diffusion and ionicity decrease with increasing chain length. Various intermolecular forces exist between the ions in the liquid phase including ion-ion, hydrogen bonding and van der Waals forces. It is expected that, as the side-chain length increases, the overall contribution of the strong, associating electrostatic (and hydrogen-bond) terms to the interactions diminishes, while the contribution of weaker, non-associating dispersion forces increases. As the size of the cations increases, the centers of charge are held farther apart on average, which

decreases Coulombic interactions.¹² As a consequence, it could be anticipated that the viscosity would decrease as the size of the nonpolar part of the cations becomes larger. Experimental results by distinct authors,^{11,13} show that it is the increase in the van der Waals interactions due to the presence of a long alkyl chain that leads to higher viscosities. The lack of a strong molecular basis for these salts has evidently created controversies quite often.

In general, the cation-anion interaction in ionic liquids is studied by matching the frequency range of these interaction energies by experimental methods such as optical heterodyne-detected Raman induced Kerr-effect spectroscopy, THz spectroscopy, and low-energy neutron scattering, FTIR and Raman studies on ionic liquids investigate the intramolecular stretching and bending modes by mid infrared range. Low frequency vibrational bands are assigned to the bending and stretching modes of the cation-anion interaction through hydrogen bond, whereas the intermolecular stretching modes are shifted to higher wave numbers with increasing ionic strength of the used anion. Thus the interpretation can be correlated to the calculated average binding energies of the ionic liquid clearly reflecting the cohesive energy between cations and anions in ionic liquids and is consistent with the *ab initio* calculate frequencies of ionic liquid clusters.

2.2 Fluidize ionic liquids

For any application of an ionic liquid, apart from non-volatility, the physical properties such as low melting point, low viscosity, high ionic conductivity and thermal/electrochemical stability, solvent behaviour are a key feature. Thus, an intense interest exists due to the wide range of possible industrial application as solvents for reactions and material processing, as extraction media or as working fluid in mechanical applications.

One of the most important properties of an IL is the viscosity, □ which stays as a barrier for several industrial applications and slow down the rate of diffusion

controlled chemical reactions. One of the lowest viscous ILs observed to date at 298 K ($\eta = 21$ cP) is $[\text{C}_2\text{mim}][(\text{CN})_2\text{N}]^{14}$, which is still more than twenty times that of water. Thus, in the synthesis of novel ILs, the search for low viscosity systems plays an essential role.^{15,16} Halide anions such as $[\text{BF}_4]^-$, $[\text{PF}_6]^-$ are strongly hygroscopic, and hydrolyse to give HF,¹⁷ in presence of moisture and thus becomes unfavourable in certain studies. It is also known that $[\text{NTf}_2]$ forms liquid salts of low viscosity with high thermal and electrochemical stability compared to other anions. In particular, when $[\text{NTf}_2]$ is replaced by its non-fluorinated homologue, bis(methanesulfonyl)amide,^{5e} there is a notable increase in viscosity and a decrease in thermal and electrochemical stability,¹⁸ that highlights the advantages of perfluorinated anions.

Various approaches to fluidize ionic liquids are shown below.

1. Weakly polar anions

By introducing weakly polar anions which strongly reduce the interaction energy between cations and anions resulting in reduced melting points and decreased viscosities.¹⁹

2. Asymmetry

Introducing asymmetry into the cations using different substituents also could lead to reduced melting point and viscosities.

For example, using different substituents at the N(1) and N(3) positions. It is reported that replacing the methyl group by an ethyl group at the C1 position in $[\text{C}_1\text{mim}][\text{NTf}_2]$ showed low viscosity.^{11, 20-21}

3. Strong, directional and localized H-bonds²²

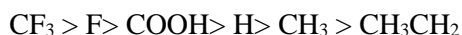
Replacing the C(2)H in imidazolium based ILs by methyl group raises melting points and increases viscosity irrespective of the anion, also coherent with documented studies.^{11,20,23}

Results from isothermographic determination of vaporization of 1-alkyl-3-methylimidazolium ILs, showed that $[C_3C_1mim][NTf_2]$ cation with a methyl group at the C(2) position possess distinctly higher enthalpies of vaporization relative to that expected for this side chain length.²⁴ This behaviour is quite interesting as the molecular volume is nearly identical for $[C_3C_1mim]$ and $[C_4mim]$ cations with a particular anion. The authors interpreted with the fact that C2 proton of C_4mim could engage in strong H-bonding with the anion of IL which is again in agreement with the strong, directional and localized H-bonds approach to liquify ILs.²²

2.2.2 Strong, directional H-bonds with inductive effect

Ludwig *et al.*²⁵ proposed a new strategy by applying an inductive effect for achieving imidazolium-based ILs with reduced melting points and lowered viscosities. Strong electron-withdrawing atoms at the C4 and C5 positions of imidazolium cations could increase the H-bond strength at C2 position. They expect that an increase in molecular volume will be overcompensated by the effect of stronger H-bonds resulting in lower viscosity. The detection of H-bonds of C2 H...A in $[C_2mim][NTf_2]$ was studied by mid infrared and far infrared spectroscopy.²³

Substituting the hydrogen atoms at the C4 and C5 positions of the imidazolium cation using different electronegative atoms shows the binding energies in the order:



Thus, the stronger the electron withdrawing inductive effect, the stronger is the H-bond whereas with electron releasing alkyl groups, the H-bond at C2 is weakened.

Thus, from this study it was strongly believed that strong, directional and localized H-bonds into the Coulomb system can fluidize ILs. However the electron-withdrawing groups such as COOH, F, CF_3 tend to increase the molecular volume of

the ILs. The resulting increase in viscosity will be overcompensated by the increasing H-bond strength at C2. Following this observations, we aimed to study the scope of inductive effect to synthesize low viscous ionic liquids. Thus we synthesised some imidazolium and pyridinium ionic liquids with some electron withdrawing groups to study their physicochemical properties.

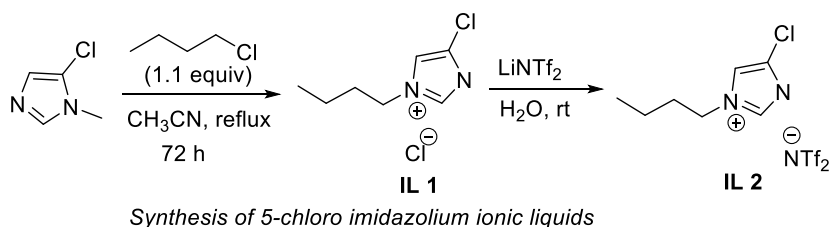
2.3 Results and discussion

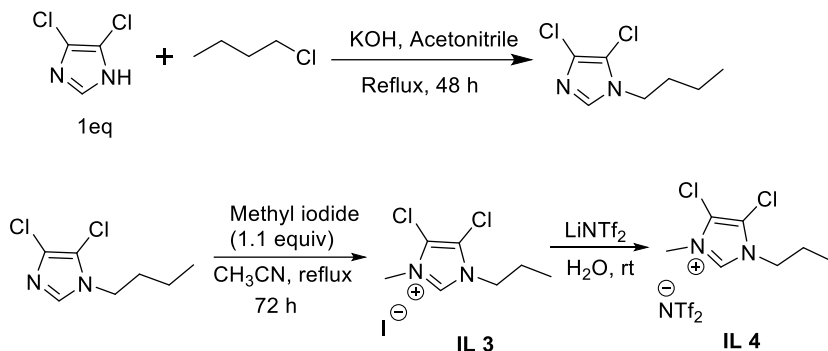
Our aim is to investigate the possibility to obtain low viscous ILs using the inductive effect. Physicochemical properties of imidazolium ILs are often well studied in comparison with other useful IL cores. Thus, we started by using imidazolium ILs, but also opened a new window with the effect of pyridinium ILs in terms of H-bond interactions.

We started our experiments by synthesizing ILs having strong electron-withdrawing inductive groups like chloride as the substituent of the imidazolium cation and fluorine in the pyridinium ring. To increase the inductive effect, we also synthesized dichloro imidazolium and difluoro pyridinium salts. The choice of anion at the first instance was halogens which then were exchanged with Lithium bistriflimide (LiNTf₂) to synthesize bistriflimide-based ILs.

2.3.1 Synthesis of new imidazolium ILs

We synthesized new imidazolium ILs with electron withdrawing groups by alkylation of 4-chloro and 4,5-dichloro imidazoles as starting materials (Scheme 2.1). The obtained imidazolium ILs possessing halogen anions were exchanged with NTf₂ anion.

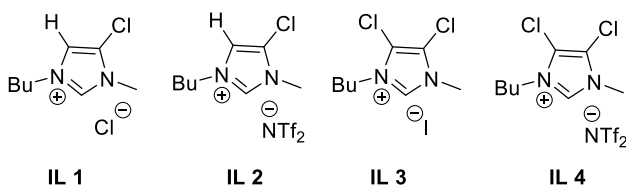




Synthesis of 4,5-dichloro imidazolium ionic liquids

Scheme 2.1 Synthesis of new imidazolium ILs

Below are the new imidazolium ILs bearing electron withdrawing groups with varying anions such as Cl, I or NTf₂. IL1 and IL2 are based on the 4-chloro imidazoles whereas IL3 and IL4 possess two electron withdrawing groups derived from 4,5-dichloroimidazoles.



All these ILs were synthesised in 5 g scale with good yield and purity with little amounts of water which was characterized by NMR. In general, the ILs were filtered through celite and silica bed filter funnel to remove any unknown impurities. Table 2.1 shows the purity of the synthesized imidazolium ILs with excellent yields on scaling up reactions.

Table 2.1 Synthesis of new imidazolium ILs

IL	Time ^a (h)	Yield (%)	Purity (%)
IL 1	95	95	95
IL 2	48	97	97

IL 3	48	98	99
IL 4	48	95	98

^aThe time varies based on the alkyl halides used for the *N*-alkylation. ^bWe used methyl iodide for alkylating 4,5-dichlorobutyl imidazole as the alkylation of 4,5-dichloromethyl imidazole did not work with butyl bromide.

The alkylation of 4-chloroimidazole took longer reaction time than 4,5-dichloroimidazoles that varied based on the alkyl halides used for the *N*-alkylation reaction. A representative ¹H NMR spectrum of the 5-chloroimidazolium bistriflimide **IL2** is shown in Figure 2.1.

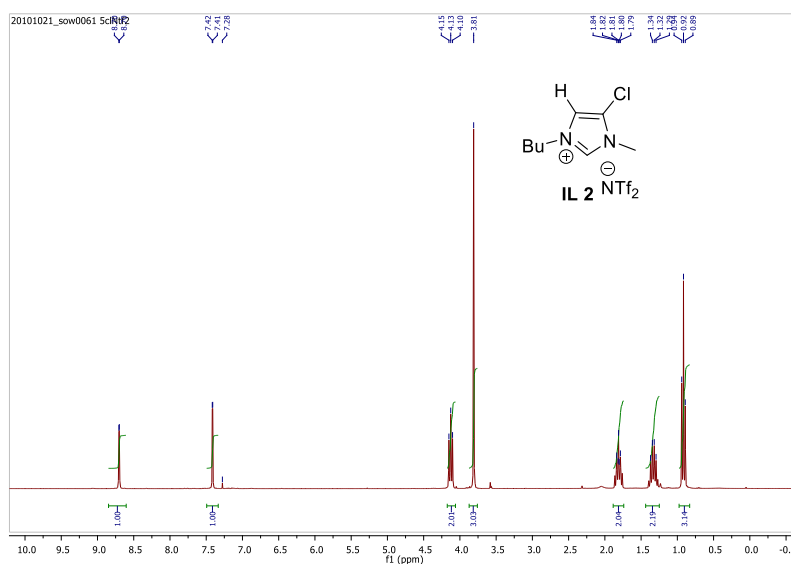
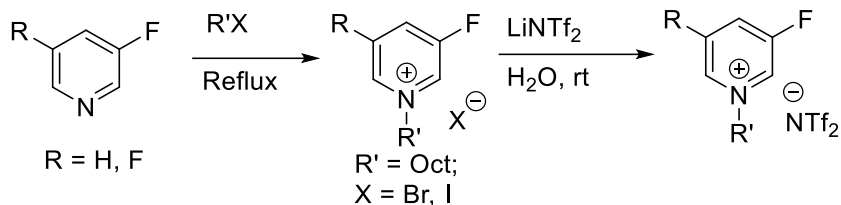


Figure 2.1 ¹H NMR of 5-chloroimidazolium bistriflimide **IL2**

2.3.2 Synthesis of new pyridinium ILs

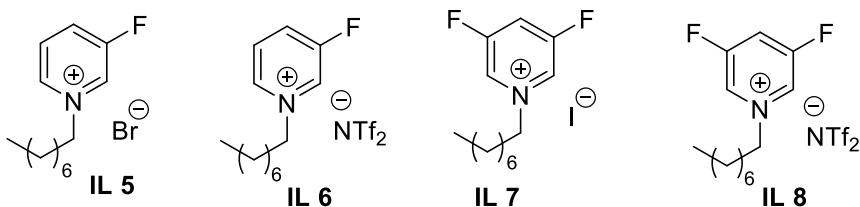
We synthesized new pyridinium ILs with electron withdrawing groups by alkylation of 3-fluoro and 3,5-difluoro pyridines as starting materials in (Scheme

2.2). The obtained pyridinium ILs possessing halogen anions were exchanged with NTf₂ anion.



Scheme 2.2 Synthesis of new pyridinium ILs

Below are the new pyridinium ILs bearing electron withdrawing groups with varying anions such as iodo or NTf₂. **IL5** and **IL6** are based on the 3-fluoropyridinies whereas **IL7** and **IL8** possess two electron withdrawing groups derived from 3,5-difluoropyridine substrates.



All these ILs were synthesised in 5 g scale with good yield and purity with little amounts of water which was characterized by NMR. In general, the ILs were filtered through celite and silica bed filter funnel to remove any unknown impurities. Table 2.2 shows the purity of the synthesized fluoro and difluoropyridinium ILs with excellent yields on scaling up reactions.

Table 2.2 Synthesis of new pyridinium ILs^a

IL	Time ^b (h)	Yield (%)	Purity (%)
IL 5	18	88	98
IL 6	48	93	97

IL 7	12	90	96
IL 8	48	96	98

^aUnless otherwise stated, the reaction was carried out in 5g scale.

^bThe time varies based on the alkyl halides used for the *N*-alkylation.

In some cases, where octyl bromide was not successful to complete reaction conversion, the option with octyl iodide was used to increase the yield with shorter reaction time. A representative ¹H NMR spectrum of the 3,5-difluoropyridinium bistriflimide **IL7** is shown in Figure 2.2.

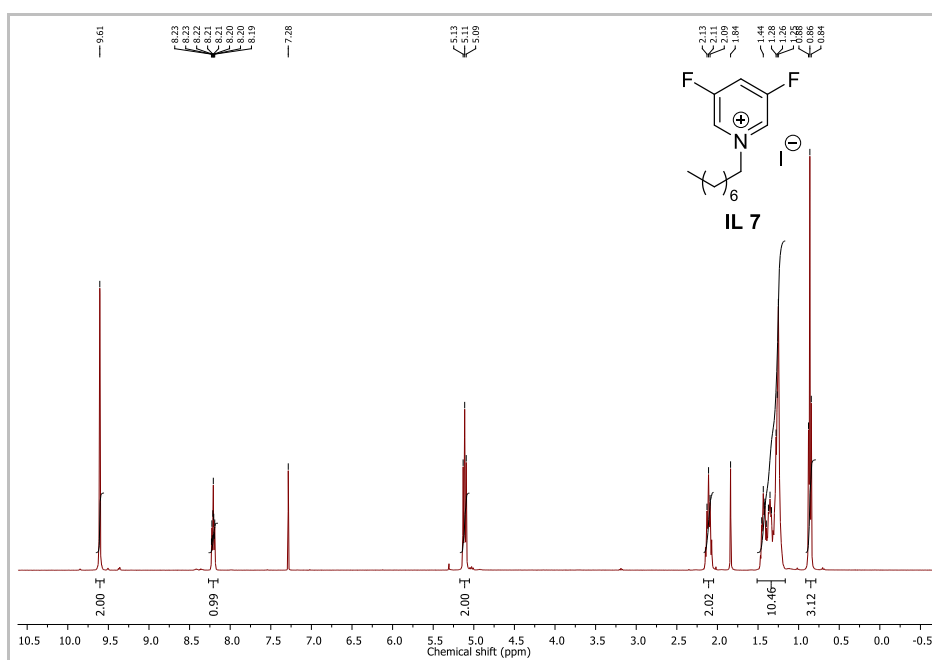


Figure 2.2 ¹H NMR of 3,5-difluoropyridinium bistriflimide **IL7**

2.3.3 Comparative viscosity study on the synthesized ionic liquids

The H-bond strength of the distinct ionic liquids used in this study was modified by making use of the inductive effect which is achieved by the transmission of charge through a chain of atoms in a molecule by electrostatic induction. By using chloride as the substituent in the C(4) and/or C(5) positions of the imidazolium

cation and fluorine in the pyridinium ring we have stronger electron-withdrawing induction groups, which strengthen the H-bond interaction. It is also known that replacing hydrogen by the strong electron-withdrawing atoms F or Cl increases the molecular volume of the proposed ILs. This fact has also a marked effect on increasing the viscosity of an ionic liquid.

The viscosity measurements were made with the synthesized imidazolium salts and the viscosity data was compared with the known standard such as [Bmim][NTf₂] ([C₄mim][NTf₂]) and the observed results are plotted as shown in Figure 2.3

In case of synthesized pyridinium salts, the viscosity measurements was compared with the known standard such as [C₈Py][NTf₂] and the observed results are plotted as shown in Figure 2.4

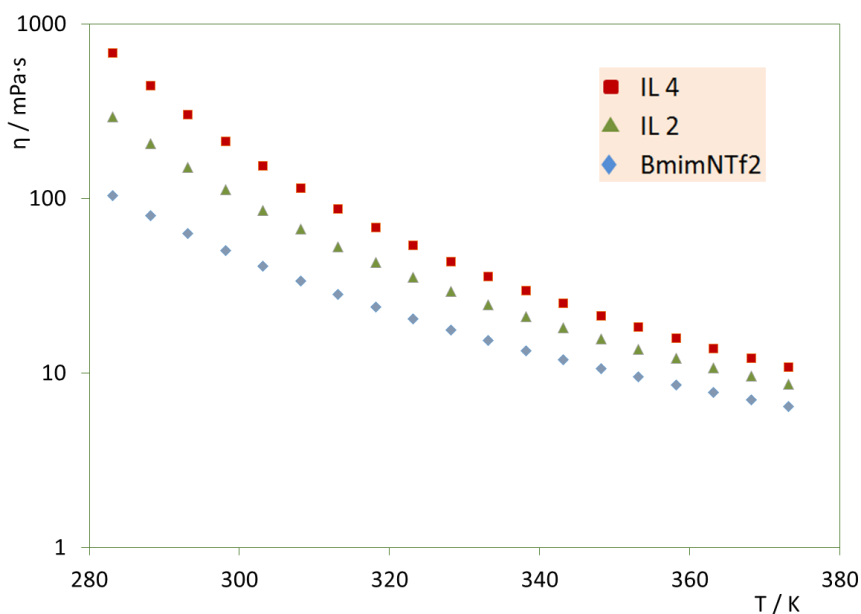


Figure 2.3 Viscosity data comparison for the synthesized imidazolium ILs

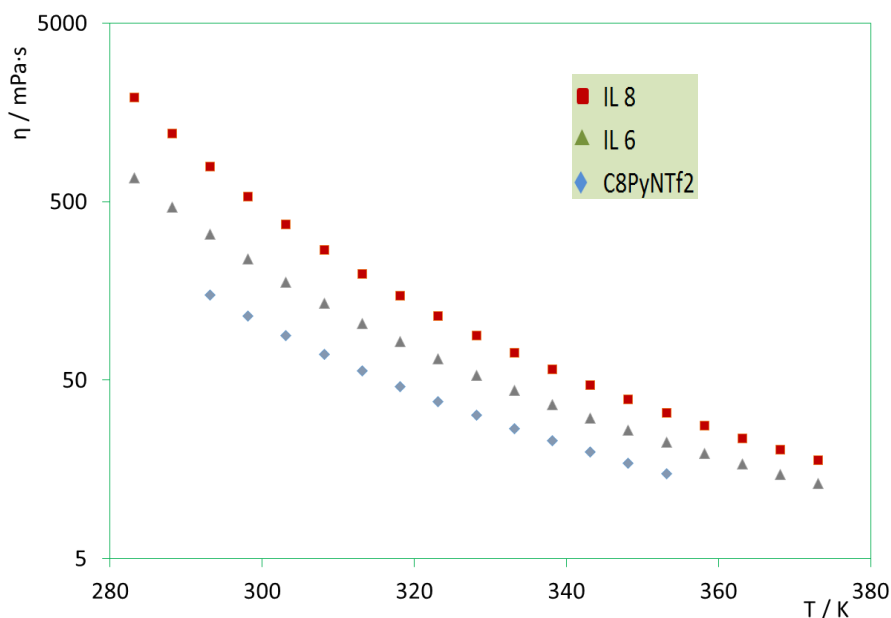


Figure 2.4 Viscosity data comparison for the synthesized pyridinium ILs

In both cases, it is clearly understood that there is a marked increase in viscosity which contrasts with the expected low viscous ILs with electron withdrawing groups. Also, the difluoro pyridinium or the dichloro imidazolium shows significant increase in viscosity by the replacement of a hydrogen atom by a halogen one. Viscosity results clearly show that the expected inductive effect, which strengthens the H-bond interaction between cation and anion, is not sufficient to compensate the increasing viscosity effect due to the size of the halogen substituents.

2.4 Conclusion

New imidazolium and pyridinium ionic liquids with one or two inductive groups were synthesised with good levels of purity for the physicochemical studies. Viscosity measurements were performed for the bistriflimide ionic liquids showed a marked increase in viscosity. This actually is contradicting the expected result where the increase in hydrogen bond strength at the C2 position would compensate the increase in molecular volume of the ILs and originate ILs with lower viscosity.

The present knowledge indicates that the molecular volume increase and the possibility of creation of distinct hydrogen bonds in the IL that would affect their structure have a stronger influence in the IL viscosity than the enhancement of the hydrogen bonding at the C2 position of the imidazolium ring. It is worth to note that other salt families may outline a highly variable behaviour which will open fascinating possibilities for the ILs over wide range of application. Molecular dynamic simulation data is currently being performed to obtain a structural explanation for this behaviour. New ionic liquids with distinct anions will also be tested to analyze if the flexibility of the bistriflimide anion is also playing a predominant role in these results.

2.5 References

1. (a) Ionic Liquids in Synthesis (Eds.: P. Wasserscheid, T. Welton), Wiley-VCH, Weinheim, **2003**; (b) P. Wasserscheid, P. A. Keim, *Angew. Chem. Int. Ed.* **2000**, *112*, 3926; (c) Forsyth, S. A.; Pringle, J. M.; MacFarlane, D. R. *Aust. J. Chem.* **2004**, *57*, 113; (d) Endres, F.; Zein El Abedin, S. *Phys. Chem. Chem. Phys.* **2006**, *8*, 2101; (e) Dupont, J.; Suarez, P. A. Z. *Phys. Chem. Chem. Phys.* **2006**, *8*, 2441; (f) Chiappe, C.; Pieraccini, D. *J. Phys. Org. Chem.* **2005**, *18*, 275; (g) Harper, J. B.; Kobrak, M. N. *Mini-Rev. Org. Chem.* **2006**, *3*, 253.
2. (a) Walden, P. *Acad. Imp. Sci. St.-Petersbourg* **1914**, *8*, 405; (b) Walden, P. *Chem. Zentralbl.* **1914**, 1800.
3. Hurley, F. H.; Wier, Jr. T. P. *J. Electrochem. Soc.* **1951**, *98*, 207.
4. (a) Welton, T. *Chem. Rev.* **1999**, *99*, 2071; (b) Hussey R. L. in *Chemistry of Nonaqueous Solutions* (Eds.: G. Mamantov, A. I. Popov), VCH, Weinheim, **1994**, 227 – 276; (c) Carlin, R. T.; Wilkes, J. S. in *Chemistry of Nonaqueous Solutions* (Eds.: G. Mamantov, Popov, A. I.), VCH, Weinheim, **1994**, 277.
5. (a) Wilkes, J. S.; Zaworotko, M. J. *J. Chem. Soc. Chem. Commun.* **1992**, 695; (b) Cooper, E. I.; Sullivan, E. J. M. *Proc. Electrochem. Soc.* **1992**, *16*,

- 386 (8th Int. Symp. Molten Salts, **1992**); (c) Chauvin, Y. Mussmann, L.; Olivier, H. *Angew. Chem. Int. Ed.* **1995**, 107, 2941; (d) Suarez, P. A. Z.; Dullius, J. E. L.; Einloft, S.; De Souza, R. F.; Dupont, . *Polyhedron* **1996**, 15, 1217; (f) BonhRte, P.; Dias, A. P.; Papageorgiou, N.; Kalyanasundaram, K.; GrStzel, M. *Inorg. Chem.* **1996**, 35, 1168. (g) Canongia Lopes, J.; Pádua, A. *J. Phys. Chem. B.* **2006**, 110, 3330. (h) Lego, A. C.; Millen, D. *J. Acc. Chem. Res.* **1987**, 20, 39.
6. (a) Welton, T. *Chem. Rev.* **1999**, 99, 2071; (b) Holbrey, J. D.; Seddon, K. R. *Clean Prod. Process.* **1999**, 1, 223; (c) Wassersheid, P.; Keim, W. *Angew. Chem. Int. Ed.* **2000**, 39, 3772; (d) Wilkes, J. S. *J. Mol. Catal. A: Chem.* **2004**, 214, 11.
7. Arce, A.; Earle, M. J.; Katdare, S. P.; Rodriguez, H; Seddon, K. R. *Chem. Commun.* **2006**, 2548.
8. Brobjer, J. T.; Murrell, J. N. *J. Chem. soc. Faraday Trans. 2* **1982**, 78, 1853.
9. (a) Buckingham, A. D.; Fowler, P. W. *Can. J. Chem.* **1985**, 63, 2018. (b) Hurst, G. J. B.; Fowler, P. W.; Stone, A. J.; Buckingham, A. D. *Int. J. Quantun Chem.* **1986**, 29, 1223.
10. (a) Hansen, J. P.; McDonald, I. R. *Theory of Simple Liquids*, 2nd ed.; Academic Press: London, **1986**. (b) Hansen, J. P.; McDonald, I. R. *Phys. Rev. A.* **1975**, 11, 2111.
11. (a) Tokuda, H.; Hayamizu, K.; Ishii, K.; Susan, M. A. B. H.; Watanabe, M. *J. Phys. Chem. B* **2005**, 109, 6103. (b) Tokuda, H.; Tsuzuki, S.; Abu Bin Hasan Susan, M.; Hayamizu, K.; Watanabe, M. *J. Phys. Chem. B* **2006**, 110, 19593.
12. Armstrong, J. P.; Hurst, C.; Jones, R. G.; Licence, P.; Lovelock, K. R. J.; Satterley, C. J.; Villar-Garcia, I. *J. Phys. Chem. Chem. Phys.* **2007**, 9, 982.
13. Bonhote, P.; Dias, A.P.; Papageorgiou, N.; Kalyanasundaram, K.; Gratzel, M. *Inorg. Chem.* **1996**, 35, 1168.

14. MacFarlane, D. R.; Golding, J.; Forsyth, S.; Deacon, G. B. *Chem. Commun.* **2001**, 1430.
15. Weingartner, H. *Angew. Chem. Int. Ed.* **2008**, *47*, 654.
16. Krossing, I.; Slattery, J.; Gaguinet, C.; Dyson, P.; Oleinikova, A.; Weingartner, H. *J. Am. Chem. Soc.* **2006**, *128*, 13427.
17. Fonseca, G. S.; Umpierre, A. P.; Fichtner, P. F. P.; Teixeira, S. R.; Dupont, J. *Chem. Eur. J.* **2003**, *9*, 3263 and references therein.
18. Pringle, J. M.; Golding, J.; Baranyai, K.; Forsyth, C. M.; Deacon, B. B.; Scott, J. L.; McFarlane, D. R. *New J. Chem.* **2003**, *27*, 1504.
19. (a) Wasserscheid, P.; Welton, T. *Ionic Liquids in Synthesis*, 2nd ed., VCH-Wiley, Weinheim, **2008**; (b) Endres, F.; El Abedin, S. Z. *Phys. Chem. Chem. Phys.* **2006**, *8*, 2101. (c) Rogers, R. D.; Seddon, K. R. *Science*. **2003**, *302*, 792. (d) Weingartner, H. *Angew. Chem. Int. Ed.* **2008**, *47*, 654; (e) Krossing, I.; Slattery, J.; Gaguinet, C.; Dyson, P.; Oleinikova, A.; Weingartner, H. *J. Am. Chem. Soc.* **2006**, *128*, 13427.
20. Bonhte, P.; Dias, A. P.; Papageorgiou, N.; Kalynasundarama, K.; Gratzel, M. *Inorg. Chem.* **1996**, *35*, 1168.
21. (a) Ngo, H. L.; LeCompte, K.; Hargens, L.; McEwen, A. B. *Thermochim. Acta* **2000**, 357; (b) Crosthwaite, J.; Muldoon, M.; Dixon, J.; Andersen, J.; Brennecke, J. *J. Chem. Thermodyn.* **2005**, *37*, 559.
22. (a) Fumino, K.; Wulf, A.; Ludwig, R. *Angew. Chem. Int. Ed.* **2008**, *120*, 3890; (b) Fumino, K.; Wulf, A.; Ludwig, R. *Angew. Chem. Int. Ed.* **2008**, *120*, 8859.
23. (a) Tokuda, H.; Tsuzuki, S.; Watanabe, M. *J. Phys. Chem. B* **2006**, *110*, 600; (b) Widegren, J. A.; Wang, Y. M.; Henderson, W. A.; Magee, J. W. *J. Phys. Chem. B* **2007**, *111*, 8959; (c) Slattery, J.; Gaguinet, C.; Dyson, P.; Schubert, J. S.; Krossing, I. *Angew. Chem. Int. Ed.* **2007**, *119*, 5480.
24. Luo, H.; Baker, G. A.; Dai, S. *J. Phys. Chem. B* **2008**, *112*, 10077.
25. Ludwig, R.; Paschek, D. *ChemPhysChem* **2009**, *10*, 516.

CHAPTER III

*Cannizzaro reaction of HMF to
valuable products*

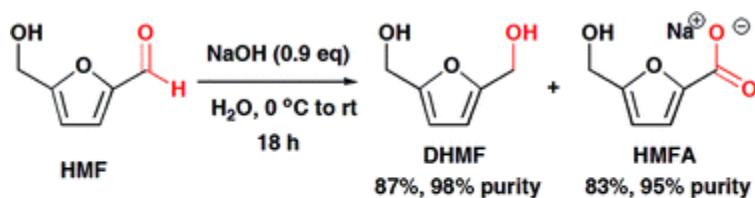
I have contributed to the planning, screening, optimization of reaction condition towards scale up synthesis, spectral characterization, and purification methods of all results described in this chapter as well as in the preparation of the manuscript.

Direct transformation of 5-hydroxymethylfurfural to the building blocks 2,5-dihydroxymethylfurfural (DHMF) and 5-hydroxymethyl furanoic acid (HMFA) *via* Cannizzaro reaction, Sowmiah Subbiah, Svilen P. Simeonov, José M. S. S. Esperança, Luís Paulo N. Rebelo and Carlos A. M. Afonso, *Green Chem.*, 2013, **15**, 2849–2853.

3. Cannizzaro reaction of HMF to valuable products

Chapter III – Summary

5-hydroxymethylfurfural (HMF), a biomass-derived platform chemical possesses two functionalities attached to a furan ring that help to convert it to several value-added compounds useful in wide variety of chemical manufacturing applications and industrial products. With the optimization of the Cannizzaro reaction conditions, an efficient, simple, scalable and atom efficient method for the synthesis of 2,5-dihydroxymethylfuran (DHMF) and 5-hydroxymethylfuranoic acid, as sodium salt (HMFA), with simple isolation by selective recrystallization is presented.



- DHMF and HMFA salt isolated by selective crystallisation;
- Transformation scaled to 12 g;
- Reaction medium and solvent crystallisation can be reused.

3.1 Introduction

The economics of biomass production have improved over the years as the growing concern about the depletion of traditional energy resources has made biomass seem a more attractive alternative both as an energy source as well for the chemical industry. 5-hydroxymethylfurfural (HMF), the so-called 'sleeping giant'¹ is one new biomass-derived platform chemical and it has great industrial potential as it is one of the new building block readily accessible from renewable resources.² The most versatile intermediate chemicals of great industrial potential that can be generated from HMF in simple large-scale transformations are as follows: 5-hydroxymethylfuranoic acid (HMFA), 2,5-furandicarboxylic acid, 2,5-dihydroxymethyl furan (DHMF), and 2,5-furandicarboxaldehyde (Figure 3.1). HMF possesses two functionalities attached to a furan ring that help to convert it to several value-added compounds useful in wide variety of chemical manufacturing applications and industrial products.^{2,3}

For example, 2,5-furancarboxaldehyde is a starting material for the preparation of Schiff bases, and 2,5-diaminomethyl furan is able to replace hexamethylenediamine in the preparation of polyamides. 2,5-Dihydroxymethylfuran (DHMF) is used in the manufacture of polyurethane foams³ and the fully saturated 2,5-dihydroxymethyl tetrahydrofuran can be used like alkane diol in the preparation of polyesters. 2,5-Dihydroxymethyl furan DHMF is used as a six-carbon monomer in a broad range of applications such as resins, polymers and artificial fibers.^{4,5}

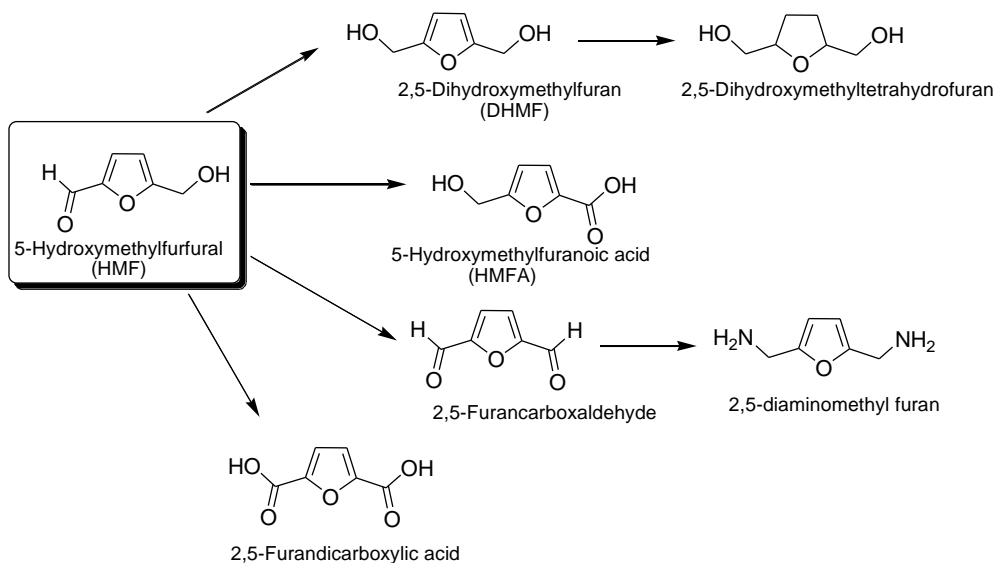


Figure 3.1 Intermediates with great industrial potential from HMF

5-hydroxymethylfuranic acid (HMFA) serves not only as a novel component in various polyesters⁶ but also as a precursor to 2,5-furandicarboxylic acid (FDCA) with many potential applications in the polymer field. 2,5-Furandicarboxylic acid can potentially replace terephthalic, isophthalic, and adipic acids that have been used to date in the manufacture of polyamides, polyesters, and polyurethanes.^{7,8} It has also been used as an intermediate in the synthesis of drugs⁹ and crown ethers.¹⁰ Moreover, HMF has been used for the production of special phenolic resins¹¹ and numerous other polymerizable furanic monomers with promising properties have been prepared.⁷ Due to the potential industrial importance of HMF, the synthetic and related interest in the chemical conversions of HMF remains undiminished. Several studies regarding DHMF synthesis have been carried out based on the catalytic reduction of HMF: its hydrogenation in the presence of nickel, copper, platinum, palladium or ruthenium catalysts, for instance.¹² Under noncatalytic conditions, the reductions with sodium borohydride have also been reported.^{10,13} Research into the conversion of HMF to HMFA has mainly focused on catalytic

oxidation.¹⁴ Using heterogeneous oxidation systems, good to excellent results have been reported.¹⁵ Very recently, oxidative studies of HMF to provide potential derivatives like HMFA, 2,5-furandicarboxaldehyde, and 2,5-furandicarboxylic acid are being explored.¹⁶

A Cannizzaro reaction is the base-induced disproportionation reaction of an aldehyde lacking a hydrogen atom at an α -position to the carbonyl group.

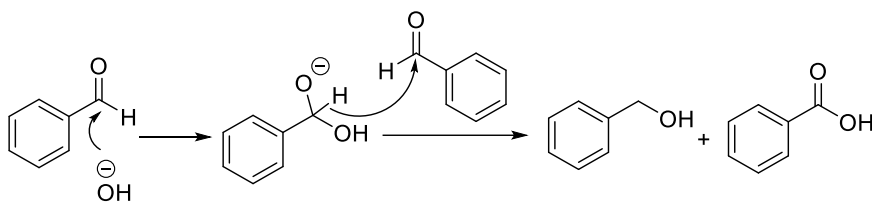
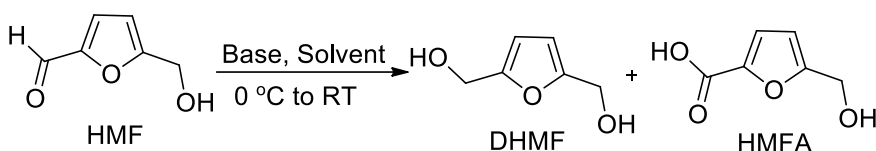


Figure 3.2 Cannizzaro reaction and mechanism

The oxidation product is a salt of a carboxylic acid and the reduction product is an alcohol. One molecule of the aldehyde acts as a hydride donor while the other functions as an acceptor, resulting in a carboxylic acid salt and an alcohol product, respectively. The Cannizzaro reaction is of limited use, as it produces an equimolar mixture of both products only one of which is not the target molecule. However, when applied to HMF, the Cannizzaro reaction would be one of the most efficient routes for the simultaneous production of DHMF and HMFA both of which are equally important potential derivatives of HMF and circumvents the need of an oxidant (for HMFA) or a reductor (for DHMF). Another advantage to the Cannizzaro reaction over the standard reduction or oxidation conditions to HMF is the relative affordability and lack of toxicity of hydroxide ions. Herein we report an efficient, operationally simple, and eco-friendly Cannizzaro reaction of HMF (Scheme 3.1). Very little research, only two studies, on the Cannizzaro reaction of HMF is available (1910, 1919), both of which employed an aqueous alkali solution.¹⁷ To the best of our knowledge, only very recently has been reported the formation of DHMF and HMFA from HMF in an ionic liquid.¹⁸

3.2 Optimization of reaction conditions

Our aim was to optimize the synthesis and purification of DHMF and HMFA *via* the Cannizzaro reaction with HMF. Initially, we started a screening with different bases to ascertain the reactivity of HMF (Table 3.1 and Scheme 3.1).



Scheme 3.1 Screening of HMF with common bases

Table 3.1 Screening with various bases^a

Entry	Base	Solvent	Time (h)	Yield ^b (%)	
				DHMF	HMFA
1	NaH	Dry THF	4	90	89
2	NaOH	Water	36	82	81
3	Li ₂ CO ₃	Water	12	7	7
4	Ba(OH) ₂	Water	12	NR	NR
5	Ca(OH) ₂	Water	12	NR	NR
6	K ₂ CO ₃	Water	12	NR	NR
7	KO ^t Bu	CH ₃ CN	12	31	34

^aGeneral conditions: 100 mg of HMF (0.8 mmol) with corresponding solvent (4 ml) at 0 °C, added base (0.88 mmol) in closed vial and stirred at room temperature and the reaction was monitored by TLC. ^bYield determined by proton NMR using 1 equiv. of (NaOAc, 0.8 mmol) as internal standard. NR represents ‘No reaction’ was observed by NMR.

Cannizzaro reaction of HMF to valuable products

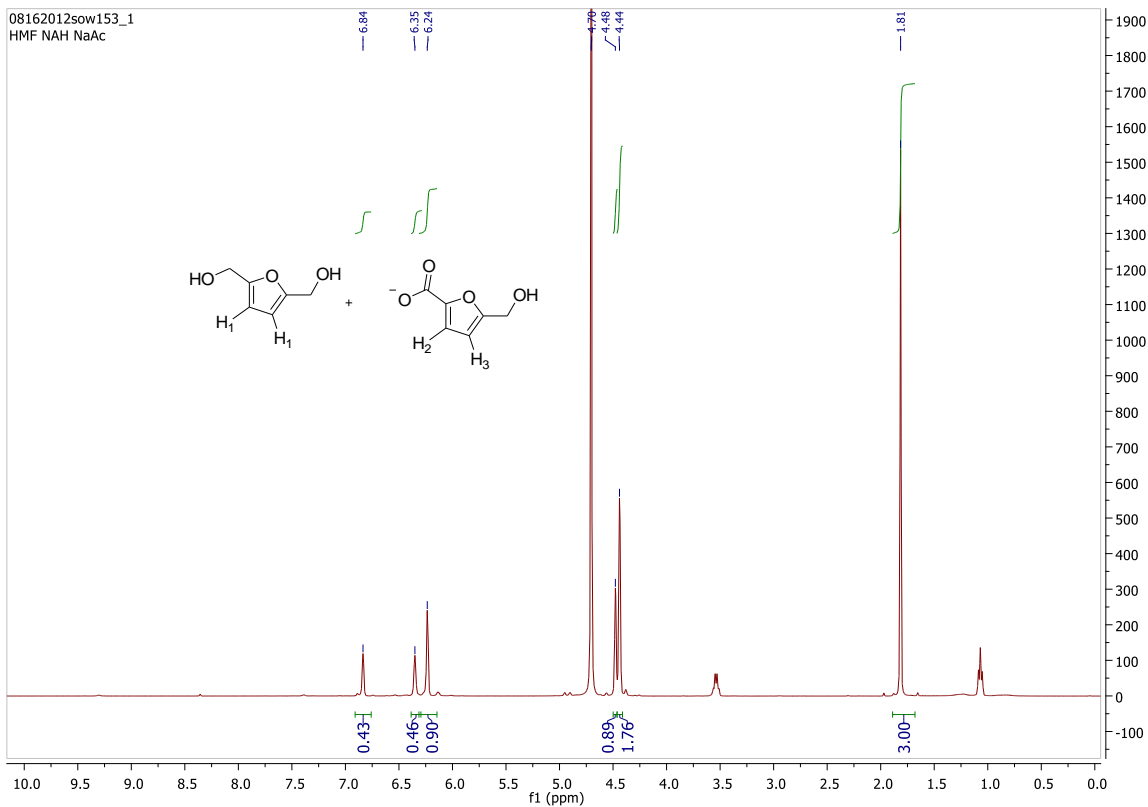
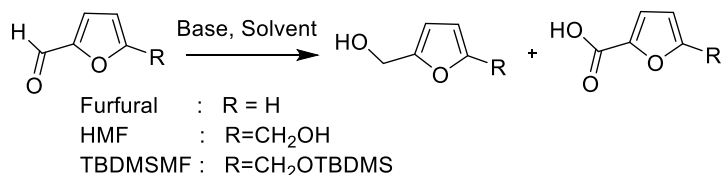


Figure 3.3 ^1H NMR(D_2O) of screening reaction with NaH

The reaction with NaH base in dry THF occurred quickly, within 4 hours, while for the NaOH base in water, it took longer. With potassium *tert*-butoxide in acetonitrile, the reaction produced 33% overall yield in 12 hours. Since promising results were obtained with NaH and NaOH, we then tried to analyse the importance of the hydroxyl group in HMF for the Cannizzaro reaction. We performed a reaction with HMF, TBDMS (*tert*-butyldimethylsilyl) protected HMF and furfural for the study with different solvents and bases (Table 3.2).

**Scheme 3.2** Screening reaction for time and temperature**Table 3.2** Screening with specific conditions

Entry	Substrate	Base	Solvent	Temp (°C)	Time (h)	Yield ^b (%)	
						DHMF	HMFA
1	HMF	NaH	THF	0 to RT	4	90	89
2	HMF	NaOH	Water	RT	18	86	87
3	HMF	NaOH	MeOH	0 to RT	22	71	69
4	HMF	NaOH	Water	40	24	62	60
5	HMF	NaOH	Water	60	24	23	21
6	TBDMSMF	NaOH	MeOH	0 to RT	12	NR	NR
7	TBDMSMF	NaOH	Water	0 to RT	12	39 ^c	20 ^c
8	TBDMSMF	NaH	THF	0 to RT	12	37	36
9	Furfural ^d	NaH	THF	0 to RT	12	68	71
10	Furfural ^d	NaOH	Water	0 to RT	12	88	83

^aGeneral conditions: To the aldehyde (0.8 mmol; 0.4 mmol for entries 2 and 3) with corresponding solvent (4 ml) of the corresponding solvent 1.1 equiv. base was added in a closed vial at the specified temperature and the reaction was monitored by TLC. ^bYield determined by proton NMR using 1 equiv. of NaOAc (0.8 mmol) as internal standard. In particular, for reactions with 50 mg HMF, 0.2 equiv. NaOAc (0.16 mmol) in entry 2, and 0.05 equiv. NaOAc (0.04 mmol) in entry 3 were used. ^cThe hydrolysis of TBDMS to

produced HMF followed by its Cannizzaro products. ^dIsolated Yields. RT- Room temperature, NR-No reaction.

While performing the reaction at higher temperatures, 40 °C and 60 °C with NaOH, the reaction for HMF produced lower yields (62% and 22%) (Table 3.2, entries 4 and 5) which is probably due to competitive known decomposition of HMF under basic conditions.^{3f,g} With TBDMS-protected HMF, the reaction of NaOH with H₂O underwent hydrolysis leading to Cannizzaro products (29%) (Table 3.2, entry 7), while the same with NaH yielded corresponding Cannizzaro products in 37% yield for 12h at 0 °C (Table 3.2, entry 8). The reaction with furfural proceeded well, producing corresponding Cannizzaro products with both NaH and NaOH bases in good yields, 70% and 86%, respectively (Table 3.2, entries 9 and 10).

From these studies, the best conditions were obtained using NaH and NaOH. To analyse the specific conditions, we compared the obtained results of NaH and NaOH at 0 °C and room temperature conditions by also varying the substrate-solvent concentration at these temperatures.

Table 3.3 Screening for specific conditions for HMF^a

Conditions	NaH		NaOH	
	0 °C to RT	RT	0 °C to RT	RT
Concentration	100 mg in 20 ml THF	50mg in 2 ml THF	100 mg in 20 ml H ₂ O	50 mg in 2 ml H ₂ O
Time (h)	1 h (0 °C) to 3h (RT)	3	1 h (0 °C) to 35h (RT)	18
Yield (%) ^b :				
DHMF	90	69	82(82)	86
HMFA	89	66	81(85)	87

^aGeneral conditions for the screening: To 100 mg of HMF (0.8 mmol) with corresponding solvent at 0 °C, the base (0.88 mmol) was added in a closed vial and stirred at room temperature; the reaction was monitored by TLC. ^bYield determined by proton NMR using 1 equiv. of NaOAc (0.8 mmol) as internal standard. In particular, for reactions with 50mg HMF at room temperature, 0.2 equiv. NaOAc (0.16 mmol) in Entry 2 were used.

As Table 3.3 illustrates, using a more concentrated reaction medium (2 ml vs 20 ml) reduced the NaH reaction efficiency from 0 °C to room temperature (90% vs 68%) whereas with NaOH, a slight improvement was obtained (82% vs 87%). The best conditions were using NaOH at room temperature in H₂O for 18 hours to give 86% yield of DHMF and 87% yield of HMFA salt; these conditions avoided the need for the organic solvent THF.

With best conditions in hand, we explored the simple purification methods to obtain both HMFA and DHMF individually without the need for column chromatography or acid-base separation techniques, since they led to significant losses of Cannizzaro products. Our simpler process is based on the recrystallization technique, in which we obtained more than 60% of 97% pure DHMF before recrystallization. Following the process, we achieved 98% pure recrystallized product HMFA (82%)¹⁹ and around 27% diol was easily purified from the mother liquor by washing with ether/hexane (total yield of DHMF = 85%, Table 3.3, results in brackets). In order to minimize the producing of NaOH waste, we explored the reaction at different equivalences of NaOH (Table 3.4). We observed a significant drop in yield using stoichiometric amount of NaOH (0.5 equiv. 32%, entry 1), 10% (43%, entry 3) or 20% excess (52%, entry 6). Using 10% excess of NaOH, longer reaction time (72h vs 48h,) originated higher overall yield (70% vs 43%, entry 4 vs entry 3). In line with the results described before (Table 3.2), the use of higher temperature (45 °C vs RT) did not improved the reaction performance (40% vs 43%, entry 5 vs entry 3). In addition, the increase of the reaction scale (500 mg vs 50 mg) provoked an erosion of the overall yield

(17% vs 31%, entry 2 and 60% vs 70%, entry 4) which was not observed when NaOH was used in higher excess. Using 0.9 and 1.1 equiv. of NaOH originated high overall yields of 80% and 86% respectively (entries 7 and 8).

Table 3.4 Screening for NaOH quantity^a

Entry	NaOH (equiv)	Time (h) / Temp (°C)	Yield ^b (%)	
			DHMF	HMFA
1	0.5	38/RT	28	35
2	0.5	18/45	30(15) ^c	32(20) ^c
3	0.55	48/RT	46	40
4	0.55	72/RT	71(61) ^c	69(60) ^c
5	0.55	48/45	38 ^c	42 ^c
6	0.6	48/RT	53	51
7	0.9	48/RT	80	81
8	1.1	18/RT	86	87

^aGeneral conditions: To 50 mg of HMF (0.4 mmol) in water (2 ml) at 0 °C, NaOH (varying equivalent) was added in a closed vial and after 1h was stirred at specific temperature; the reaction was monitored by TLC. ^bYield determined by proton NMR using 0.15 equiv. of NaOAc (0.04 mmol) as an internal standard. After reaction, the water was evaporated and the mixture was washed with diethylether and dried before preparing NMR sample to remove any unreacted HMF. ^cObserved yields (in brackets) using 500 mg of HMF.

3.3 Scale up and product isolation

Besides the use of an excess of NaOH that implies less green chemistry credits due to the need of more base and the generation of more waste, we selected 0.9 equivalent of NaOH as the most appropriate compromise for the following studies of reaction and product isolation at a higher reaction scale (Table 3.5). As can be

seen, the transformation can be efficiently performed under different concentrations (40 mM to 0.8 M) and scales to up to 12 g (95 mmol) of HMF, providing isolated 85% yield of DHMF and 82% of HMFA salt (entry 6). Those conditions correspond to an E-factor of 0.3 since the reaction medium (water) and the solvent of crystallization can be reused by distillation.

Table 3.5 Cannizzaro reaction of HMF and product isolation^a

Entry	HMF scale	Water (mL) / concentration (M)	Yield ^b (%)	
			DHMF	HMFA
1	0.1 g	20 mL/40 mM	82	85
2	0.1 g	4 mL/0.2 M	88	84
3	1 g	60 mL/0.13 M	90	85
4	3 g	120 mL/0.2 M	85	83
5	3 g	30 mL/0.8 M	87	83
6	12 g	200 mL/0.5 M	85	82

^aGeneral conditions: To HMF (0.4 mmol) in water at 0 °C, NaOH (0.9 equiv.) was added in a closed vial and after 1h was stirred at room temperature for 18h; the reaction was monitored by TLC. ^bIsolated yield.

3.3.1 Representative procedure for the Cannizzaro reaction of HMF and product isolation

3 g of HMF (24 mmol) were dissolved in water (30 ml) and then cooled to 0 °C. After the addition of 0.87g (22 mmol) of NaOH at 0 °C, the resulting mixture was stirred at room temperature in a closed vessel for about 18h and the reaction completion was confirmed by TLC. After evaporating the water from the reaction mixture, ethyl acetate (2×50 ml) was added to the solid to separate the DHMF diol (0.85g, 60%). Carboxylate salt HMFA was isolated by recrystallization with ethanol (approx. 2 ml)/ethyl acetate (100 ml) yielding an HMFA salt (1.4 g, 83%

yield) as hygroscopic solid which was stored in a refrigerator. After evaporation of the mother liquor, DHMF (0.4g, 27% yield) was isolated.

Isolated DHMF: 87% yield, 98% purity; Isolated HMFA salt: 83% yield, 95% purity;

The diol DHMF can be further purified by washing with ether/hexane to remove any remaining non-polar impurities. Several batch experiments were successfully performed at different quantities of HMF with this purification process under distinct conditions (Table 3.5).

3.3.2 Representative spectra on the isolation of products

The isolated products were analysed by NMR and some of the representative spectra of the isolated products are shown below.

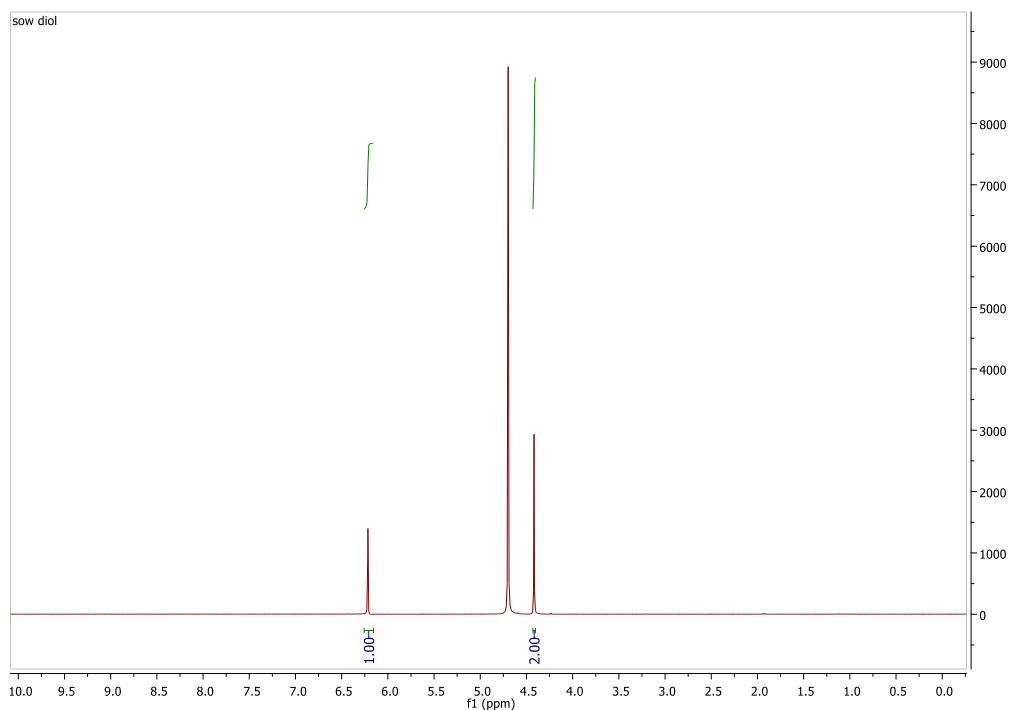


Figure 3.4 ^1H NMR(D_2O) of isolated DHMF from Cannizzaro reaction

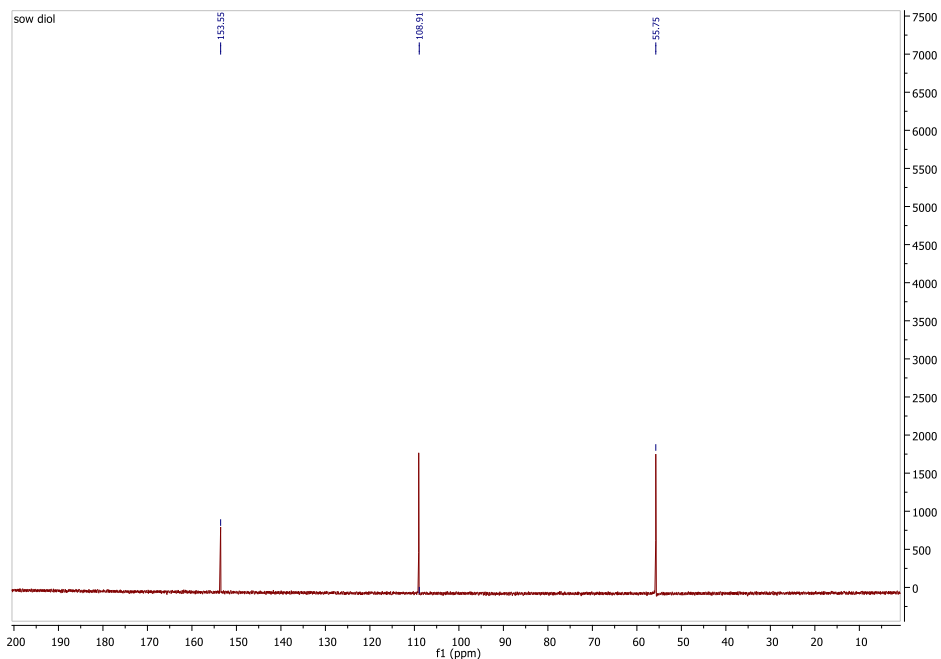


Figure 3.5 ^{13}C NMR(D_2O) of isolated DHMF from Cannizzaro reaction

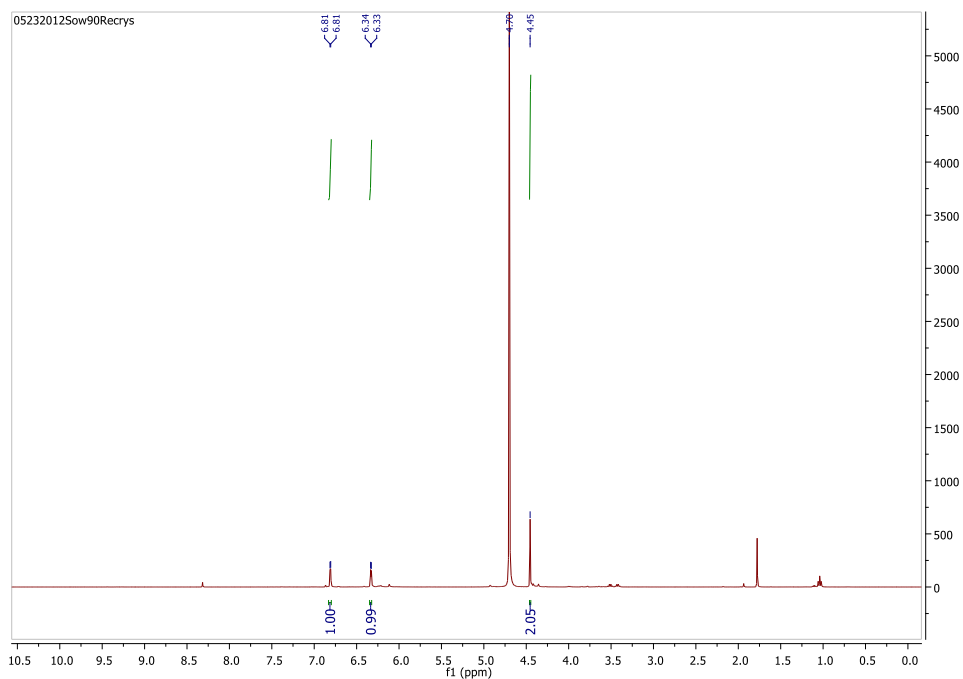


Figure 3.6 ^1H NMR(D_2O) of isolated HMFA from Cannizzaro reaction

Cannizzaro reaction of HMF to valuable products

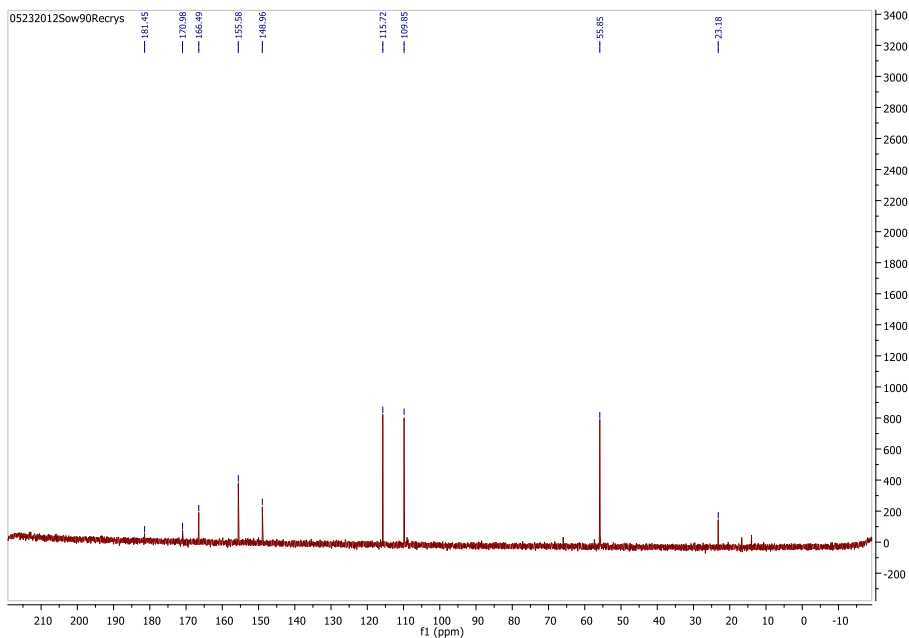


Figure 3.7 ^{13}C NMR(D_2O) of isolated HMFA from Cannizzaro reaction

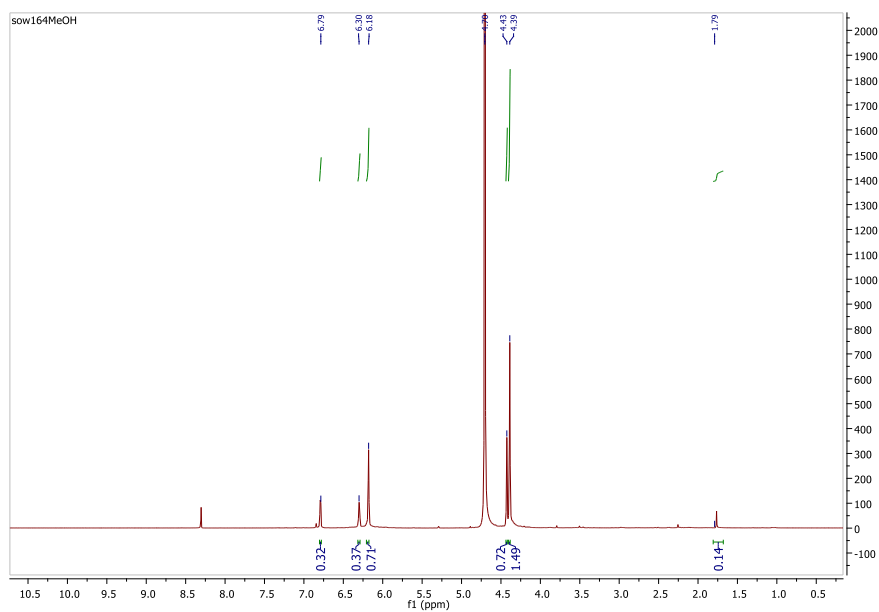


Figure 3.8 ^1H NMR(D_2O) of HMF reacting with NaOH in CH_3OH (Table 3.2, Entry 3).

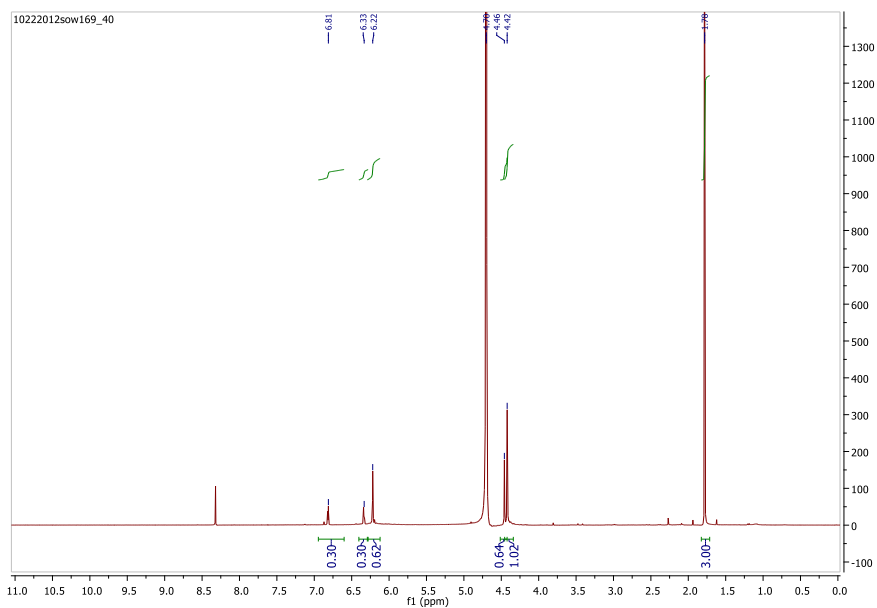


Figure 3.9 ^1H NMR(D_2O) of HMF reacting with NaOH at 40 °C (Table 3.2, Entry 4).

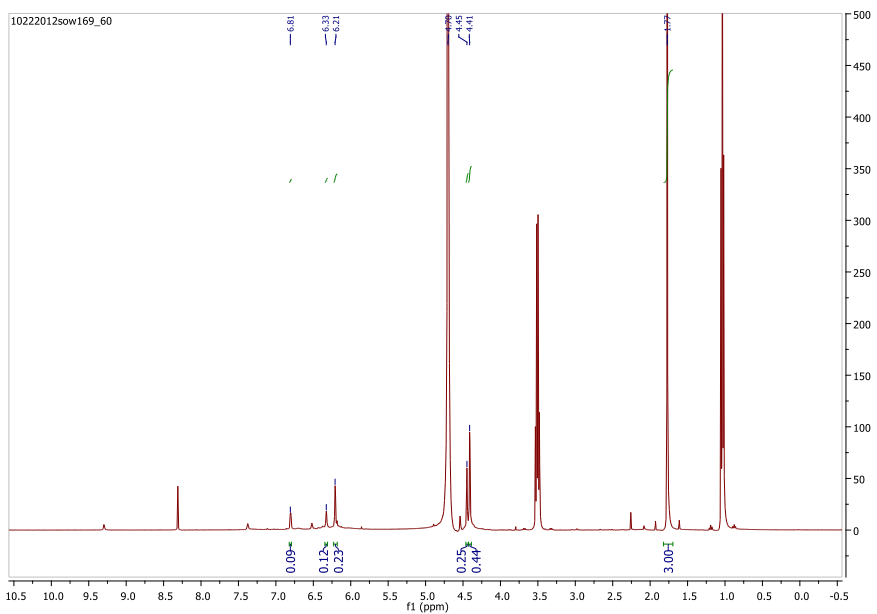


Figure 3.10 ^1H NMR(D_2O) of HMF reacting with NaOH at 60 °C (Table 3.2, Entry 5).

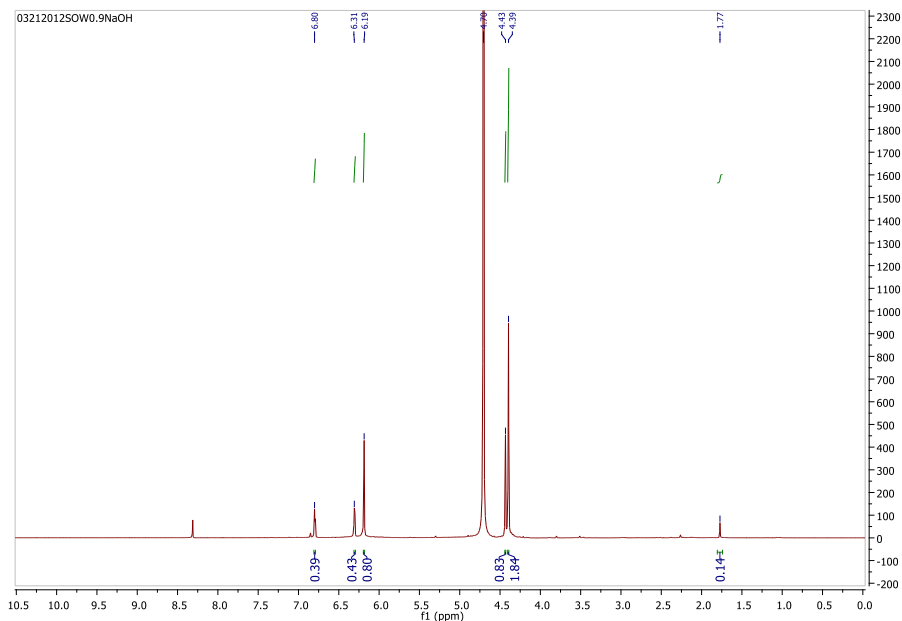


Figure 3.11 ¹H NMR(D₂O) of HMF reaction with (0.9 eq) NaOH (Table 3.4, Entry 7).

3.4 Conclusion

In conclusion, we have developed an efficient and eco-friendly Cannizzaro reaction of HMF for the simultaneous synthesis of both DHMF and HMFA. The Cannizzaro reaction of HMF ensures an economical process to effectively isolate both DHMF and HMFA by crystallization rather than an acid base extraction. A scalable, simply purified, high yield reaction would make the present process even more useful and attractive.

3.5 References

1. M. Bicker, D. Kaiser, L. Ott, H. Vogel, *J. Supercrit. Fluids*, **2005**, *36*, 118.
2. (a) F. W. Lichtenthaler, E. Cuny, D. Martin, S. Rönninger, in: F. W. Lichtenthaler (Ed.), *Carbohydrates as Organic Raw Materials*, VCH, Weinheim/NewYork, **1991**, p.214; (b) L. Bing, Z. Zhang, K. Deng, *Ind. Eng.*

- Chem. Res.* **2012**, *51*, 15331; (c) S. P. Simeonov, J. A. S. Coelho and C. A. M. Afonso, *ChemSusChem* **2012**, *5*, 1388; (d) A. D. Sutton, F. D. Waldie, R. Wu, M. Schlaf, L. A. ‘Pete’ Silks III, J. C. Gordon, *Nature Chem.* **2013**, *5*, 428.
3. W. J. Pentz, GB Patent 2131014, **1984**; Reviews: (b) J. Lewkowski, *Arkivoc* **2001**, 17-54; (c) G. W. Huber, S. Iborra and A. Corma, *Chem. Rev.*, **2006**, *106*, 4044; (d) A. Corma, S. Iborra and A. Veltym, *Chem. Rev.*, **2007**, *107*, 2411; (e) T. Stahlberg, W. J. Fu, J. M. Woodley, A. Riisager, *Chemsuschem* **2011**, *4*, 451-458; (f) A. A. Rosatella, S. P. Simeonov, R. F. M. Frade, C. A. M. Afonso, *Green Chemistry* **2011**, *13*, 754-793; (g) M. E. Zakrzewska, E. Bogel-Lukasik, R. Bogel-Lukasik, *Chemical Reviews* **2011**, *111*, 397-417; (h) S. Dutta, S. De, B. Saha, *Chempluschem* **2012**, *77*, 259-272; (i) T. Buntara, S. Noel, P. H. Phua, I. Melian-Cabrera, J. G. de Vries, H. J. Heeres, *Topics in Catalysis* **2012**, *55*, 612-619; (j) R. J van Putten, J. C. van der Waal, Ed de Jong, C. B. Rasrendra, H. J. Heeres, and J.G. de Vries, *Chem. Rev.* **2013**, *113*, 1499.
 4. British Petroleum Co., Process for production of furfural and 5-(hydroxymethyl)-furfural and corresponding hydrogenated derivatives, FR2556344 14, **1985**. June.
 5. A. Gandini, *ACS Symp. Ser.* **1990**, *433*, 195.
 6. H. Hirai, *J. Macromol. Sci. Chem.* A21, **1984**, A21, 1165.
 7. (a) A. Gandini, M. N. Belgacem, *Prog. Polym. Sci.*, **1997**, *22*, 1203; (b) A. Gandini, *Green Chem*, **2011**, *13*, 1061.
 8. (a) C. Moreau, M. N. Belgacem, A. Gandini, *Top. Catal.*, **2004**, *27*, 11;. (b) S. Dutta, S. De, and B. Saha, *ChemPlusChem*, **2012**, *77*, 259;. (c) T. Buntara, S. Noel, P. H. Phua, I. M-Cabrera, J. G. de Vries, H. J. Heeres, *Top Catal.* **2012**, *55*, 612.
 9. I. Matsumoto, K. Nakagawa, K. Horiuchi, *Jpn. Kokai* , **1973**, *73*, 763.
 10. J. M. Timko, D. J. Cram, *J. Am. Chem. Soc.*, **1974**, *96*, 7159.

11. H. Koch, F. Krause, R. Steffan, H. U. Woelk, *Stärke (Starce)* **1983**, 35, 304.
12. (a) A. Faury, A. Gaset, J. P. Gorrichon, *Inf. Chim.*, **1981**, 214, 203; (b) V. Schiavo, G. Descotes, J. Mentech, *Bull. Soc. Chim. Fr.*, **1991**, 704; (c) G. C. A. Luijkx, N. P. M. Huck, H. V. Bekkum, F. V. Rantwijk, L. Maat, *Heterocycles*, **2009**, 77, 1037; (d) M. Chidambaram, A. T. Bell, *Green Chem.*, **2009**, 12, 1253; (e) Furanix Technologies B. V., 5-Substituted 2-(alkoxymethyl)furans, WO2009/30509, March 12, **2009**; (f) Battelle Memorial Institute, Hydroxymethylfurfural reduction methods and methods of producing furandimethanol, US2007/287845, December 13, **2007**.
13. (a) C. J. Moye, *Rev. Pure Appl. Chem.*, **1964**, 14, 161; (b) P. A. Finan, *J. Chem. Soc.*, **1963**, 3917; (c) L. Cottier, G. Descotes, Y. Soro, *Synth. Commun.*, **2004**, 33, 4285; (d) S. Goswami, S. Dey, S. Jana, *Tetrahedron*, **2008**, 64, 6358.
14. (a) J. J. Blanksma, *Chem. Zentralbl.*, **1910**, 81, 539; (b) T. E. Hajj, A. Masroua, J. Martin, G. Descotes, *Bull. Soc. Chim. Fr.*, **1987**, 5, 855; (c) L. Cottier, G. Descotes, J. Lewkowski, R. Skowronski, *Polish J. Chem.*, **1994**, 68, 693; (d) S. Solvay, R. Saladino, A. Farina, **2010**. Process for the oxidation of alcohol and/ or aldehyde groups, WO2010/7139, January 21; (e) J. Kiermayer, *Chemiker-Zeitung, Chem. Apparatur*, **1895**, 19, 1004.
15. (a) T. Reichstein, *Helv. Chim. Acta*, **1926**, 9, 1066; (b) B. W. Lew, *Atlas Chem. Ind.*, **1968**. Method of producing dehydromucic acid, US3326944, June 20, **1967**; *Chem. Abstr.*, **1968**, 68, P49434n; (c) H. V. Bekkum, *Carbohydrates as Organic Raw Materials III, VCH, Weinham*, **1994**; (d) P. Vinke, Ph.D. Thesis, Technical University in Delft, Delft, **1991**.
16. (a) A. Villa, M. Schiavoni, S. Campisi, G. M. Veith, L. Prati, *ChemSusChem* **2013**, 6, 609; (b) M. Krystof, M. P-Sanchez, P. D. de Maria, *ChemSusChem*, **2013**, 6, 826.
17. (a) J. J. Blanksma, *Rec. Trav. Chim.*, **1910**, 29, 403; (b) J. A. Middendorp, *Rec. Trav. Chim.*, **1919**, 38, 42.

Chapter III

18. E. S. Kang, D. W. Chae, B. Kim, Y. G. Kim, *J. Ind. Eng. Chem*, **2012**, *18*, 174.
19. During the purification process was observed that the excess of NaOH in the reaction mixture interfered in the recrystallization process with ethylacetate by precipitating sodium acetate as solid. In order to avoid this, we used only 0.9 equivalent NaOH which greatly minimized this impurity making way for an easier purification process.

CHAPTER IV

*Synthesis of N-alkyl pyridinium salts
from HMF*

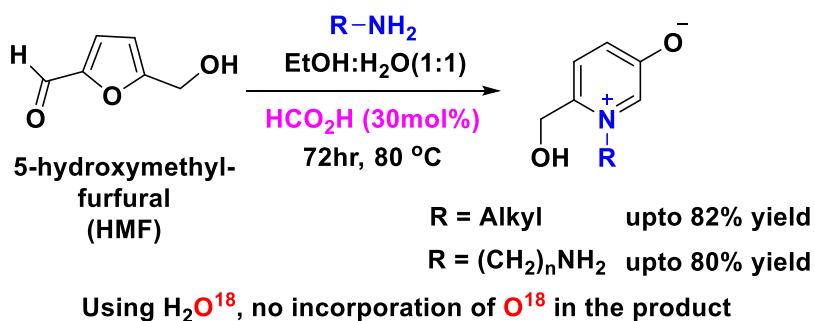
I have been responsible for most of this work such as screening catalysts, optimization of reaction condition, substrate scopes, and spectral analysis including isotopic study for revealing the mechanistic details as well as to the preparation of the manuscript. Thanks to Prof. Luis. F. Veiros for helping with the DFT calculations described in this chapter.

Organocatalyzed one-step synthesis of functionalized *N*-alkylpyridinium Salts from biomass derived 5-hydroxymethylfurfural, Subbiah Sowmiah, Luís F. Veiros, José M. S. S. Esperança, Luís Paulo N. Rebelo, and Carlos A. M. Afonso, *Org. Lett.* **2015**, *17*, 5244–5247.

4. Synthesis of functionalized *N*-alkylpyridinium salts from biomass derived HMF

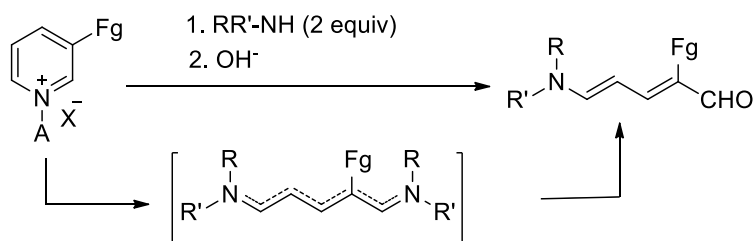
Chapter IV - Summary

*This chapter describes the efforts made to develop an efficient and scalable method for the synthesis of *N*-alkyl pyridinium salts from biomass derived 5-hydroxymethylfurfural (HMF). Optimization of the reaction conditions, the liability of the approach with different substrates such as alkyl amines or alkyl diamines and their characterisation was studied in detail. Moreover, the mechanism for the formation of pyridinium salts was also studied. This successful protocol represents a new way to explore the properties, reactivities and applications of *N*-alkyl pyridinium salts.*



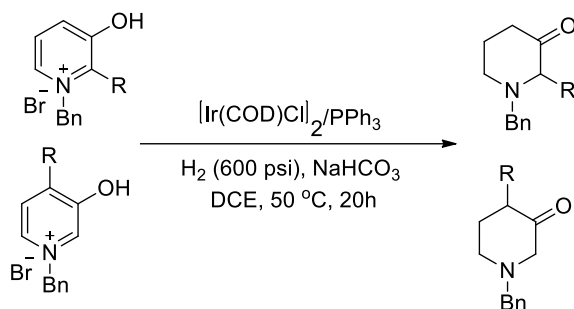
4.1 Introduction

Pyridinium salts (Pyr) are privileged scaffolds found in many natural and bioactive compounds.¹ Pyr containing natural products such as Njaoaminiums and Pachychalines are well known for their wide occurrence in marine sponges of the Haplosclerida order.^{2,3} In general, Pyr are known to exhibit many applications such as acylating agents, phase transfer catalysts, biocides such as antimicrobial agents, dyes and cationic surfactants.⁴ Moreover, they have high synthetic value as key intermediates for the production of a broad range of pharmacologically relevant piperidine, dihydro and tetrahydropyridine frameworks.⁵ Pyr that are liquid at room temperature, so called “pyridinium ionic liquids”,^{4b} such as 1-alkylpyridinium salts, are potential solvents in synthesis and catalysis.^{4b} The classical routes to synthesise Pyr involve the reaction of pyridine with organic halides or quaternization of the pyridine nitrogen using chloromethylalkyl ethers or sulphides.^{4a} Current reports on the synthesis of Pyr by catalytic C-H activation⁶ and the utility of pyridinium salts to originate conjugated dienals, a highly useful synthetic precursor for constructing natural products,⁷ reveals the high demand of pyridinium salts in synthetic chemistry.



Scheme 4.1 Ring opening of 3-substituted pyridinium salts to give Zincke aldehydes

Also 3-hydroxy pyridinium salts can be transformed with great effect for piperidine-3-ol/one functionalization (Scheme 4.2).



Scheme 4.2 Ir-catalyzed selective hydrogenation of 3-hydroxypyridinium salts

For example, Zhou *et al.* recently reported effective Iridium catalyzed hydrogenation of 3-hydroxy pyridinium salts to give piperidine-3-ones.⁸

This class of salts is known to exhibit biological activity including cytotoxicity and ichthyotoxicity.⁹ A few examples of pyridinium salts containing natural products are shown in Figure 4.1.

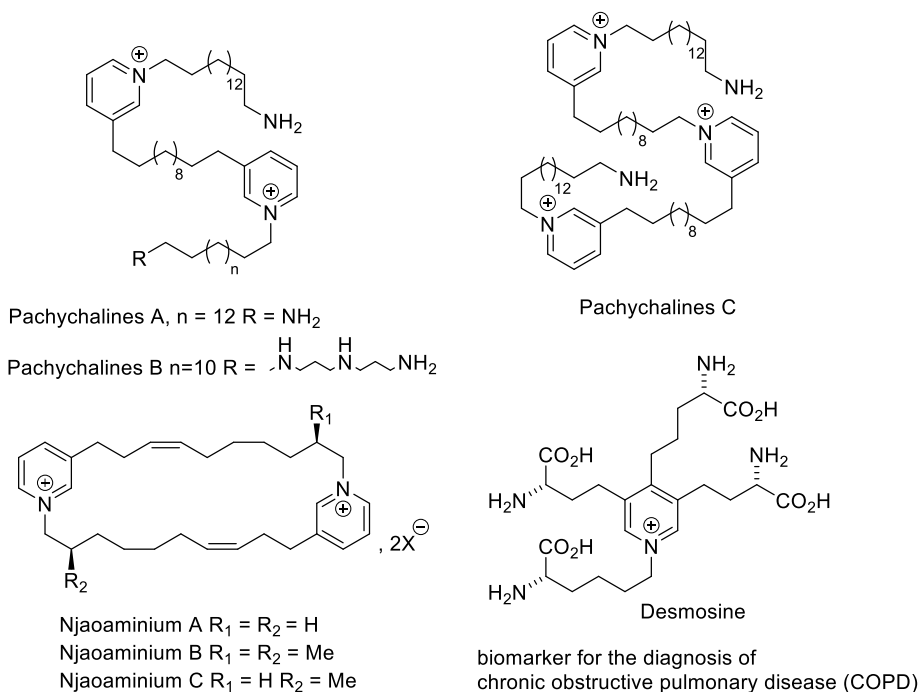


Figure 4.1. Natural products containing pyridinium salts¹⁰

Several efforts have been successfully made in the construction of natural products on different core moieties using pyridinium salts as the key substrate. Figure 4.2 shows some examples of natural products synthesised using pyridinium salt.

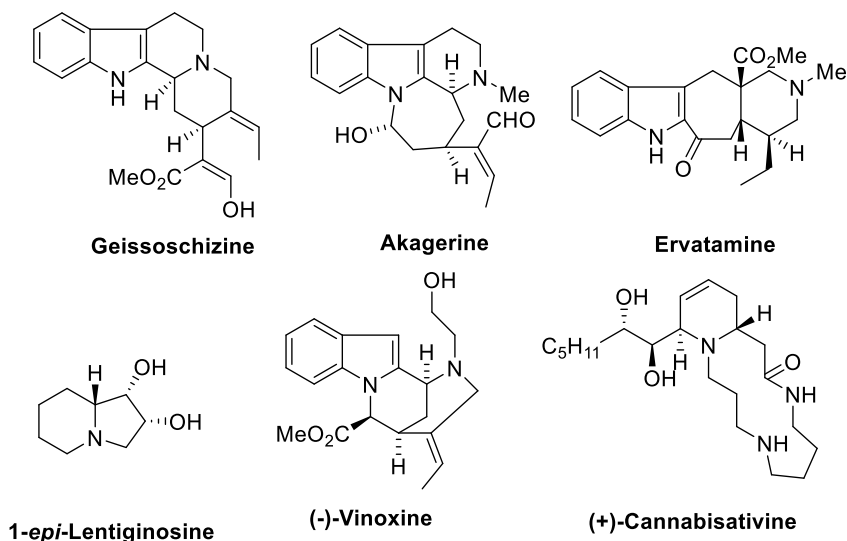
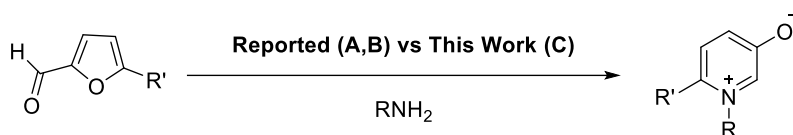


Figure 4.2 Natural products derived using pyridinium salts¹¹

On the other hand, with the increasing demand on biorenewable resources as an alternative feedstock for the production of fuels and bulk chemicals,¹² 5-hydroxymethylfurfural (HMF) gained considerable attention as it is derived from renewable resources such as fructose, glucose or cellulose. HMF acts as a bridging molecule linking biomass to fuels and chemicals and is also very useful for the production of the biofuel dimethylfuran and other important commodities.¹³

In line with our ongoing research on the preparation of HMF¹⁴ and transformation of furfural and HMF to useful building blocks,¹⁵ in this work we present a novel strategy for the implementation of a new and competitive platform for the production of *N*-alkyl-5-hydroxy-2-(hydroxymethyl)pyridinium (HPyr)¹⁶ from HMF. Optimization of the synthetic pathway leads on to the establishment of efficient reaction conditions and purification methods as the key transformation

from HMF to HPyr using various alkyl amines and alkyl diamines to promote the exclusive formation of mono *N*-alkylpyridinium salts (Scheme 4.3C). Some HPyr derived from aminoacids were already reported as potential bitter inhibitors. Low yields (32 % for alanine) were obtained by reaction of aminoacid with HMF (Scheme 4.3A).¹⁶ An alternative reported route involves a three step synthesis *via* imine reduction followed by oxidative rearrangement with bromine.¹⁶ Recently a more efficient 3 steps approach was described on furfural using NaBH₄ and HCl/H₂O₂ for respectively the imine reduction and oxidative rearrangements steps (Scheme 4.3B).¹⁷



A: Reported¹⁶: EtOH/H₂O (1:1), pH = 9.4, reflux, 24 h; R' = CH₂OH(HMF), alanine; yield 32%.

B: Reported¹⁷: R' = H(furfural), step 1) aminoacid (1 equiv), MeOH, NaOH, 60 °C, 0.5 h; step 2) NaBH₄, 0 °C, 1 h; step 3) 3 M HCl, H₂O₂ (2 equiv), 100 °C, 0.5 h, yield 55%-quant.

C: This work: R' = CH₂OH(HMF), alkylamines, terminal diamines, EtOH/H₂O (1:1), formic acid (30 mol %), 80 °C, 48 h; up to 82%.

Scheme 4.3 Overview of reported *vs* this work synthetic routes for the synthesis of 3-hydroxypyridinium salts.

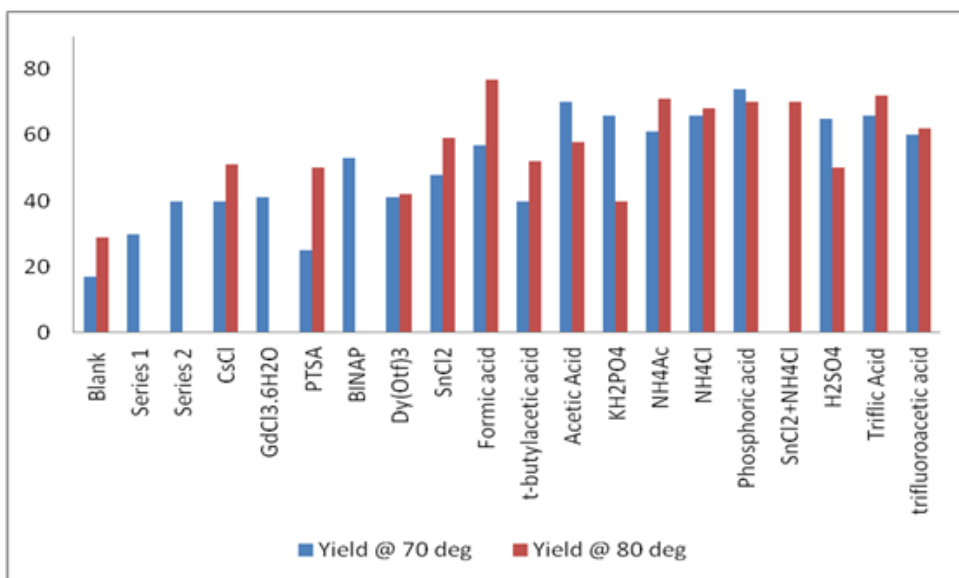
4.2 Optimization of reaction conditions

4.2.1 Catalyst screening

With an efficient and cheap starting material, fructose, we synthesized HMF for our screening reactions using our previously reported method.^{14a} With the synthesized HMF, the screening of various solvents was performed for the product formation at 70 °C for 2 days using butylamine as model substrate. The reaction progress was monitored by TLC and the best results obtained with EtOH:H₂O (1:1) ratio. Few other protic solvents such as 1-propanol, methanol, H₂O led to the formation of the product whereas other organic solvents like dichloromethane,

acetonitrile only showed starting materials. Also our initial efforts to analyse the product formation with HPLC studied were not convincing due to the formation of polymeric products and observation of multiple peaks. Thus, we carried out the screening of these reactions by NMR using acetonitrile as internal standard.

Our preliminary screening reactions were performed with solvents and the best results were obtained on using EtOH:H₂O (1:1 ratio). We then screened the product conversion with the presence of some inorganic bases having Li, K, Na, Ca as catalysts (30 mol %) using butylamine as the model substrate for the reaction. The results show that they are ineffective for this reaction. Some of the potential catalysts such as 2,6-Lutidine, DBU, HCO₂Na, urea, Ca(OH)₂, N(Et)₃Br, NaOAc, Na₂HPO₄, KOAc, MgO, CuCl₂ · 2H₂O, HCl, Cu(OTf)₂, CsCl, *t*-butylacetic acid, also showed ineffective results on varying temperatures.

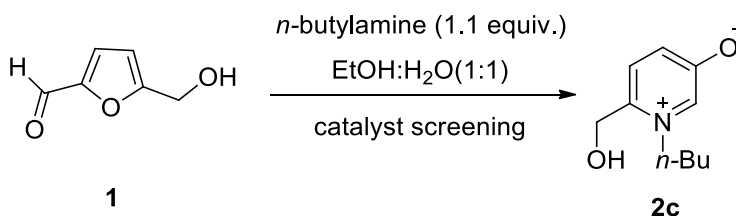


Series 1: 2,6-Lutidine, DBU, HCO₂Na, Urea, Ca(OH)₂, N(Et)₃Br, NaOAc, Na₂HPO₄

Series 2: KOAc, MgO, CuCl₂ · 2H₂O, HCl, Cu(OTf)₂, CsCl, *t*-butylacetic acid

Figure 4.3 Screening of the catalysts at various temperatures

Significant yield improvement was observed using 30 mol % of NH_4Cl , NH_4OAc and SnCl_2 as catalysts giving, respectively, yields of 66%, 61% and 48% at 70 °C and 68%, 71%, and 59% yields at 80 °C. On a 2 days reaction using 30 mol % of acetic acid, or phosphoric acid the variation of temperature from 70 °C to 80 °C gave reduced yields of reaction from 70% to 58% and from 73% to 70% respectively. Under the same conditions, only a 2% and 4% increase was found using trifluoro acetic acid and triflic acid respectively on moving from 70 °C to 80 °C. When using 30 mol % of formic acid as catalyst, the yields were raised significantly from 57% to 77% while increasing the temperature from 70 °C to 80 °C. Despite the small variations observed, interesting results were achieved using catalysts such as trifluoroacetic acid, phosphoric acid, acetic acid, formic acid, or triflic acid at different temperatures. We decided to use these catalysts for further screening to obtain optimized reaction condition.

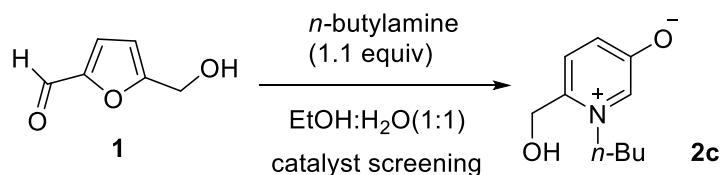


Scheme 4.4 Screening of catalysts

4.2.2 Screening of catalysts for specific time and temperature

HMF decomposes quickly at higher temperatures with no product observation. At lower temperatures below 70 °C, the reaction proceeds slowly and does not lead to completion even after 4 days. With those acidic catalysts that provided better yields for this reaction at 70 °C and 80 °C, we continued our optimization varying the reaction time. Experiments show that reaction times above 3 days generate poor reaction yields even increasing the catalyst amount. The gummy reaction

mixture at this stage after 3 days hinders the stirring process of the reaction with no increase in efficiency.



Scheme 4.5 Screening of catalysts

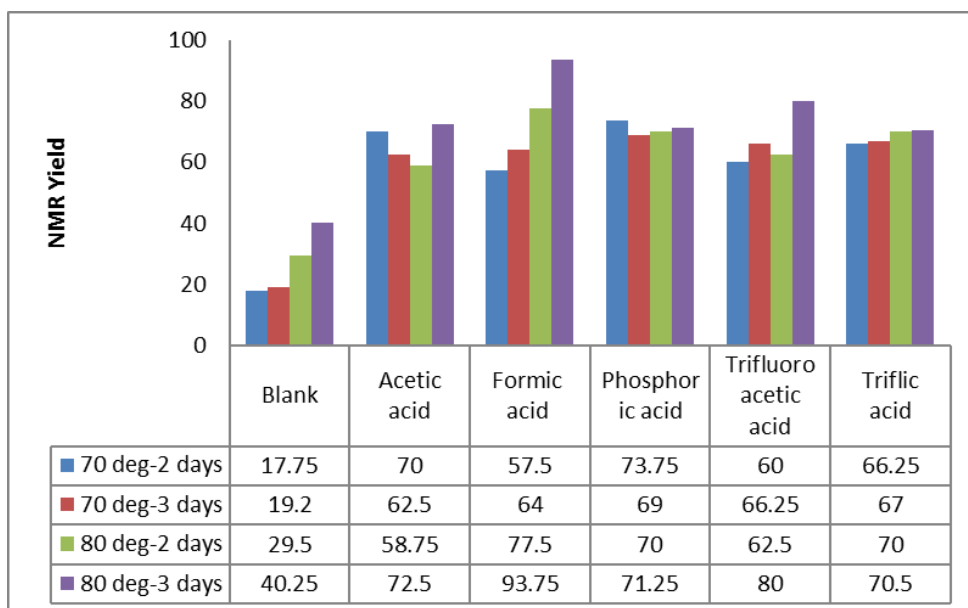


Figure 4.4 Screening of catalysts for specific time and temperature

Below are the representative spectra showing the effectiveness of the reaction at 80 °C for 3 days a) with acetic acid catalyst shown in Figure 4.5, b) with formic acid as catalyst shown in Figure 4.6.

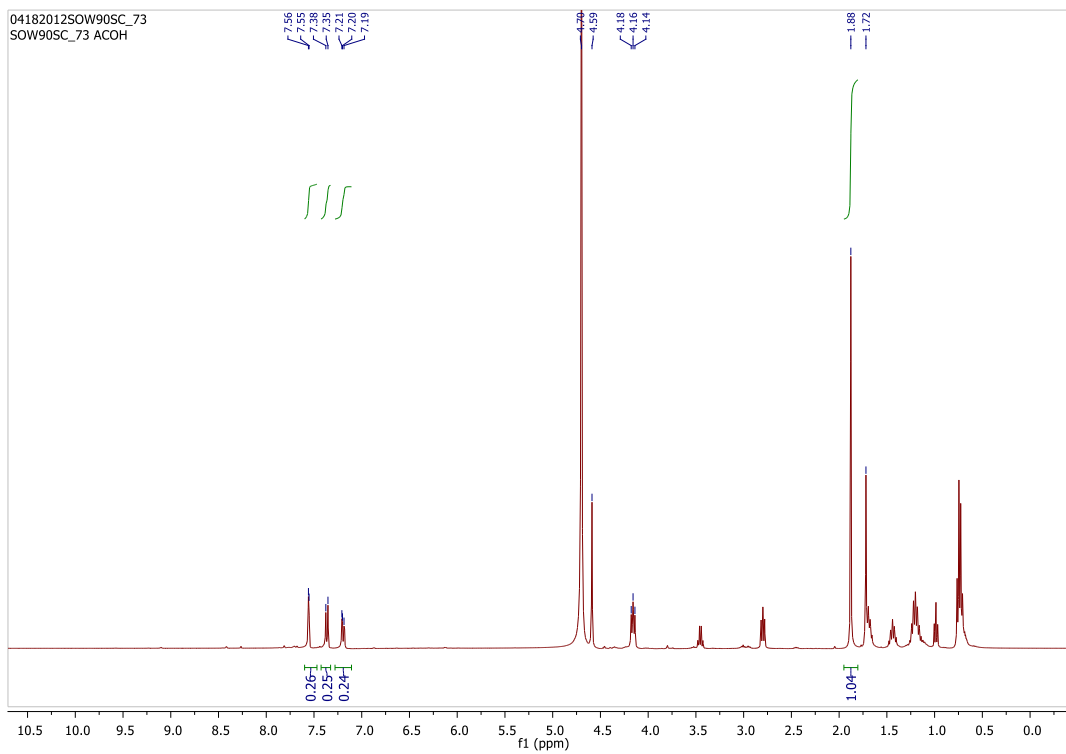


Figure 4.5 ^1H NMR(D_2O) of catalyst screening (AcOH, 80 °C, 3 days)

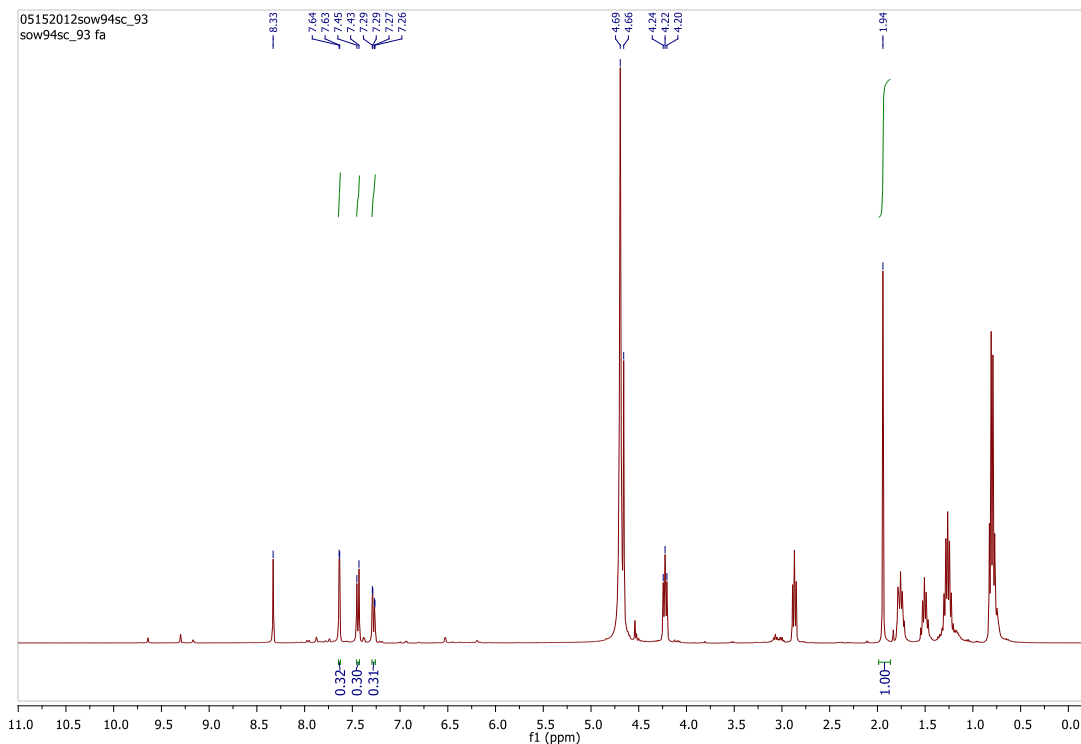


Figure 4.6 ^1H NMR(D_2O) of catalyst screening (HCO_2H , $80\text{ }^\circ\text{C}$, 3 days)

Varying the reaction conditions from $70\text{ }^\circ\text{C}/2\text{days}$ to $70\text{ }^\circ\text{C}/3\text{days}$ we observed either a decrease in the yield (for acetic acid or, phosphoric acid as catalysts) or small effect (with the other acid catalysts) (Figure 4.3). A negligible effect of increasing the reaction time from 2 to 3 days was also observed with phosphoric acid or triflic acid at $80\text{ }^\circ\text{C}$. However, the reaction yield improves significantly when changing the reaction time from 2 days to 3 days at $80\text{ }^\circ\text{C}$ using acetic acid, trifluoroacetic acid or formic acid as catalysts. While changing the reaction time from 2 days to 3 days at $80\text{ }^\circ\text{C}$ we observed an increase in the yield from 58% to 72% for acetic acid, from 62% to 80% for trifluoroacetic acid and from 77% to 94% for formic acid. Thus, the optimized condition for the reaction was set as $80\text{ }^\circ\text{C}/3\text{days}$ using 30 mol % of formic acid and the yield was 94 %. We also varied the amount of catalyst and the results show that at 10 mol % and 20 mol % of

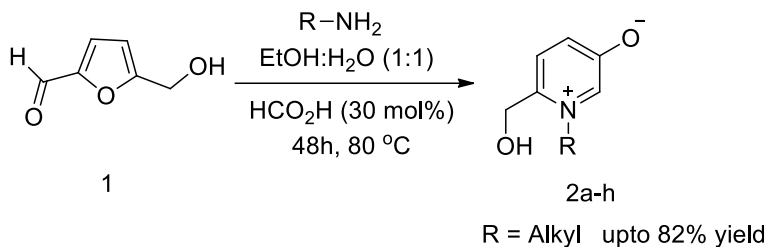
formic acid (with *n*-butylamine) provided, respectively, yields of 69% and 50%, whereas any increase above 30 mol % in the catalyst did not affect the reaction.

4.3 Substrate scope studies

Using the optimized reaction conditions we performed the reaction with various alkyl amines (Table 4.1). For most cases, the reaction completion was observed at 80 °C/2days. However, for amines with longer alkyl chains, the reactions take place slowly and 80 °C/3days are needed for the reaction to complete. For example, the isolated yield using hexylamine was 34% for an incomplete reaction at 80 °C/2days, increasing to 55% of yield if we allow the reaction to proceed for 3 days (Table 4.1, entry 5).

Several attempts were performed with aryl amines; however, the reaction yields were poor. In contrast, shorter alkyl amines, such as, methylamine, propylamine, butylamine, or pentylamine gave better isolated yields of about 70-80% (Table 4.1, entries 1-4), whereas longer alkyl chain amines like hexyl or octyl amines gave lower yields, namely, 55% and 13%, respectively (Table 4.1, entries 5, 6).

The reaction with longer alkylamines were comparatively slow showing only the presence of unreacted amines but not HMF which already lead to decomposition and not improving the yield. On a 5g scale up reaction of HMF with methyl amine we observed an isolated yield of 80%. In the case of octylamine, 1 equiv. of formic acid was used intentionally for longer reaction time to improve the yield (30% vs 13%, entry 6). In some cases, an excess of unreacted amines turned to be inseparable from the final pyridinium salt.



Scheme 4.6 Substrate scope with alkyl amines

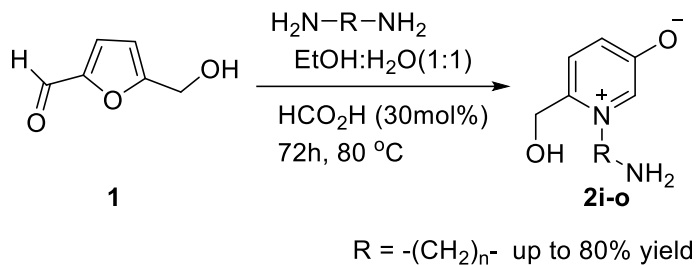
Table 4.1 Substrate scope with various alkyl amines

Entry	R	Time (h)	Temp (°C)	product	yield (%)
1	Methyl-	48	80	2a	78
2	Ethyl-	48	80	2b	81
3	<i>n</i> -Propyl-	48	80	2c	82
4	<i>n</i> -Butyl-	48	80	2d	72
5	<i>n</i> -Hexyl-	48	80	2e	34
		72	80		55
6	<i>n</i> -Octyl-	72	80	2f	13
		72 ^a	80		30
7	Allyl-	48	80	2g	77
8	3-methoxypropyl-	48	80	2h	62

Reaction condition: To 100 mg of HMF (0.8 mmol) in EtOH/H₂O (1:1, 10 mL), was added 1.1 equiv. of respective amine, HCO₂H (30 mol%) and the mixture was heated in a closed high pressure vessel at 80 °C for 2 days. ^aWas used 1 equiv. of HCO₂H.

Interestingly, the reaction with hexyl diamines exclusively formed monopyridinium salts (Table 4.2) even with 2 mol equiv of HMF (Table 4.2, entry

4). This fact expanded the substrate scope and we were able to isolate various pyridinium salts from different alkyl diamines in good yields.



Scheme 4.7 Substrate scope with alkyl diamines

Table 4.2 Substrate scope with various alkyl diamines

Entry	R	Time (h)	Temp (°C)	product	yield (%)
1	$-(\text{CH}_2)_3-$	72	80	2i	61
2	$-(\text{CH}_2)_4-$	72	80	2j	72
3	$-(\text{CH}_2)_5-$	72	80	2k	80
4	$-(\text{CH}_2)_6-$				
	HMF:amine 1:1 ^a	72	80	2l	70
	HMF:amine 2:1 ^b	72	80		74
5	$-(\text{CH}_2)_7-$	72	80	2m	69
6	$-(\text{CH}_2)_8-$	72	80	2n	63
7	$-(\text{CH}_2)_{12}-$	72	80	2o	59

Reaction condition: To 100 mg of HMF (0.8 mmol), in EtOH/H₂O (1:1, 10 mL), was added 1.1 equivalent of respective amine, HCO₂H (30 mol%) and the mixture was heated

in a closed high pressure vessel at 80 °C for 3 days. ^aused 1:1 molar ratio of HMF/diamine. ^bused 2:1 molar ratio of HMF/diamine.

Also longer chain diamines gave higher yields in comparison with simple alkyl amines. For instance, octyl amine provided only 13% yield whereas octyldiamine under similar conditions originated 63% yield (Table 4.1, entry 6 vs Table 4.2, entry 6).

A representative procedure for the key transformation

To a mixture of 100 mg of HMF (0.8 mmol) and ethanol:water (1:1, 10 mL), 1.1 equivalent of alkyl amine and a catalytic amount of formic acid 30 mol% was added. The resulting mixture was heated in a closed high pressure vessel at 80 °C for specified time. The reaction was monitored by TLC (ethylacetate/methanol 3:7). After the reaction was complete, the reaction mixture is diluted with 50 mL water and stirred well with activate charcoal and then filtered through celite. The filtrate is clear from the coloured impurities and water is evaporated under reduced pressure to give the corresponding pyridinium derivatives. In some cases, we observed some known impurities along with the products such as the starting amines. The spectral data of these isolated derivatives are from the filtrate without further purification.

Representative Spectra:

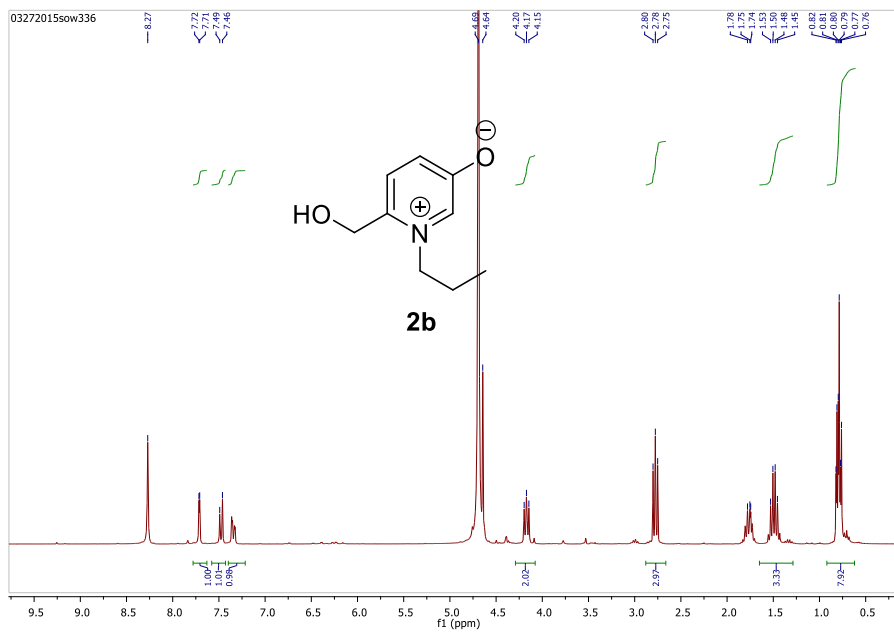


Figure 4.7 ¹H NMR(D₂O) of propylamine pyridinium salt.

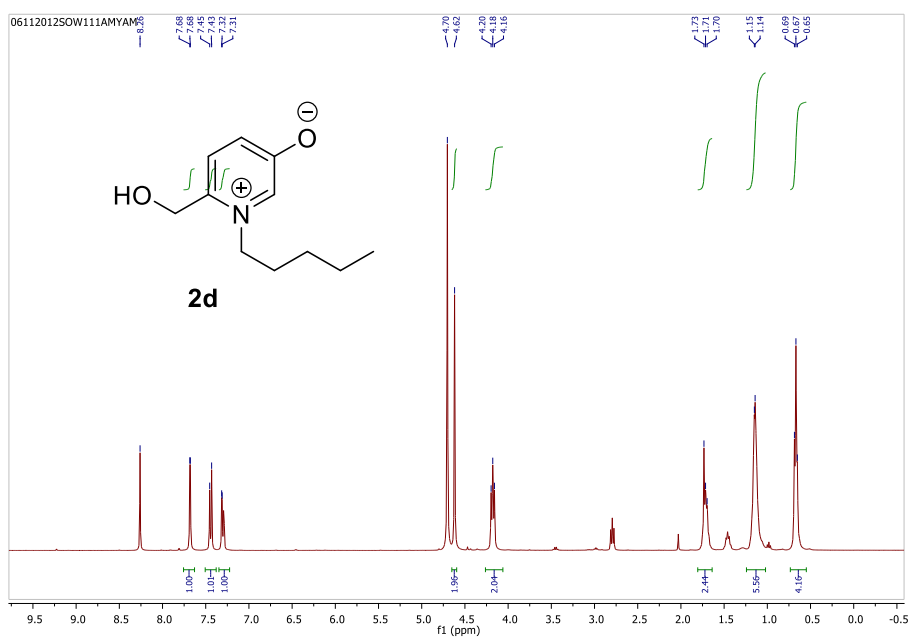


Figure 4.8 ¹H NMR(D₂O) of pentylamine pyridinium salt.

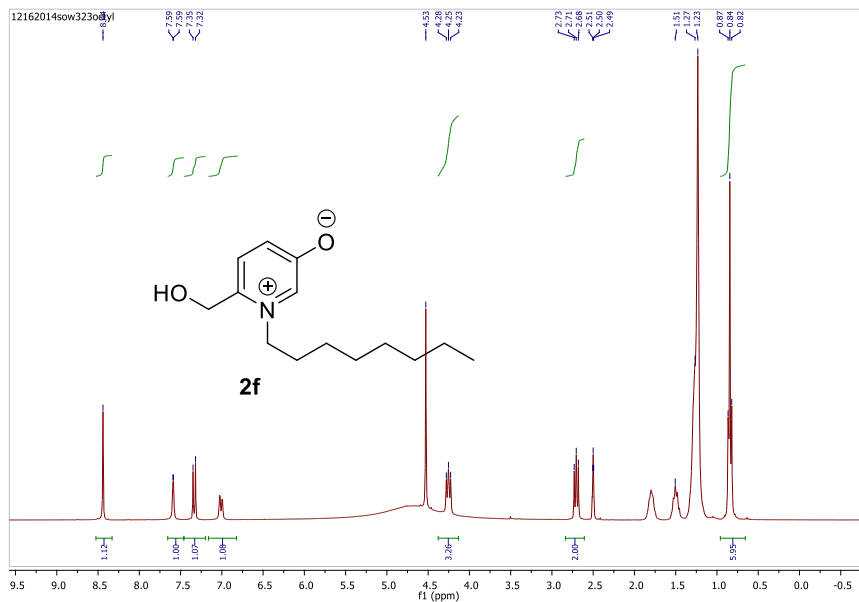


Figure 4.9 ^1H NMR(D_2O) of octylamine pyridinium salt.

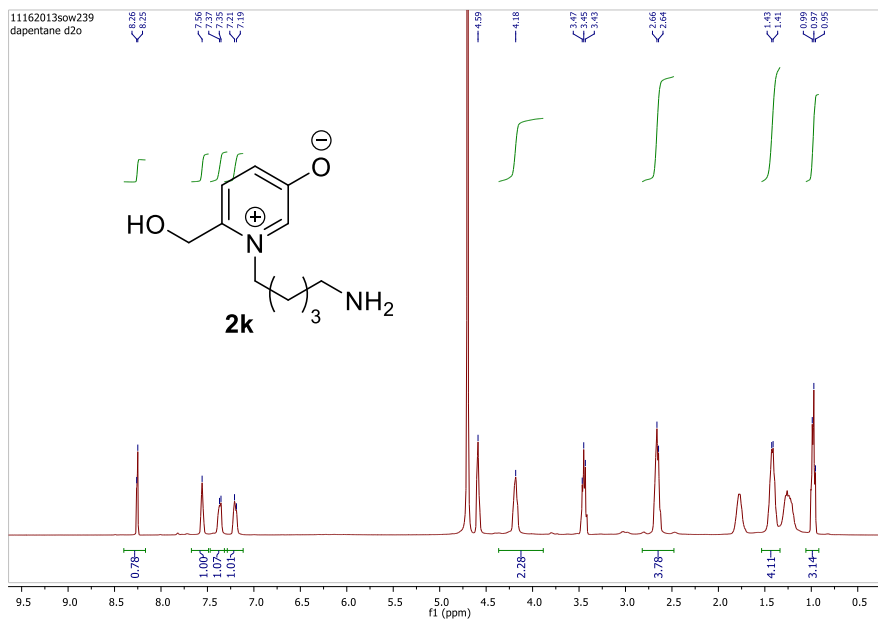


Figure 4.10 ^1H NMR(D_2O) of pentylamine pyridinium salt.

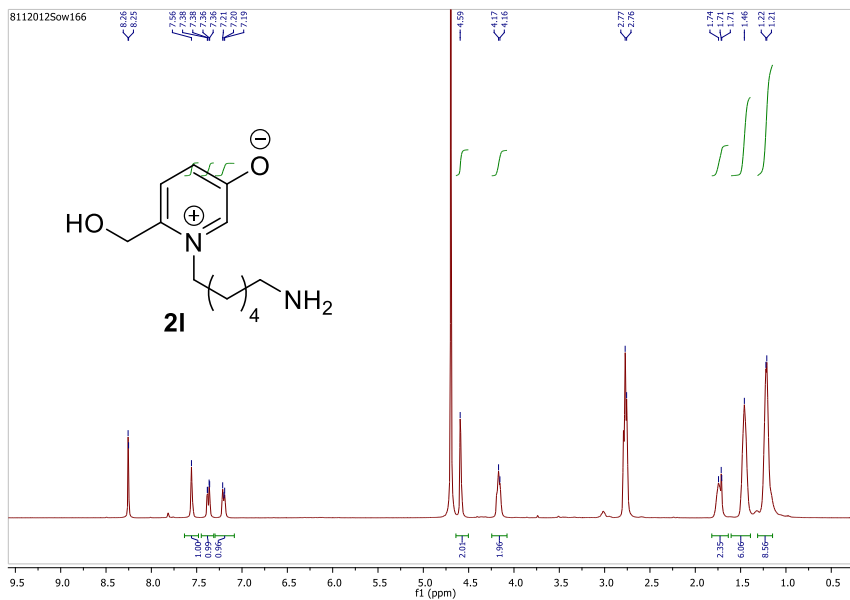


Figure 4.11 ^1H NMR(D_2O) of hexyldiamine pyridinium salt.

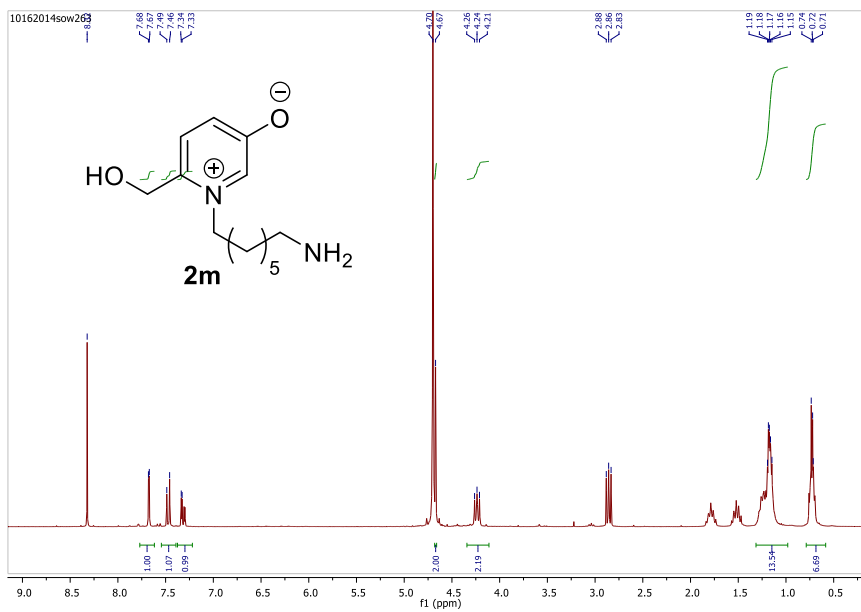


Figure 4.12 ^1H NMR(D_2O) of heptyldiamine pyridinium salt.

4.4 Study on the mechanistic details

With the purpose of disclosing the involved mechanism, an isotope water experiment using 99% H₂O¹⁸ was performed. In order to minimize the amount of used H₂O¹⁸ some experiments were conducted using H₂O in variable H₂O:EtOH ratios using *n*-butylamine as model substrate, allowing to identify the weighed quantity of H₂O:EtOH (0.167 g: 0.322 g) as the minimum quantity of water to be used. Under those conditions, by replacing H₂O by H₂O¹⁸ the observed HRMS of the product **2c** revealed that there is no incorporation 18-labelled isotopic oxygen (See SI) which is consistent with the mechanistic approach for the formation of pyridinium betaine *via* intermediate **D** (Figure 4.7). In principle, HMF **1** forms an imine with respective amine and water attacks at the C5 carbon resulting in the ring opening of furan to form an intermediate **D**. The obtained intermediate undergoes an intramolecular nucleophilic attack of nitrogen onto C2-carbonyl group leading to the ring closure to form 6-membered ring **E**, which follows a dehydration reaction to give the final pyridinium betaine compound **2**.

DFT calculations using methylamine as substrate are also consistent with this proposed reaction pathway. Two explicit water molecules (solvent) were considered in the computational model, in order to have a reasonable description for the solvent assistance on the various proton transfer steps along the mechanism. The complete energy profile obtained for the reaction is represented in supporting information Figures S131 and S132. The highest observed barriers are for **A/B**, **B/C**, **C/D** and **F/G** intermediate steps. In addition, the **A/B** and **F/G** steps are clearly endoenergetic while **G/2** is a highly exoenergetic step derived from the aromaticity gain associated with the formation of the pyridinium cation.

The larger values obtained for the individual barriers along the path are 27 kcal/mol and the highest point in the profile (TSC'D) is 33 kcal/mol above the initial reactants which is in reasonable agreement with the experimental conditions

of the reaction (2 days at 80 °C). Nevertheless, it is important to notice that the accuracy of the energy values is somewhat limited by the modesty of the model used in the calculations, with only two explicit water molecules in a mechanism where that solvent plays a decisive part. The mechanism proposed in Scheme 2 was reproduced by the DFT calculations. In the path obtained water plays a crucial role, not only as a proton carrier, assisting all the proton transfer steps, but also as an active participant in the reaction, being added to the furan ring of the initial iminium salt and lost in the final steps that lead to the pyridinium product **2**

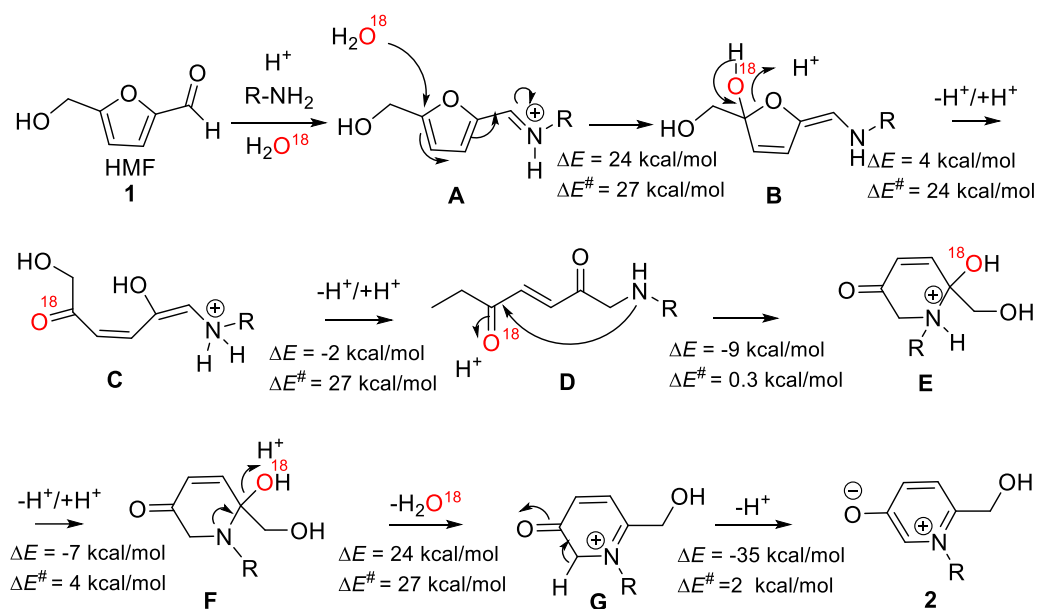


Figure 4.7 Plausible reaction mechanism and selected DFT results

4.5 Conclusion

In conclusion, an efficient organocatalyzed transformation under mild conditions of the bioplatfrom HMF to *N*-alkyl-5-hydroxy-2-(hydroxymethyl)pyridinium (HPyr) salts by reaction with a range of alkylamines is described. In particular, it was also proven that in the case of using terminal alkyldiamines there is an exclusive formation of mono-HPyr. In addition, no incorporation of H_2O^{18} was

observed from the reaction medium. This synthetic route opens the possibility to consider those highly functionalized pyridinium salts as useful building blocks derived from biomass.

4.6 References

1. (a) Laville, R.; Amade, P.; Thomas, O. P. *Pure Appl. Chem.* **2009**, *81*, 1033; (b) Temraz, T. A.; Houssen, W. E.; Jaspars, M.; Woolley, D. R.; Wease, K. N.; Davies, S. N.; Scott, R. H. *BMC Pharmacology* **2006**, *6*, 10; (c) Dasari, V. R. R. K.; Muthyala, M. K. K.; Nikku, M. Y.; Donthireddy, S. R. R. *Microbiol. Res.* **2012**, *167*, 346; (d) Laville, R.; Genta-Jouve, G.; Urda, C.; Fernández, R.; Thomas, O. P.; Reyes, F.; Amade, P. *Molecules* **2009**, *14*, 4716; (e) Reyes, F.; Fernández, R.; Urda, C.; Francesch, A.; Bueno, S.; de Eguilior, C.; Cuevas, C. *Tetrahedron* **2007**, *63*, 2432.
2. See review: Sepcik, K. *J. Toxicol.* **2000**, *19*, 139.
3. Andersen, R.J.; van Soest, R.W.; Kong, F. *Alkaloids Chemical and Biological Perspectives*. Pelletier, S.W., Ed.; Elsevier Science: Oxford, UK, **1996**, *10*, 301.
4. (a) Śliwa, W. *N-Substituted Salts of Pyridine and Related Compounds, Synthesis, Properties, Applications*. Academic Press: Częstochowa, Poland, **1996**; (b) Welton, T. *Chem. Rev.* **1999**, *99*, 2071; (c) Coe, B. J.; Harris, J. A.; Asselberghs, I.; Wostyn, K.; Clays, K.; Persoons, A.; Brunschwig, B. S.; Coles, S. J.; Gelbrich, T.; Light, M. E.; Hursthouse, M. B.; Nakatani, K. *Adv. Funct. Mater.* **2003**, *13*, 347; (d) Madaan, P.; Tyagi, V. K. *J. Oleo Sci.* **2008**, *57*, 197.
5. (a) Lyle, R. E. *In Pyridine and its Derivatives*. Wiley: New York, NY, **1974**, *1*, 137; (b) Review: Silva, E. M. P.; Varandas, P. A. M. M.; Silva, A. M. S.; *Synthesis*, **2013**, *45*, 3053.

6. Luo, C. Z.; Jayakumar, J.; Gandeepan, P.; Wu, Y. C.; Cheng, C. H. *Org. Lett.* **2015**, *17*, 924.
7. Nolsoe, J. M. J.; Aursnes, M.; Tungen, J. E.; Hansen, T. V. *J. Org. Chem.*, **2015**, *80*, 5377.
8. (a) Huang, W. X.; Wu, B.; Gao, X.; Chen, M. W.; Wang, B.; Zhou, Y. G. *Org. Lett.* **2015**, *7*, 1640; (b) Ye, Z. S.; Chen, M. W.; Chen, Q. A.; Shi, L.; Duan, Y.; Zhou, Y. G. *Angew. Chem. Int. Ed.* **2012**, *51*, 10181.
9. Sepcik, K.; Turk, T. *Prog. Mol. Subcell. Biol.* **2006**, *42*, 105.
10. (a) Laville, R.; Thomas, O. P.; Berrue, F.; Reyes, F.; Amade, P.; *Eur. J. Org. Chem.* **2008**, 121; (b) Suzuki, R.; Yanuma, H.; Hayashi, T.; Yamada, H.; Usuki, T.; *Tetrahedron* **2015**, *71*, 1851.
11. (a) Bennasar, M. L.; Jiménez, J. M.; Vidal, B.; Sufi, B. A.; Bosch, J. *J. Org. Chem.* **1999**, *64*, 9605; (b) Bennasar, M. L.; Zulaica, E.; Alonso, Y.; Vidal, B.; Vázquezb, J. T.; Bosch, J. *Tetrahedron Asymmetry* **2002**, *13*, 95; (c) Focken, T.; Charette, A. B. *Org. Lett.* **2006**, *8*, 2985; (d) Azzouz, R.; Fruit, C.; Bischoff, L.; Marsais, F. *J. Org. Chem.* **2008**, *73*, 1154; (e) Kuethe, J. T.; Comins D. L. *J. Org. Chem.* **2004**, *69*, 5219; (f) Bennasar, M. L.; Zulaica, E.; Yuan, C.; Alonso, Y.; Bosch, J. *J. Org. Chem.* **2002**, *67*, 7465; (g) Bennasar, M. L.; Vidal, B.; Bosch, J. *J. Org. Chem.* **1997**, *62*, 3597.
12. (a) Corma, A.; Iborra, S.; Velty, A.; *Chem. Rev.* **2007**, *107*, 2411; (b) Tuck, C.O.; Pérez, E.; Horváth, I.T.; Sheldon, R.A.; Poliakov, M.; *Science* **2012**, *337*, 695; (c) Takagaki, A.; Nishimura, S.; Ebitani, K.; *Catal. Surv. Asia*, **2012**, *16*, 164..
13. (a) Rosatella, A. A.; Simeonov, S. P.; Frade, R. F. M.; Afonso, C. A. M. *Green Chem.* **2011**, *13*, 754; (b) van Putten, R.-J.; van der Waal, J. C.; de Jong, E.; Rasrendra, C. B.; Heeres, H. J.; de Vries, J. G. *Chem. Rev.* **2013**, *113*, 1499.

14. (a) Simeonov, S. P.; Coelho, J. A. S.; Afonso, C. A. M.; *ChemSusChem*, **2012**, *5*, 1388; (b) Simeonov, S. P.; Coelho, J. A. S.; Afonso, C. A. M.; *ChemSusChem*, **2013**, *6*, 1997; (c) Simeonov, S. P.; Afonso, C. A. M.; *J. Chem. Educ.* **2013**, *90*, 1373.
15. (a) Nunes, J. P. M.; Afonso, C. A. M.; Caddick, S.; *RSC Adv.*, **2013**, *3*, 14975; (b) Subbiah, S.; Simeonov, S. P.; Esperança, J. M. S. S.; Rebelo, L. P. N.; Afonso, C. A. M.; *Green Chem.*, **2013**, *15*, 2849.
16. (a) Villard, R.; Robert, F.; Blank, I.; Bernardinelli, G.; Soldo, T.; Hofmann, T.; *J. Agric. Food. Chem.*, **2003**, *51*, 4040; (b) Soldo, T.; Hofmann, T. *J. Agric. Food. Chem.*, **2005**, *53*, 9165.
17. Kirchhecker, S.; Tröger Müller, S.; Bake, S.; Antonietti, M.; Taubert, A.; Esposito, D.; *Green Chem.* **2015**, *17*, 4151.

CHAPTER V

*Studies on the new biomass derived
pyridinium salts*

I have produced all the results revealed in this chapter to understand the chemical properties of pyridinium salts. Thanks to Dr. Raquel Frade for guiding/assisting me on the biological activity studies.

5. Studies on new biomass derived pyridinium salts

CHAPTER V- Summary

Pyridinium salts are assessed with their potential synthetic value in the construction of pharmacologically relevant piperidine, dihydro- and tetrahydropyridines framework to natural products. Their study in various material and biological applications ranging from dyes, surfactants, sensors, electrolytes to potent inhibitors, anti-microbial agents, gene delivery etc.

In this chapter we studied the possible chemical reactivity under various acidic and basic reaction conditions of the synthesized pyridinium salts. Furthermore, we also tested these compounds for biological activity. These studies provide the basic understanding of these new compounds to develop them as stable substrates suitable for future applications.

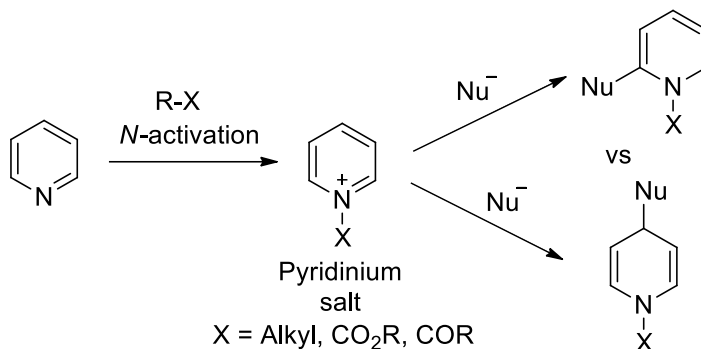
5.1 Chemical reactivity of pyridinium salts

5.1.1 Introduction

The addition of a broad variety of nucleophiles to pyridinium salts is, probably, the method of choice for the preparation of functionalized dihydro-, tetrahydropyridines, as well as piperidines. All these heterocycles are important intermediates in the synthesis of piperidine containing biologically active molecules and alkaloids. Thus these pyridinium salts possess high synthetic value as key intermediate for the production of wide range of pharmacologically relevant piperidine, dihydro, tetrahydropyridine frameworks.^{1,2}

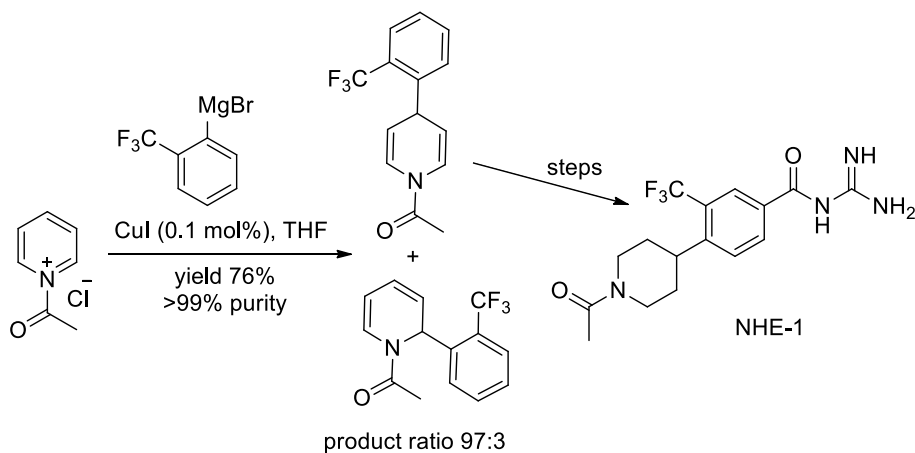
Due to the aromatic character of the pyridine heterocycle, its basicity and the electron-attracting influence of the nitrogen atom, pyridinium salts are found to be of versatile chemical reactivity. The nucleophilic additions to pyridinium salts for the synthesis of dihydropyridines and 2,3-dihydro-4-pyridones have been studied systematically.^{3,4}

Pyridinium cations can behave as electrophiles and 1,3-dipoles to take part in condensation, Michael addition, 1,3-dipolar addition, nuclear substitution and arrangement reactions, and find vast applications to organic syntheses. Pyridinium salts contain reactive electrophilic sites at the 2, 4 and 6-positions of the heterocyclic ring. Upon addition of nucleophile, mixtures of substituted 1,2- and 1,4-dihydropyridines are frequently obtained (Scheme 5.1).



Scheme 5.1 Functionalization of *N*-activated pyridinium salts.

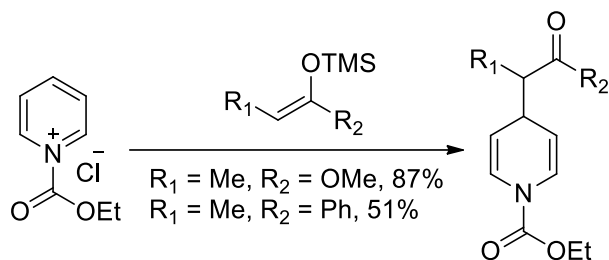
Recently, a facile and economical five-step process for the synthesis of a sodium–hydrogen exchange type I inhibitor (NHE-1) was developed from readily available starting materials in 43% overall yield (Scheme 5.2).⁵ The key transformation is efficient copper-catalyzed conjugate addition of 2-trifluoromethylphenyl Grignard reagents to acetyl pyridinium salts.



Scheme 5.2 Synthesis of NHE-1

Softer mixed Cu–Zn species have been derived from alkyl and aryl Zinc reagents with copper sources.^{6,7} These have been employed to achieve high-yielding 4-selective addition, for example, in the synthesis of 4-substituted

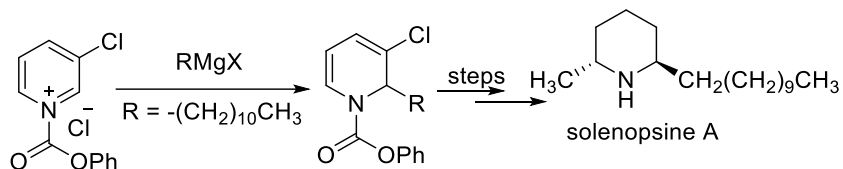
piperidine derivatives. Recently, Arndtsen and co-workers reported that mild organoindium reagents add to pyridinium salts formed *in situ* in the presence of chloroformates under copper catalysis with moderate to good C-4 selectivity.⁸ Silyl enol ethers generated from ketones and silyl ketene acetals, which are soft nucleophiles, add with high regioselectivity to the 4-position in the presence of ethyl chloroformate (Scheme 5.3).⁹



Scheme 5.3 Selective addition of silyl enol ethers to 4-position

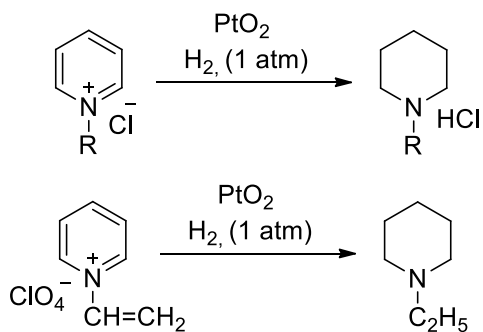
Other nucleophiles that add selectively at the 4-position include benzylic tin reagents¹⁰ and Phosphonates¹¹ which provided high yields of pyridine-4-phosphonates. The addition of trialkylalkynylborates to *N*-acetylpyridine also provided a 4-selective addition.

The introduction of an easily removable bulky group can control the regioselectivity of nucleophile addition. Subsequent removal of the blocking group can reveal the desired unsubstituted dihydropyridine. Adding a blocking group to the 4-position ensures addition to the 2-position. Chloride has been used for this purpose and removed by hydrogenation to allow access to (±)-solenopsine A and (±)-dihydropinidine¹² as well as alkaloids from the quinolizidine family (Scheme 5.4).



Scheme 5.4 Synthesis of solenopsine A

There are data in the literature on the catalytic reduction of pyridinium salts both under normal conditions and at elevated temperature and hydrogen pressure with various metals (Raney Ni, Pd/C, Ru/C, Rh/C, Ni/Ru) and their oxides (PtO₂, PtO, RuO₂, PdO) as catalysts. The direction of the reaction and its stereochemical effect depend on the number, nature, and character of substituents in the substrate and on the selected conditions.¹³ The catalytic reduction of pyridinium salts at platinum black (Adam's catalyst) for the production of *N*-substituted piperidines was first realized in 1928 (Scheme 5.5).

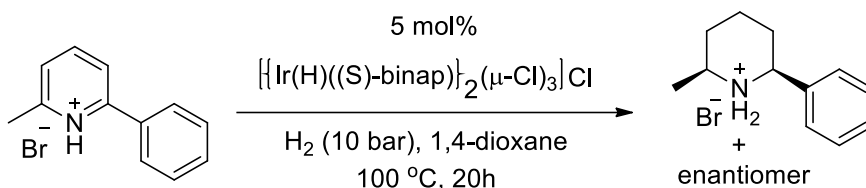


Scheme 5.5 Catalytic reduction of pyridinium salts

It is worth to state that pyridinium salts with alkyl, aryl, and functionally substituted radicals at the nitrogen atom are reduced more readily than pyridinium hydrochloride. The reason could be the existence of an

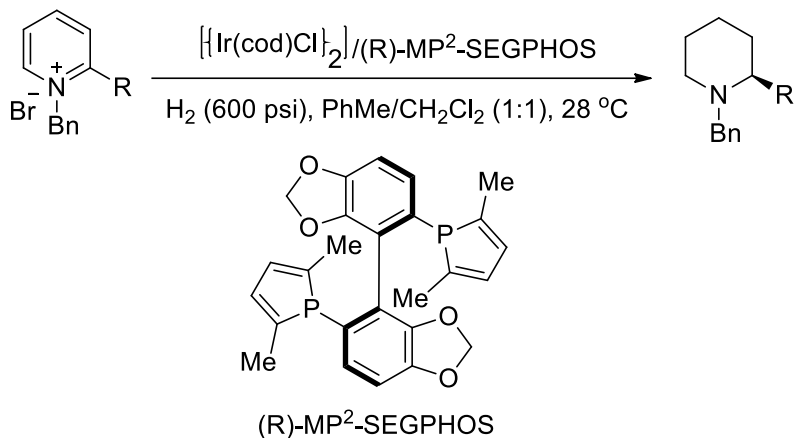
equilibrium between the free base and the pyridinium salt in the solution. The free base, gets adsorbed on the catalyst through the electron pair of the nitrogen atom, leads to deactivation and displaces the equilibrium toward the pyridine base.

A salt formation strategy for asymmetric hydrogenation of pyridines is described in Scheme 5.6. Poly-substituted pyridinium salts were successfully hydrogenated using chiral iridium dinuclear complexes to afford substituted piperidines with multiple stereogenic centers after a simple basic workup.



Scheme 5.6 Ir-catalyzed asymmetric hydrogenation of di-substituted pyridinium salts

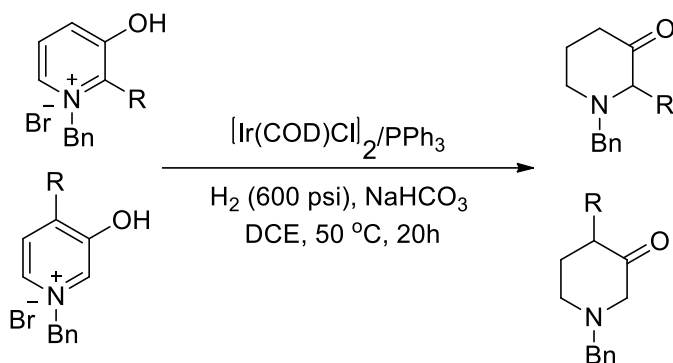
Zhang and his co-workers have developed a highly efficient enantioselective hydrogenation of *N*-alkyl-2-arylpyridinium salts (Scheme 5.7).¹⁴ This protocol represents a significant advance over previous methods in that a directing group is not required. With this constraint removed, this new method tolerates a variety of *N*-benzyl as well as simple *N*-alkyl groups, which greatly increases the scope and applicability of this approach in synthesis.



Scheme 5.7 Asymmetric hydrogenation of pyridinium salts with an iridium phosphole catalyst

In addition, this work provides the unique example of using a chiral-phosphole-based ligand for highly efficient asymmetric catalysis. The unique electronic and structural aspects of the phosphole unit should inform future ligand design for asymmetric catalysis.

The selective hydrogenation of 3-hydroxypyridinium salts has been achieved using a homogeneous Iridium catalyst, providing a direct access to 2- and 4- substituted piperidin-3-one derivatives with high yields, which are important organic synthetic intermediates and the prevalent structural motifs in pharmaceutical agents. Mild reaction conditions, high chemoselectivity, and easy scalability make this reaction highly practical for the synthesis of piperidin-3-ones (Scheme 5.8).¹⁵



Scheme 5.8 Iridium-catalyzed selective hydrogenation of 3-hydroxypyridinium salts

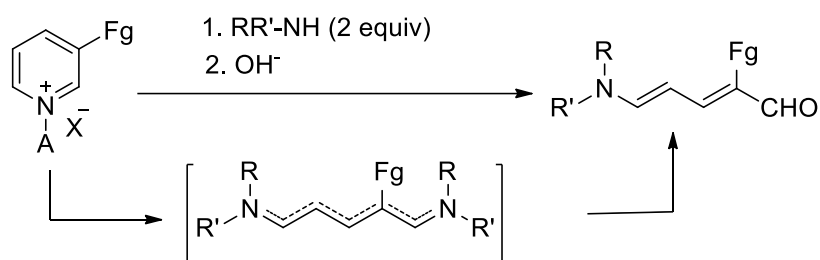
Donohoe *et al.* reported the addition of two electrons to a pyridinium salt turns it into a nucleophile.¹⁶ The intermediate generated by the reduction of such salts can react successfully with a range of different alkyl halides, and the intermediate hydrolyzed *in situ* to provide a wide range of dihydropyridones. Each position on the dihydropyridone ring is then accessible using standard synthetic manipulations. Moreover they defined a highly versatile method for introducing groups α to the nitrogen with great potential for broader synthetic application. They have also shown that these molecules can be derivatized at every position around the ring, enhancing their utility to organic chemists.

Further, transformation of pyridinium compounds into functionalized conjugated dienes can be adapted to natural product synthesis with great effect. Pyridines carrying a formal positive charge on the nitrogen atom can undergo nucleophilic addition to the adjacent position and subsequent ring-opening through an apparent disrotatory electrocyclic mechanism. Thus in this case, disruption of the aromatic π -system will lead to the formation of

functionalized conjugated dienes. Considering the variations possible, in terms of functional pattern on the pyridinium salt and the types of nucleophiles available, the transformation represents a powerful strategy to manufacture five-carbon units containing a dienal moiety.

In its most fundamental form, reacting a pyridinium salt with 2 equivalents of a secondary amine will result in the corresponding 5-aminopenta-2,4-dienal upon basic hydrolysis (Scheme 5.9). The compounds formed in this manner are commonly referred to as Zincke aldehydes. The secondary amine need not be symmetric and can incorporate a number of functional patterns.

Nevertheless, it is found that pyridinium salts functionalized in the 3-position preferentially give rise to the corresponding 2-substituted Zincke aldehydes.¹⁷



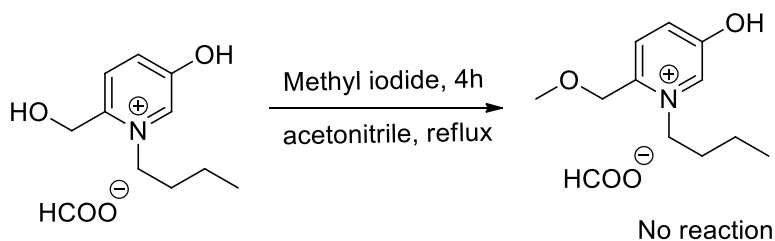
Scheme 5.9 Ring-opening of 3-substituted pyridinium salts

The literature available explains effectively the potential reactivity of biomass derived pyridinium salts that could be useful to a greater extent. Thus studying their stability and reactivity is of interest and we carried out step-by-step analysis to the studies on the newly synthesized biomass derived pyridinium salts.

5.2 Reactivity of synthesized pyridinium salts

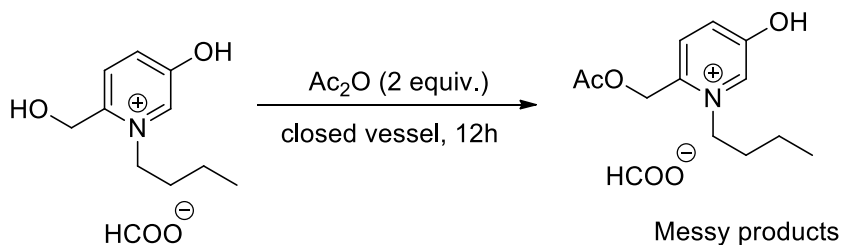
5.2.1 Reactivity with protecting groups

With the synthesized pyridinium salts, to explore more on their reactivity, we started with a simple methylation reaction using methyl iodide in acetonitrile under reflux and found traces of decomposed product with no progress to the expected product (Scheme 5.10).



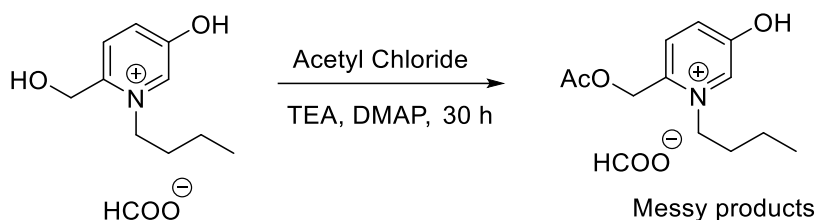
Scheme 5.10 Reaction of pyridinium salt with methyl iodide

Longer reaction time under similar condition did not provide the desired product. Thus to control the substrate reactivity, we aimed to protect the labile hydroxyl group using acetyl or TBDMS groups. Accordingly, the acetylation reaction was carried out using 5 equiv. of acetic anhydride in closed vessel at 80 °C for 12h. ¹H NMR analysis of reaction mixture shows the formation of complex mixture (Scheme 5.11).



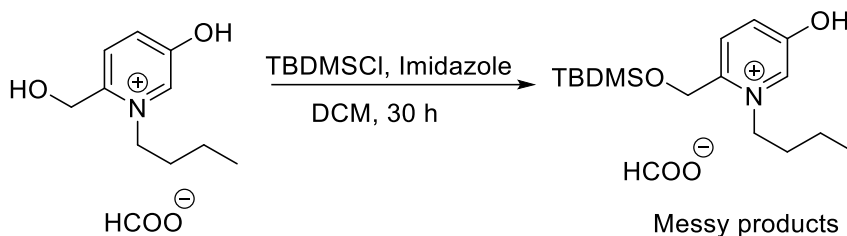
Scheme 5.11 Reaction of pyridinium salt with acetic anhydride

When the reaction was performed using acetyl chloride and trimethylamine with catalytic amount of DMAP for longer reaction time at room temperature gave messy products (Scheme 5.12).



Scheme 5.12 Reaction of pyridinium salt with acetyl chloride

We further performed reactions under mild basic condition. To protect the hydroxyl group, we have carried out the reaction using 1 equiv. of TBDMSCl and 1.2 equiv. of imidazole as a base in dichloromethane for longer reaction time (Scheme 5.13).

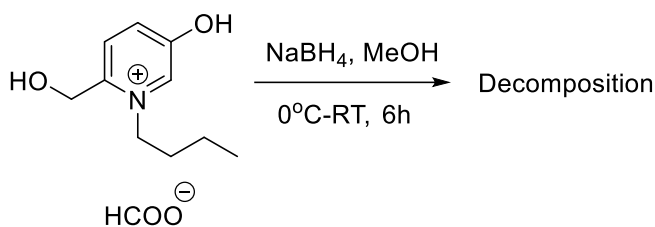


Scheme 5.13 Reaction of pyridinium salt with TBDMSCl

Again, we observed the decomposition of pyridinium salt under these conditions providing messy products which can be seen by appearance of several peaks in the NMR analyses of the reaction mixture. The less stability could be due to the acidic and basic reaction conditions used for these reactions and thus we were curious to know its liability towards neutral conditions.

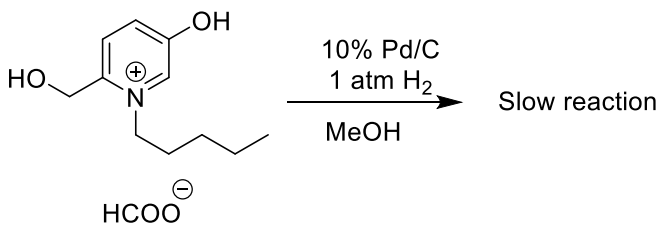
5.2.2 Hydrogenation reactions

A pyridinium salt was subjected to reduction with NaBH₄ at 0°C under room temperature for 6 h in methanol as solvent (Scheme 5.14). Even in this case, we observed complete decomposition of the starting materials, which might be due to the generated harsh basic conditions. Actually these results with classical reaction conditions were unexpected, but revealed the instability of the substrate.



Scheme 5.14 Reduction of pyridinium salt with sodium borohydride

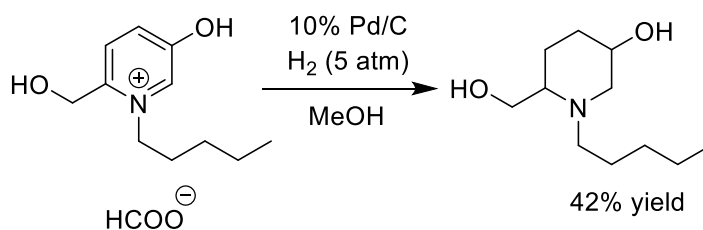
At this point, based on our attempts to various distinct reactions, we could conclude that the pyridinium substrate tends to decompose quickly under acidic or basic conditions. We were also interested to investigate their reactivity under neutral conditions such as hydrogenation with 1atm H₂ pressure using catalytic amount of 10% Pd on Carbon (Scheme 5.15).



Scheme 5.15 Reduction of pyridinium salt using Pd/C with 1 atm H₂

Though the reaction was slow, the transformation to expected product was identified by ¹H NMR analysis of the reaction mixture. We then performed

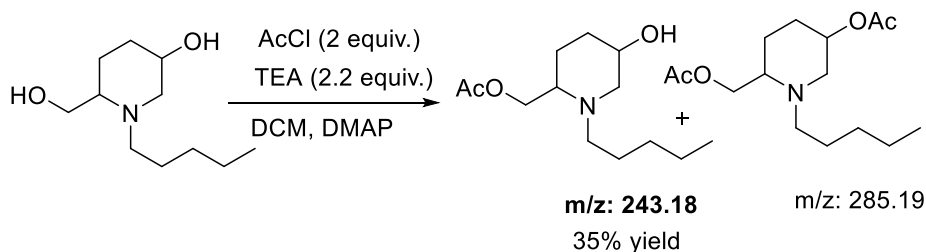
the hydrogenation reaction with 10% Pd/C under 5 atm H₂ pressure in methanol solvent for 48h (Scheme 5.16). Interestingly we observed the complete hydrogenation along with other side product. The hydrogenated product was isolated using column chromatography.



Scheme 5.16 Reduction of pyridinium salt using Pd/C under 5 atm H₂

5.2.3 Reactions with piperidine derivatives

The obtained piperidine product was subjected to acetylation reactions using Ac₂O or AcCl in dry dichloromethane in the presence of DMAP. (Scheme 5.17) and observed the monoacetylated product which was confirmed by mass analysis data (Figure 5.1).



Scheme 5.17 Reaction of piperidine with acetyl chloride

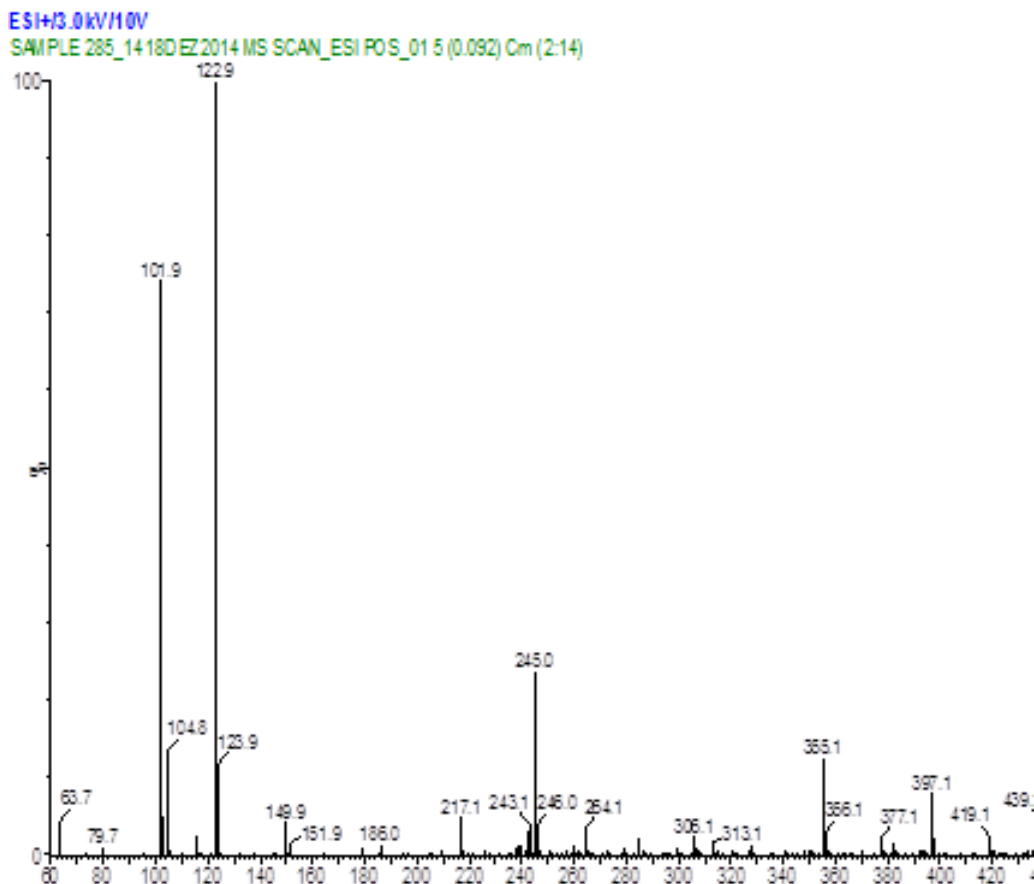
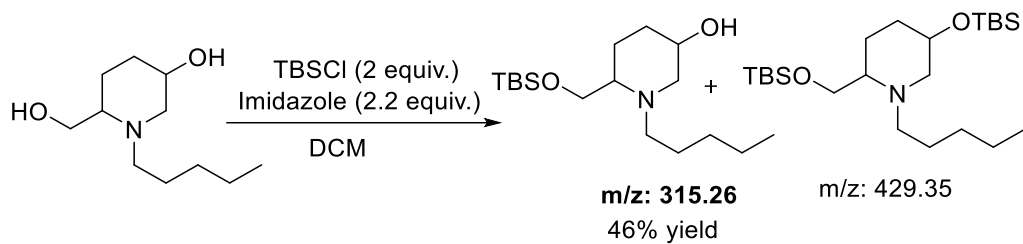


Figure 5.1 LCMS analysis of acetylation reaction with piperidine

Moreover, the obtained piperidine substrate on reaction with 2 equiv. of TBS chloride and 2.2 equiv. of imidazole as base in dichloromethane as solvent, provided monoprotected product (Scheme 5.18) which was confirmed by LCMS analysis (Figure 5.2).



Scheme 5.18 Reaction of piperidine with TBSCl

ESI+3.0kV/20V

SAMPLE 283_1418DEZ2014 MS SCAN_ESI POS_01 9 (0.166) Cm (1:14)

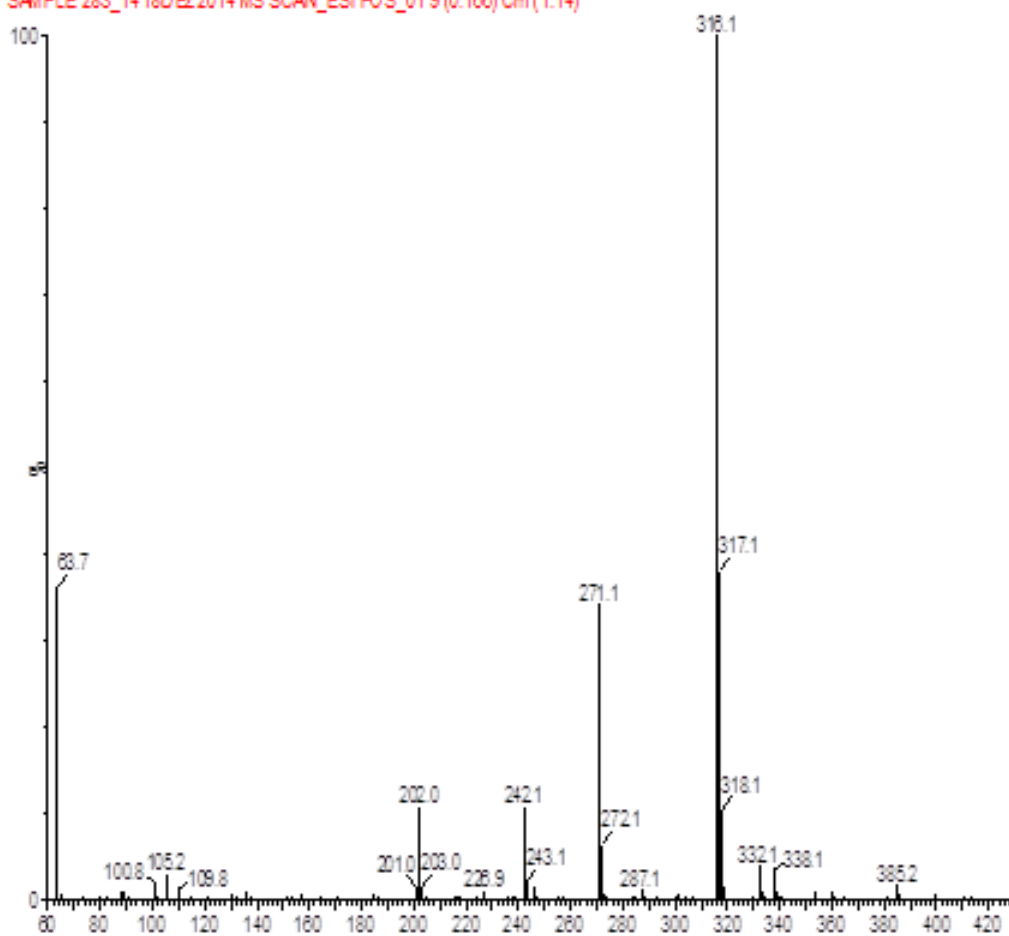
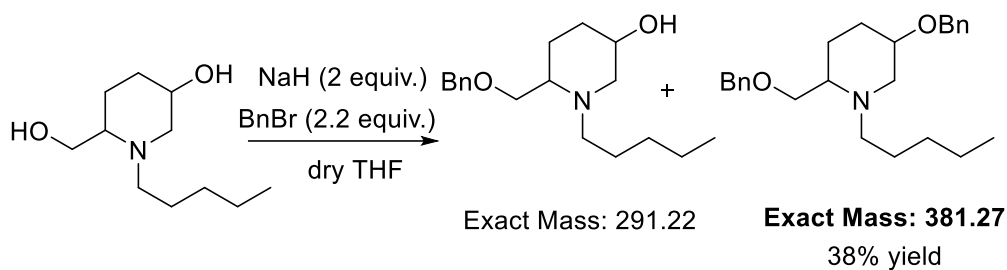


Figure 5.2 LCMS analysis of silylation reaction with piperidine

Further, we subjected the piperidine substrate to benzylation reaction using 2 equiv. benzyl bromide and 2.2 equiv. of sodium hydride in dry THF (Scheme 5.19). We have observed the formation of dibenzylated product by LCMS analysis (Figure 5.3).



Scheme 5.19 Reaction of piperidine with benzyl bromide

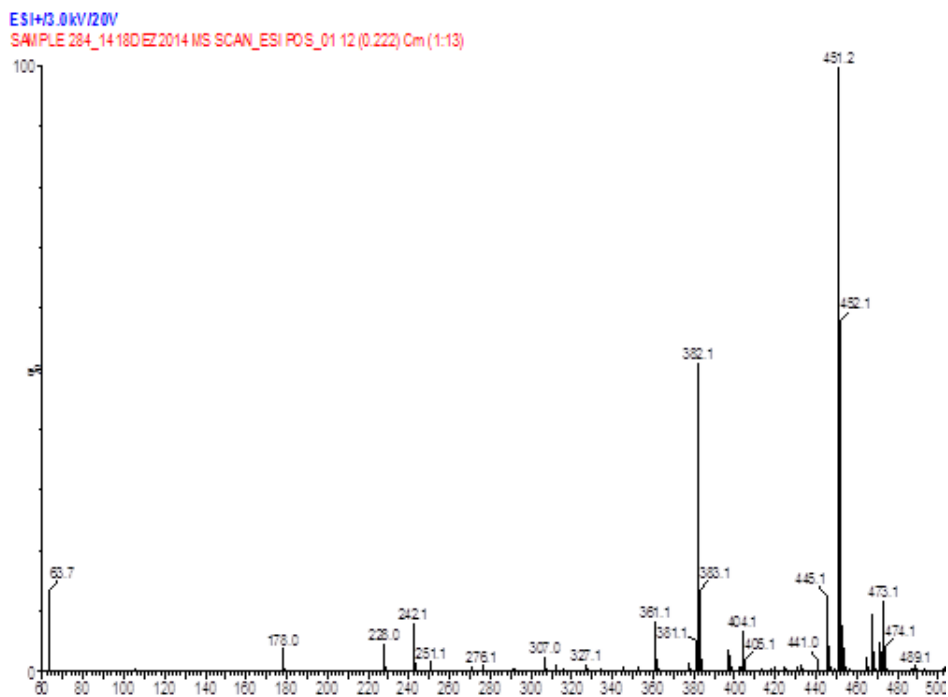
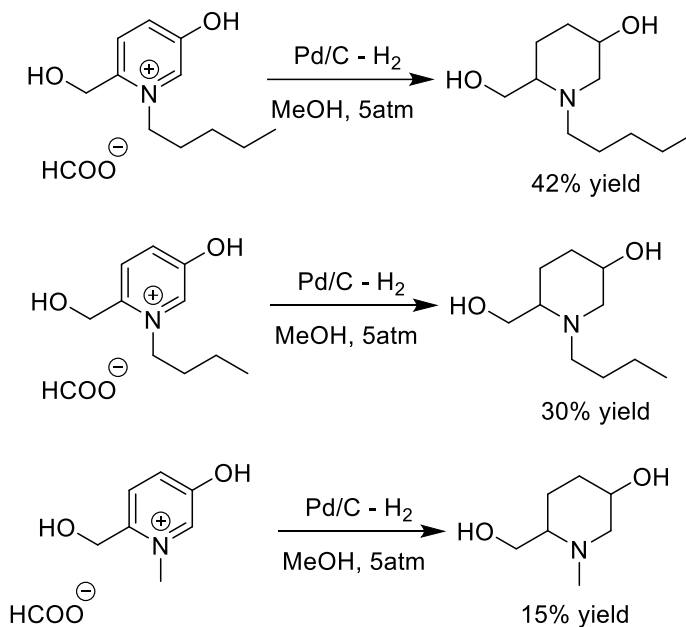


Figure 5.3 LCMS analysis of benzylation reaction with piperidine

5.2.4 Reduction of synthesized pyridinium substrates

Following the studies on piperidine substrates, we intended to study the substrate scope on reduction of various pyridinium salts (Scheme 5.20).



Scheme 5.20 Reduction reaction with various pyridinium substrates

We isolated the piperidine products from various biomass derived pyridinium substrate. With pentylpyridinium salt, under 5 atm H₂ pressure, we observed 42% isolated yield whereas with *N*-butylpyridinium salt under similar condition, we obtained 30% yield. With methylpyridinium salt, only 15% product was obtained. In all these cases, the isomeric products were not separated and the lower isolated yield was due to the formation of other unidentified side products in the reaction. Thus, further studies on the careful optimization of the reaction *via* screening of reducing agents, the reaction time could yield selective product with high yield.

5.3 Biological activity of pyridinium salts

Pyridinium salts are known to inhibit the growth of various microorganisms such as bacteria, viruses, fungi etc. Their effectiveness against microorganisms is employed as antimicrobial agents to our daily life in various ways such as sterilizing surgical instruments, as disinfectant for sanitizer in dairy industry, for the treatment of urological infections, Cetylpyridinium chloride formulated medicines such as griseofluvin for effective skin treatment¹⁸ and controls supragingival plaque and gingivitis. They also exhibit anti-inflammatory activity by inhibiting several matrix metalloproteinase proteins that causes inflammation. Moreover they become an important ingredient in cosmetic products including skin creams, body lotions, hair conditioner etc.¹⁹ Cytotoxic agents such as 12-methacryloyloxydodecylpyridinium bromide (MDPB) and cetylpyridinium chloride (CPC), is used extensively for the treatment of oral infections.²⁰

1(10-aminodecyl)-Pyridinium salt was isolated from a marine actinomycetes shows antibacterial activities against Gram-positive and Gram-negative bacteria and has *in vitro* cytotoxic activity profile against cervix, breast, brain cell lines.²¹ Compounds such as 4-amino-1-alkyl pyridinium bromides are simple and easy for larger scale synthesis are shown to exhibit interesting antimicrobial activity and biological activities such as anti-bacterial activity against *Escherichia coli* and *Staphylococcus aureus*, germ tube inhibition against *C. albicans*.²² Certain *N-Alkyl*- and *N*-prenylpyridinium based ions found to be potent and specific inhibitors against *Candida albicans* oxidosqualene-lanosterol cyclase and also exhibits anti-fungal activity.

Pyridinium based AChE inhibitors already has attention as multipotent Alzheimer's disease modifying agents.²³ F. Baharloo *et al.* reported benzofuranone-based compounds containing benzylpyridinium moiety as acetylcholinesterase inhibitors.²⁴ The *N*-benzylpyridinium moiety contributes to inhibitor activity on interaction with catalytic site while the aromatic part of benzofuranone ring participates in pepstacking with the PAS of AchE. Simplifying this lead by replacing the benzofuranone moiety with benzofuran ring and the results showed in vitro anti-AchE activity with IC50 value of 4.1nM, 7-fold more potent than donepezil.²⁵

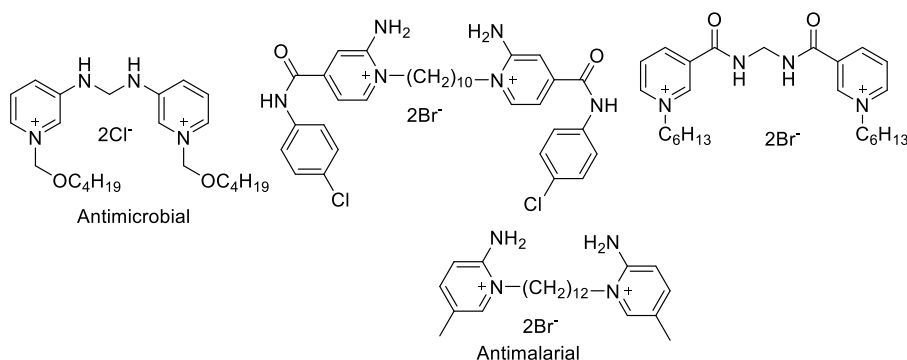


Figure 5.4 Bispyridinium salts with antimicrobial, antimalarial activity

Gene therapy is highly promising in the treatment of wide range of diseases such as AIDS, Parkinson's, arthritis, cardiovascular arteriosclerosis including several types of cancer. The efficiency of therapy is its overall gene delivery into the diseased target cell through the introduction of foreign DNA using reliable transfection agents. Pyridinium amphiphiles as efficient transfection agent for non-toxic *in-vitro* gene delivery was reported by Engberts' group in 1997 which then surpassed both the *in-vitro* and *in-vivo* transfection efficiency of formulated commercial cationic lipid maintaining low cytotoxicity across different cell lines.²⁶ These pyridinium

lipid/cholesterol also transfect several cancer cell lines similar to its tetraalkyl ammonium congener.²⁷ Certain pyridinium surfactants are shown to promote efficient, non-toxic DNA transfection and enhance *in vitro* gene delivery.²⁸

Ilies *et al.* designed supramolecular assemblies using pyridinium cations with dialkoxyphenyl structure *via* an ether linker as an efficient gene delivery and was able to transfect neurons selectively among primary neuronal/glial cells cocultures (Figure 5.5).²⁹

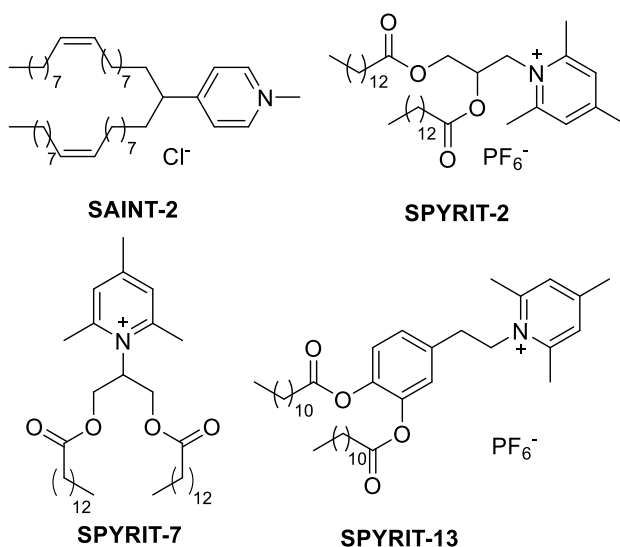


Figure 5.5 Synthetic pyridinium gene delivery systems

5.4 Biological studies on biomass derived pyridinium salts

The assessment of environmental impact of Ionic Liquids (ILs) has mainly centered on the evaluation of their toxicity,^{30,31} however it is known that a refractory organic substance, if released into the environment, would bioaccumulate and may eventually lead to chronic toxic effects.³² Earlier investigations have also indicated that structural features, such as alkyl chain length, that can decrease resistance to microbial attack may also increase the toxicity of the ILs.³³ As suitable structural design has helped integrate low toxicity with high biodegradability in some commercial products in the past (e.g. drilling fluids), we aimed to understand the toxicity behaviour of our newly synthesized compounds believing that appropriately designing the ILs may lead to the solvents with desired attributes that would not pose problems to the environment³³ rather could be a potential entity for biological activity. Thus a series of the synthesized pyridinium salts were subjected to biological testing comprising the evaluation of the compounds on different cell lines from tumoral and non-tumoral origin.

5.4.1 Testing compounds with neutral red assay

The assay used for testing our compounds is the neutral red uptake assay that provides a quantitative estimation of the number of viable cells in a culture. It is one of the most used cytotoxicity tests with many biomedical and environmental applications. Cells are seeded in 96-well tissue culture plates and are treated for the appropriate period with the test compounds, after approximately 24 hours. The plates are then washed and incubated for 3 h with a medium containing neutral red. The cells are subsequently

washed, the dye is extracted in each well and the absorbance is read using a spectrophotometer. The procedure is cheaper and more sensitive to determine between viable, damaged and dead cells than other cytotoxicity tests (tetrazolium salts, enzyme leakage or protein content). Once the cells have been treated, the assay can be completed successfully. The quantity of dye incorporated into cells is measured by spectrometry at 540 nm, and is directly proportional to the number of cells with an intact membrane. The assay can be used to evaluate cytotoxicity by determination of the IC₅₀ (50% inhibiting concentration).

5.4.2 Experimental procedure

The neutral red method of monitoring *in vitro* cytotoxicity is well suited for use with multiwell plates. Each test also included a blank containing complete medium without cells.

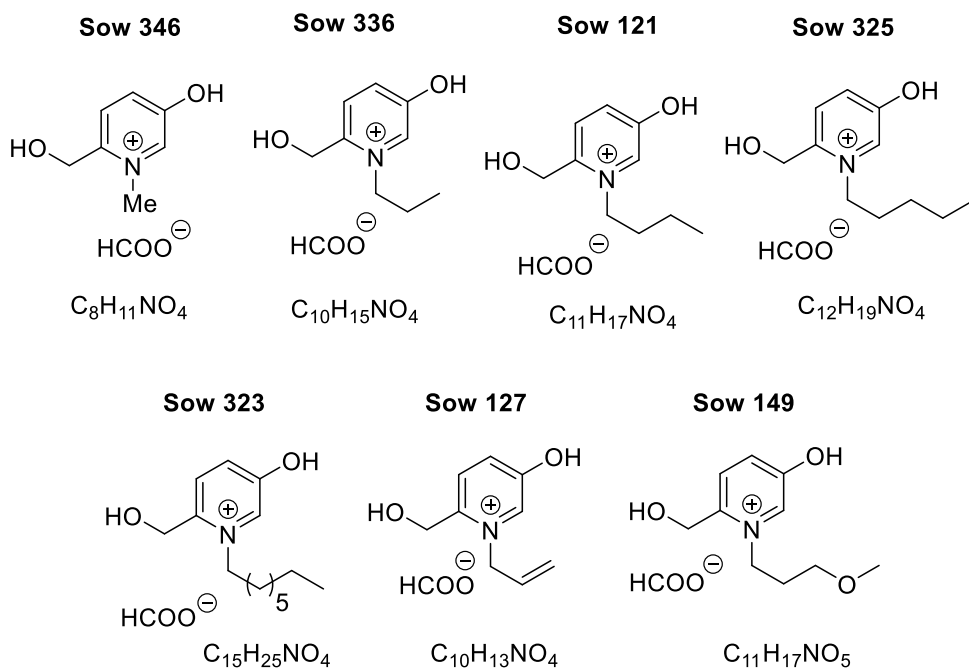
1. Remove cultures from incubator into laminar flow chamber hood.
2. Added 0.33% Neutral Red Solution [N-2889] in an amount equal to 10% of the culture medium volume and placed the cultures to the incubator for 2-4 hrs.
3. At the end of the incubation period, the medium is carefully removed and the cells quickly rinsed with Hank's Buffer Salt Solution HBSS and incubated with 0.5% FBS cell culture medium containing 50 µg/ml neutral red for 2-3 hrs.
4. Cells were washed again with HBSS and the amount of neutral red retained by the cells were extracted with organic solvent (20 ml distilled water, 20 ml ethanol and 400 µl glacial acetic acid)

5. Absorbance of the samples were measured at 540nm in a plate reader after gentle shake by Spectrophotometer.

Viability was determined by the ratio of absorbance of treated and untreated cells (control). Triplicates were done for each tested experimental condition and presented results are the average \pm standard deviation

5.4.3 Results and discussion

Viability tests were performed with the compounds shown in Figure 5.6 representing the sample names, structures and molecular formula.



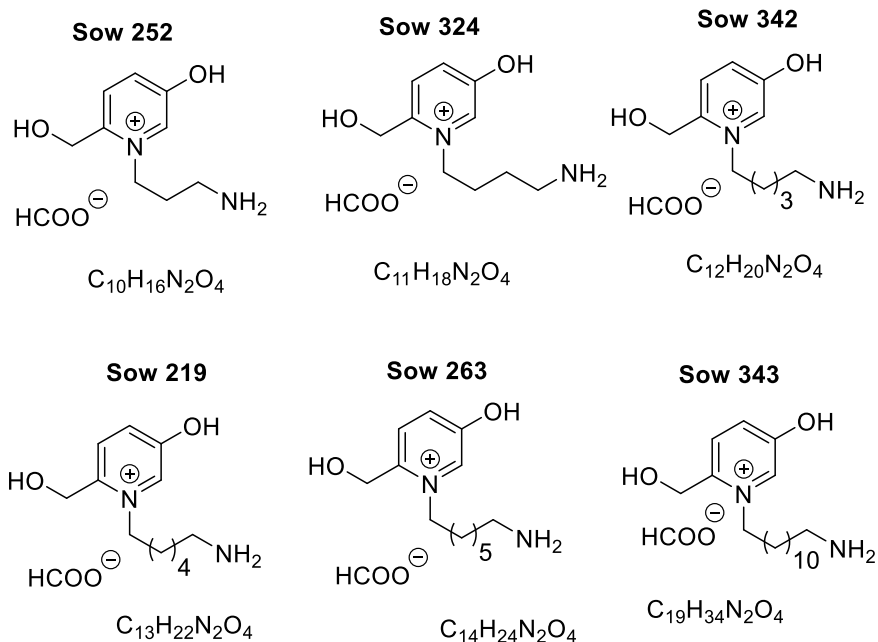


Figure 5.6 Test compounds for viability assays

CHOK1 cells were seeded at a density of 5×10^4 cells/well and incubated the following day with the several compounds at a concentration of 20 micromolar. Compounds were in contact with the cells for 48 hours before assessment of the viability with neutral red. Viability of CHOK1 cells upon exposure to the compounds for 48 hours was determined and the results are shown in Figure 5.7

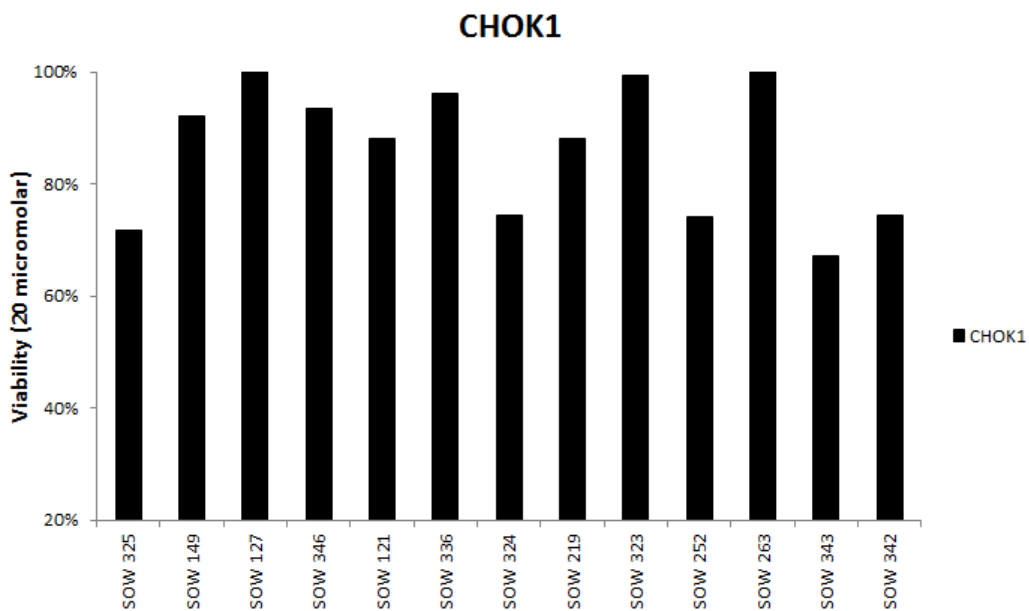


Figure 5.7 Viability of CHOK1 cells upon exposure to the compounds for 48 hours.

None of the compounds reduced significantly the viability of this cell line since determined viability is above 60% in all tested experimental conditions. Therefore, all the compounds were carried out to a second screening step where a tumoral cell line was used as model. Figure 5.8 shows the viability study of the synthesized compounds to lung cancer cell line NCI-H460.

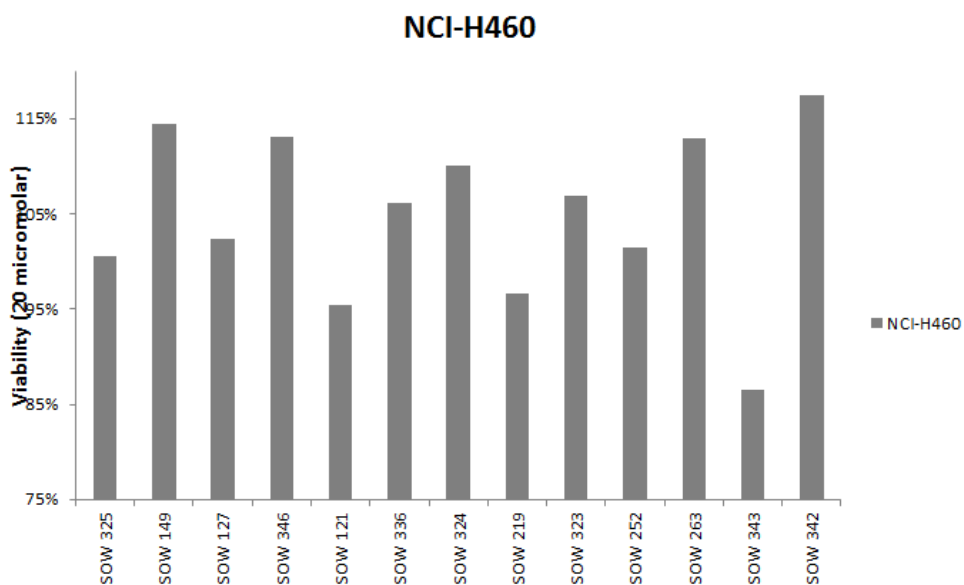


Figure 5.8 Viability of NCI-H460 cells upon exposure to the compounds for 48 hours.

Figure 5.9 corresponds to the viability study of the synthesized compounds to colon cancer cell line HT 29 and is shown below.

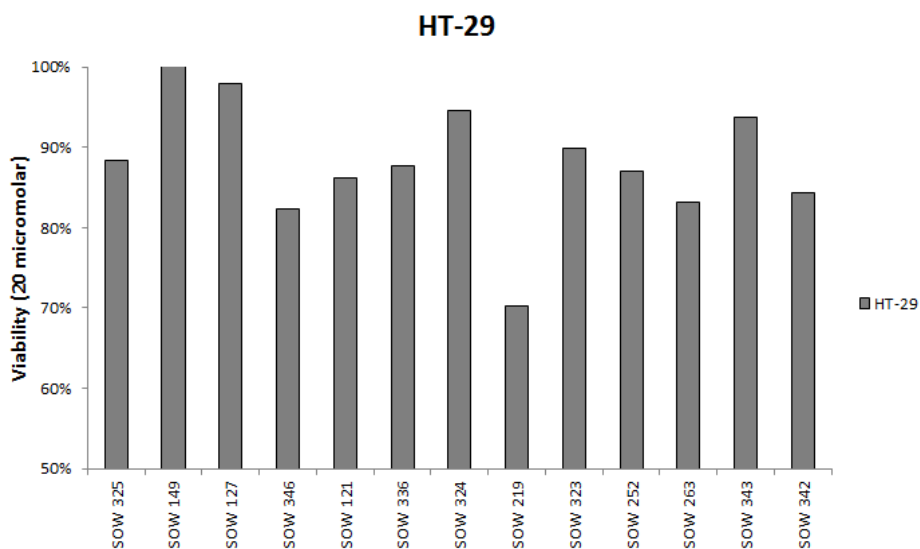


Figure 5.9 Viability of HT-29 cells upon exposure to the compounds for 48 hours.

Figure 5.10 corresponds to the viability study of the synthesized compounds to breast cancer cell line MCF-7.

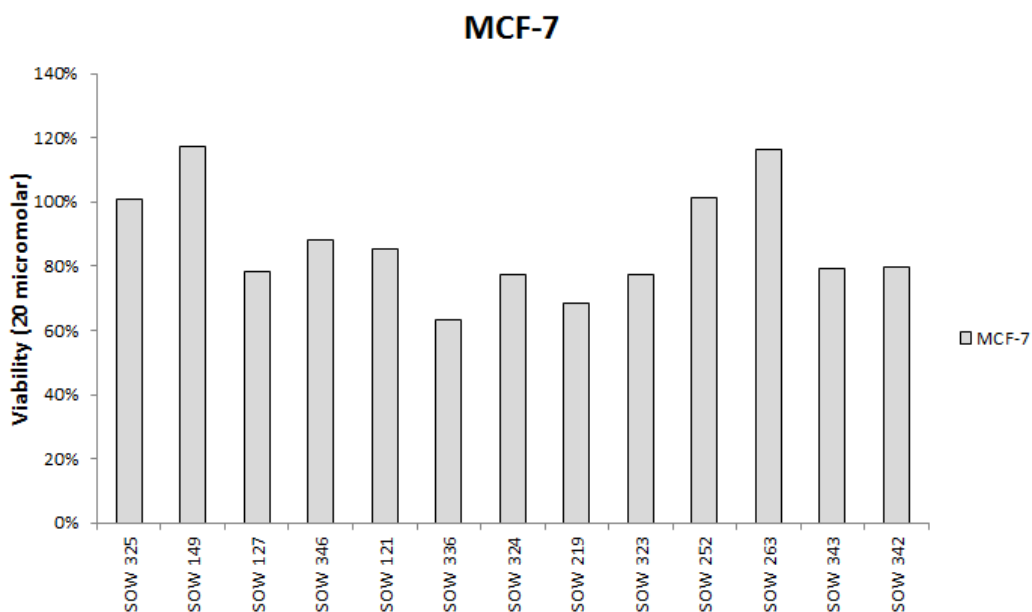


Figure 5.10 Viability of MCF-7 cells upon exposure to the compounds for 48 hours.

As illustrated in Figures 5.8-5.10, none of the studied experimental conditions shows a significant decrease of the tumoral cells viability up to a 20 micromolar concentration. This concentration was used as the maximum concentration because bearing in mind that an interesting IC₅₀ (concentration needed to decrease viability in 50%) must be in the nanomolar range, the used concentration is still considerably high. The tested compounds did not possess anticancer activities which might be due

to the fact that they are not sufficient lipophilic to cross biological membranes.

5.5 Conclusion

Further studies to reveal the promising reactivity with enhanced substrate stability, and test on other biological activity of the compounds are in progress. Enormous challenges on this biomass derived pyridinium substrates are still in its infancy and the constant study on these substrate will provide a sustainable approach for the synthesis of pyridinium substrate from HMF which in turn evolve potential synthesis of several heterocyclic compounds and natural products amplifying their advances in medicinal and biological applications of these unique substrates in modern sustainable research.

5.6 References

1. Lyle, R. E. *In Pyridine and its Derivatives*. Wiley: New York, NY, **1974**, *1*, 137.
2. Goldman, S.; Stoltefuss, J. *Angew. Chem., Int. Ed.* **1991**, *30*, 1559. (b) Sunkel, C. E.; FaudeCasa, J, M.; Santos, L.; Gomes, M. M.; Villarroya, M.; Gonzalez, M.M. A.; Priego, J. G.; Ortega, M. P. *J. Med. Chem.* **1990**, *33*, 3205. (c) Jaing, J. L.; Li, A. H.; Jang, S. Y.; Chang, L.; Melman, N.; Moro, S.; Ji, X.; Lobkovsky, E.; Clardy, J.; Jacobson, K. *A. J. Med. Chem.* **1999**, *42*, 3055.
3. Lavilla, R. J. *J. Chem. Soc., Perkin Trans. I* **2002**, 1141.

4. Bull, J. A.; Mousseau, J. J.; Pelletier, G.; Charette, A. B. *Chem. Rev.* **2012**, *112*, 2642.
5. Tang, W.; Patel, N. D.; Wei, X.; Byrne, D.; Chitroda, A.; Narayanan, B.; Sienkiewicz, A.; Nummy, I. J.; Sarvestani, M.; Ma, S.; Grinberg, N.; Lee, H.; Kim, S.; Li, Z.; Spinelli, E.; Yang, B. S.; Yee, N.; Senanayake, C. H. *Org. Process Res. Dev.* **2013**, *17*, 382.
6. Chia, W. L.; Shiao, M. J. *Tetrahedron Lett.* **1991**, *32*, 2033.
7. Le Gall, E.; Gosmini, C.; Nede'lec, J. Y.; Pe'richon, J. *Tetrahedron* **2001**, *57*, 1923.
8. Beveridge, R. E.; Black, D. A.; Arndtsen, B. A. *Eur. J. Org. Chem.* **2010**, 3650.
9. Akiba, K. Y.; Nishihara, Y.; Wada, M. *Tetrahedron Lett.* **1983**, *24*, 5269.
10. Yamaguchi, R.; Moriyasu, M.; Kawanisi, M. *Tetrahedron Lett.* **1986**, *27*, 211.
11. Akiba, K.; Matsuoka, H.; Wada, M. *Tetrahedron Lett.* **1981**, *22*, 4093.
12. Comins, D. L.; Mantlo, N. B. *J. Org. Chem.* **1991**, *56*, 2506.
13. *Chemistry of Heterocyclic Compounds*, **2001**, *37*, 797.
14. Chang, M.; Huang, Y.; Liu, S.; Chen, Y.; Krska, S.W.; Davies, I. W.; Zhang, X. *Angew. Chem. Int. Ed.* **2014**, *53*, 12761.
15. Huang, W. X.; Wu, B.; Gao, X.; Chen, M. W.; Wang, B.; Zhou, Y. G. *Org. Lett.* **2015**, *17*, 1640.
16. Donohoe, T. J.; Johnson, D. J.; Mace, L.H.; Bamford, M. J.; Ichihara, O. *Org. Lett.* **2005**, *7*, 435
17. Michels, T. D.; Rhee, J. U.; Vanderwal, C. D. *Org. Lett.* **2008**, *10*, 4787.

18. Said, S.; Mahrous, H.; Kassem, A. *Infection* **1976**, *4*, 49.
19. (a) Nakamura, K.; Nakamura, K. *U.S. Pat 66*, **2003**, *04*, 531. (b) Gross, P.; Keller, W. *U.S. Pat 47*, **1998**, *19*, 930. (c) Bartuska, W.R.; Silverman, P. *U.S. Pat 41*, **1980**, *83*, 366.
20. Sreenivasan, P.; Gaffar, A. *J. Clin. Periodontol.* **2002**, *29*, 965.
21. Dasari, V. R. R. K.; Muthyala, M. K. K.; Nikku, M. Y.; Donthireddy, R. R. *Microbiol Res* **2012**, *167*, 346.
22. Ilangovan, A.; Venkatesan, P.; Sundararaman, M.; Kumar, R. R. *Med Chem Res* **2012**, *21*, 694.
23. P. Kapkova, V. Alptüzün, P. Frey, E. Erciyas, U. Holzgrabe, *Bioorg. Med. Chem.* **2006**, *14*, 472.
24. Nadri, H.; Hamedani, M. P.; Shekarchi, M.; Abdollahi, M.; Sheibani, V.; Amanlou, M.; Shafiee, A.; Foroumadi, A. *Bioorganic & Medicinal Chemistry* **2010**, *18*, 6360.
25. Baharloo, F.; Moslemin, M. H.; Nadri, H.; Asadipour, A.; Mahdavi, M.; Emami, S.; Firoozpour, L.; Mohebat, R.; Shafiee, A.; Foroumadi, A. *Eur. J. Med. Chem.* **2015**, *93*, 196.
26. (a) van der Woude, I.; Visser, H. W.; Ter Beest, M. B. A.; Wagenaar, A. Ruiters, M. H. J.; Engberts, J. B. F. N.; Hoekstra, D. *Biochim. D. Biophys. Acta.* **1995**, *124*, 34; (b) Van der Woude, I.; Wagenaar, A.; Meekel, A. A. P.; Ter Beest, M. B. A.; Ruiters, M. H. J.; Engberts, N.; Hoekstra, D. *Proc. Natl. Acad. Sci. USA.* **1997**, *94*, 1160; (c) Meekel, A. A. P.; Wagenaar, A.; Bosgraaf, B.; Stuart, M. C. A.; Brisson, A.; Ruiters, M. H. J.; Engberts, J. B. F. N.; Hoekstra, D. *Eur. J. Org. Chem.* **2000**, 665.

27. Ilies, M. A.; Johnson, B. H.; Makori, F.; Miller, A.; Seitz, W. A.; Thompson, E. B.; Balaban, A. *Arch. Biochem. Biophys.* **2005**, *435*, 217.
28. VanderWoude, I.; Wagenaar, A.; Meekel, A. A. P.; Ter Beest, M. B. A.; Ruiters, M. H. J.; Engberts Jan, B. F. N.; Hoekstra, D. *Proc. Natl. Acad. Sci. USA* **1997**, *94*, 1160.
29. Savarala, S.; Brailoiu, E.; Wunder, S. L.; Ilies, M. A. *Biomacromolecules* **2013**, *14*, 2750
30. Ranke, J.; Stolte, S.; Stoermann, R.; Arning J.; Jastorff, B. *Chem. Rev.*, **2007**, *107*, 2183.
31. (a) Matsumoto, M.; Mochiduki, K.; Kondo, K. *J. Biosci. Bioeng.*, **2004**, *98*, 344; (b) Pretti, C.; Chiappe, C.; Pieraccini, D.; Gregori, M.; Abramo, F.; Monni G.; Intorre, L. *Green Chem.*, **2006**, *8*, 238; (c) Stolte, S.; Matzke, M.; Arning, J.; Boeschen, A.; Pitner, W. R.; Welz-Biermann, U.; Jastorff, B.; Ranke, J. *Green Chem.*, **2007**, *9*, 1170.
32. Boethling, R. S.; Sommer E.; DiFiore, D. *Chem. Rev.*, **2007**, *107*, 2207.
33. (a) Docherty, K. M.; Kulpa, C. *Abstracts of Papers, 231st ACS National Meeting*, Atlanta, GA, United States, **2006**, IEC-174; (b) Ranke, J.; Moelter, K.; Stock, F.; Bottin-Weber, U.; Poczobutt, J.; Hoffmann, J.; Filser, J.; Jastorff, B. *Ecotoxicol. Environ. Safe.* **2004**, *58*, 396.

CHAPTER VI

*Concluding remarks & Future
perspectives*

6. Concluding remarks & Future perspectives

6.1 Concluding remarks

Revealing from its extensive investigations since discovery, **Pyridinium salts (1)**, the subject of this thesis, preserves itself some of its physical, chemical and biological properties (represented in chapter I). The synthesis of new halogenated imidazolium and pyridinium ionic liquids in chapter II opened fascinating possibilities concerning the study of the properties of ILs.

On the other hand, the increasing attention in biorenewable resources as an alternative feedstock for the production of fuels and bulk chemicals, motivated us to present **HMF (2)**, a useful building block for the synthesis of biofuel dimethylfuran and other important commodities. The present study in chapter III, evidences the simple, efficient and cost-effective method of obtaining value added products such as 5-hydroxymethylfuranic acid (HMFA), and 2,5-dihydroxymethyl furan (DHMF) through Cannizzaro reaction of HMF in high yields.

Further, combining the uniqueness of these broad research themes **(1)** and **(2)**, we developed an optimized reaction condition demonstrating successfully the organo-catalyzed one-step synthesis of functionalized *N*-alkylpyridinium salts from HMF as explained in Chapter IV. We also took up further challenges on exploring the reactivity of derived pyridinium salts and turned out with interesting preliminary results to transform them into piperidine cores that are highly privileged structural motif in many natural products and pharmaceutical drugs. Our approach discussed in chapter V,

for the synthesis of piperidines under Pd/C reactions proves to be a good initiative but the work is still in infancy and great results can be achieved from this juncture. Further studies on screening for best catalytic conditions, improving yield and product isolation to have this valuable piperidine core from HMF platform chemical will be continued. For this purpose, it is also important to enhance the stability of these pyridinium salts with possible functionalization. Undoubtedly, succeeding from these pyridinium salts to ionic liquids for specific applications would also be desirable.

Thus, our step-by-step investigation on the synthesis of pyridinium salts from biomass HMF is successful and will endure certainly as a breakthrough approach in near future for the construction of organic cores such as dienals *via* ring opening, dihydropyridines or piperidines *via* partial reduction or complete reduction which are discussed below highlighting the perspectives in this area.

6.2 Future perspectives

6.2.1 Synthetic manipulations

The versatility of pyridinium salts and their high synthetic value in the construction of various structural cores has been always interesting among organic chemists. Some of the highly valuable approaches which would make this biomass derived pyridinium salts a promising component for the development of sustainable chemicals are discussed below in Figure 6.1.

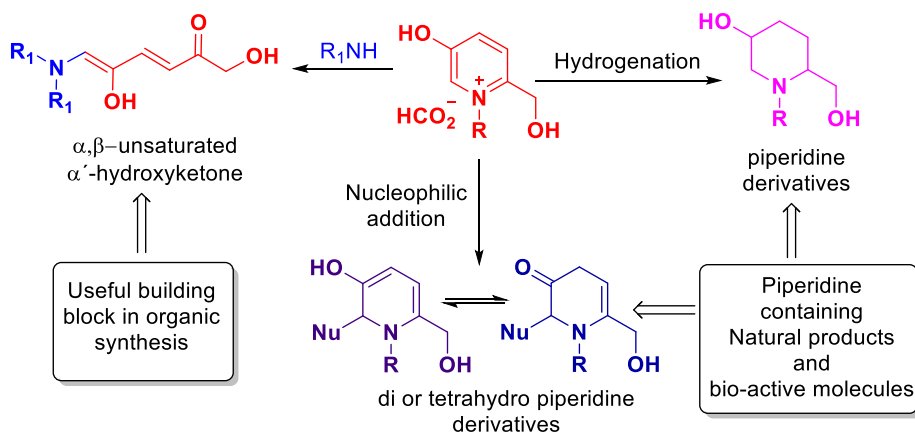
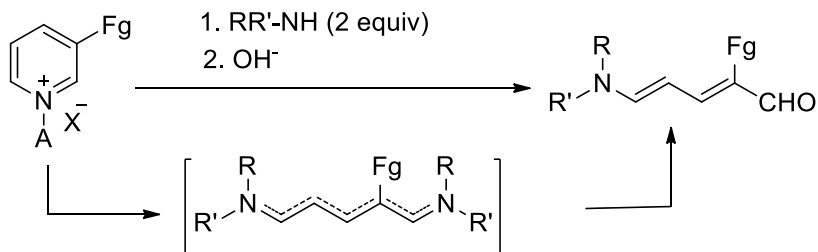


Figure 6.1 Scope of new biomass derived pyridinium salts

In continuation with this, we herein discuss the possibility of these approaches with prevailing literatures that demonstrates its effectiveness in organic and medicinal chemistry.

6.2.2 Zincke aldehyde

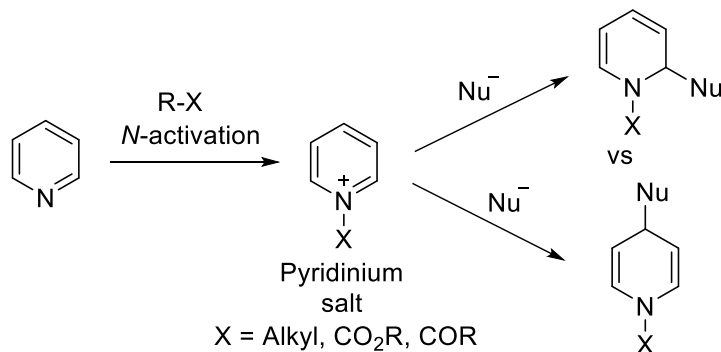
In its most fundamental form, reacting a pyridinium salt with secondary amine will result in the corresponding 5-aminopenta-2,4-dienal upon basic hydrolysis (Scheme 6.1). The compounds formed in this manner are commonly referred to as Zincke aldehydes. The secondary amine does not need to be symmetric and can incorporate a number of functional patterns. Nevertheless, it is found that pyridinium salts functionalized in the 3-position preferentially give rise to the corresponding 2-substituted Zincke aldehydes.¹



Scheme 6.1 Ring opening of 3-substituted pyridinium salts

6.2.3 Reactivity of *N*-alkyl pyridinium salts

In principle, pyridinium salts are highly reactive species in comparison with pyridine heterocycles. It undergoes various nucleophilic addition reactions with variety of nucleophiles for the preparation of functionalized dihydro, tetrahydropyridines, as well as piperidines. All these heterocycles are important intermediates for the synthesis of piperidine containing biologically active molecules and alkaloids.



Scheme 6.2 Functionalization of *N*-activated pyridinium salts

Pyridinium salt contains reactive electrophilic sites at the 2 and 4 positions of the ring. Thus, mixtures of substituted 1,2- and 1,4-dihydropyridines are obtained when nucleophile attacks (Scheme 6.2).

The addition of organometallic reagents to pyridinium salts is mostly used to study the regioselectivity of nucleophilic addition and the HSAB (Hard-Soft-Acid-Base) model has been used to rationalize the regioselectivity. The nature of nucleophile, and reaction conditions can afford selective 1,2- or 1,4-additions (Figure 6.2). In general, harder nucleophiles such as Grignard reagents add at the 2-position whereas softer organometallic reagents, such as organocuprates, generally add to the 4-position. In all cases, the combination of the nucleophile and the acylating agent are important in determining regio- and stereoselectivity. The nature and position of substituents on pyridine ring also determine the position of incoming nucleophile.

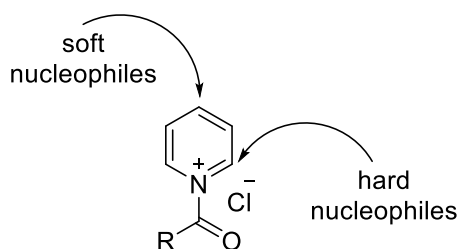


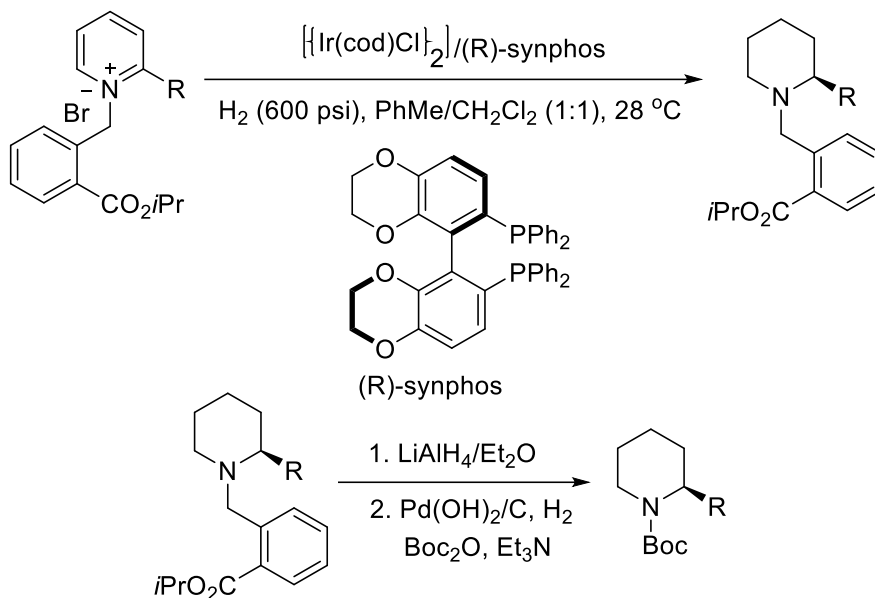
Figure 6.2 Electrophilic sites of pyridinium salt

However, several of these studies were performed with *N*-acyl pyridinium salts and substituted pyridine derivatives. The addition of Grignard reagents to unsubstituted pyridinium salts studied with a variety of activating agents.

6.2.4 Piperidine derivatives by reduction reactions

Zhou *et al.* have successfully developed a highly efficient iridium-catalyzed hydrogenation of 2-substituted pyridinium salts, to provide chiral piperidines with high enantioselectivity (Scheme 6.3).⁵ The key feature of this strategy was the activation of simple pyridines as the pyridinium bromide, thus efficiently avoiding inhibition of the catalyst by the substrate

and improving the reactivity of the substrate. Moreover, the stoichiometric hydrogen bromide generated *in situ* is believed to effectively inhibit coordination ability of the desired product.



Scheme 6.3 Ir-catalyzed asymmetric hydrogenation of pyridinium salts

Few examples of this type of reduction reactions to piperidine derivatives are already explained in chapter V, Scheme 5.5- Scheme 5.8. The scope of these pyridinium salts from biomass HMF is not only on the synthetic point but also evidence itself from applications learned through literature ranging from dyes, surfactants, sensors, electrolytes and biological excellence as antimicrobials, acetylcholinesterase inhibitors, their permeability in biological membranes, gene delivery etc. The applicability of pyridinium salts with surfactant property is employed in various industrial processes such as textile softeners, flotation chemicals, dye removal processes, antistatic agents, petroleum additives and much more. It will be of great use

to perform the physicochemical studies on these pyridinium salts to know the parameters such as viscosity, density, diffusion coefficient, miscelle concentration etc. for selective applications possible.

6.3 References

1. Michels, T. D.; Rhee, J. U.; Vanderwal, C. D. *Org. Lett.* **2008**, *10*, 4787.
2. Vanderwal, C. D.; Vosburg, D. A.; Weiler, S.; Sorensen, E. J. *J. Am. Chem. Soc.* **2003**, *125*, 5393.
3. Bian, Z.; Marvin, C.C.; Martin, S. F. *J. Am. Chem. Soc.*, **2013**, *135*, 10886.
4. Tsukanov, S. V.; Comins, D. L. *J. Org. Chem.* **2014**, *79*, 9074.
5. Ye, Z. S.; Chen, M.W.; Chen, Q.; Shi, L.; Duan, Y.; Zhou, Y. G. *Angew. Chem. Int. Ed.* **2012**, *51*, 10181.

Appendix I

List of Abbreviations

Ac	:	Acetyl
AcOH	:	Acetic acid
Ac ₂ O	:	Acetic anhydride
AChE	:	anti-cholinesterase
Bn	:	Benzyl
BF ₃ .OEt ₂	:	Boron trifluoride diethyl etherate
BF ₄	:	Boron tetrafluoride
[Bupy][BF ₄]	:	<i>n</i> -butylpyridinium tetrafluoroborate
[BuPy]Cl	:	<i>N</i> -butylpyridinium chloride
[BuPy]FeCl ₄	:	<i>N</i> -butylpyridiniumiron(IV) chloride
[BuPy][NO ₃]	:	<i>N</i> -butylpyridinium nitrate
[C ₃ CNpy] ⁺	:	butyronitrile pyridinium cation
CH ₂ Cl ₂	:	Dichloromethane
Cu	:	Copper
Cu(OAc) ₂	:	Copper(II) acetate
CPC	:	cetylpyridinium chloride
DABCO	:	1,4-Diazabicyclo[2.2.2]octane
DCM	:	Dichloromethane
DIAD	:	Diisopropyl azodicarboxylate
2,4-DTBP	:	2,4-di- <i>tert</i> -butylphenol
DMAP	:	<i>N,N</i> -Dimethylaminopyridine
DMF	:	<i>N,N</i> -Dimethylformamide
DMSO	:	Dimethyl sulphoxide
DNA	:	Deoxyribonucleic acid
Et	:	Ethyl

Appendix I

List of Abbreviations

[EPy][BF ₄]	:	<i>N</i> -ethylpyridinium tetrafluoroborate
Equiv	:	equivalent
H-bond	:	Hydrogen bond
HBr	:	Hydrogen bromide
HMF	:	5-Hydroxymethylfurfural
h	:	hour(s)
IL	:	Ionic liquid
NaH	:	Sodium hydride
NaOH	:	Sodium hydroxide
PMB	:	<i>p</i> -Methoxy benzyl
Pd	:	Palladium
PF ₆	:	hexafluorophosphate
Ph	:	Phenyl
PPh ₃	:	Triphenylphosphine
PyILs	:	Pyridinium ionic liquids
Rh(III)	:	Rhodium(III)
RTILs	:	Room temperature ionic liquids
S _N 2	:	bimolecular nucleophilic substitution
TBDMS	:	<i>tert</i> -butyl dimethyl silyl
TBDPS-Cl	:	<i>tert</i> -butyl diphenyl silyl
TBP	:	<i>tert</i> -butylphenol
TBS	:	<i>tert</i> -butyl dimethyl silyl
TEA	:	Triethyl amine
TFA	:	Trifluoroacetic acid
Tf ₂ N	:	bis(trifluoromethylsulfonyl)imide
THF	:	Tetrahydrofuran
THP	:	Tetrahydropyranyl
TESOTf	:	Triethylsilyl trifluoromethanesulfonate
TMSOTf	:	Trimethylsilyl trifluoromethanesulfonate

Appendix I

Appendix II

List of Publications

Thesis Publications

1. Sowmiah Subbiah, Carlos A. M. Afonso, José M. S. S. Esperança and Luís Paulo N. Rebelo, Pyridinium Salts: From synthesis to reactivity and applications. *Chem. Soc. Rev. Manuscript to be submitted*, **2016**.
2. Sowmiah S, Luis M. Veiros, Carlos A. M. Afonso, José M. S. S. Esperança and Luís Paulo N. Rebelo, Organocatalyzed one-step synthesis of functionalized *N*-alkyl-pyridinium salts from biomass derived 5-hydroxymethylfurfural. *Organic Letters*, **2015**, *17*, 5244-5247.
3. Sowmiah Subbiah, Svilen P. Simeonov, José M. S. S. Esperança, Luís Paulo N. Rebelo and Carlos A. M. Afonso Direct transformation of 5-hydroxymethylfurfural to the building blocks 2,5-dihydroxymethylfurfural (DHMF) and 5-hydroxymethyl furanoic acid(HMFA) *via* Cannizzaro reaction. *Green Chem.*, **2013**, *15*, 2849-2853.

Other Publications

4. Ranu, B. C; Jana. R; Sowmiah. S. An improved procedure for the three-component synthesis of highly substituted pyridines using ionic liquid *J. Org. Chem.* **2007**, *72*, 3152.

Appendix II

5. Sowmiah. S; Srinivasadesikan. V; Ming-Chung Tseng and Yen-Ho Chu. On the chemical stability of ionic liquid. *Molecules* **2009**, *14*, 3780.
6. Sowmiah S, Cathy I. Cheng and Yen-Ho Chu. Ionic liquids for green organic synthesis. *Current Organic Synthesis*, **2012**, *9*, 74-95.

ANNEXURE

Supporting Details

Chapter II

Supporting Information

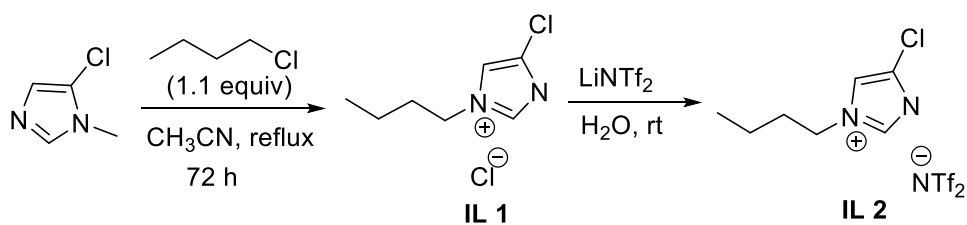
Studies on halogenated imidazolium and pyridinium ILs

2.1 General Information

All reagents were purchased from Sigma-Aldrich, Alfa Aesar and Merck and were used without further purification. The compounds were characterized by NMR in a Bruker Avance II 400 Ultrashield Plus; NMR bruker 300

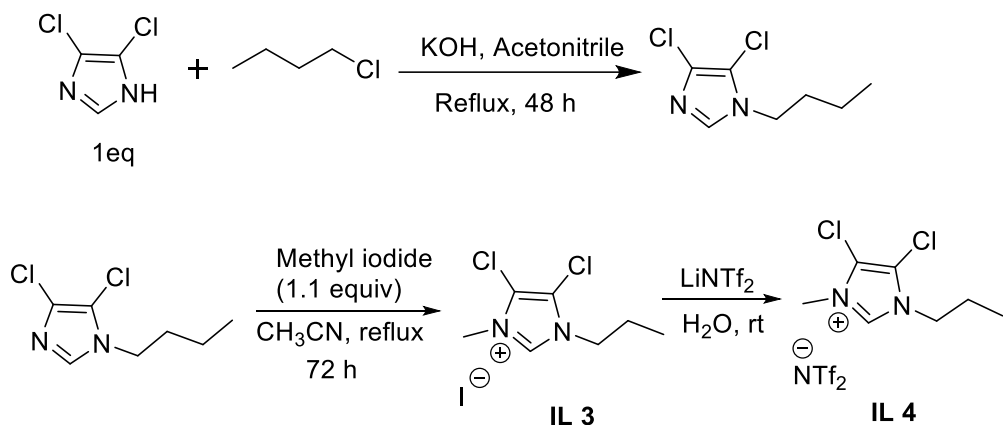
2.2 Experimental Procedure

2.2.1 Synthesis of 5-chloro imidazolium ionic liquids



5-chloro-methyl imidazole (100mg, 0.86 mmol) was dissolved in acetonitrile and added 1.1 equivalent of butyl chloride (1.1 equiv, 0.95 mmol) in a closed vessel and then refluxed for 3 days. The reaction was monitored by TLC. After the completion of reaction, the solvent was completely evaporated and the reaction mixture is washed with diethyl ether (2x10 mL) afforded the 3-butyl-5-chloro-1-methyl imidazolium chloride (**IL 1**) in 95 % yield. To the obtained ionic liquid **IL 1**, 1.5 equiv of lithium bistriflimide, LiNTf₂ is added with water as solvent medium and the reaction is allowed to stir at room temperature for 24h. To the reaction mixture, dichloromethane was added and the organic layer was separated from the aqueous phase. On evaporating the solvent and dried under vacuum afforded 3-butyl-5-chloro-1-methyl imidazolium bistriflimide (**IL2**) in 98% yield. The purity of the ionic liquids were enhanced by filtration through celite using methanol solvent to give 95% pure ILs and analysed using NMR.

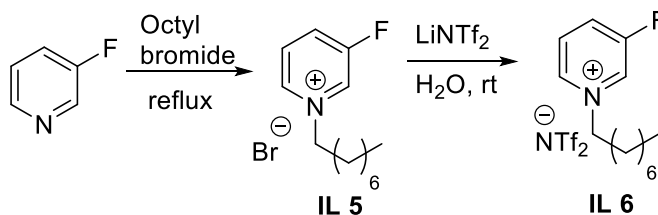
2.1.2 Synthesis of 4,5-dichloro imidazolium ionic liquids



4,5-dichloro imidazole (100mg, 0.75 mmol) was dissolved in acetonitrile and added powdered KOH (1.1 equiv, 0.83 mmol) which was then allowed to stir for about 48 h. The reaction was monitored by TLC and the solvent was evaporated, dried in vacuum and characterized by NMR (Fig SI 2.7 - 2.9). To the obtained 3-butyl-4,5-dichloro imidazole in acetonitrile, was added methyl iodide (2 equiv, 1.1 mmol) in a closed vessel and then refluxed for 4h. On evaporating the solvent, the reaction mixture was washed with diethyl ether (2x10 mL) afforded 3-butyl-4,5-dichloro-1-methyl imidazolium chloride (**IL 3**) in 95 % yield. To the obtained ionic liquid **IL3**, 1.5 equiv of lithium bistriflimide, LiNTf₂ was added with water

as solvent medium and the reaction is allowed to stir at room temperature for 24h. To the reaction mixture, dichloromethane was added and the organic layer was separated from the aqueous phase. On evaporating the solvent and dried under vacuum afforded 3-butyl-4,5-dichloro-1-methyl imidazolium bistriflimide (**IL 4**) in 98% yield. The purity of the ionic liquids were enhanced by filtration through celite using methanol solvent to give above 95% pure ILs and analysed by NMR.

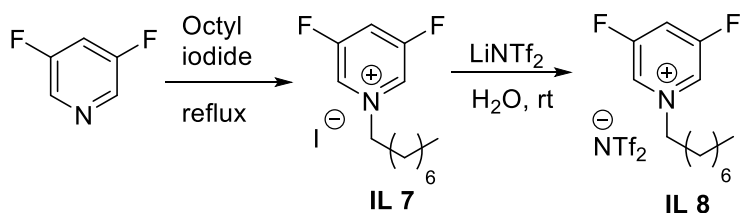
2.1.3 Synthesis of 3-fluoro pyridinium ionic liquids



With the fluoro-substituted pyridines (100mg, 0.1mmol) was corresponding octyl bromide(1.1 equiv, 0.11 mmol) and refluxed for about 24h. The completion of the reaction was monitored by TLC. On evaporating the solvent from the reaction mixture, it was then washed with diethyl ether (2x10 mL) to give 3-fluoro pyridinium bromide (**IL 5**) in 90% yield. To the obtained ionic liquid **IL 5**, 1.5 equiv of lithium bistriflimide, LiNTf₂ was

added with water as solvent medium and the reaction was allowed to stir at room temperature for 24 h. To the reaction mixture, added dichloromethane and the organic layer was separated from the aqueous phase. On evaporating the solvent and dried under vacuum afforded 3-fluoro pyridinium bistriflimide (**IL 6**) in 98% yield. The reaction was scaled upto 5g and the purity of the ionic liquids were enhanced through celite filtration using methanol solvent to give the ILs in 95% purity and were characterized by NMR.

2.1.3 Synthesis of 3,5-difluoro pyridinium ionic liquids

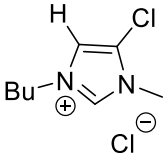


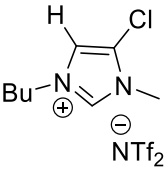
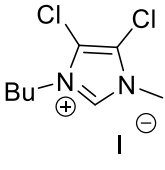
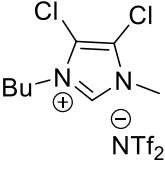
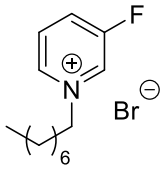
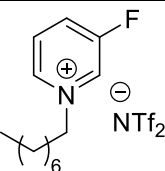
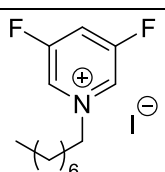
To the 3,5-difluoro pyridines (100mg, 0.1mmol) was added octyl iodide(1.1 equiv, 0.11 mmol) and refluxed for about 24h. The completion of the reaction was monitored by TLC. On evaporating the solvent from the reaction mixture, it was then washed with diethyl ether (2x10 mL) to give 3,5-difluoro pyridinium iodide (**IL 7**) in 90% yield. To the obtained ionic liquid **IL 7**, 1.5 equiv of lithium bistriflimide, LiNTf₂ was added with water

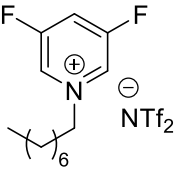
as solvent medium and the reaction was allowed to stir at room temperature for 24h. To the reaction mixture, added dichloromethane and the organic layer was separated from the aqueous phase. On evaporating the solvent and dried under vacuum afforded 3,5-difluoro pyridinium bistriflimide (**IL 8**) in 98% yield. The reaction was scaled upto 5g and the purity of the ionic liquids were enhanced through celite filtration using methanol solvent to give the ILs in 95% purity and were characterized by NMR.

As mentioned, for the comparative study of viscosity measurements of halo-substituted ILs in respect with the simple ILs, the reactions were efficiently scaled up to obtain 5 g of the required IL in high yield and purity.

Table SI 1.1 Synthesis of imidazolium and pyridinium ionic liquids (**IL1-IL8**)

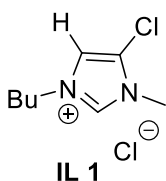
S. No	Compound	Structure	Yield (%)	Purity (%)	Fig SI ref
1.	IL 1		95	95	Fig SI 2.1 - 2.3

2.	IL 2		97	97	Fig SI 2.4 - 2.6
3.	IL 3		98	99	Fig SI 2.10 - 2.12
4.	IL 4		95	98	Fig SI 2.13 - 2.15
5.	IL 5		88	98	Fig SI 2.16 - 2.18
6.	IL 6		93	97	Fig SI 2.19 - 2.21
7.	IL 7		90	96	Fig SI 2.22 - 2.24

8.	IL 8		96	98	Fig SI 2.25 - 2.27
----	------	---	----	----	--------------------

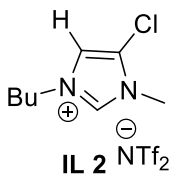
2.3 NMR spectral data of synthesized compounds

3-butyl-5-chloro-1-methyl-1H-imidazolium chloride (IL 1)



^1H NMR (400 MHz, CDCl_3) δ 10.62 (d, $J = 5.8$ Hz, 1H), 7.81-7.59 (m, 1H), 4.31 (t, $J = 6.8$ Hz, 2H), 3.94 (s, 3H), 1.95-1.68 (m, 2H), 1.30 (dd, $J = 13.0, 6.8$ Hz, 2H), 0.97-0.76 (m, 3H); ^{13}C NMR (101 MHz, CDCl_3) δ 137.9, 122.2, 118.8, 50.5, 33.9, 31.7, 19.2, 13.3; ^{13}C NMR (101 MHz, CDCl_3) δ 137.9, 118.9, 118.8, 50.5, 33.9, 31.8, 19.2, 13.3.

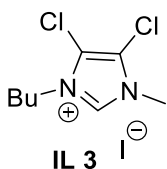
3-butyl-5-chloro-1-methyl-1H-imidazolium bis((trifluoromethyl)sulfonyl)amide (IL 2)



^1H NMR (300 MHz, CDCl_3) δ 8.70 (d, $J = 1.4$ Hz, 1H), 7.41 (d, $J = 1.9$ Hz, 1H), 4.13 (t, $J = 7.5$ Hz, 2H), 3.81 (s, 3H), 1.92-1.66 (m, 2H), 1.33 (m, 2H), 0.92 (t, $J = 7.3$ Hz, 3H); ^{13}C NMR (75 MHz, CDCl_3) δ 135.7, 123.0, 121.7, 119.2, 117.5, 50.6, 33.7, 31.4, 19.0, 12.9; ^{13}C

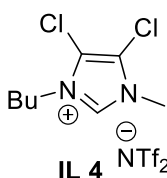
DEPT (75 MHz, CDCl₃) δ 135.7, 119.2, 50.6, 33.7, 31.4, 19.0, 12.9.

3-butyl-4,5-dichloro-1-methyl-1H-imidazolium iodide (IL 3)



¹H NMR (400 MHz, CDCl₃) δ 10.47 (s, 1H), 4.35 – 4.21 (m, 2H), 4.01 (s, 3H), 1.97 – 1.84 (m, 2H), 1.48 – 1.33 (m, 2H), 0.92 (t, J = 7.4 Hz, 3H); ¹³C NMR (101 MHz, CDCl₃) δ 136.4, 119.6, 118.6, 48.8, 35.7, 30.6, 19.2, 13.1; ¹³C NMR (101 MHz, CDCl₃) δ 136.4, 48.8, 35.7, 30.6, 19.2, 13.1.

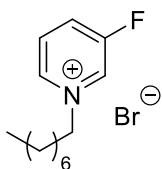
3-butyl-4,5-dichloro-1-methyl-1H-imidazolium bis((trifluoromethyl)sulfonyl)amide (IL 4)



¹H NMR (400 MHz, CDCl₃) δ 9.00 (s, 1H), 4.29 – 4.14 (m, 2H), 3.93 (s, 3H), 1.94 – 1.80 (m, 2H), 1.43 (m, 2H), 1.00 (t, J = 7.4 Hz, 3H); ¹³C NMR (101 MHz, CDCl₃) δ 135.7, 121.2, 120.3, 119.4, 118.1, 49.2, 35.2, 31.0, 19.3, 13.2; ¹³C DEPT (101 MHz, CDCl₃) δ 135.7, 49.2, 35.2, 31.0, 19.3, 13.2.

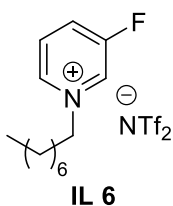
3-fluoro-1-octylpyridinium bromide (IL 5)

¹H NMR (400 MHz, CDCl₃) δ 9.80 (s, 1H), 9.41 (d, J = 5.9 Hz, 1H), 8.30 (m, 2H), 4.99 (t, J = 7.5 Hz, 2H), 1.96 (dd, J = 15.0, 7.6 Hz, 2H), 1.43-0.93 (m, 10H), 0.73 (t, J = 6.9 Hz, 3H); ¹³C NMR (101 MHz, CDCl₃) δ 161.1,



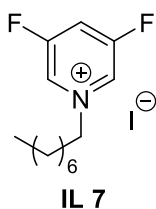
158.6, 142.2, 142.2, 134.9, 134.6, 132.9, 132.7, 129.9, 129.9, 62.2, 31.7, 31.4, 28.7, 28.7, 25.7, 22.3, 13.8; ^{13}C DEPT (101 MHz, CDCl_3) δ 142.2, 142.2, 134.9, 134.6, 132.9, 132.7, 129.9, 129.9, 62.2, 31.7, 31.4, 28.7, 28.6, 25.7, 22.3, 13.0.

3-fluoro-1-octylpyridinium bis((trifluoromethyl)sulfonyl)amide (IL 6)



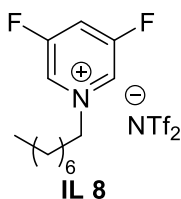
^1H NMR (400 MHz, CDCl_3) δ 8.84-8.69 (m, 2H), 8.33-8.22 (m, 1H), 8.12 (dt, $J = 8.9, 5.6$ Hz, 1H), 4.73-4.55 (m, 2H), 2.10-1.93 (m, 2H), 1.45-1.18 (m, 10H), 0.88 (t, $J = 6.8$ Hz, 3H); ^{13}C NMR (101 MHz, CDCl_3) δ 161.9, 159.3, 141.6, 133.2, 133.0, 130.1, 130.0, 121.3, 118.1, 63.3, 31.5, 31.4, 28.8, 28.7, 25.8, 22.5, 13.9. ^{13}C DEPT (101 MHz, CDCl_3) δ 141.6, 133.2, 133.0, 130.1, 130.0, 63.3, 31.5, 31.4, 28.8, 28.7, 25.8, 22.5, 13.9.

3,5-difluoro-1-octylpyridinium iodide (IL 7)



^1H NMR (400 MHz, CDCl_3) δ 9.61 (s, 2H), 8.21 (m, 1H), 5.11 (t, $J = 7.6$ Hz, 2H), 2.11 (t, $J = 7.6$ Hz, 2H), 1.51-1.16 (m, 10H), 0.86 (t, $J = 6.9$ Hz, 3H); ^{13}C NMR (101 MHz, CDCl_3) δ 161.6, 161.5, 159.0, 158.9, 132.7, 132.4, 122.0, 121.7, 121.6, 63.3, 31.6, 31.5, 28.9, 25.8, 22.5, 14.0; ^{13}C DEPT (101 MHz, CDCl_3) δ 132.7, 132.4, 122.0, 121.7, 121.6, 63.3, 31.6, 31.5, 28.9, 28.8, 25.8, 22.5, 14.0

3,5-difluoro-1-octylpyridinium bis((trifluoromethyl)sulfonyl)amide (IL 8)



^1H NMR (400 MHz, CDCl_3) δ 8.62 (s, 2H), 8.11-7.85 (m, 1H), 4.62-4.39 (m, 2H), 2.02-1.76 (m, 2H), 1.19 (m, 10H), 0.77 (dd, $J = 14.7, 8.3$ Hz, 3H); ^{13}C NMR (101 MHz, CDCl_3) δ 162.3, 162.2, 159.7, 159.6, 132.0, 131.6, 121.8, 121.2, 117.9, 64.1, 31.5, 31.1, 28.7, 28.6, 25.7, 22.4, 13.8; ^{13}C DEPT (101 MHz, CDCl_3) δ 132.0, 131.6, 121.9, 121.7, 121.6, 64.1, 31.5, 31.1, 28.7, 28.6, 25.7, 22.4, 13.8.

2.4 NMR spectral of synthesized compounds

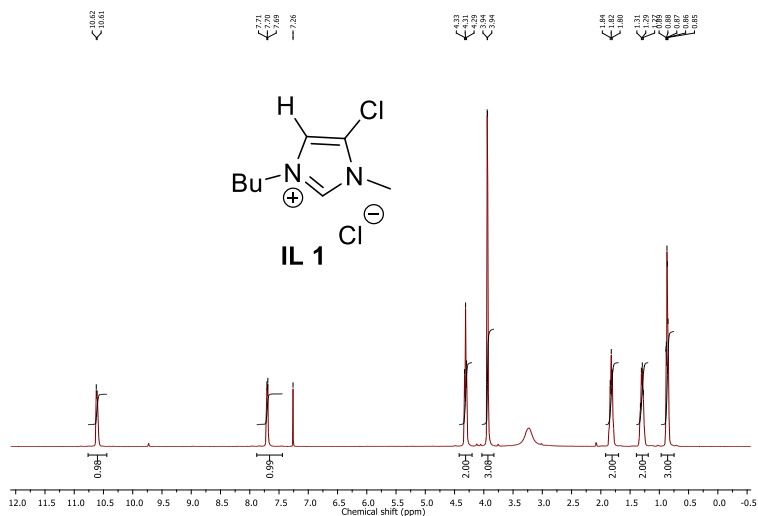


Fig SI 2.1: $^1\text{H NMR}$ of 3-butyl-5-chloro-1-methyl-1H-imidazolium chloride

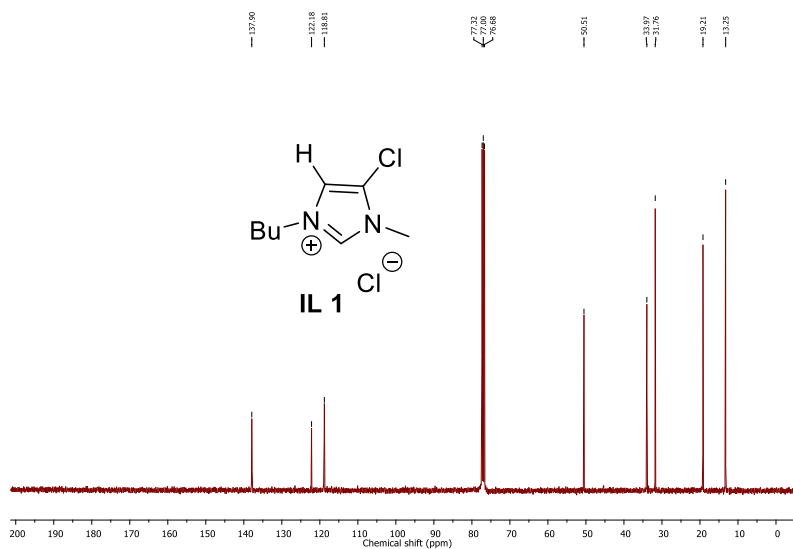


Fig SI 2.2: $^{13}\text{C NMR}$ of 3-butyl-5-chloro-1-methyl-1H-imidazolium chloride

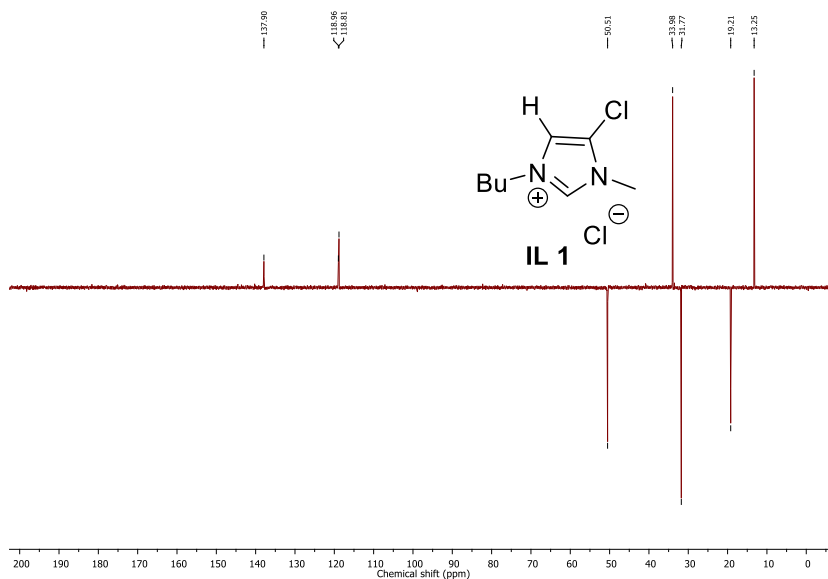


Fig SI 2.3: ^{13}C DEPT of 3-butyl-5-chloro-1-methyl-1H-imidazolium chloride

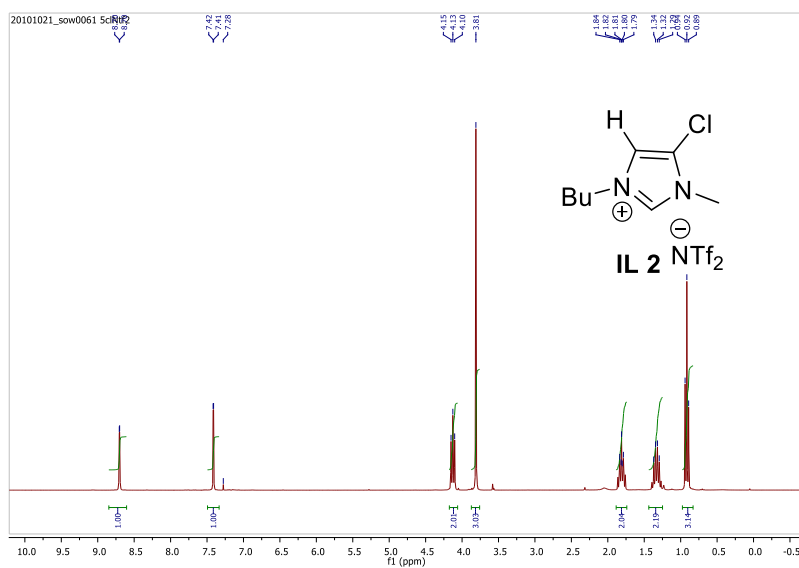


Fig SI 2.4: ^1H NMR of 3-butyl-5-chloro-1-methyl-1H-imidazolium bis((trifluoromethyl) sulfonyl)amide

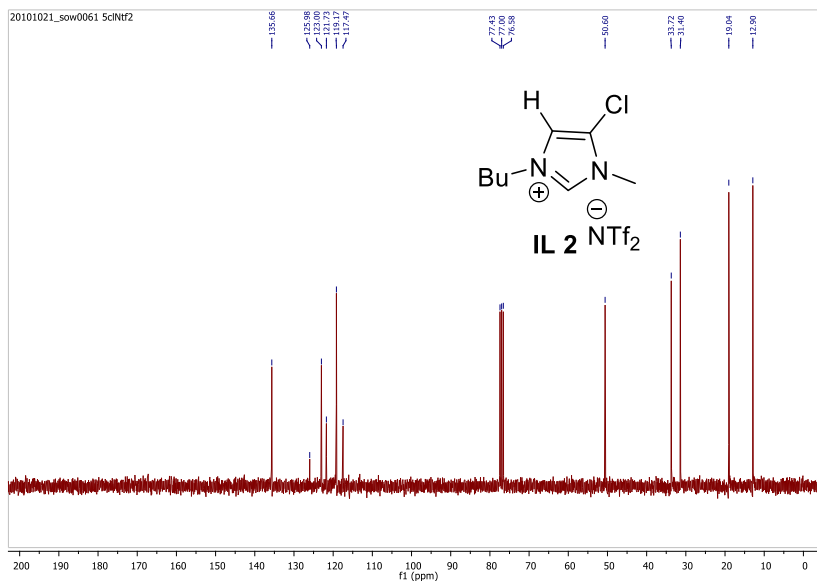


Fig SI 2.5: ^{13}C NMR of 3-butyl-5-chloro-1-methyl-1H-imidazolium bis((trifluoromethyl) sulfonyl)amide

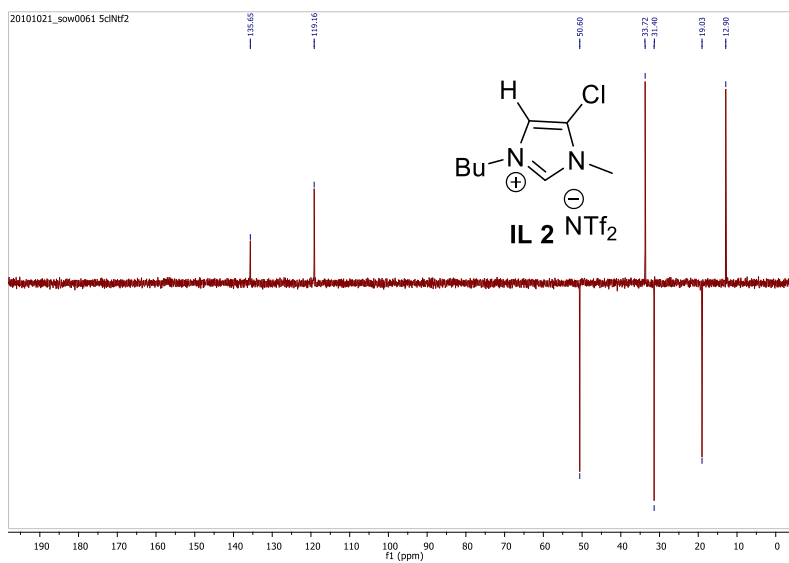


Fig SI 2.6: ^{13}C DEPT of 3-butyl-5-chloro-1-methyl-1H-imidazolium bis((trifluoromethyl) sulfonyl)amide

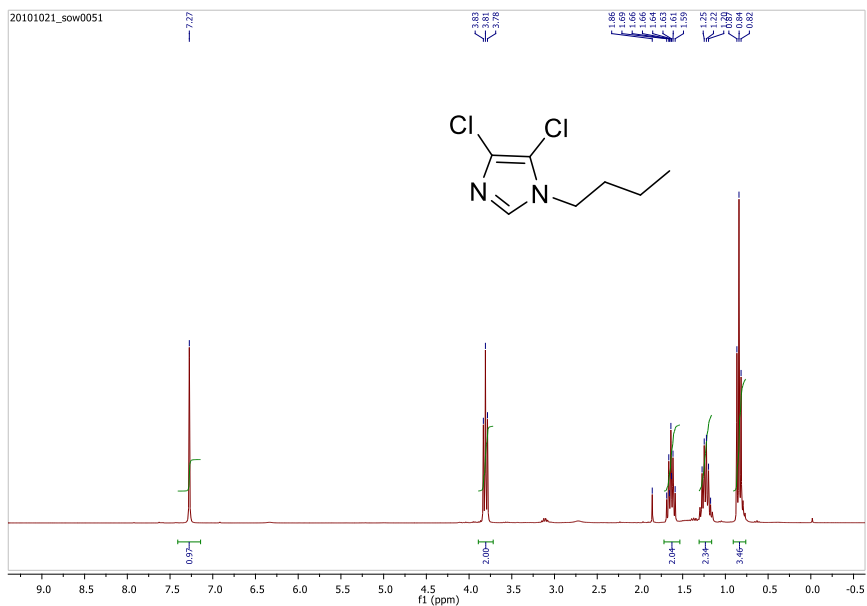


Fig SI 2.7: ^1H NMR of 1-butyl-4,5-dichloro-1H-imidazole

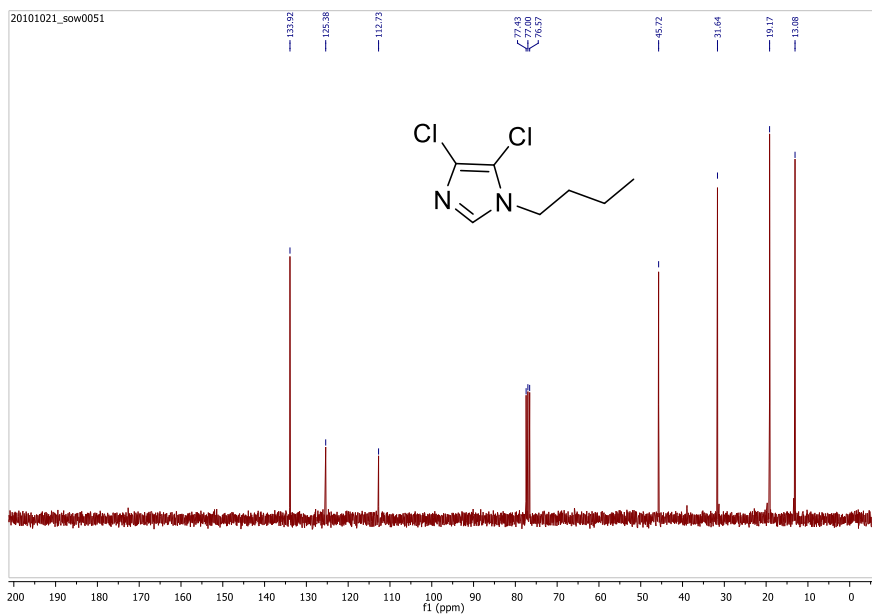


Fig SI 2.8: ^{13}C NMR of 1-butyl-4,5-dichloro-1H-imidazole

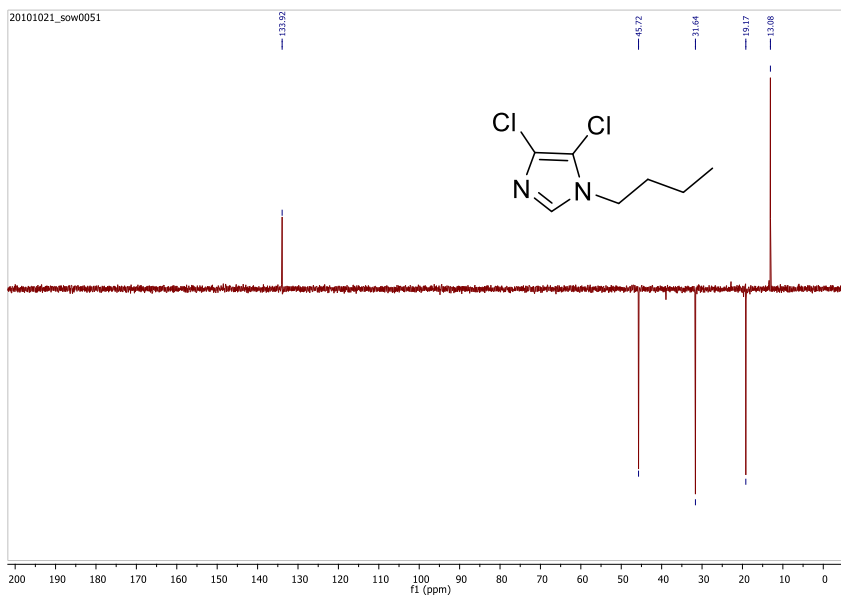


Fig SI 2.9: ^{13}C DEPT of 1-butyl-4,5-dichloro-1H-imidazole

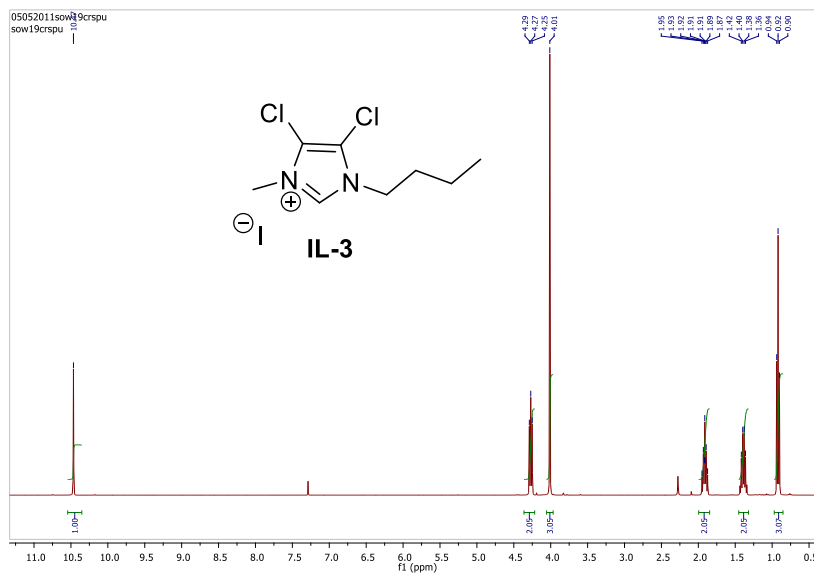


Fig SI 2.10: ^1H NMR of 1-butyl-4,5-dichloro-3-methyl-1H-imidazol-3-ium iodide

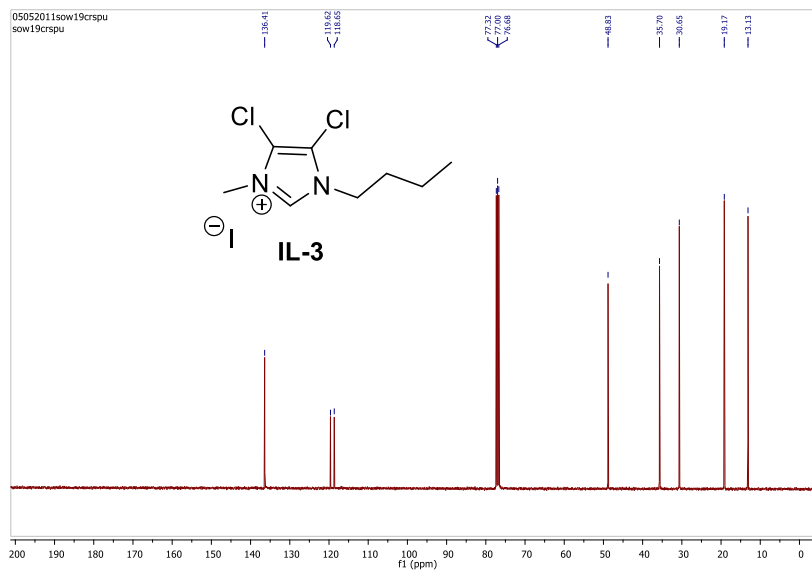


Fig SI 2.11: ^{13}C NMR of 1-butyl-4,5-dichloro-3-methyl-1H-imidazol-3-ium iodide

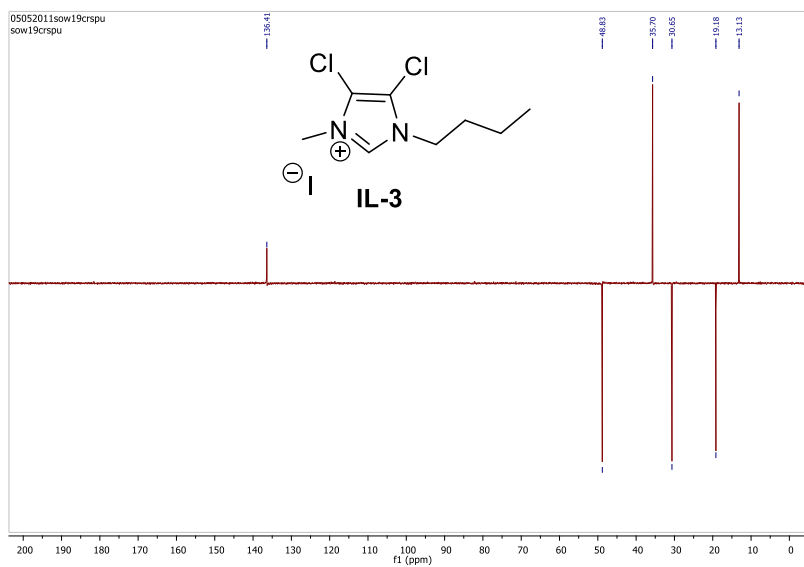


Fig SI 2.12: ^{13}C DEPT of 1-butyl-4,5-dichloro-3-methyl-1H-imidazol-3-ium iodide

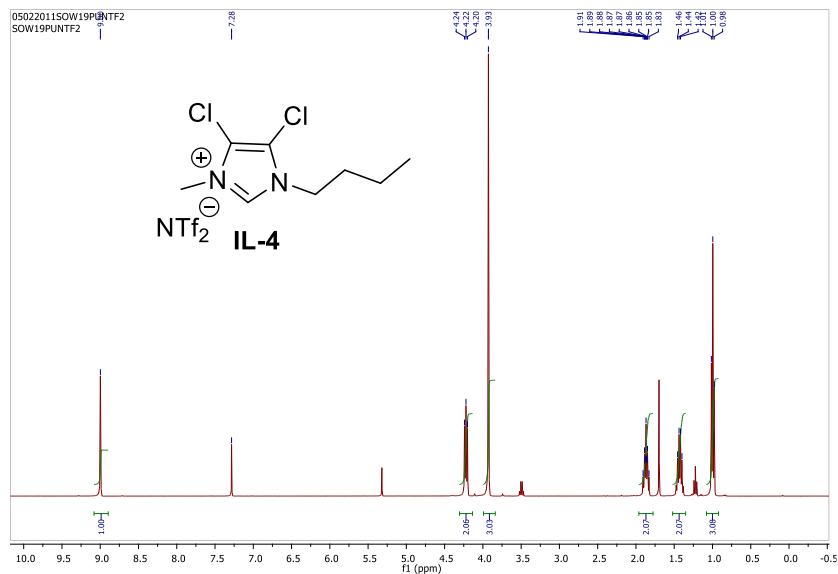


Fig SI 2.13: ^1H NMR of 1-butyl-4,5-dichloro-3-methyl-1H-imidazol-3-ium bis((trifluoromethyl)sulfonyl)amide

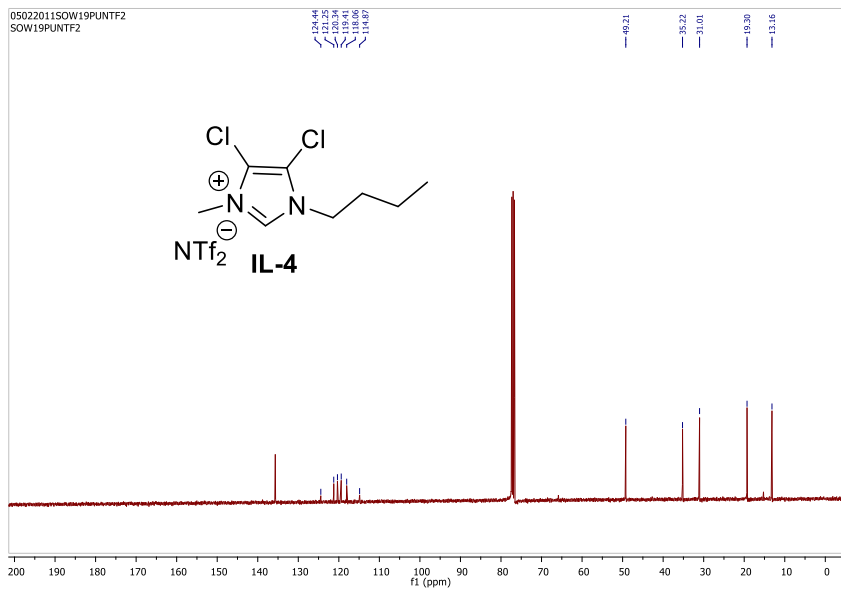


Fig SI 2.14: ^{13}C NMR of 1-butyl-4,5-dichloro-3-methyl-1H-imidazol-3-ium bis((trifluoromethyl)sulfonyl)amide

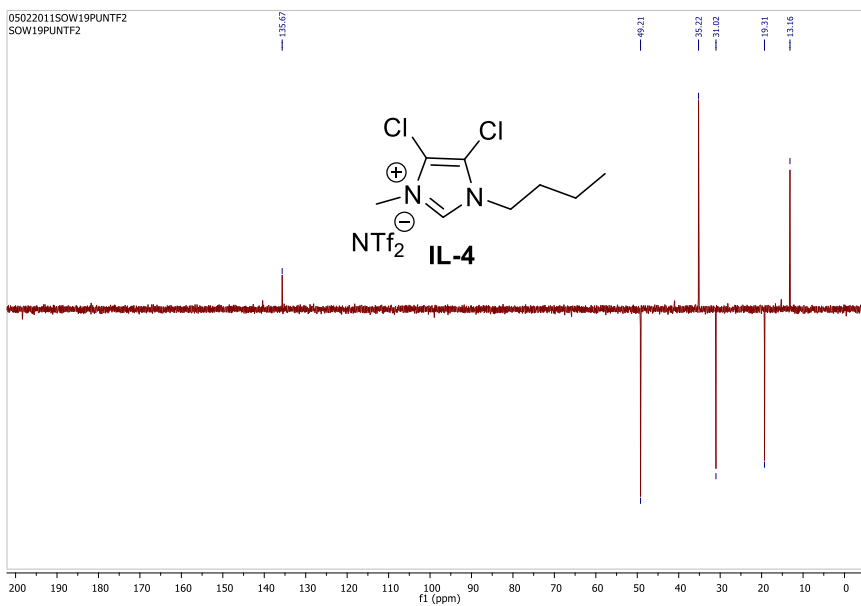


Fig SI 2.15: ¹³C DEPT of 1-butyl-4,5-dichloro-3-methyl-1H-imidazol-3-ium bis((trifluoromethyl)sulfonyl)amide

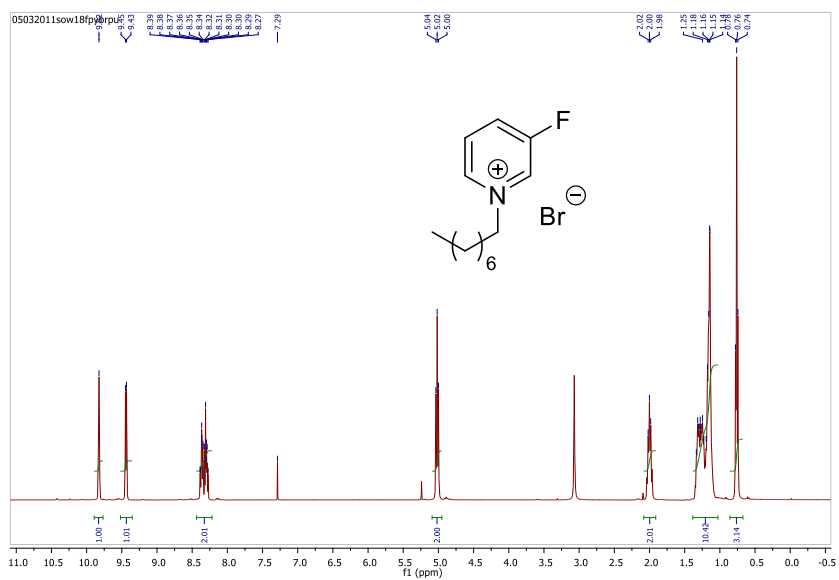


Fig SI 2.16: ¹H NMR of 3-fluoro-1-octylpyridinium bromide (IL 5)

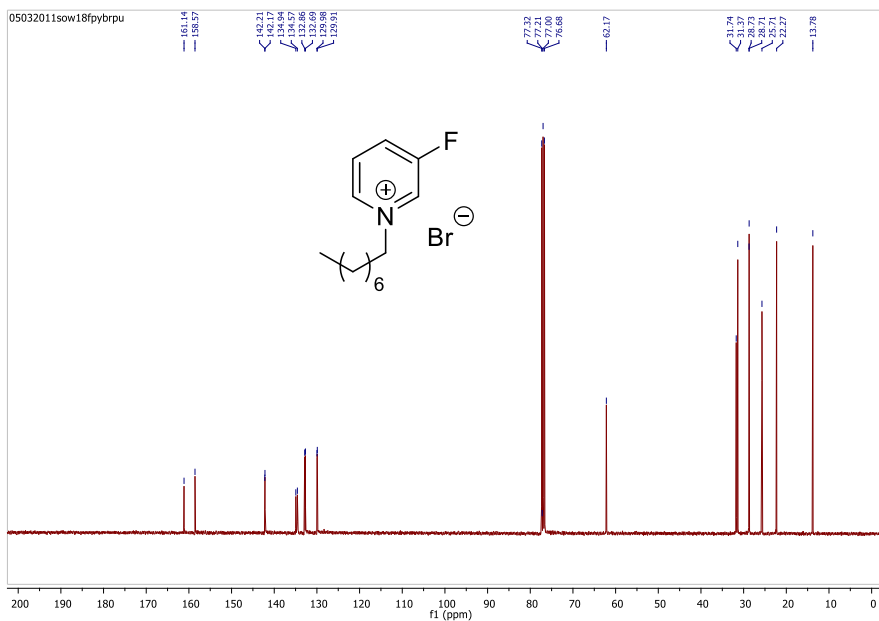


Fig SI 2.17: ^{13}C NMR of 3-fluoro-1-octylpyridinium bromide (IL 5)

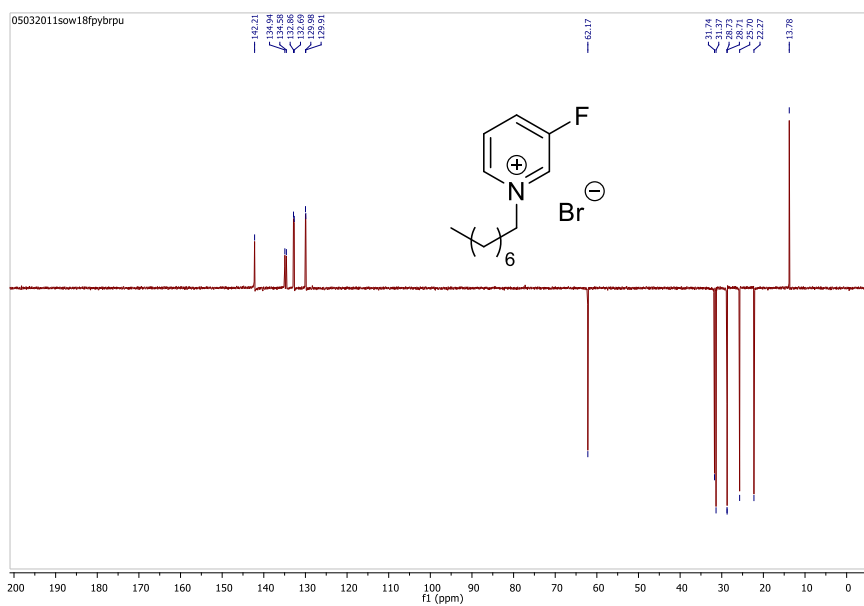


Fig SI 2.18: ^{13}C DEPT of 3-fluoro-1-octylpyridinium bromide (IL 5)

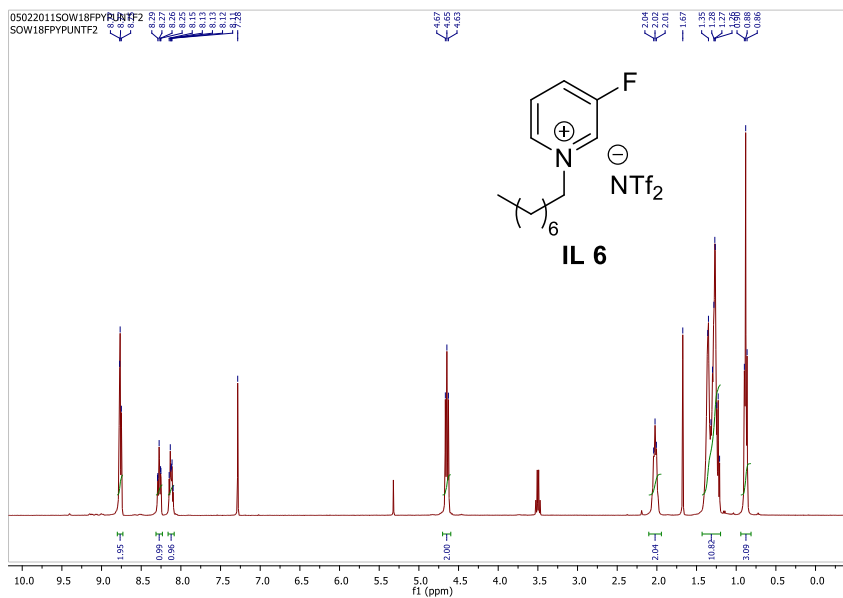


Fig SI 2.19: ^1H NMR of 3-fluoro-1-octylpyridinium bis((trifluoromethyl)sulfonyl) amide (IL 6)

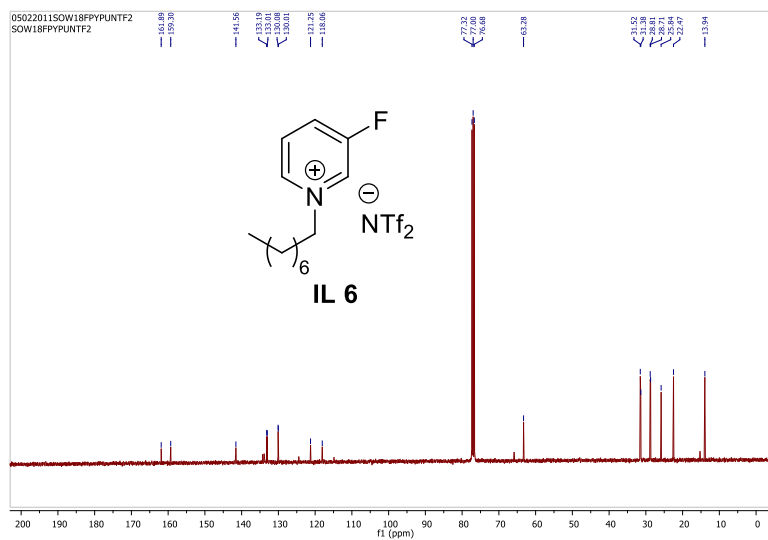


Fig SI 2.20: ^{13}C NMR of 3-fluoro-1-octylpyridinium bis((trifluoromethyl)sulfonyl)amide (IL 6)

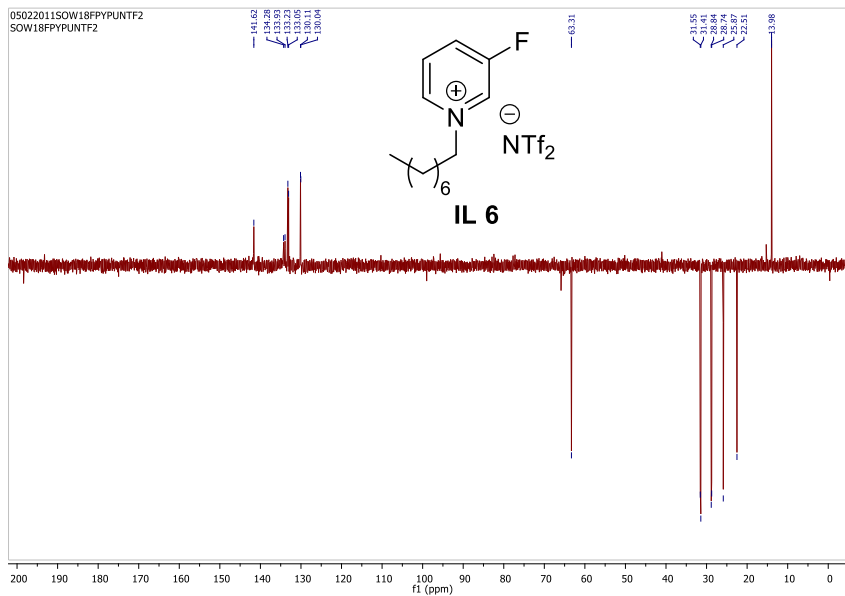


Fig SI 2.21: ^{13}C DEPT of 3-fluoro-1-octylpyridinium bis((trifluoromethyl)sulfonyl) amide (IL 6)

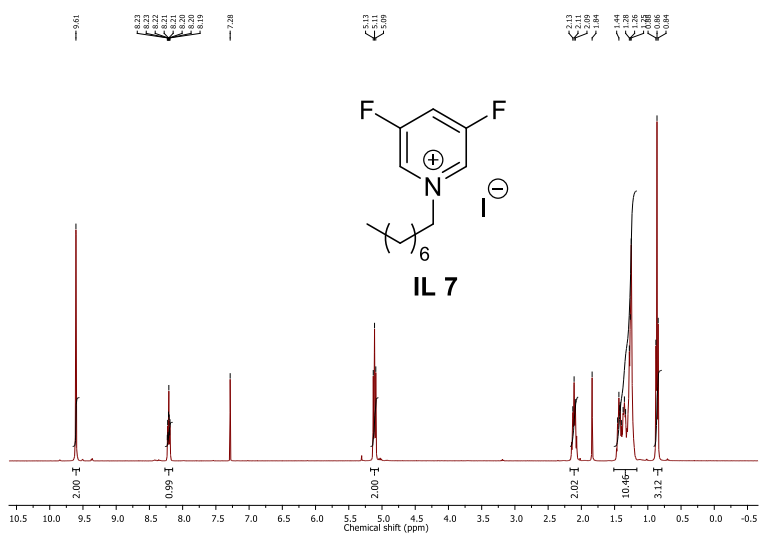


Fig SI 2.22: ^1H NMR of 3,5-difluoro-1-octylpyridinium iodide (IL 7)

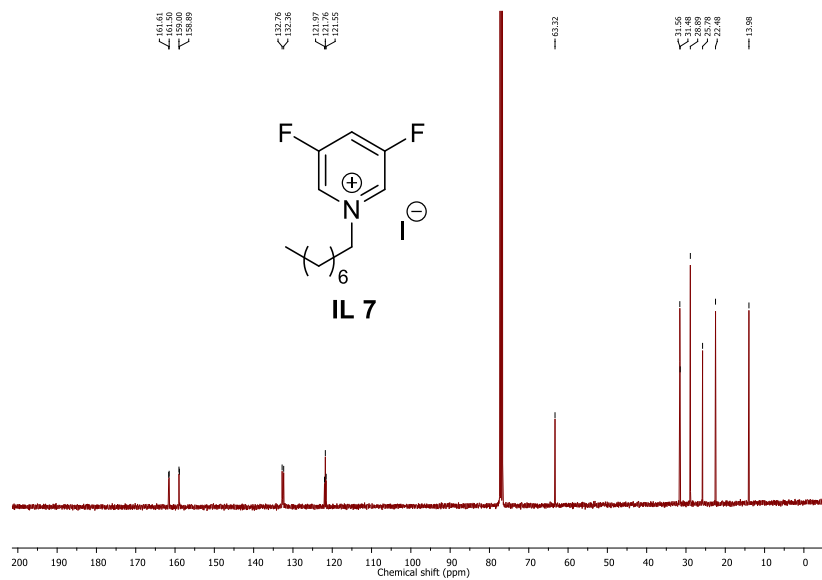


Fig SI 2.23: ^{13}C NMR of 3,5-difluoro-1-octylpyridinium iodide (IL 7)

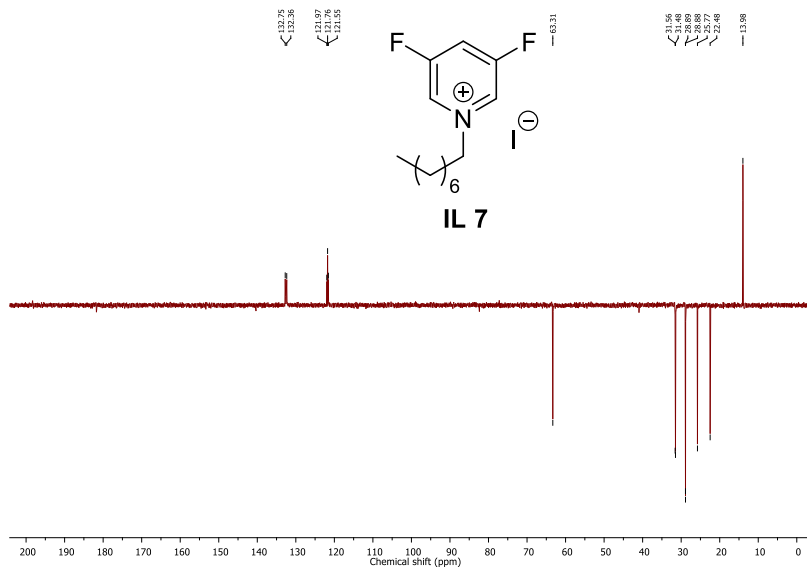


Fig SI 2.24: ^{13}C DEPT of 3,5-difluoro-1-octylpyridinium iodide (IL 7)

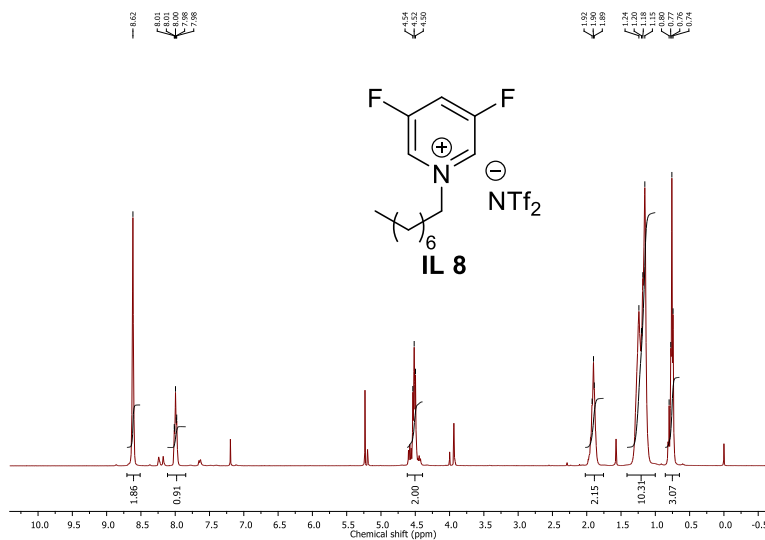


Fig SI 2.25: ¹H NMR of 3,5-difluoro-1-octylpyridinium bis((trifluoromethyl)sulfonyl)amide

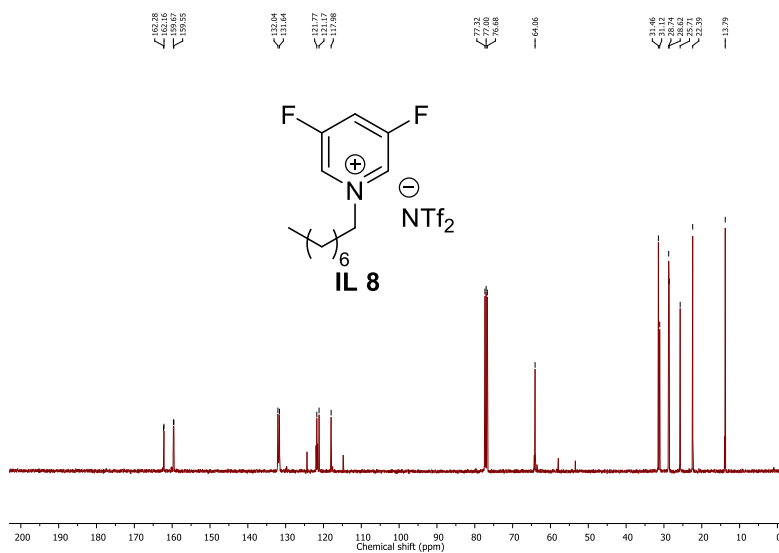


Fig SI 2.26: ¹³C NMR of 3,5-difluoro-1-octylpyridinium bis((trifluoromethyl)sulfonyl)amide

Supporting details

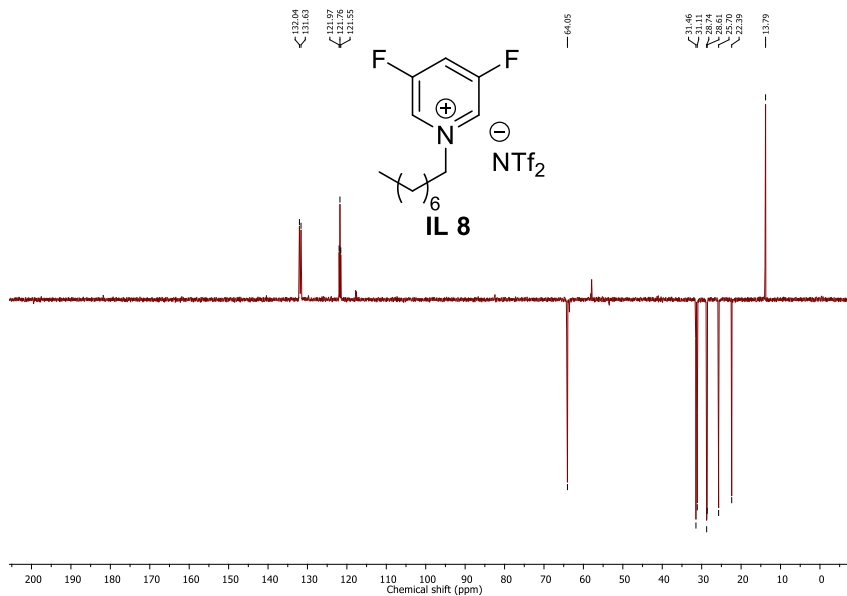


Fig SI 2.27: ^{13}C DEPT of 3,5-difluoro-1-octylpyridinium bis((trifluoromethyl)sulfonyl)amide

Chapter III

Supporting Information

Direct transformation of 5-hydroxymethylfurfural to the building blocks 2,5-dihydroxymethylfurfural (DHMF) and 5-hydroxymethyl furanoic acid (HMFA) via Cannizzaro reaction

Sowmiah Subbiah^{a,b}, Svilen P. Simeonov^b José M.S.S. Esperança^a, Luís Paulo N. Rebelo^a and Carlos A. M. Afonso^{*,b}

^a Instituto de Tecnologia Quimica e Biologica, Universidade Nova de Lisboa, Av. da Republica, 2780-157 Oeiras

^b iMed. UL, Faculdade de Farmacia da Universidade de Lisboa, Av. Prof. Gama Pinto, 1649-003, Lisboa, Portugal, E-mail: carlosafonso@ff.ul.pt, Fax: +351 21 7946476.

Experimental:

General:

All reagents were purchased from Sigma-Aldrich, Alfa Aesar and Merck and were used without further purification. 5-hydroxymethyl furfural was synthesised in the laboratory using commercially available fructose¹. The

Supporting details

compounds were characterized: a) by NMR in a Bruker Avance II 400 Ultrashield Plus; b) by elemental analysis performed in a Flash 2000 CHNS-O analyser (Thermoscientific, UK) at the Faculty of Pharmacy, University of Lisbon; c) by measuring the melting point in a Stuart SMP10 apparatus; and d) by MS/MS experiments performed on Micromass® Quattro Micro triple Quadrupole (Waters®, Ireland) with an electrospray (ESI) ion source.

Preparation of 5-Hydroxymethylfurfural (5-HMF) ¹:

Water (0.9mL) was added to 9.1g of Et₄NBr (1% water content w/w). and the resulting mixture (10g, 10% water content w/w) was mixed with 2g of fructose (available from local commerce) and 0.2g of smashed Amberlyst-15® (10% w/w). The mixture was placed at 80 °C and heated upto 100 °C for 10 min and was then stirred at 100 °C for 15 min. Next, the mixture was cooled down to room temperature and the water was evaporated. The resulting solid was washed with EtOAc (50 ml). The solvent was decanted and the solid was dissolved in hot EtOH (2 mL) and then EtOAc (200mL) was added under vigorous stirring. The resulting precipitate was filtered out and the combined solutions were filtered through a pad of silica gel (10g)

and evaporated to yield a brown liquid of HMF (1.25g, 91%) 97% pure as determined by NMR.

^1H NMR for HMF (CDCl_3 , 400 MHz): δ 9.56 (s, 1H), 7.51, 6.59 (d, 2H), 4.54 (s, 2H)

Preparation of TBDMS protected HMF(TBDMSMF):

Imidazole, 0.6 g (8.8mmol), was mixed with 1g (8 mmol) of HMF in dichloromethane (20 mL) and allowed to stir for 15 mins. Then 1.3g (8.4mmol) TBDMSCl was added and stirred overnight at room temperature under argon atmosphere. Water was then added and the organic layers were separated using dichloromethane. The combined organic extracts are dried over MgSO_4 , filtered, and the solvent removed by rotary evaporation to deliver a yellow solid without any chromatography purification (1.7g, 92% yield).

^1H NMR (CDCl_3 , 400 MHz): δ 9.58(s, 1H), 7.22(d, $J=3.3\text{Hz}$, 1H), 6.48(d, $J=3.3\text{Hz}$, 1H), 4.74(s, 2H), 0.93(s, 9H), 0.11(s, 6H); ^{13}C NMR (CDCl_3 , 101 MHz): δ 177.4, 161.3, 152.1, 109.6, 58.4, 25.8, 18.4, 5.39. ESI(+) MS: m/z 241.57. $\text{C}_{12}\text{H}_{20}\text{O}_3\text{Si}$: Calcd C 59.96, H 8.39; found C 60.41, H 8.38.

A representative procedure for the Cannizzaro reaction of HMF and product isolation

3g of HMF (24 mmol) were dissolved in water (30mL) and then cooled to 0 °C. After 0.87g (22 mmol) of NaOH at 0 °C were added, the resulting mixture was stirred at room temperature in a closed vessel for about 18h; TLC confirmed the completion of the reaction. After evaporating the water, ethyl acetate (2x50mL) was added to the solid residue to separate the DHMF diol (0.85g, 60%). From the remaining solid, carboxylate salt HMFA was isolated by recrystallization with ethanol (approx 2mL)/ethylacetate (100mL), yielding HMFA salt (1.4g, 83% yield) hygroscopic solid which was stored in a refrigerator. More DHMF (0.4g, 27% yield) was isolated after evaporation of the mother liquor.

Isolated DHMF: 87% yield, 98% purity

Isolated HMFA salt: 83% yield, 95% purity

The diol DHMF can be further purified by washing with ether/hexane and hexane to remove any non-polar impurities retained after the recrystallization process.

For the 12g scale of HMF, during the HMFA isolation, a few drops of water were initially added to dissolve the residue followed by the addition, first, of

25 mL ethanol and then ethyl acetate leading to the formation of a HMFA salt.

Several batch experiments were successfully performed at different quantities of HMF following the above-mentioned purification process during our optimization studies.

Batch experiments performed by this isolation procedure:

entry	HMF Quantity	Reaction Conditions ^a 0 °C to RT	Isolated Yield (%)	
			DHMF	HMFA
1	100mg	NaH, Dry THF (20 mL)	80	88
	100mg	NaOH, Water		
2	Trial I	Water (20 mL)	82	85
3	Trial II	Water (4 mL)	88	84
4	1g	NaH, Dry THF (60 mL)	77	80
5	1g	NaOH, Water (60 mL)	90	85
6	3g	NaOH, Water (120mL)	85	83
7	3g	NaOH, Water (30mL)	87	83
8	12g	NaOH , Water (200 mL)	85	82
9	6.5 g ^b	NaOH (0.56 eq.), EtOH (1 mL)	51	61

^a Reactions were performed with 1.1equiv of NaH and 0.9 equiv of NaOH wherever mentioned; reaction time 18 h (entry 9, 4 days). ^b Observed conversion of 65%.

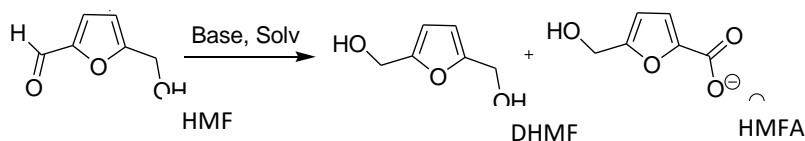
Cannizzaro products DHMF and HMFA were isolated based on the optimized procedure from our studies under the described conditions.

Supporting details

2,5-dihydroxymethylfuran (DHMF) : Initial purification by recrystallization and further cleansing by washing with diethylether yielded an off-white solid DHMF; mp 76 °C (lit. mp 76– 78 °C)²; ¹H NMR(400MHz, D₂O): δ 6.22 (s, 2H), 4.42 (s, 4H); ¹³C NMR(400MHz, D₂O): δ 153.6, 108.9, 55.8. ESI(+)-MS: m/z 127.89; 111.04 (C₆H₇O₂).

5-hydroxymethylfuranate (HMFA sodium salt): Purification by recrystallization in ethanol/ethyl acetate produced a brown hygroscopic solid. ¹H NMR(400MHz, D₂O): δ 6.81(d, J = 3.3Hz, 1H), 6.33 (d, J = 3.3Hz, 1H), 4.45 (s, 2H); ¹³C NMR(400MHz, D₂O): δ 166.3, 155.8, 149.0, 115.4, 109.9, 55.7; ESI (-) MS: m/z 140.89.

Screening with various bases (Table 1)

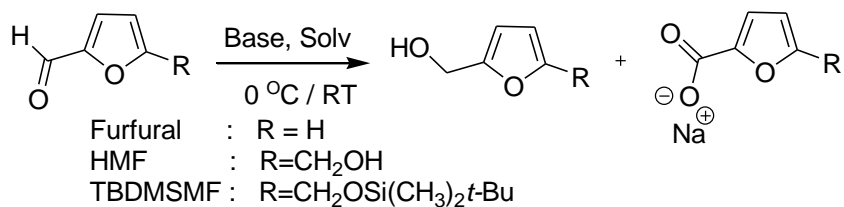


Experimental Procedure:

A solvent was added to 100 mg of HMF (0.100g, 0.8mmol) and the mixture was stirred at 0 °C; then the base (0.88 mmol) was added in and after 1 h

was continually stirred at room temperature. The reaction was monitored by TLC (ethylacetate/hexane 8:2). After the reaction was complete, the solvent was evaporated completely from the reaction mixture and sodium acetate NaOAc (0.8mmol, 1 equiv) was added to serve as an internal standard for proton NMR analysis.

Screening with Specific Conditions (Table 2)



Experimental Procedure:

HMF (0.100g, 0.8mmol; for entries 2 and 3: 0.4 mmol) were dissolved on the appropriate solvent (4 mL) and stirred at 0 °C (entry 1 and 3, and 6-10) and base (0.88mmol) was added and after 1 h was stirred at room temperature. For entries 2, 4, 5, the addition of the base and the stirring were carried out at the specific temperature. The reaction was monitored by TLC (ethylacetate/hexane 8:2). After the reaction was complete, the solvent

Supporting details

was completely evaporated and NaOAc (0.8mmol, 1 equiv) was added to serve as an internal standard for proton NMR analysis.

Entry 2 received 0.2 equiv NaOAc (0.16mmol) and Entry 3 got 0.05equiv NaOAc (0.04mmol) as the internal standard. Entries 9 and 10 saw their isolated yields determined.

Screening for specific conditions for HMF (Table 3)

Experimental Procedure:

Reaction at 0°C temperature

HMF (0.100g, 0.8mmol) were dissolved in 20mL of corresponding solvent and stirred at 0 °C. A base (0.88mmol) was added in a closed vessel under argon atmosphere. The reaction mixture was stirred at 0 °C for 1 hour and then continued at room temperature. After the reaction was complete (by TLC), the solvent was completely evaporated and NaOAc (0.8mmol, 1 equiv) added as an internal standard for proton NMR analysis.

Reaction at room temperature

HMF (50mg, 0.4mmol) was dissolved in 2mL of corresponding solvent and stirred at room temperature. To this, base (0.44mmol) was added in a closed

vessel under argon atmosphere and was continually stirred at room temperature. After the reaction was complete (TLC), the solvent was completely evaporated and NaOAc (0.16mmol, 0.2 equiv) was added as an internal standard for proton NMR analysis.

Screening for NaOH quantity (Table 4)

Experimental Procedure:

HMF (50mg, 0.4mmol) were dissolved in 2mL of water at 0 °C, then a varying equivalent of base was added in a closed vial and after 1 hr was stirred at room temperature during the amount of time identified in table 4. The reaction was monitored by TLC. After 48 hours of reaction time, the solvent was completely evaporated and the reaction mixture was washed with diethylether to remove unreacted HMF, dried in vacuo and NaOAc (0.04mmol, 0.15 equiv) was added as an internal standard for proton NMR analysis.

Supporting details



Recrystallization of HMFA sodium salt using 3g of HMF



Recrystallization of HMFA Salt with 12g HMF producing a brown colored HMFA sodium salt.

References:

1. S. P. Simeonov, J. A. S. Coelho and C. A. M. Afonso, *ChemSusChem* 2012, **5**, 1388.
2. S. Goswami, S. Dey, S. Jana, *Tetrahedron*, 2008, **64**, 6358.

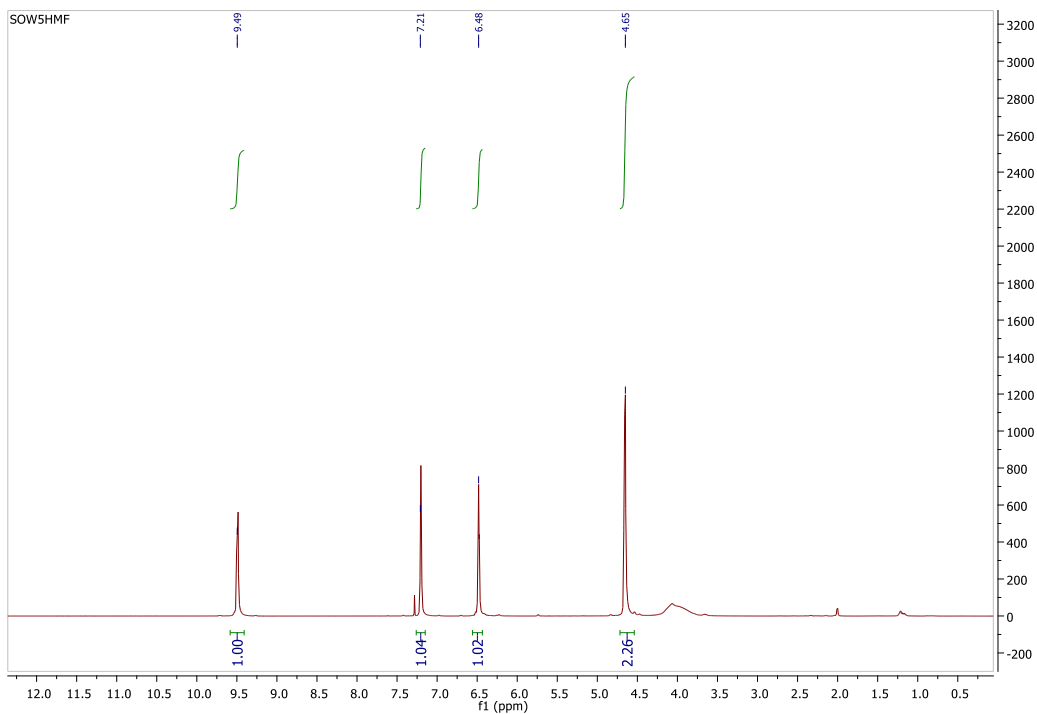


Fig S1: ¹H NMR(CDCl₃) of synthesized 5-hydroxymethyl furfural (HMF).

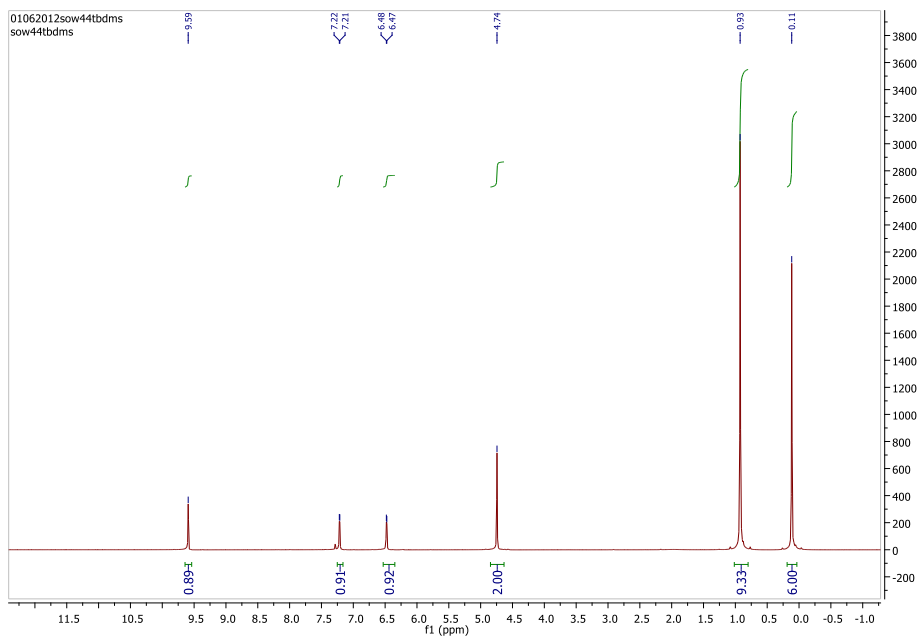


Fig S2: ^1H NMR(CDCl_3) of TBDMS protected HMF.

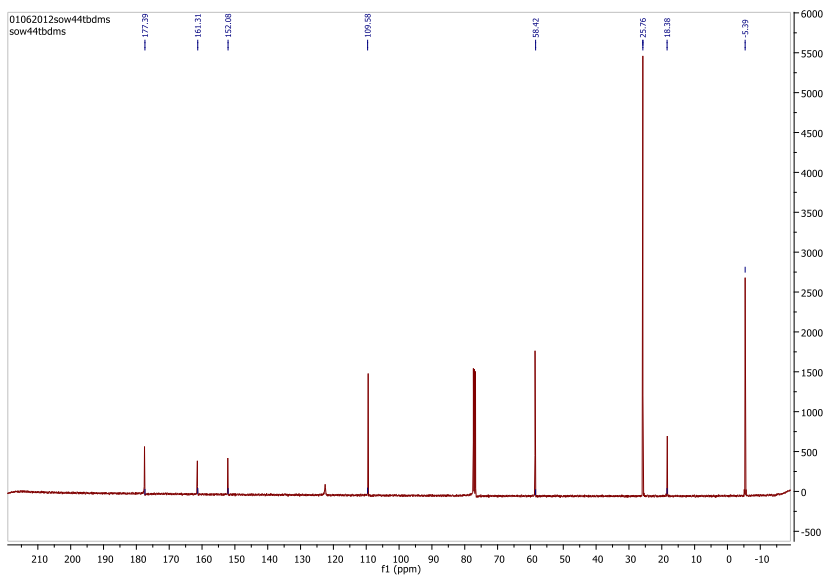


Fig S3: ^{13}C NMR(CDCl_3) of TBDMS protected HMF.

Supporting details

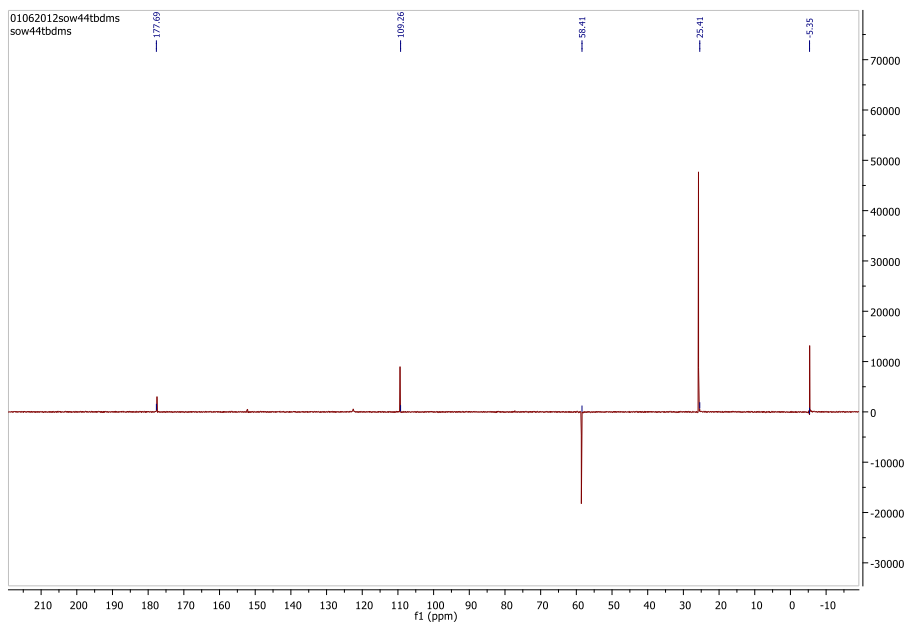


Fig S4: ^{13}C -DEPT NMR(CDCl_3) of TBDMS protected HMF.

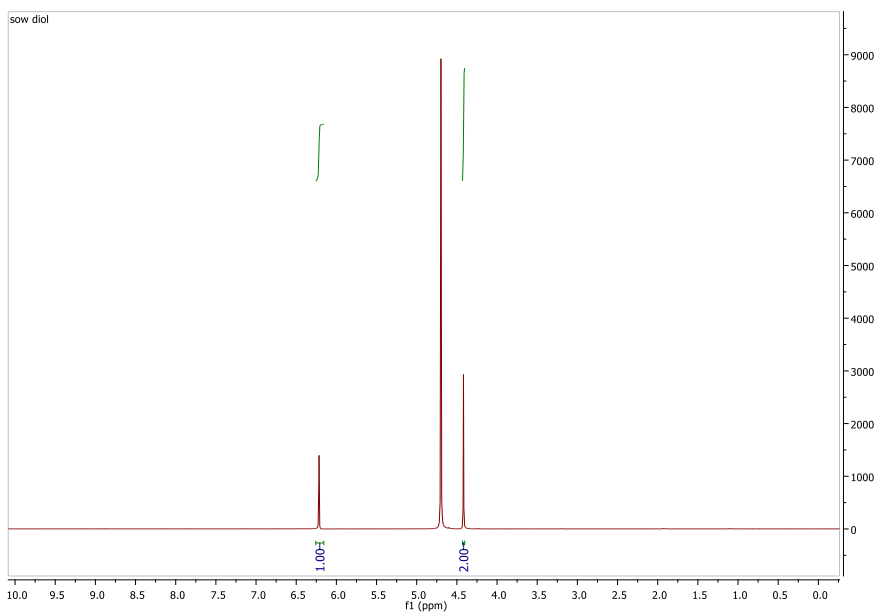


Fig S5: ^1H NMR(D_2O) of isolated DHMF from Cannizzaro reaction.

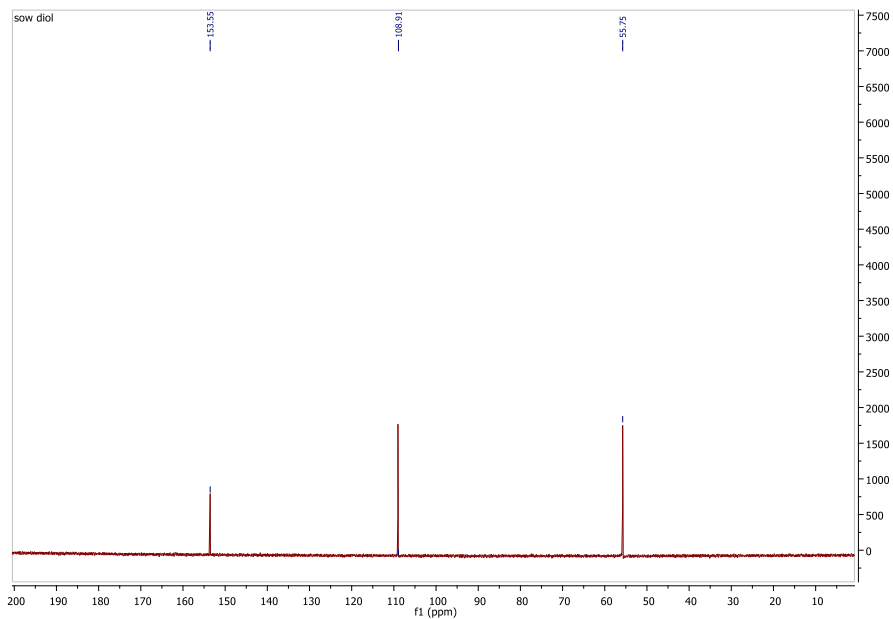


Fig S6: ^{13}C NMR(D_2O) of isolated DHMF from Cannizzaro reaction

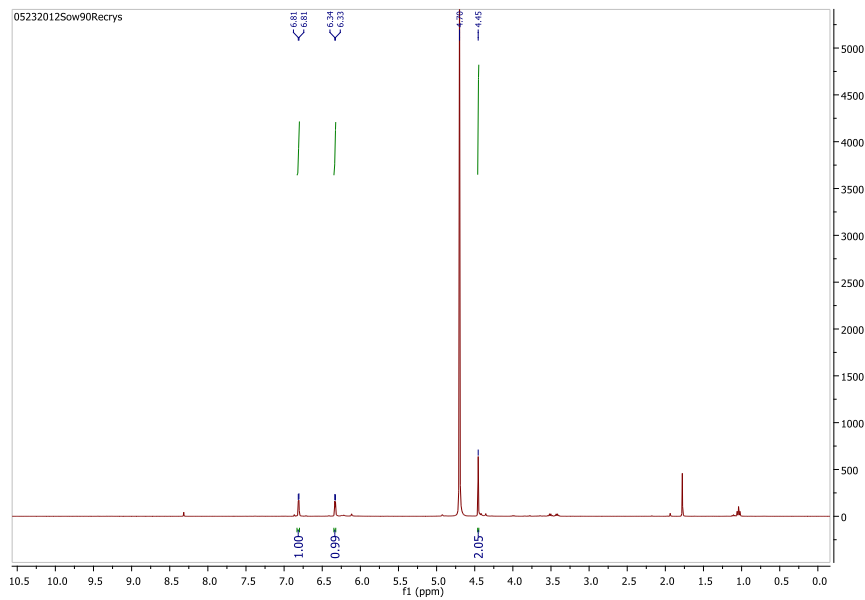


Fig S7: ^1H NMR(D_2O) of isolated HMFA from Cannizzaro reaction

Supporting details

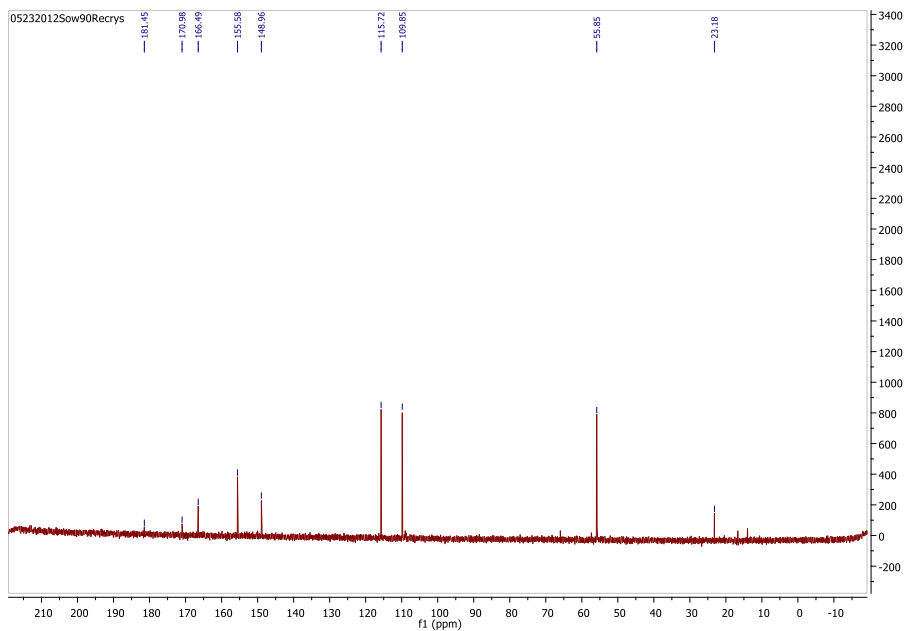


Fig S8: ^{13}C NMR(D_2O) of isolated HMFA from Cannizzaro reaction.

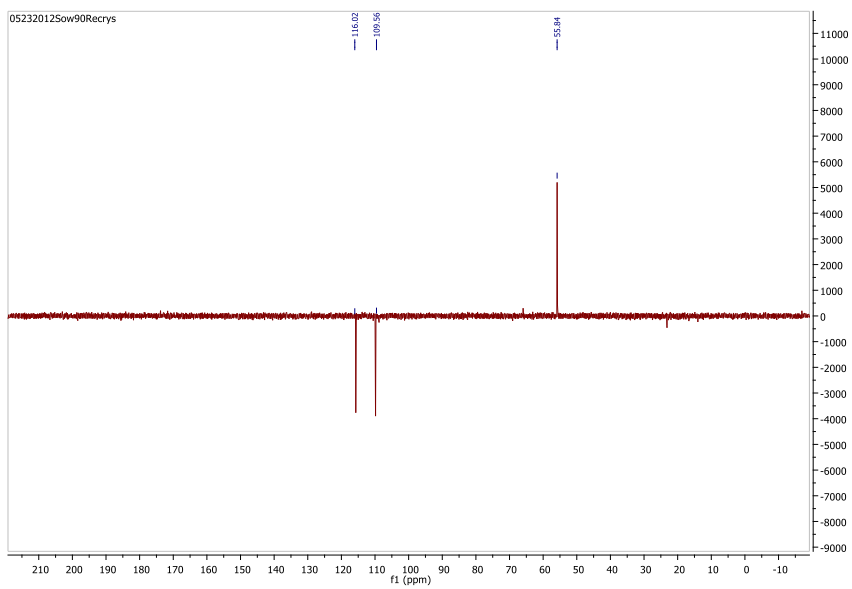


Fig S9: ^{13}C -DEPT NMR(D_2O) of isolated HMFA from Cannizzaro reaction.

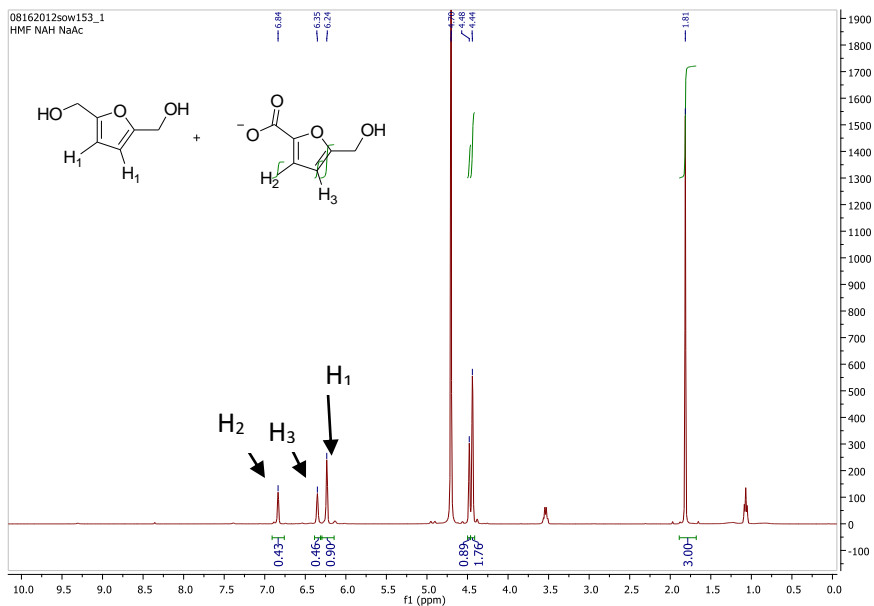


Fig S10: ^1H NMR(D_2O) of screening reaction with NaH (Table 1, Entry 1).

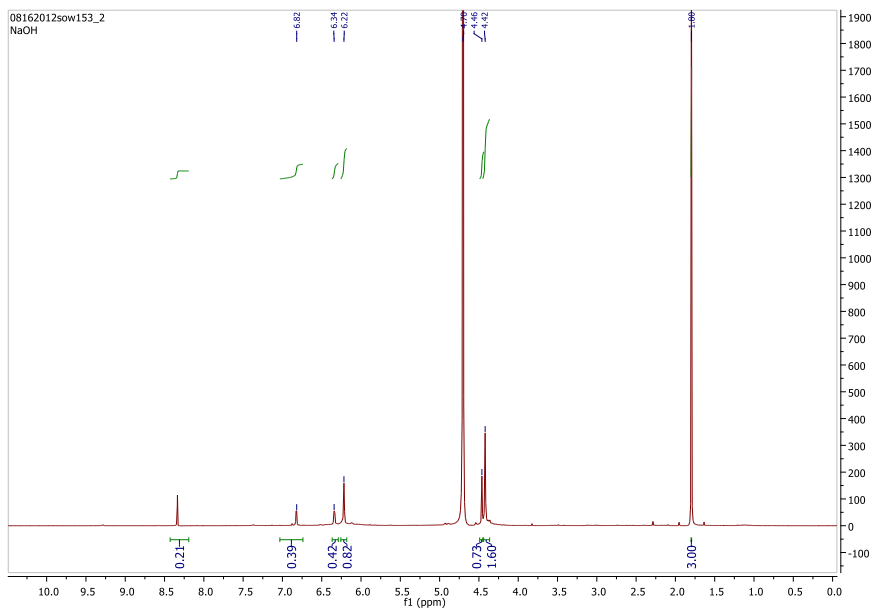


Fig S11: ^1H NMR(D_2O) of screening reaction with NaOH (Table 1, Entry 2).

Supporting details

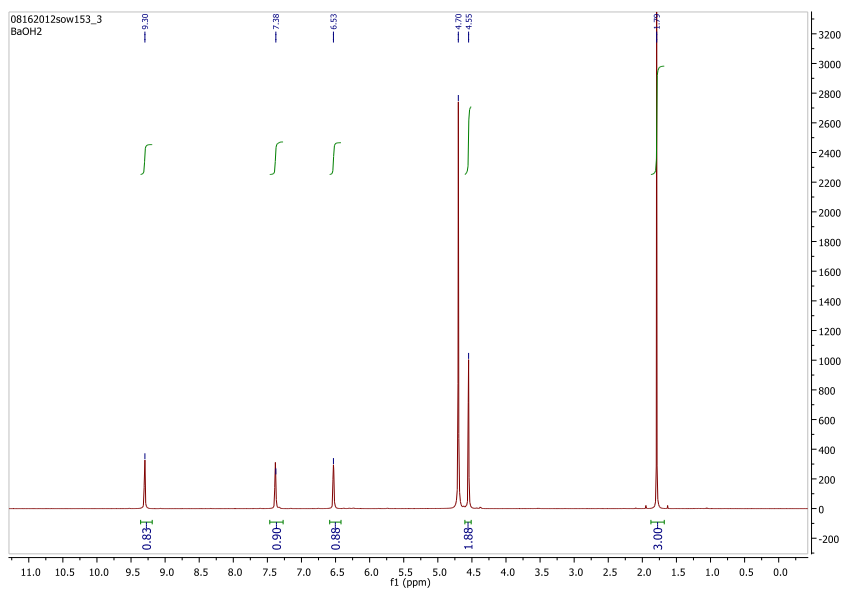


Fig S12: ¹H NMR(D₂O) of screening reaction with Ba(OH)₂ (Table 1, Entry 3).

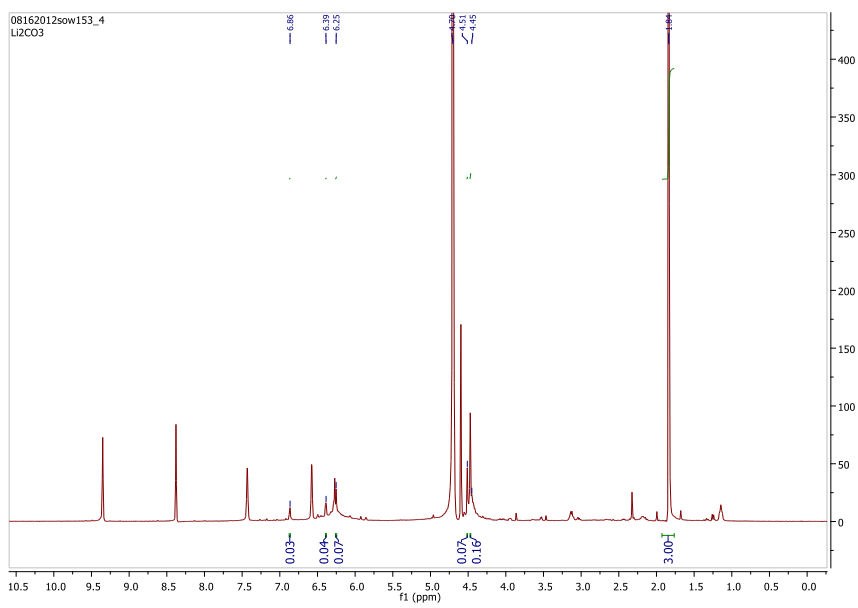


Fig S13: ¹H NMR(D₂O) of screening reaction with Li₂CO₃ (Table 1, Entry 4).

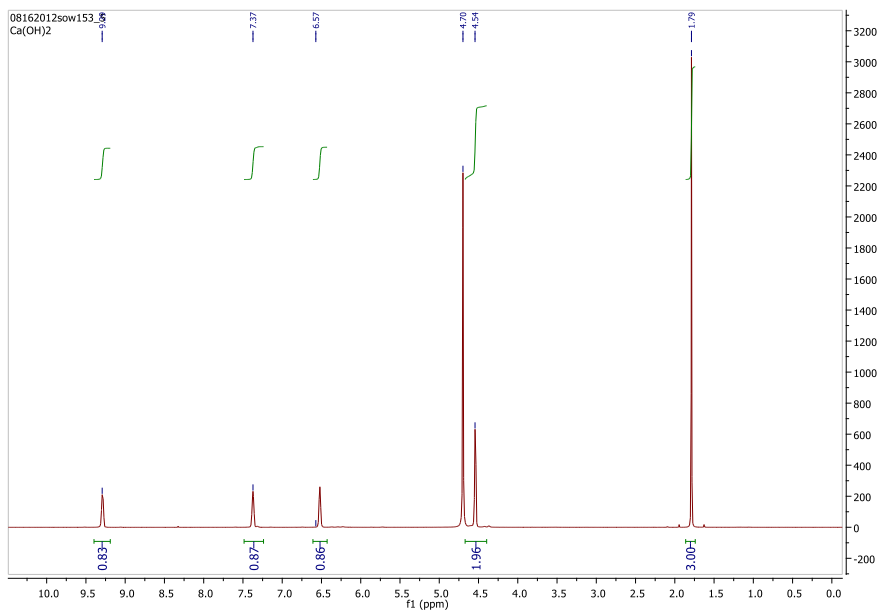


Fig S14: ¹H NMR(D₂O) of screening reaction with Ca(OH)₂ (Table 1, Entry 5).

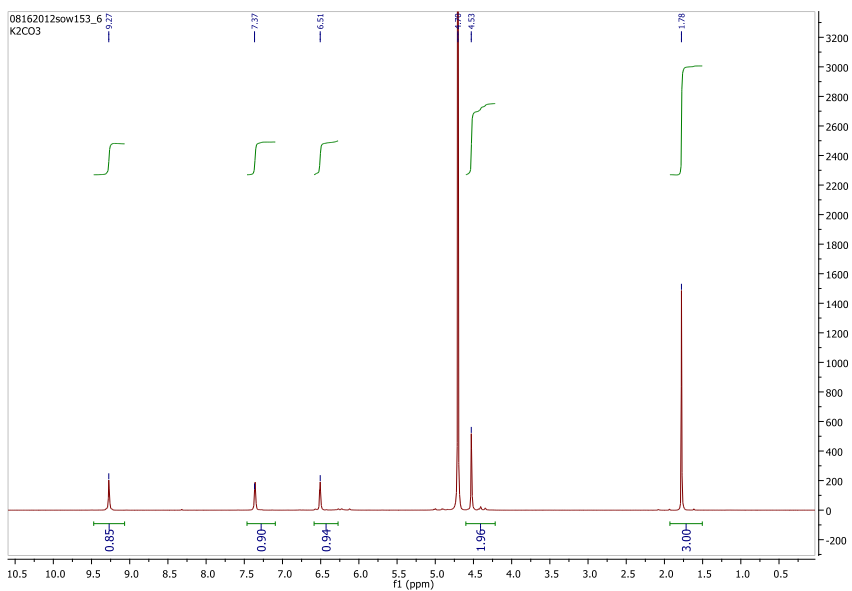


Fig S15: ¹H NMR(D₂O) of screening reaction with K₂CO₃ (Table 1, Entry 6).

Supporting details

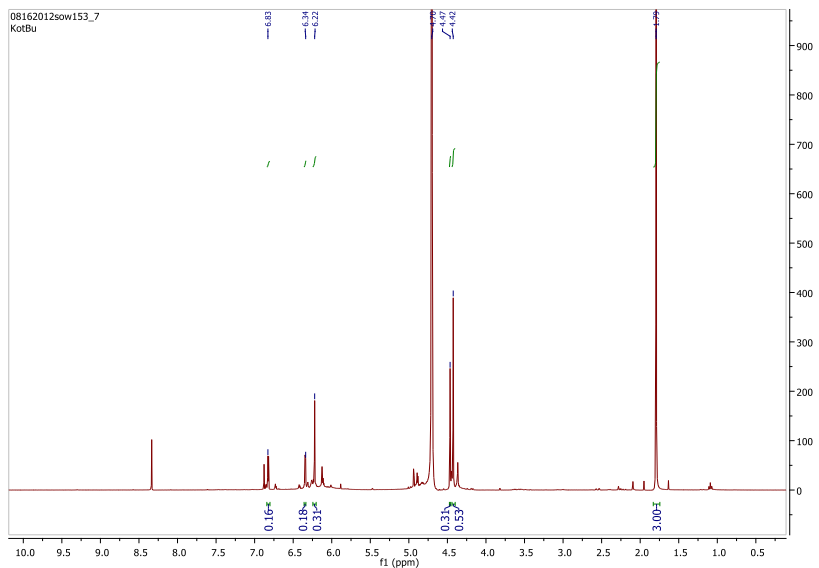


Fig S16: $^1\text{H NMR}$ (D_2O) of screening reaction with KO^tBu (Table 1, Entry 7).

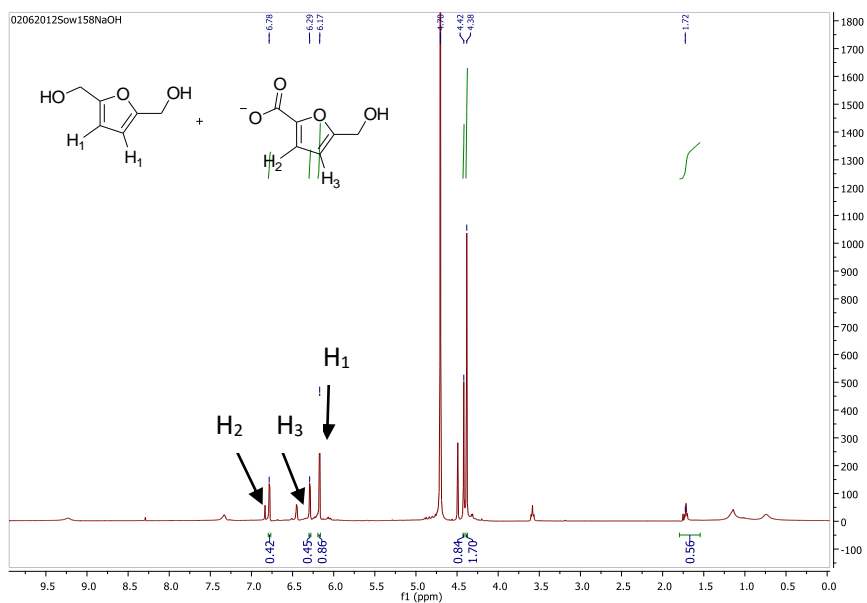


Fig S17: $^1\text{H NMR}$ (D_2O) of 50 mg HMF with NaOH (Table 3, 87% yield); (Table 2, Entry 2); (Table 4, Entry 1)

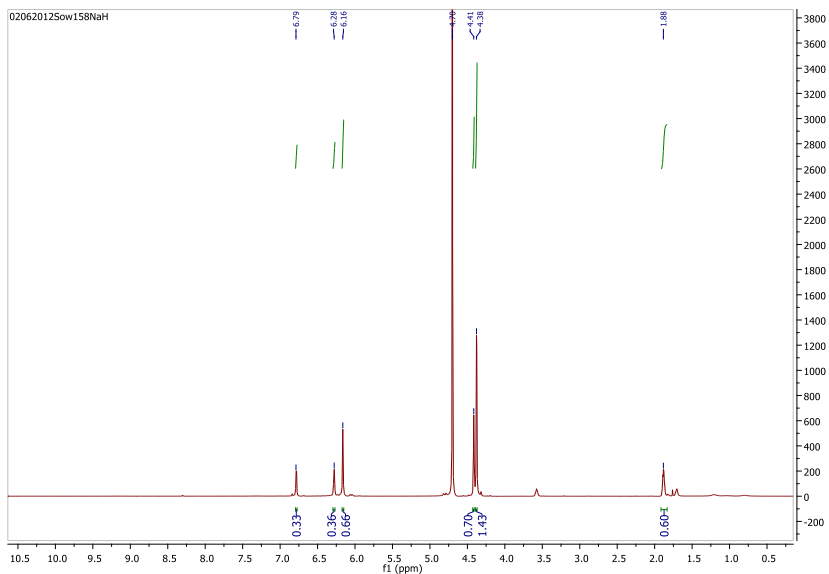


Fig S18: ^1H NMR(D_2O) of 50mg HMF with NaH(Table 3, 68% yield)

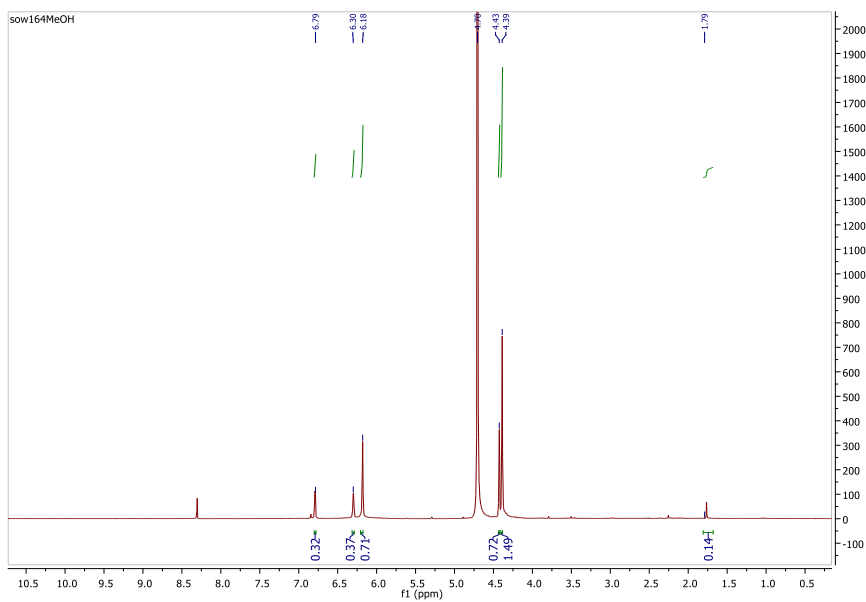


Fig S19: ^1H NMR(D_2O) of HMF reacting with NaOH in CH_3OH (Table 2, Entry 3).

Supporting details

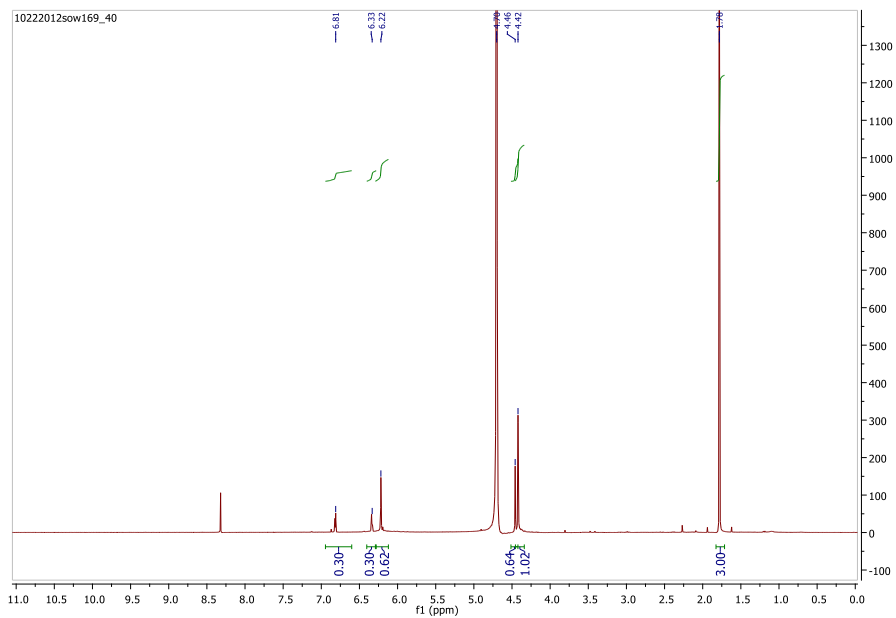


Fig S20: ^1H NMR(D_2O) of HMF reacting with NaOH at 40 °C (Table 2, Entry 4).

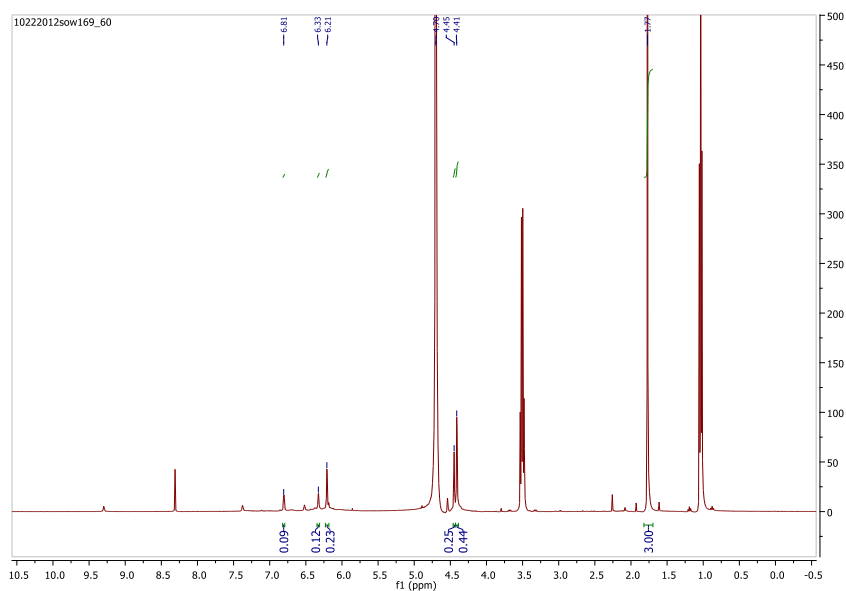


Fig S21: ^1H NMR(D_2O) of HMF reacting with NaOH at 60 °C (Table 2, Entry 5).

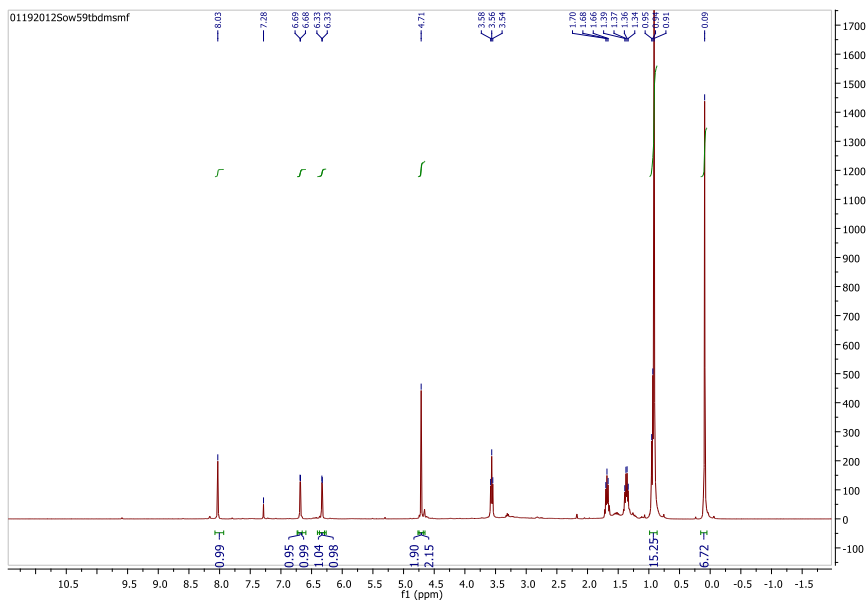


Fig S22: ^1H NMR(CDCl_3) of TBDMSMF reacting with NaOH in CH_3OH (Table 2, Entry 6).

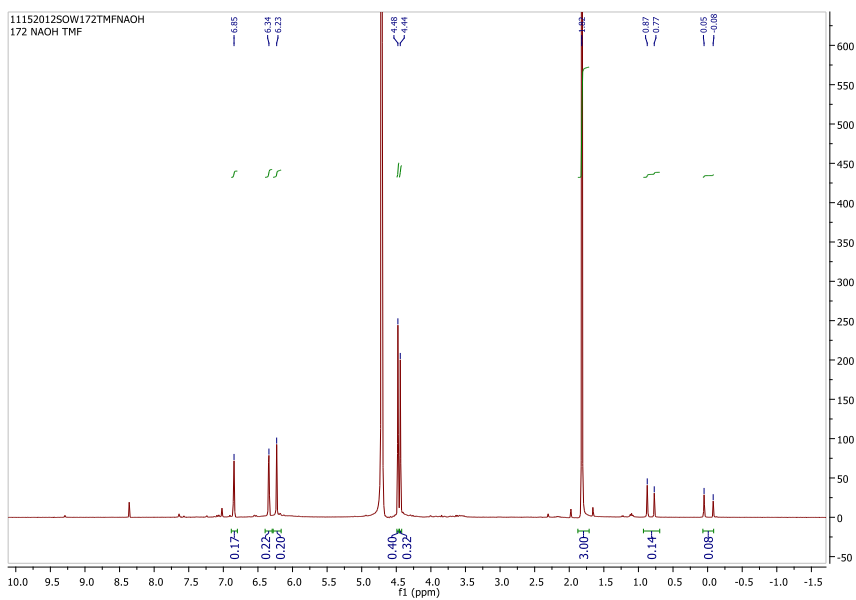


Fig 23: ^1H NMR(D_2O) of TBDMSMF reacting with NaOH in H_2O (Table 2, Entry 7).

Supporting details

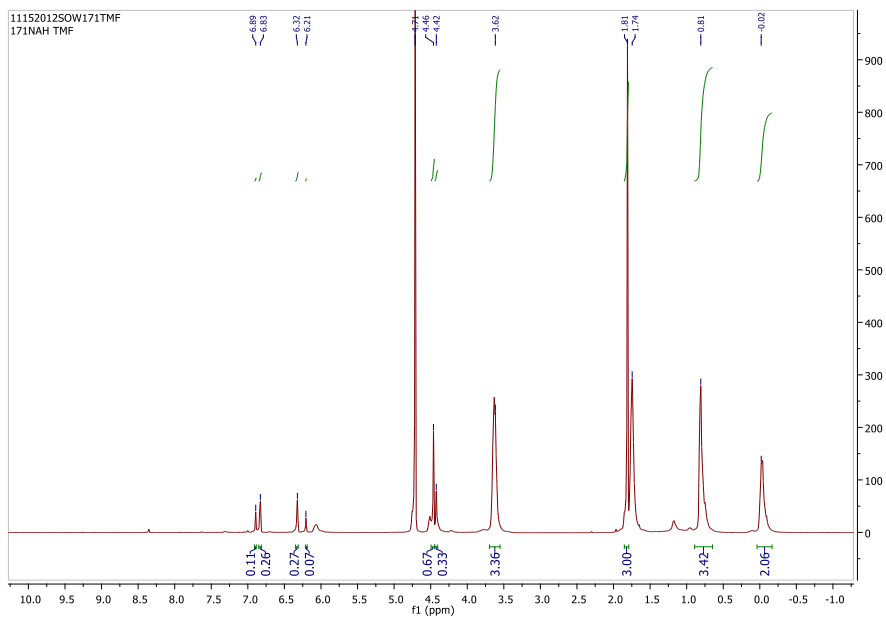


Fig S24: ^1H NMR(D_2O) of TBDMSMF reacting with NaH in dry THF (Table 2, Entry 8).

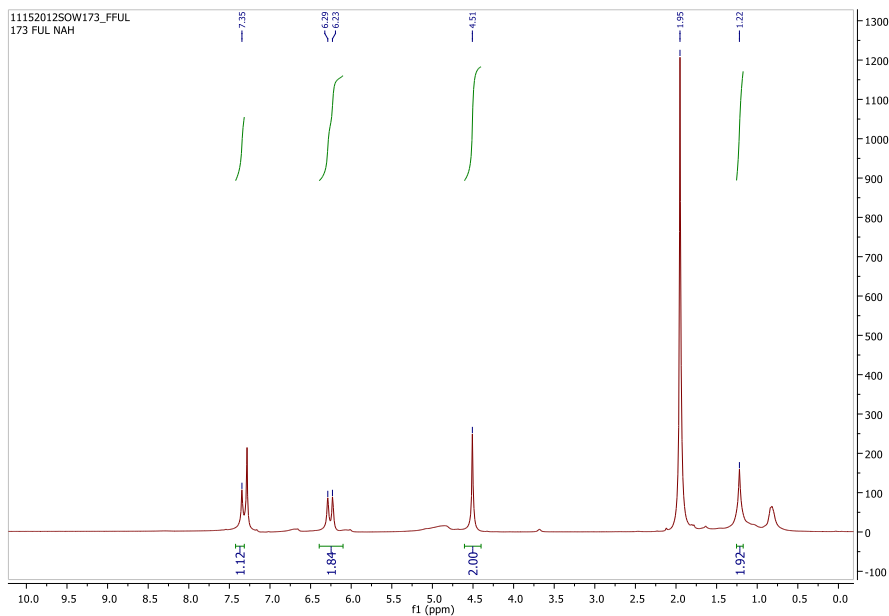


Fig S25: ^1H NMR(CDCl_3) of Furfural reacting with NaH (Table 2, Entry 9).

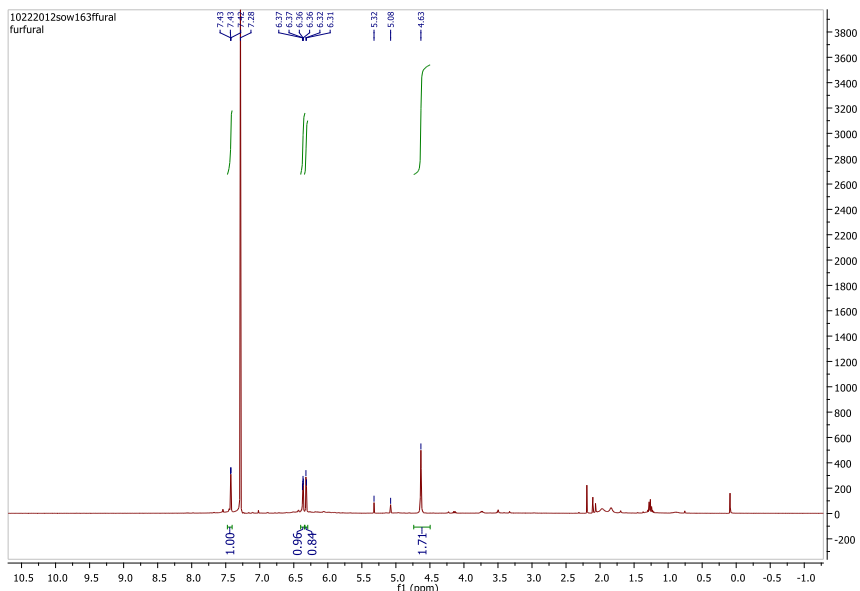


Fig S26: $^1\text{H NMR}_{(\text{CDCl}_3)}$ of furfural reacting with NaOH (Table 2, Entry 10).

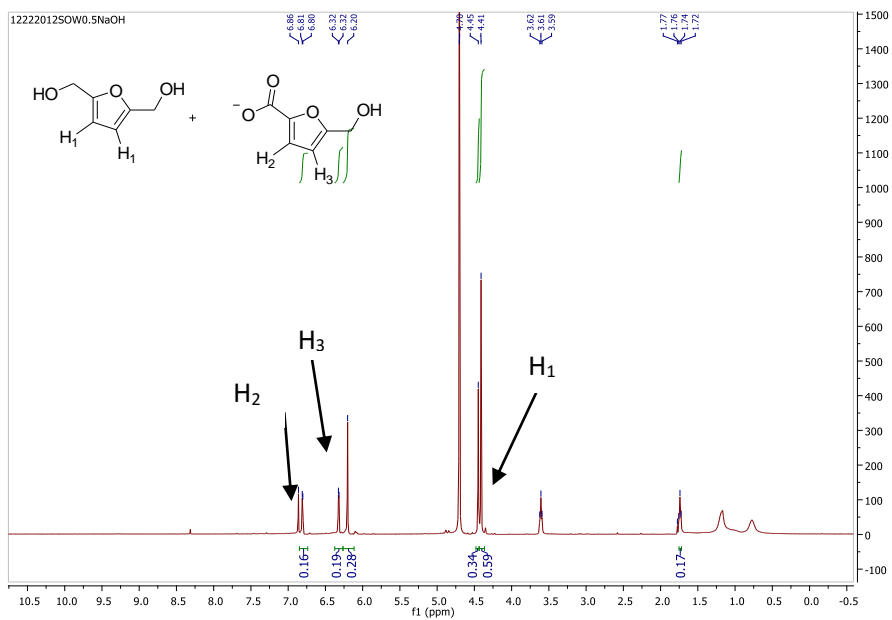


Fig S27: $^1\text{H NMR}_{(\text{D}_2\text{O})}$ of HMF reaction with (0.5 eq) NaOH (Table 4, Entry 2).

Supporting details

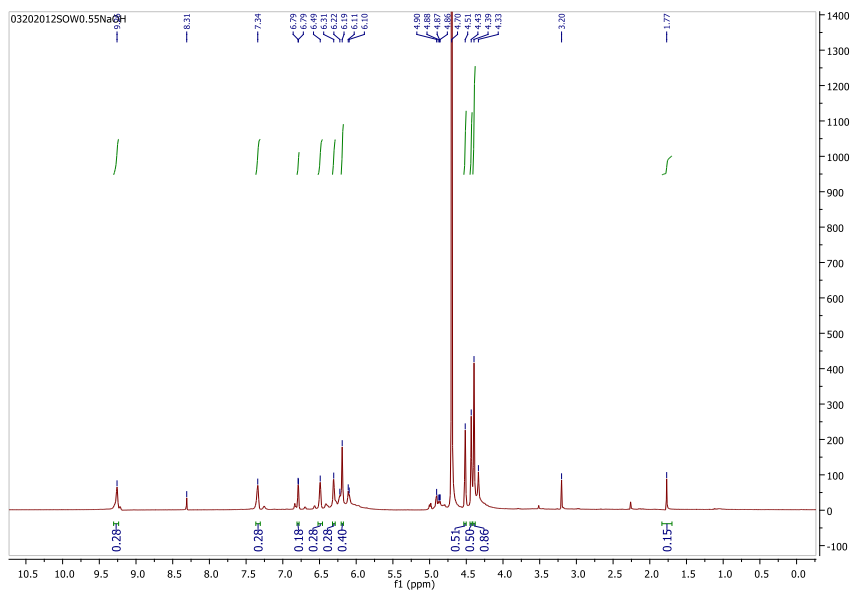


Fig S28: ^1H NMR(D_2O) of HMF reaction with (0.5 eq) NaOH (Table 4, Entry 3).

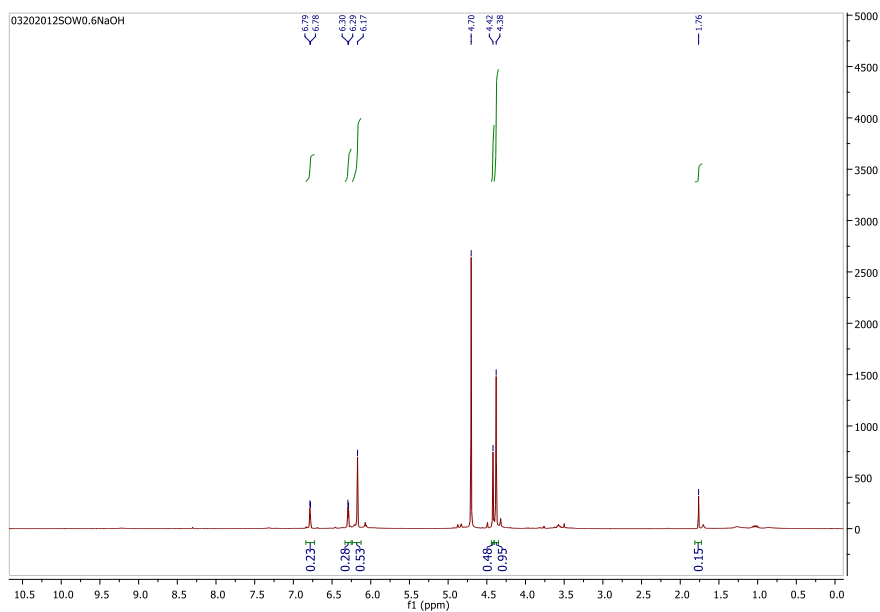


Fig S29: ^1H NMR(D_2O) of HMF reaction with (0.6 eq) NaOH (Table 4, Entry 4).

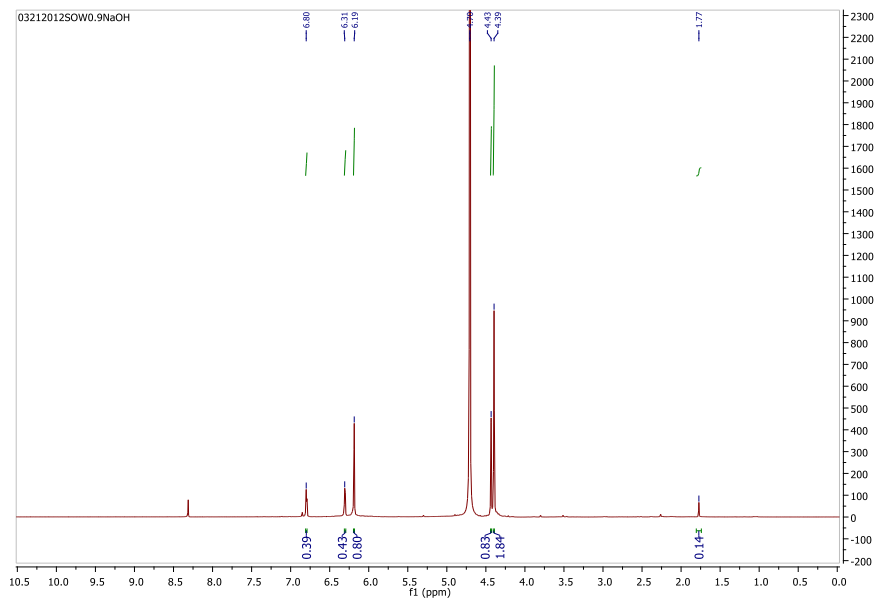


Fig S30: ^1H NMR(D_2O) of HMF reaction with (0.9 eq) NaOH (Table 4, Entry 5).

Chapter IV

Supporting Information

Organocatalyzed one-step synthesis of functionalized N-alkyl-pyridinium salts from biomass derived 5-hydroxymethylfurfural

Subbiah Sowmiah,^{a,b} Luís F. Veiros,^c José M. S. S. Esperança,^a Luís P.N. Rebelo,^a Carlos A.M. Afonso,^{b,*}

*^aInstituto de Tecnologia Química e Biológica António Xavier, Universidade Nova de Lisboa, Av. da República, 2780-157 Oeiras, Portugal. ^biMed. UL, Faculdade de Farmácia da Universidade de Lisboa, Av. Prof. Gama Pinto, 1640-003 Lisboa, Portugal. ^cCentro de Química Estrutural, Complexo I, Instituto Superior Técnico, Universidade de Lisboa, Av. Rovisco Pais 1, 1049-001 Lisboa, Portugal
Email: carlosafonso@ff.ul.pt*

Experimental:

General:

All reagents were purchased from Sigma-Aldrich, Alfa Aesar and Merck and were used without further purification. 5-hydroxymethyl furfural was synthesised in the laboratory using commercially available fructose¹. The

¹ Simeonov, S. P.; Coelho, J. A. S.; Afonso, C. A. M.; *ChemSusChem*, **2012**, *5*, 1388.

compounds were characterized: a) by NMR in a Bruker Avance II 400 Ultrashield Plus; NMR Bruker 300; b) by elemental analysis performed in a Flash 2000 CHNS-O analyser (ThermoScientific, UK) at the Faculty of Pharmacy, University of Lisbon; c) by measuring the melting point in a Stuart SMP10 apparatus; and d) by MS/MS experiments performed on Micromass® Quattro Micro triple Quadrupole (Waters®, Ireland) with an electrospray (ESI) ion source and by d) HRMS experiments performed in a LTQ Orbitrap XL mass spectrometer (Thermo Fischer Scientific, Bremen, Germany) controlled by LTQ Tune Plus 2.5.5 and Xcalibur 2.1.0. The capillary voltage of the electrospray ionization (ESI) was set to 3000 V. The capillary temperature was 275°C. The sheath gas flow rate (nitrogen) was set to 5 (arbitrary unit as provided by the software settings). The capillary voltage was 36 V and the tube lens voltage 110 V.

Preparation of 5-Hydroxymethylfurfural (5-HMF) ¹:

Water (0.9ml) was added to 9.1g of Et₄NBr (1% water content w/w). and the resulting mixture (10g, 10% water content w/w) was mixed with 2g of fructose (available from local commerce) and 0.2g of smashed Amberlyst-15® (10% w/w). The mixture was placed at 80 °C and heated up to 100 °C for 10 min and was then stirred at 100 °C for 15 min. Next, the mixture was cooled down to room temperature and the water was evaporated. The resulting solid was washed with EtOAc (50 ml). The solvent was decanted and the solid was dissolved in hot EtOH (2 ml) and then EtOAc (200ml) was added under vigorous stirring. The resulting precipitate was filtered out and the combined solutions were filtered through a pad of silica gel (10g)

Supporting details

and evaporated to yield a brown liquid of HMF (1.25g, 91%) with a purity of 97% as determined by NMR (Fig S1).

^1H NMR for HMF (CDCl_3 , 400 MHz): δ 9.56 (s, 1H), 7.51, 6.59 (d, 2H), 4.54 (s, 2H)

Optimization of reaction condition

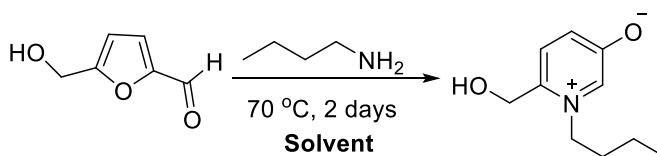
1.1 Solvent Screening:

With the synthesized HMF, the screening of various solvents was performed for the product formation at 70 °C for 2 days using *n*-butylamine as model substrate.

A representative procedure for solvent screening:

To a series of sample vials was added 100 mg of HMF (0.100g, 0.8 mmol) in each vial, followed by the solvent (2 mL), 1.1 equivalent of butylamine. The pH of the reaction mixture was measured and the mixture was heated in a closed vial at 70 °C for 2 days. The reaction was monitored by TLC (ethylacetate/methanol 3:7) to analyse the product formation (assigned as Yes in the Table SI-1).

Table SI-1: Solvents screening



Entry	Solvent	Reaction pH	Observation
1	EtOH	9.5	Yes

2	H ₂ O	9.5	Yes
3	EtOH:H ₂ O (1:1)	12	Yes
4	Ethylacetate*	9.5	No
5	Acetonitrile*	9.5	No
6	Butylamine	12	No
7	Dichloromethane*	9.5	No
8	EtOH:Butylamine (1:1)	10	No
9	t-Butanol*	6	No
10	t-Butanol:Butylamine (1:1)	10	No
11	1-Propanol	9.5	Yes
12	MeOH:H ₂ O (1:1)	11	Yes

*excess of butylamine was added to enhance the reaction completion.

1.2 Screening of Catalysts:

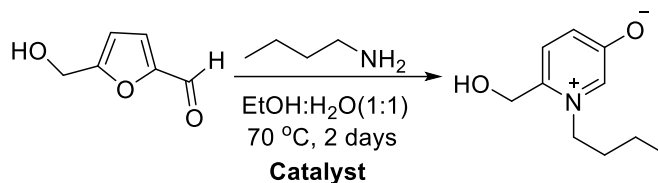
We screened some inorganic bases having Li, K, Na, Ca as catalysts for the reactions and observed ineffective results with no product formation. We then performed a screening with several Lewis acids, inorganic salts and acids to obtain better reaction conditions.

A representative procedure for catalyst screening:

To a series of sample vials was added 100 mg of HMF (0.100g, 0.8 mmol) in EtOH:H₂O as solvent (2 mL) in each vial, added 1.1 equivalent of butylamine and catalyst (30 mol %) and the mixture was heated in a closed

vial at 70 °C for 2 days. The reaction was monitored by TLC (ethylacetate/methanol 3:7). After the reaction was complete, the solvent was evaporated completely from the reaction mixture and acetonitrile (0.8 mmol, 1 equiv) was added to serve as an internal standard for proton NMR analysis.

Table SI-2. Screening of Catalysts



Entry	Catalyst (30 mol %)	NMR Yield at 70 deg (%)	Reference Spectras
1	Blank	17-20	<i>Fig S2</i>
2	KHCO ₃	18	<i>Fig S3</i>
3	K ₂ CO ₃	6	<i>Fig S4</i>
4	Ca(OH) ₂	22	<i>Fig S5</i>
5	MgO	33	<i>Fig S6</i>
6	CsCl	40	<i>Fig S7</i>
7	NaHCO ₃	11	<i>Fig S8</i>
8	NaOH*	11	<i>Fig S9</i>
9	CH ₃ ONa	3	<i>Fig S10</i>
10	Li ₂ CO ₃ *	NR	-
11	DBU	18	<i>Fig S11</i>

12	Cinchonidine	13	<i>Fig S12</i>
13	Urea	20	<i>Fig S13</i>
14	2,6 Lutidine	15	<i>Fig S14</i>
15	MnO ₂	7	<i>Fig S15</i>
16	CuCl ₂ .2H ₂ O	33	<i>Fig S15</i>
17	LaCl ₃ .2H ₂ O	40	<i>Fig S17</i>
18	SnCl ₂ .2H ₂ O	48	<i>Fig S18</i>
19	ZnCl ₂ *	0	-
20	Dy(OTf) ₃	41	<i>Fig S19</i>
21	Cu(OTf) ₂	34	<i>Fig S20</i>
22	GdCl ₃ .6H ₂ O	41	<i>Fig S21</i>
23	CeCl ₃ .7H ₂ O	39	<i>Fig S22</i>
24	FeCl ₃ .6H ₂ O*	NR	-
25	KBO ₂ 1.5H ₂ O	8	<i>Fig S23</i>
26	KH ₂ PO ₄	66	<i>Fig S24</i>
27	K ₃ PO ₄	7	<i>Fig S25</i>
28	BINAP	53	<i>Fig S26</i>
29	NH ₄ Cl	66	<i>Fig S27</i>
30	NH ₄ Ac	61	<i>Fig S28</i>
32	HCOONa	20	<i>Fig S29</i>

Supporting details

32	KOAc	32	<i>Fig S30</i>
33	NaOAc*	22	<i>Fig S31</i>
34	Na ₂ HPO ₄	27	<i>Fig S32</i>
35	Sod. Citrate	16	<i>Fig S33</i>
36	N(Et) ₃ Br	22	<i>Fig S34</i>
37	N(Bu) ₄ I*	12	<i>Fig S35</i>
38	Acetic acid	70	<i>Fig S36</i>
39	H ₃ BO ₃ (Boric Acid)*	8	<i>Fig S37</i>
40	tertbutylacetic acid	40	<i>Fig S38</i>
41	trifluoroacetic acid	60	<i>Fig S39</i>
42	Formic acid	57	<i>Fig S40</i>
43	Hydrochloric acid	35	<i>Fig S41</i>
44	Sulphuric acid	65	<i>Fig S42</i>
45	4-toluene sulphonic acid	25	<i>Fig S43</i>
46	Phosphoric acid	74	<i>Fig S44</i>
47	Triflic Acid	66	<i>Fig S45</i>

*excess of butylamine was added to enhance the reaction completion

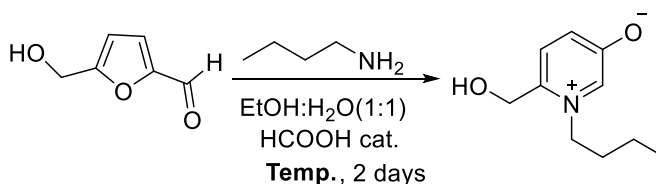
1.3 Screening of catalysts with varying temperature

With those catalysts that provided better yields, we continued to screen by varying temperatures that doesnot lead to the decomposition of HMF (70-80 °C).

A representative procedure for screening:

To a series of sample vials added 100 mg of HMF (0.100g, 0.8 mmol) in EtOH:H₂O as solvent (2 mL) in each, added 1.1 equivalent of butylamine and catalyst (30 mol %) and the mixture was heated in a closed vial at 80 °C for 2 days. The reaction was monitored by TLC (ethylacetate/methanol 3:7). After the reaction was complete, the solvent was evaporated completely from the reaction mixture and acetonitrile (0.8 mmol, 1 equiv) was added to serve as an internal standard for proton NMR analysis.

Table SI-3. Screening of catalysts with varying temperature



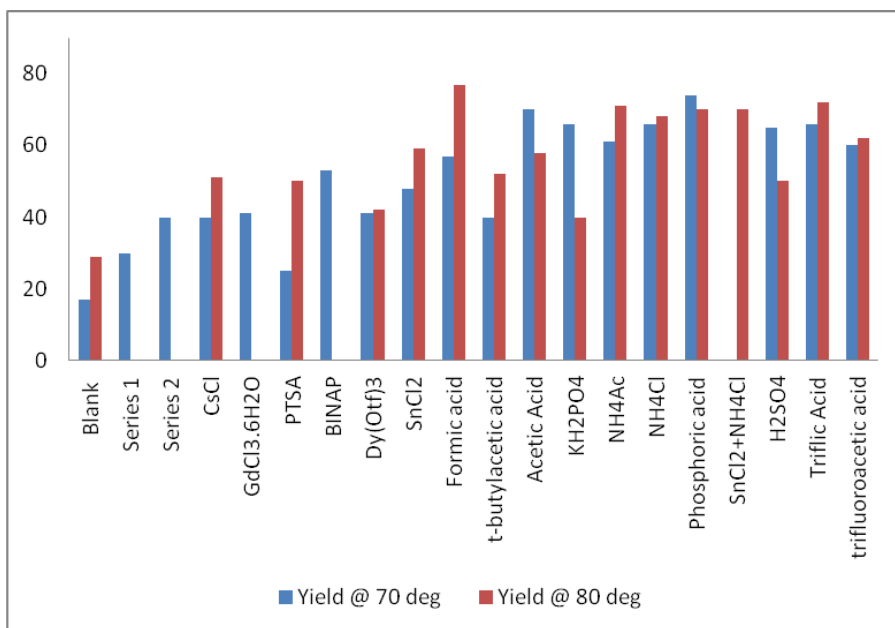
S. No	Catalyst (30 mol%)	NMR Yield at 70 °C, 2 days	NMR Yield at 80 °C, 2 days	Reference Spectras
1	Blank	17-20	29	<i>Fig S46</i>
2	Acetic Acid	70	58	<i>Fig S47</i>

Supporting details

3	Formic acid	57	77	<i>Fig S48</i>
4	Phosphoric acid	74	70	<i>Fig S49</i>
5	Trifluoro acetic acid	60	62	<i>Fig S50</i>
6	Triflic Acid	66	72	<i>Fig S51</i>
7	NH ₄ Ac	61	71	<i>Fig S52</i>
8	SnCl ₂ +NH ₄ Cl	-	70	<i>Fig S53</i>
9	SnCl ₂	48	59	<i>Fig S54</i>
10	NH ₄ Cl	66	68	<i>Fig S55</i>
11	Sulphuric acid	65	50	<i>Fig S56</i>
12	t-butylacetic acid	40	52	<i>Fig S57</i>
13	KH ₂ PO ₄	66	40	<i>Fig S58</i>
14	PTSA	25	50	<i>Fig S59</i>
15	Dy(Otf) ₃	41	42*	<i>Fig S60</i>
16	CsCl	40	51*	<i>Fig S61</i>

*excess of butylamine was added to enhance the reaction completion.

Overview of selected catalyst screening



Series 1: 2,6-Lutidine, DBU, HCO₂Na, Urea, Ca(OH)₂, N(Et)₃Br, NaOAc, Na₂HPO₄

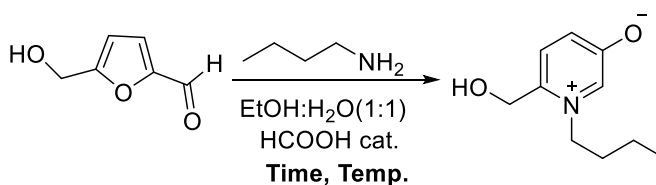
Series 2: KOAc, MgO, CuCl₂. 2H₂O, HCl, Cu(OTf)₂, CsCl, t-butylacetic acid

1.4 Screening of catalysts for specific time and temperature:

With those catalysts that provided better yields, we continued to screen for specific conditions by varying time and temperature to obtain the more efficient reaction conditions.

A representative procedure for specific time and temperature

To a series of sample vials added 100 mg of HMF (0.100g, 0.8 mmol) in EtOH:H₂O as solvent (2 mL) in each, added 1.1 equivalent of butylamine and catalyst (30 mol %) and the mixture was heated in a closed vial at specified temperature (70 °C/80 °C) for 2/3 days as mentioned. The reaction was monitored by TLC (ethylacetate/methanol 3:7). After the reaction was complete, the solvent was evaporated completely from the reaction mixture and acetonitrile (0.8 mmol, 1 equiv) was added to serve as an internal standard for proton NMR analysis. **Table SI-4.** Screening of catalysts for specific time and temperature



Catalyst (30 mol %)	70 deg @ 2 days	70 deg @ 3 days	80 deg @ 2 days	80 deg @ 3 days
Blank	17	21 <i>Fig S62</i>	29	34 <i>Fig S68</i>
Acetic acid	70	63 <i>Fig S63</i>	58	75 <i>Fig S69</i>
Formic acid	57	64 <i>Fig S64</i>	77	93 <i>Fig S70</i>
Phosphoric acid	74	69 <i>Fig S65</i>	70	72 <i>Fig S71</i>
Trifluoroacetic acid	60	66 <i>Fig S66</i>	62	80 <i>Fig S72</i>
Triflic acid	66	67 <i>Fig S67</i>	72	76 <i>Fig S73</i>

Substrate Scope Study:

2.1 Reactions with alkyl amines

With the optimized reaction conditions, we were also able to synthesize new ionic liquids by varying the amine substrates.

A representative procedure for substrate with alkyl amines:

To 100 mg of HMF (0.100g, 0.8mmol) in ethanol:water(1:1, 10 mL), 1.1 equivalent of alkyl amine and catalytic amount of formic acid (30 mol %) were added. The mixture was heated in a closed high pressure vessel at 80 °C. The reaction was monitored by TLC (ethylacetate/methanol 3:7). After the reaction was complete, the reaction mixture is diluted with 50ml water and stirred well with activate charcoal and then passed through the celite filter funnel. The filtrate is cleared from the coloured impurities and water is completely evaporated to give the isolated derivative. In some cases, we observed some known impurities along with the products such as starting material amines. The spectral data of these isolated derivatives are from the filtrate without further purification.

Table SI-5. Reactions with various alkyl amines

$\text{HMF (1)} \xrightarrow[\text{HCOOH (30 mol \%), 80 }^\circ\text{C}]{\text{EtOH:H}_2\text{O(1:1), R-NH}_2} \text{2a-h}$

entry	R	Time h	Temp °C	Yield %	Ref. data
1	$\text{H}_3\text{C-NH}_2$	48	80	78	Fig. S74- Fig S77
2		48	80	81	Fig S78- Fig S81
3		48	80	82	Fig S82- Fig S85
4		48	80	72	Fig S86- Fig S89
5		72	80	55	Fig S90- Fig S93
6		72 ^a	80	30	Fig S94- Fig S97
7		48	80	77	Fig S98- Fig S101
8		48	80	62	Fig S102- Fig S104

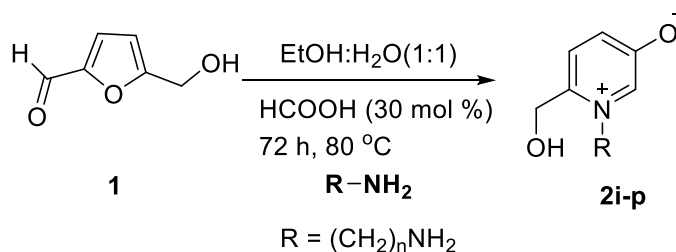
Reaction condition: To 100 mg of HMF (0.8 mmol) in EtOH/H₂O (1:1, 10 mL), was added 1.1 equiv of respective amine, HCO₂H (30 mol %) and the mixture was heated in a closed high pressure vessel at 80 °C for 2 days. ^a 1 equiv of HCOOH was used.

2.2 Reactions with alkyl diamines

A representative procedure for substrate with alkyl diamines:

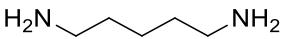
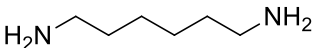
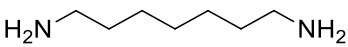
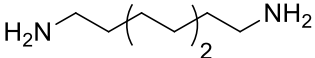
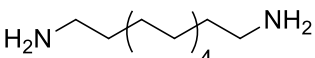
To 100 mg of HMF (0.100g, 0.8mmol) in ethanol:water(1:1, 10 mL), added 1.1 equivalent of alkyl diamine, catalytic amount of formic acid (30 mol %) and the mixture was heated in a closed high pressure vessel at 80 °C for 3 days. The reaction was monitored by TLC (ethylacetate/methanol 3:7). After the reaction was complete, the reaction mixture is diluted with 50ml water and stirred well with activate charcoal and then passed through the celite filter funnel. The filtrate is clear from the coloured impurities and water is completely evaporated to give the isolated derivative. In some cases, we observed some known impurities along with the products such as starting material amines. The spectral data of these isolated derivatives are from the filtrate without further purification.

Table SI-6. Substrate scope with various diamines



Entry	R	Time h	Temp °C	Yield %	Ref. data
9		72	80	61	Fig S105-Fig S107
10		72	80	72	Fig S108-Fig S111
11		72	80	80	Fig S112-Fig

Supporting details

					S114
12		72	80	70	Fig S115-Fig S117
13		72	80	69	Fig S118-Fig S121
14		72	80	63	Fig S122-Fig S125
15		72	80	59	Fig S126-Fig S129

Reaction condition: To 100 mg of HMF (0.8 mmol), in EtOH/H₂O (1:1, 10 mL), was added 1.1 equiv of respective amine, HCO₂H (30 mol %) and the mixture was heated in a closed high pressure vessel at 80 °C for 3 days.

Isotopic water experiment:

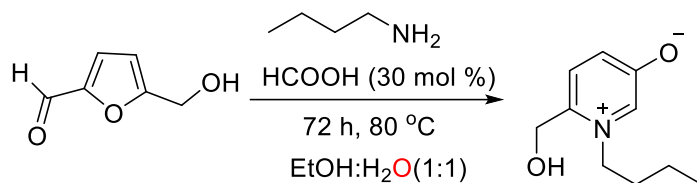
A series of experiments were performed in order to calculate the minimal amount of water necessary to obtain the product.

Representative procedure for isotopic experiment:

To 100 mg of HMF (0.100g, 0.8 mmol), added 1.1 equivalent of butyl amine, catalytic amount of formic acid (30 mol %) with ethanol: 99% H₂O¹⁸ (1:1) solvent and the mixture was heated in a closed vial at 80 °C for specified time. For comparison purpose, we simultaneously performed a blank reaction with distilled H₂O. In both set of experiments, weighed quantity of H₂O/(H₂O¹⁸):EtOH were used. The minimal quantity of isotope

water to be used for the product formation was analyzed by a small screening with non-isotope water.

Table SI-7. Screening for minimal water



S.No	EtOH	Water	Temp (°C)	Time (h)	Reaction
1*	1 drop*	1 drop	80	48	NR
2	1ml	1 drop	80	48	NR
3	1ml	2 drops	80	48	NR
4	1ml	3 drops	80	48	NR
5*	1drop	1drop	80	48	NR
6	2drops	2 drops	80	48	NR
7	4drops	4drops	80	24	traces
8	4drops (0.167g)	4 drops (0.322g)	80	12	Complete
9	0.5 ml (0.0471 g)	0.25 ml (0.0338 g)	80	12	Complete
10	0.5ml	0.6ml	80	RT (1hr), Heat 4hr	Reaction not completed
11	2 drops	4 drops	80	12	Complete
12	4drops (0.167g)	4 drops[#] (0.322g)	80	12	Complete (Fig S130)

Reaction Conditions: To 20 mg of HMF (0.02 g, 0.16 mmol), added 1.1 equiv of butylamine with weighed solvent and the mixture was heated in a closed vial at 80 °C for specified time. *Reaction performed with 10 mg HMF with similar reaction conditions. NR – No reaction observed. # Reaction with 99% H₂O¹⁸.

Spectral data

6-(hydroxymethyl)-1-methylpyridinium-3-olate 2a

(86.8 mg, 78% yield); Pale yellow liquid; ^1H NMR (300 MHz, D_2O): δ ^1H NMR (400 MHz, D_2O) δ 8.32 (s, 1H), 7.73 (d, $J = 2.0$ Hz, 1H), 7.50 (d, $J = 8.9$ Hz, 1H), 7.42 – 7.35 (m, 1H), 4.68 (s, 2H), 4.01 (s, 3H). ^{13}C NMR (100 MHz, D_2O): δ 170.0, 141.0, 135.0, 132.7, 127.0, 118.8, 58.3, 43.9. HRMS - MS-CI: m/z Found 140.0710 for $\text{C}_7\text{H}_{10}\text{NO}_2$

6-(hydroxymethyl)-1-propylpyridinium-3-olate 2b

(108.4 mg, 81% yield); Pale yellow liquid; ^1H NMR (300 MHz, D_2O): δ ^1H NMR (400 MHz, D_2O) δ 8.30 (s, 1H), 7.79 (s, 1H), δ 7.54 (d, $J = 8.8$ Hz, 1H), 7.41 (d, $J = 8.6$ Hz, 1H), 4.71 (s, 2 H) 4.22 (t, $J = 7.6$ Hz, 2H), 1.97 (m, 2H), 0.91 – 0.71 (t, $J = 7.6$, 3H). ^{13}C NMR (100 MHz, D_2O): δ 170.0, 141.0, 134.8, 133.8, 128.4, 118.8, 60.4, 59.2, 25.9, 11.1. HRMS - MS-CI: m/z Found 167.0948 for $\text{C}_9\text{H}_{13}\text{NO}_2$

6-(hydroxymethyl)-1-butylpyridinium-3-olate 2c

(118.9 mg, 82% yield); Yellow liquid; ^1H NMR (300 MHz, D_2O): δ 8.30 (s, 1H), 7.67 (s, 1H), 7.46 (d, $J = 8.8$ Hz, 1H), 7.31 (d, $J = 8.9$ Hz, 1H), 4.66 (s, 2H), 4.22 (t, $J = 7.4$ Hz, 2H), 1.77 (m, 2H), 1.44 (m, 2H), 1.04 (t, $J = 7.4$ Hz, 3H), ^{13}C NMR (100 MHz, D_2O): δ 170.7, 164.48, 138.56, 135.07, 134.03, 128.46, 58.72, 56.67, 32.6, 18.9, 12.7. HRMS - MS-CI: m/z Found 182.1171 for $\text{C}_{10}\text{H}_{16}\text{NO}_2$

6-(hydroxymethyl)-1-pentylpyridinium-3-olate 2d

(112.5 mg, 72% yield); Yellow liquid; ^1H NMR (400 MHz, D_2O) δ 8.26 (s, 1H), 7.68 (d, $J = 2.4$ Hz, 1H), 7.44 (d, $J = 8.9$ Hz, 1H), 7.30 (dd, $J = 8.9, 2.4$ Hz, 1H), 4.62 (s, 2H), 4.18 (t, $J = 7.4$ Hz, 2H), 1.77 – 1.66 (m, 2H), 1.15 (m, 4H), 0.67 (t, $J = 6.7$ Hz, 3H). ^{13}C NMR (100 MHz, D_2O): δ 170.7, 163.6, 139.2, 134.8, 133.8, 128.4, 58.7, 56.9, 30.3, 27.7, 21.5, 13.1. HRMS - MS-CI: m/z Found 196.1329 for $\text{C}_{11}\text{H}_{18}\text{NO}_2$

6-(hydroxymethyl)-1-hexylpyridinium-3-olate 2e

(92.1 mg, 55% yield); Brown liquid; ^1H NMR (400 MHz, D_2O) δ 8.28 (s, 1H), 8.07 (d, $J = 1.8$ Hz, 1H), 7.67 (m, 2H), 4.73 (s, 2H), 4.30 (t, $J = 7.4$ Hz, 2H), 1.72 – 1.82 (m, 2H), 1.38 – 1.4 (m, 2H), 1.1 – 1.18 (m, 4H), 0.7 – 0.82 (t, 3H). ^{13}C NMR (100 MHz, D_2O): δ ^{13}C NMR (75 MHz, D_2O) δ 170.5, 165.5, 137.6, 134.9, 134.2, 128.5, 58.7, 56.6, 30.8, 30.5, 26.7, 25.3, 13.3. HRMS - MS-CI: m/z Found 210.1484 for $\text{C}_{12}\text{H}_{20}\text{NO}_2$

6-(hydroxymethyl)-1-octylpyridinium-3-olate 2f

(57 mg, 30% yield); Pale yellow liquid; ^1H NMR (300 MHz, D_2O) δ 8.44 (s, 1H), 7.59 (d, $J = 2.7$ Hz, 1H), 7.33 (d, $J = 8.9$ Hz, 1H), 7.01 (dd, $J = 8.9, 2.5$ Hz, 1H), 4.65 (s, 2H), 4.38 – 4.09 (m, 2H), 1.79 (m, 2H), 1.49 (m, 2H), 1.26 (m, 8H), 0.98 – 0.56 (t, 3H). ^{13}C NMR (100 MHz, D_2O): δ 170.6, 157.18, 141.71, 134.8, 134.3, 128.7, 58.85, 56.75, 31.65, 29.06, 28.99, 28.96, 27.25, 22.94, 14.02. HRMS - MS-CI: m/z Found 238.1796 for $\text{C}_{14}\text{H}_{24}\text{N}_2\text{O}_2$

1-allyl-6-(hydroxymethyl)pyridinium-3-olate 2g

(101.8 mg, 77% yield); Yellow liquid; ^1H NMR (400 MHz, D_2O) δ 8.29 (s, 1H), 7.74 (s, 1H), 7.54 (d, $J = 8.8$ Hz, 1H), 7.42 (d, $J = 8.7$ Hz, 1H), 5.92 (m, 1H), 5.27 (t, $J = 10.3$ Hz, 1H), 5.04 – 4.83 (m, 3H), 4.65 (s, 2H). ^{13}C NMR (100 MHz, D_2O): δ 170.8, 163.3, 140.1, 135.0, 134.2, 130.5, 128.2, 119.4, 58.7, 58.6. HRMS - MS-Cl: m/z Found 166.0836 for $\text{C}_9\text{H}_{12}\text{NO}_2$

6-(hydroxymethyl)-1-(3-methoxypropyl)pyridinium-3-olate 2h

(97.8 mg, 62% yield); Yellow liquid; ^1H NMR (400 MHz, D_2O) δ 8.33 (s, 1H), 7.68 (d, $J = 2.0$ Hz, 1H), 7.49 (d, $J = 8.9$ Hz, 1H), 7.39 – 7.28 (m, 1H), 4.65 (s, 2H), 4.36 (t, $J = 7.3$ Hz, 2H), 3.47 (t, $J = 5.8$ Hz, 2H), 3.24 (s, 3H), 2.10 (q, $J = 8$ Hz, 2H). ^{13}C NMR (100 MHz, D_2O): δ 170.9, 165.0, 138.4, 135.3, 134.5, 128.6, 69.7, 68.40, 58.76, 57.97, 29.98. HRMS - MS-Cl: m/z Found 198.1121 for $\text{C}_{10}\text{H}_{16}\text{NO}_3$

1-(3-aminopropyl)-6-(hydroxymethyl)pyridinium-3-olate 2i

(88.9 mg, 61% yield); Pale Yellow liquid; ^1H NMR (400 MHz, D_2O) δ 8.30 (s, 1H), 7.78 (d, $J = 2.6$ Hz, 1H), 7.54 (d, $J = 8.9$ Hz, 1H), 7.41 (dd, $J = 8.8, 2.7$ Hz, 1H), 4.70 (s, 2H), 4.30 – 4.10 (m, 2H), 1.89 – 1.62 (m, 2H), 1.54 (m, 2H). ^{13}C NMR (100 MHz, D_2O): δ 170.9, 164.0, 139.2, 134.9, 133.9, 128.5, 58.8, 56.8, 39.2, 29.2. HRMS - MS-Cl: m/z Found 183.1111 for $\text{C}_9\text{H}_{15}\text{N}_2\text{O}_2$

1-(4-aminobutyl)-6-(hydroxymethyl)pyridinium-3-olate 2j

(113 mg, 72% yield); Dark yellow liquid; ^1H NMR (400 MHz, D_2O) δ 8.29 (s, 1H), 7.58 (s, 1H), 7.37 (d, $J = 3.9$ Hz, 1H), 7.22 (s, 1H), 4.60 (s, 2H),

4.20 (t, $J = 7.4$ Hz, 2H), 1.76 (m, 2H), 1.33 (m, 4H). ^{13}C NMR (100 MHz, D_2O): δ 170.79, 165.7, 137.7, 135.1, 134.6, 128.7, 58.7, 55.8, 37.1, 27.5, 25.3. HRMS - MS-CI: m/z Found 197.1279 for $\text{C}_{10}\text{H}_{17}\text{N}_2\text{O}_2$

1-(5-aminopentyl)-6-(hydroxymethyl)pyridinium-3-olate 2k

(134.6 mg, 80% yield); Dark yellow liquid; ^1H NMR (400 MHz, D_2O) δ 8.26 (s, 1H), 7.56 (s, 1H), 7.36 (d, $J = 6.2$ Hz, 1H), 7.20 (d, $J = 8.4$ Hz, 1H), 4.59 (s, 2H), 4.18 (t, $J = 7.4$ Hz, 2H), 3.44 (m, 2H), 1.77 (d, $J = 5.2$ Hz, 2H), 1.42 (m, 4H), 1.35 – 1.12 (m, 2H). ^{13}C NMR (100 MHz, D_2O): δ 170.9, 165.6, 137.6, 135.3, 134.3, 128.5, 58.8, 56.8, 30.3, 27.7, 21.5, 13.0. HRMS - MS-CI: m/z Found 211.1436 for $\text{C}_{11}\text{H}_{19}\text{N}_2\text{O}_2$

1-(6-aminohexyl)-6-(hydroxymethyl)pyridinium-3-olate 2l

(125.6 mg, 70% yield); Yellow liquid; ^1H NMR (400 MHz, D_2O) δ 8.25 (s, 1H), 7.56 (s, 1H), 7.37 (dd, $J = 8.4, 1.9$ Hz, 1H), 7.25 – 7.11 (m, 1H), 4.59 (s, 2H), 4.16 (d, $J = 6.0$ Hz, 2H), 1.83 – 1.65 (m, 2H), 1.46 (m, 4H), 1.22 (m, 4H). ^{13}C NMR (100 MHz, D_2O): δ 170.7, 163.8, 134.9, 133.9, 128.5, 118.9, 58.7, 56.9, 39.4, 26.6, 25.2, 21.7, 13.2. HRMS - MS-CI: m/z Found 225.1605 for $\text{C}_{11}\text{H}_{21}\text{N}_2\text{O}_2$

1-(7-aminoheptyl)-6-(hydroxymethyl)pyridinium-3-olate 2m

(131.6 mg, 69% yield); Brown liquid; ^1H NMR (400 MHz, D_2O) δ 8.32 (s, 1H), 7.68 (d, $J = 2.7$ Hz, 1H), 7.47 (d, $J = 8.9$ Hz, 1H), 7.32 (dd, $J = 8.9, 2.8$ Hz, 1H), 4.67 (s, 2H), 4.30 – 4.17 (m, 2H), 2.92 – 2.79 (m, 2H), 1.90 – 1.67 (m, 2H), 1.64 – 1.41 (m, 8H), 0.85 – 0.56 (m, 4H). ^{13}C NMR (101 MHz,

Supporting details

D₂O) δ 170.6, 165.6, 137.5, 135.1, 134.2, 128.5, 58.6, 56.6, 41.1, 39.3, 30.4, 29.3, 27.5, 26.7, 25.2. HRMS - MS-CI: m/z Found 239.18 for C₁₃H₂₃N₂O₂

1-(8-aminooctyl)-6-(hydroxymethyl)pyridinium-3-olate 2n

(127.2, 63% yield); Brown liquid; ¹H NMR (400 MHz, D₂O) δ 8.28 (s, 1H), 7.56 (s, 1H), 7.38 (d, *J* = 8.9 Hz, 1H), 7.20 (d, *J* = 8.9 Hz, 1H), 4.59 (s, 2H), 4.17 (t, *J* = 7.5 Hz, 2H), 2.67 (dd, *J* = 12.6, 5.6 Hz, 2H), 1.71 (d, *J* = 6.7 Hz, 2H), 1.39 (m, 2H), 1.12 (m, 8H). ¹³C NMR (101 MHz, D₂O) δ 170.54, 165.68, 137.38, 135.06, 134.19, 128.48, 58.62, 57.21, 56.63, 39.57, 30.56, 27.96, 27.91, 27.89, 27.84, 27.79, 25.49, 25.44, 25.34, 16.78. HRMS - MS-CI: m/z Found 253.1902 for C₁₄H₂₅N₂O₂

1-(12-aminododecyl)-6-(hydroxymethyl)pyridinium-3-olate 2o

(145.6 mg, 59% yield); Brown liquid; ¹H NMR (400 MHz, D₂O) δ 8.25 (s, 2H), 7.55 (d, *J* = 2.5 Hz, 1H), 7.37 (d, *J* = 8.9 Hz, 1H), 7.20 (dd, *J* = 8.9, 2.4 Hz, 1H), 4.58 (s, 2H), 4.16 (t, *J* = 7.6 Hz, 2H), 2.77 (m, 2H), 1.72 (d, *J* = 7.4 Hz, 2H), 1.44 (m, 6H), 1.17 (m, 13H). ¹³C NMR (101 MHz, D₂O) δ 170.76, 165.55, 137.59, 135.18, 134.26, 128.54, 58.73, 56.65, 39.37, 30.39, 27.54, 26.64, 26.60, 25.24, 25.2. HRMS - MS-CI: m/z Found 309.2529 for C₁₈H₃₃N₂O₂

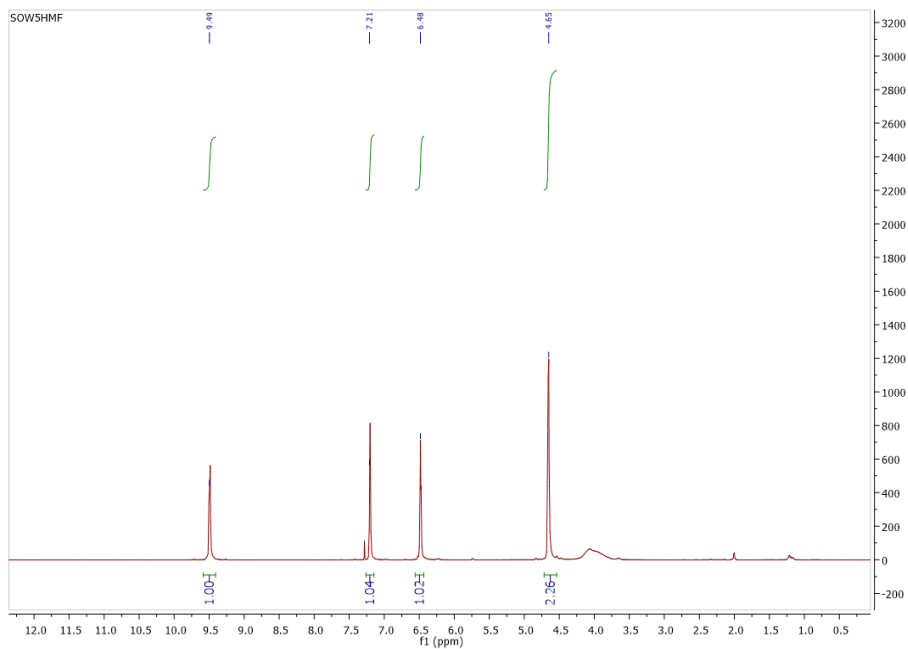


Fig S1: ^1H NMR(CDCl_3) of synthesized 5-hydroxymethyl furfural (HMF).

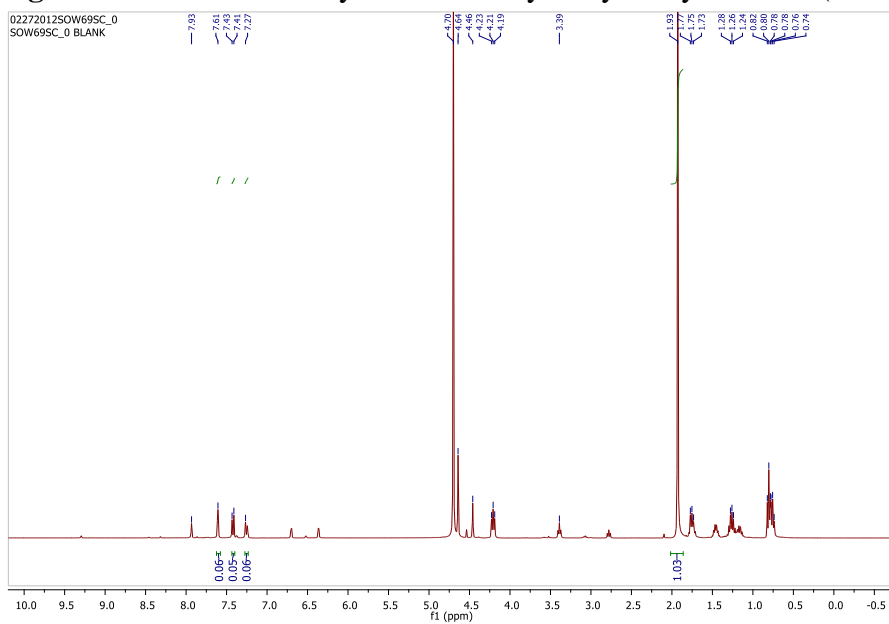


Fig S2: ^1H NMR(D_2O) of catalyst screening without any catalyst added.

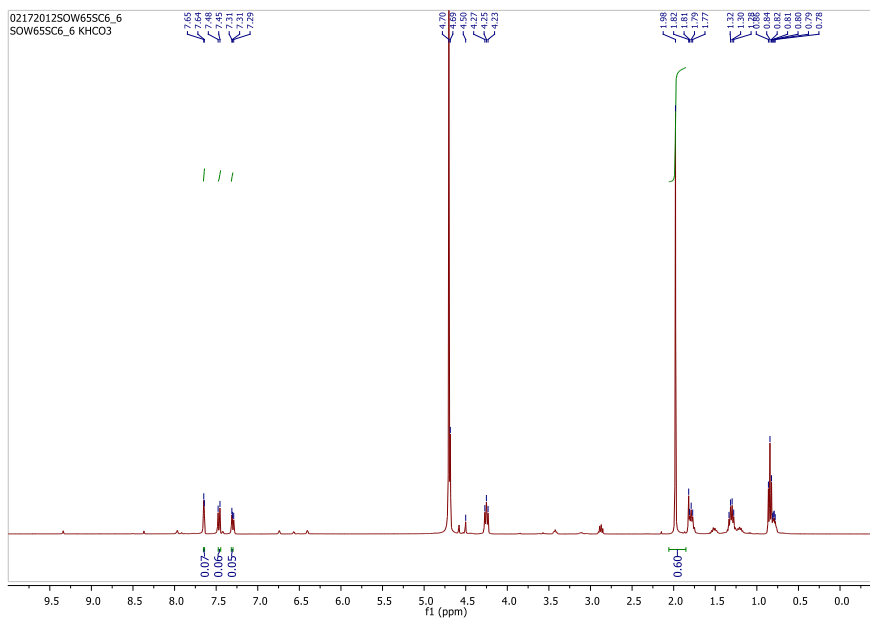


Fig S3: $^1\text{H NMR}_{(\text{D}_2\text{O})}$ of catalyst screening with KHCO_3 as catalyst.

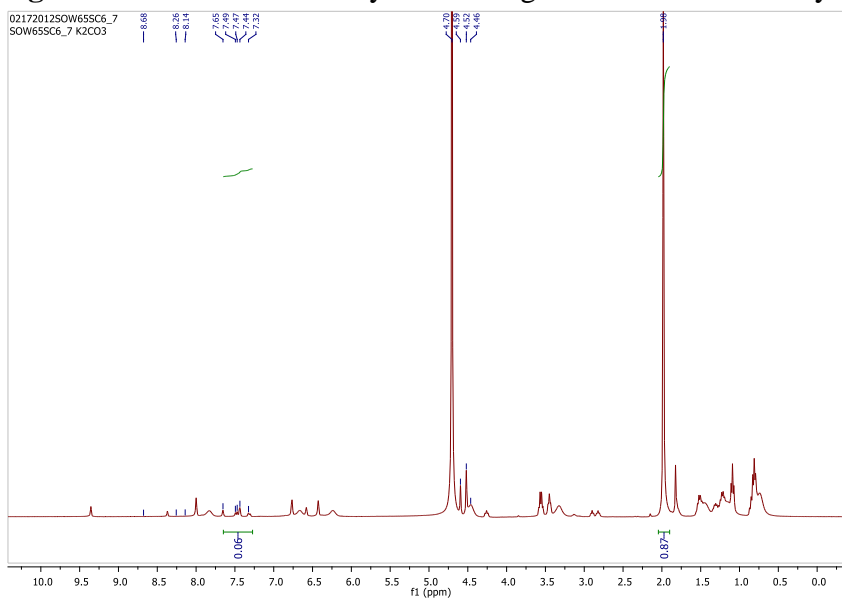


Fig S4: $^1\text{H NMR}_{(\text{D}_2\text{O})}$ of catalyst screening with K_2CO_3 as catalyst.

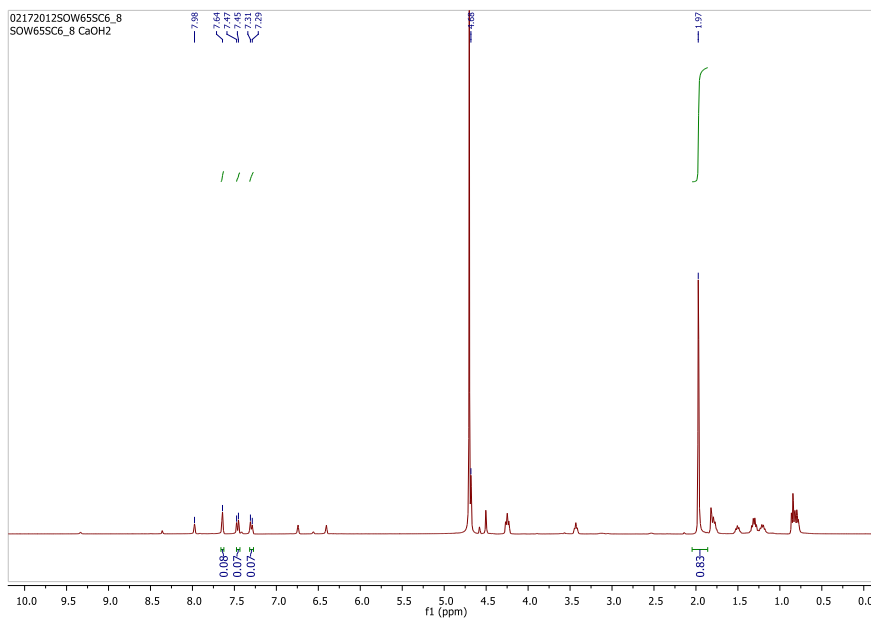


Fig S5: $^1\text{H NMR}_{(\text{D}_2\text{O})}$ of catalyst screening with $\text{Ca}(\text{OH})_2$ as catalyst

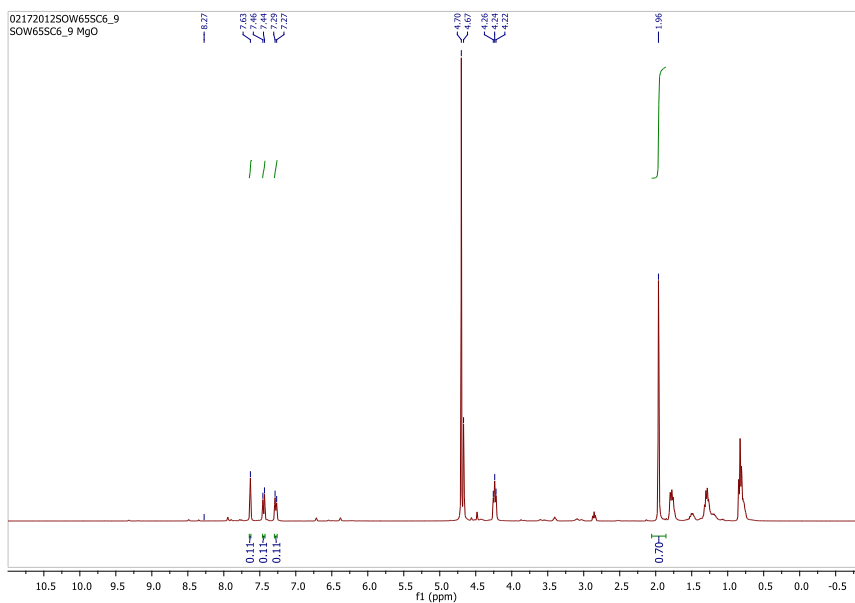


Fig S6: $^1\text{H NMR}_{(\text{D}_2\text{O})}$ of catalyst screening with MgO as catalyst

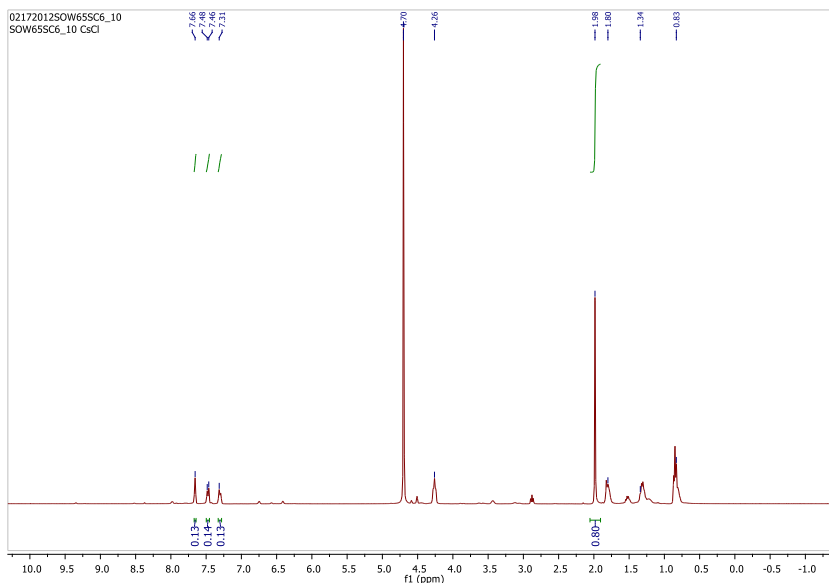


Fig S7: $^1\text{H NMR}_{(\text{D}_2\text{O})}$ of catalyst screening with CsCl as catalyst

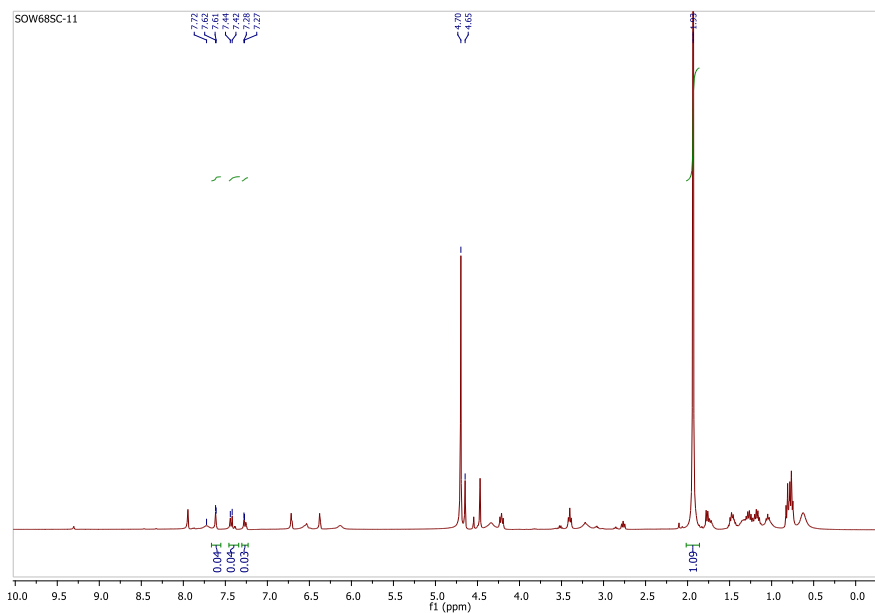


Fig S8: $^1\text{H NMR}_{(\text{D}_2\text{O})}$ of catalyst screening with NaHCO_3 as catalyst

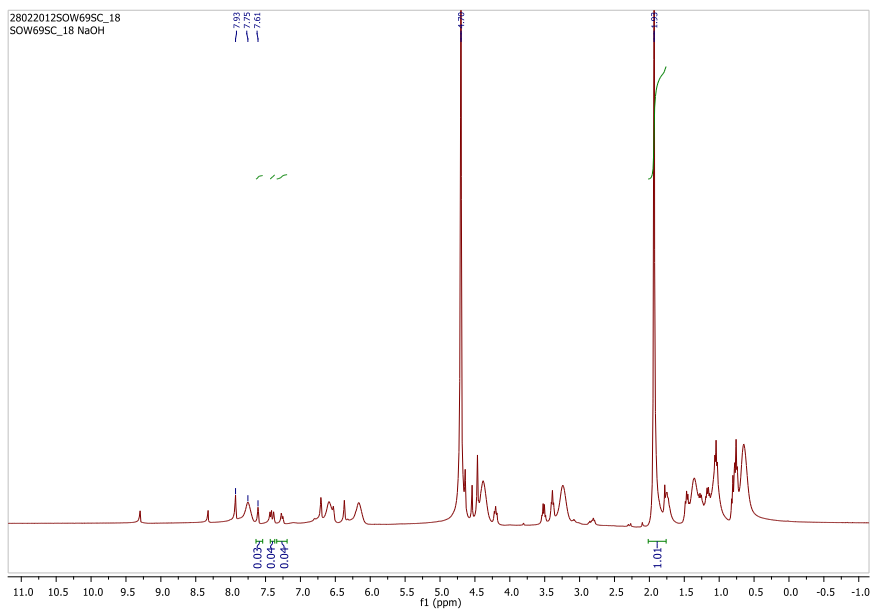


Fig S9: $^1\text{H NMR}_{(\text{D}_2\text{O})}$ of catalyst screening with NaOH as catalyst

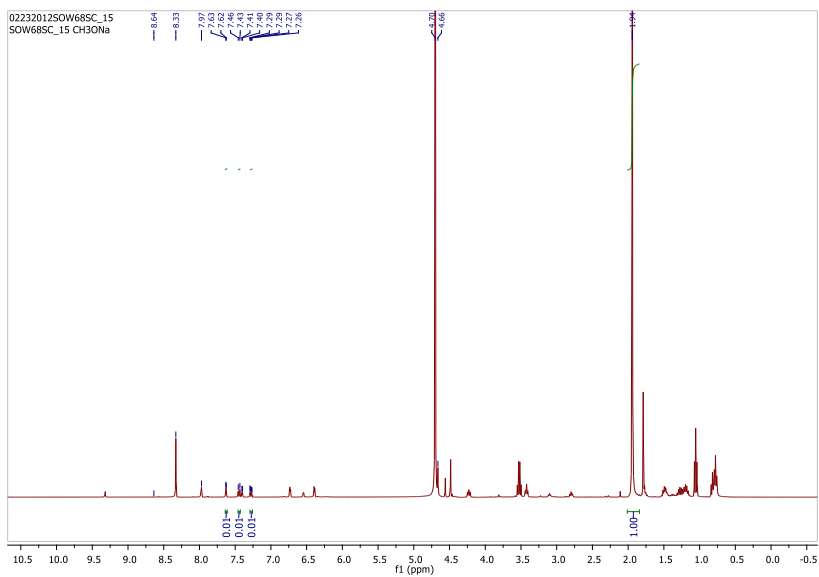


Fig S10: $^1\text{H NMR}_{(\text{D}_2\text{O})}$ of catalyst screening with CH_3ONa as catalyst

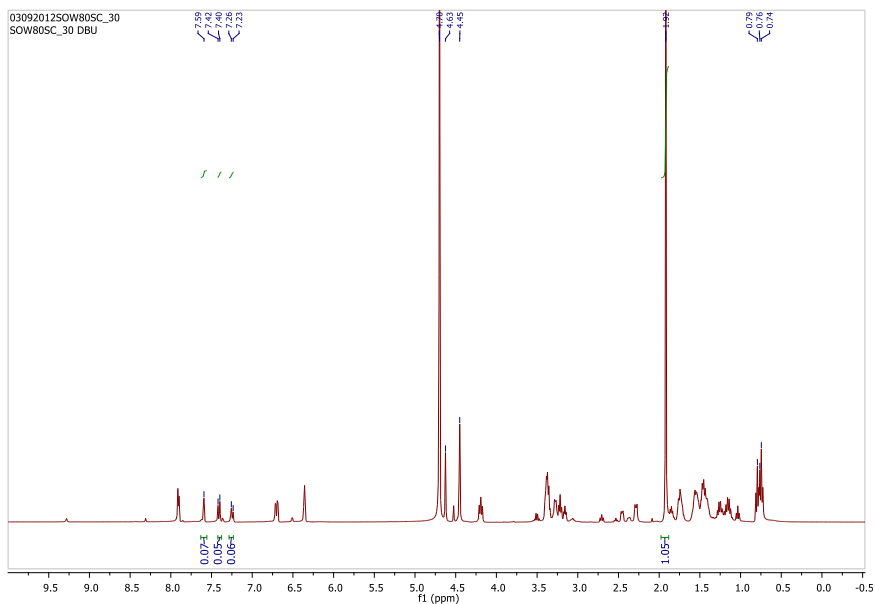


Fig S11: $^1\text{H NMR}_{(\text{D}_2\text{O})}$ of catalyst screening with DBU as catalyst

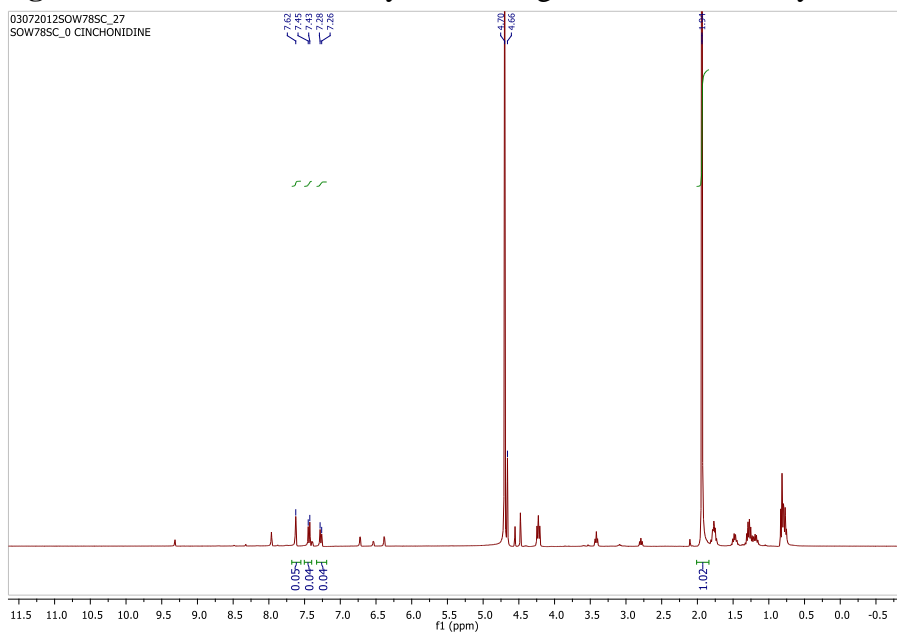


Fig S12: $^1\text{H NMR}_{(\text{D}_2\text{O})}$ of catalyst screening with Cinchonidine as catalyst

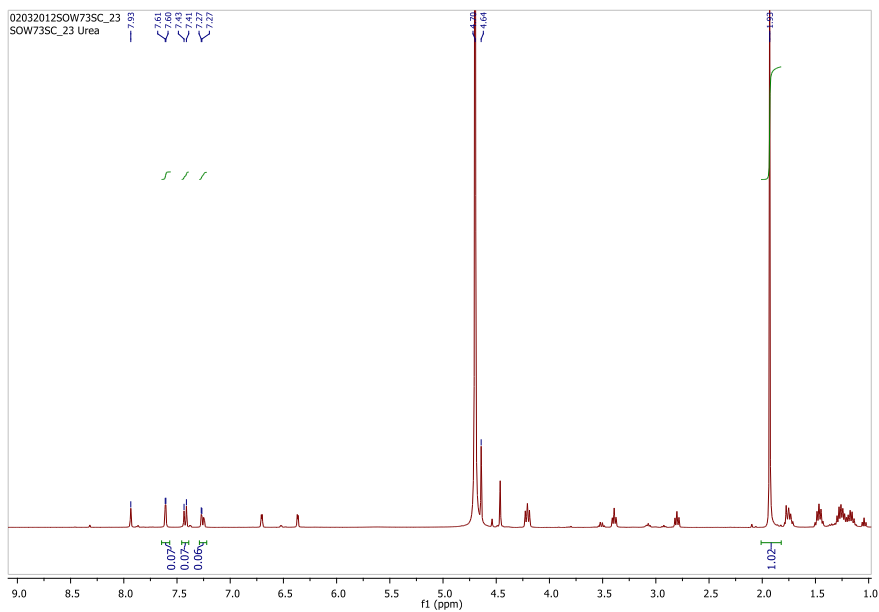


Fig S13: $^1\text{H NMR}_{(\text{D}_2\text{O})}$ of catalyst screening with Urea as catalyst

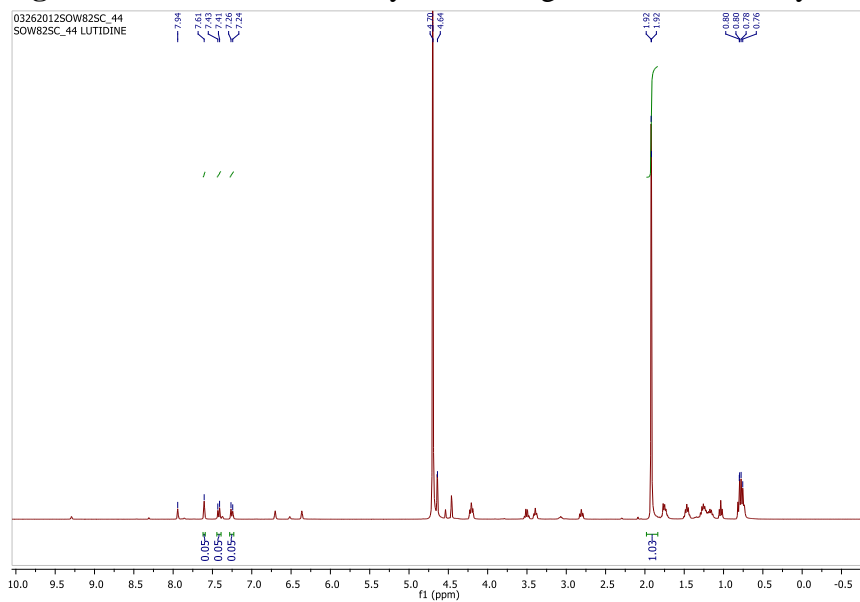


Fig S14: $^1\text{H NMR}_{(\text{D}_2\text{O})}$ of catalyst screening with Lutidine as catalyst

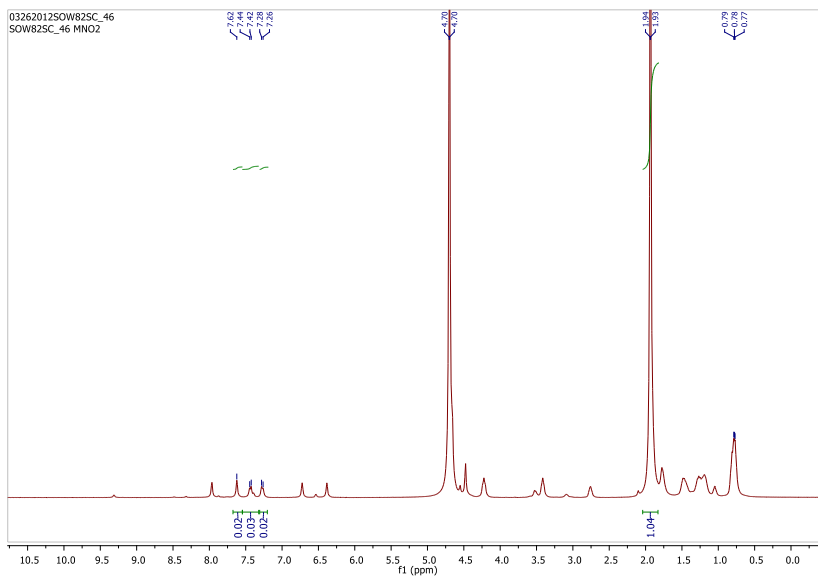


Fig S15: $^1\text{H NMR}_{(\text{D}_2\text{O})}$ of catalyst screening with MnO_2 as catalyst

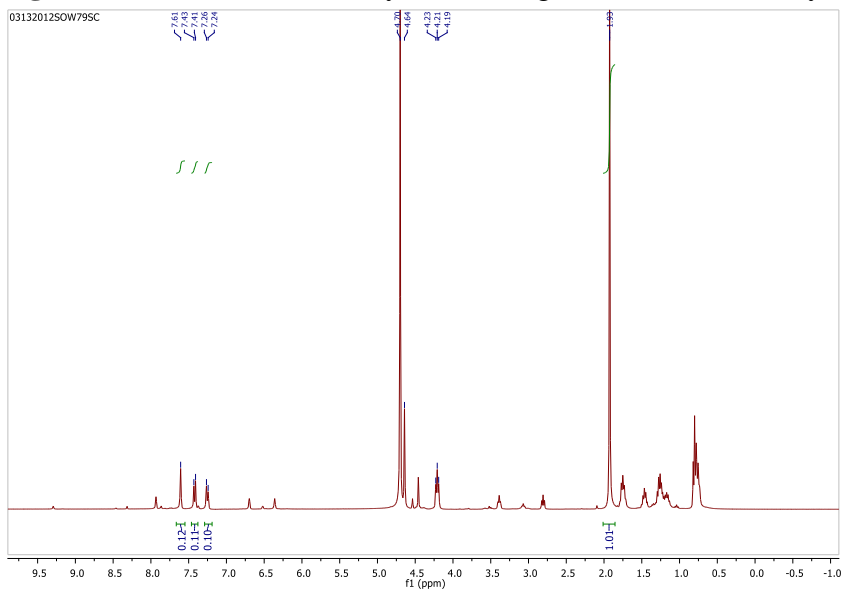


Fig S16: $^1\text{H NMR}_{(\text{D}_2\text{O})}$ of catalyst screening with $\text{CuCl}_2 \cdot 2\text{H}_2\text{O}$ as catalyst

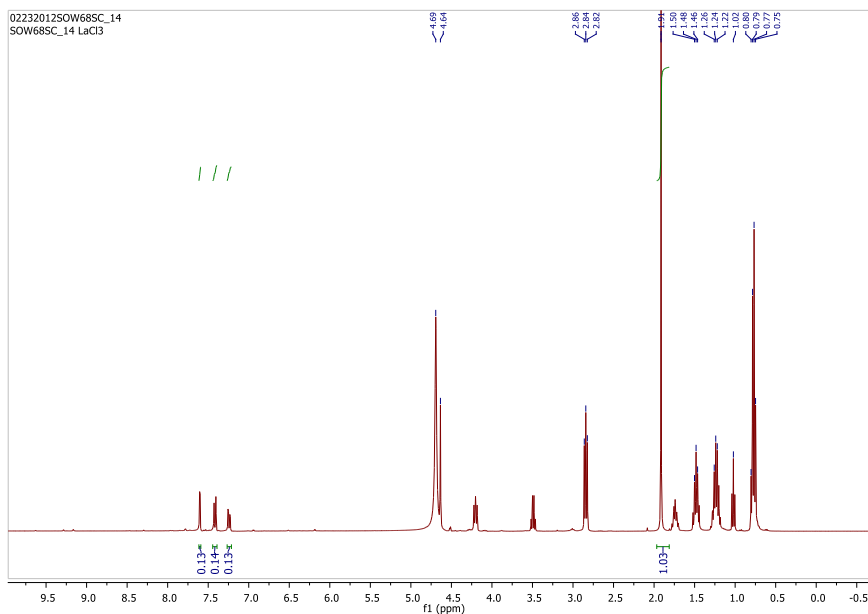


Fig S17: $^1\text{H NMR}_{(\text{D}_2\text{O})}$ of catalyst screening with $\text{LaCl}_3 \cdot 2\text{H}_2\text{O}$ as catalyst

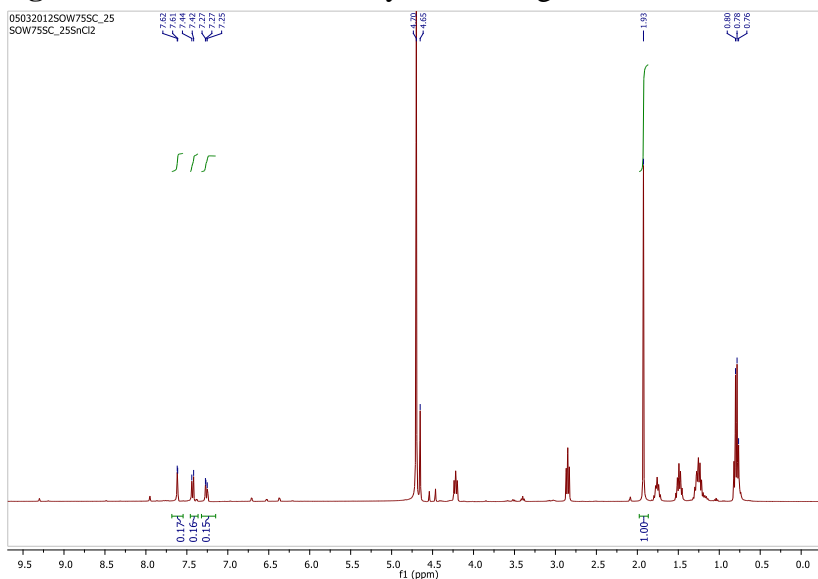


Fig S18: $^1\text{H NMR}_{(\text{D}_2\text{O})}$ of catalyst screening with $\text{SnCl}_2 \cdot 2\text{H}_2\text{O}$ as catalyst

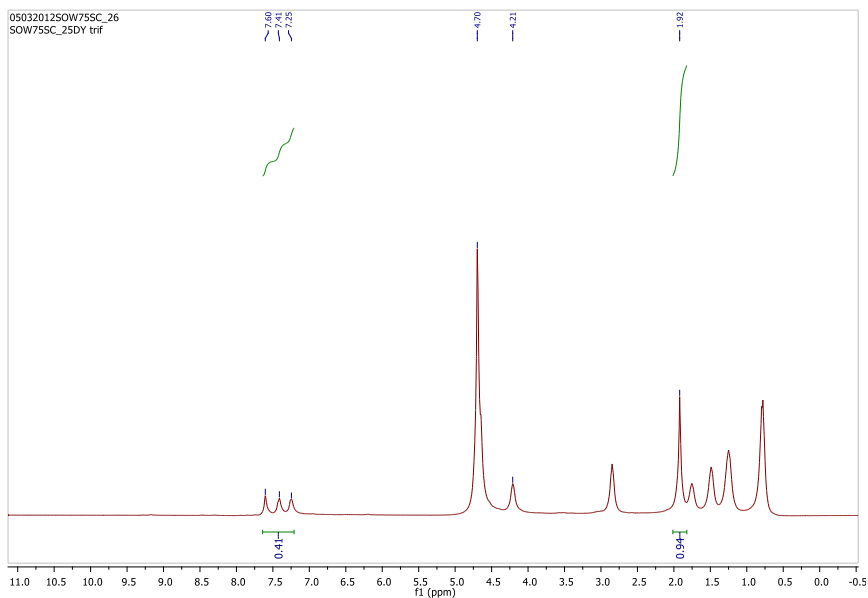


Fig S19: ^1H NMR(D_2O) of catalyst screening with $\text{Dy}(\text{OTf})_3$ as catalyst

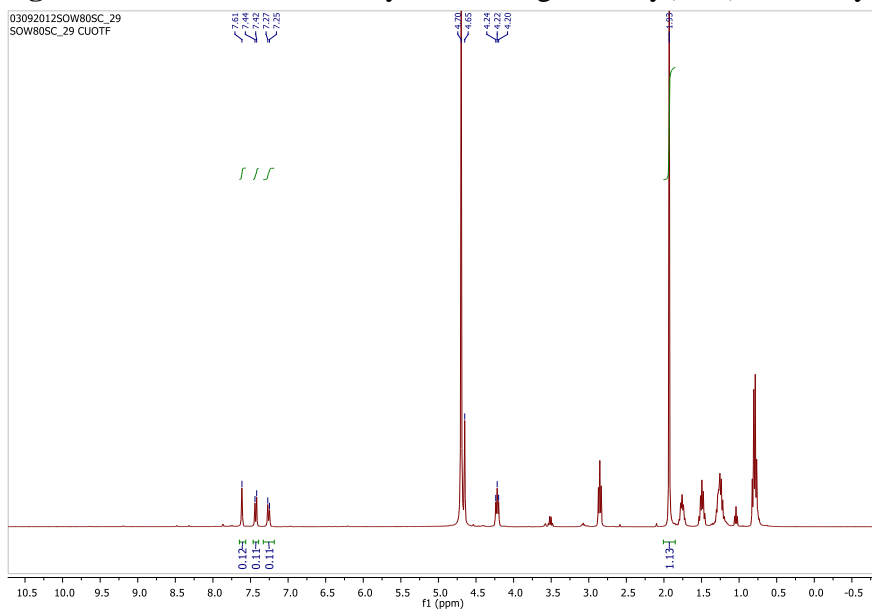


Fig S20: ^1H NMR(D_2O) of catalyst screening with $\text{Cu}(\text{OTf})_2$ as catalyst

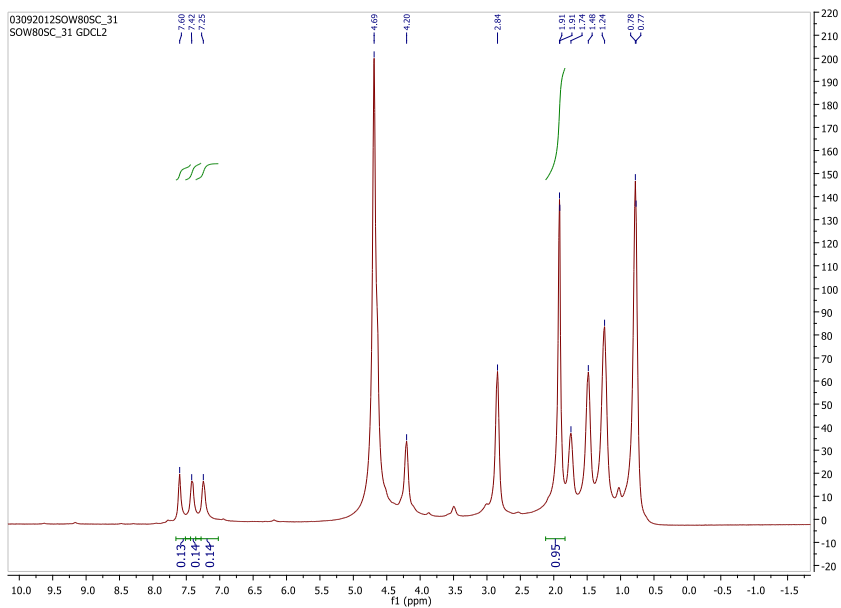


Fig S21: $^1\text{H NMR}_{(\text{D}_2\text{O})}$ of catalyst screening with $\text{GdCl}_3 \cdot 6\text{H}_2\text{O}$ as catalyst

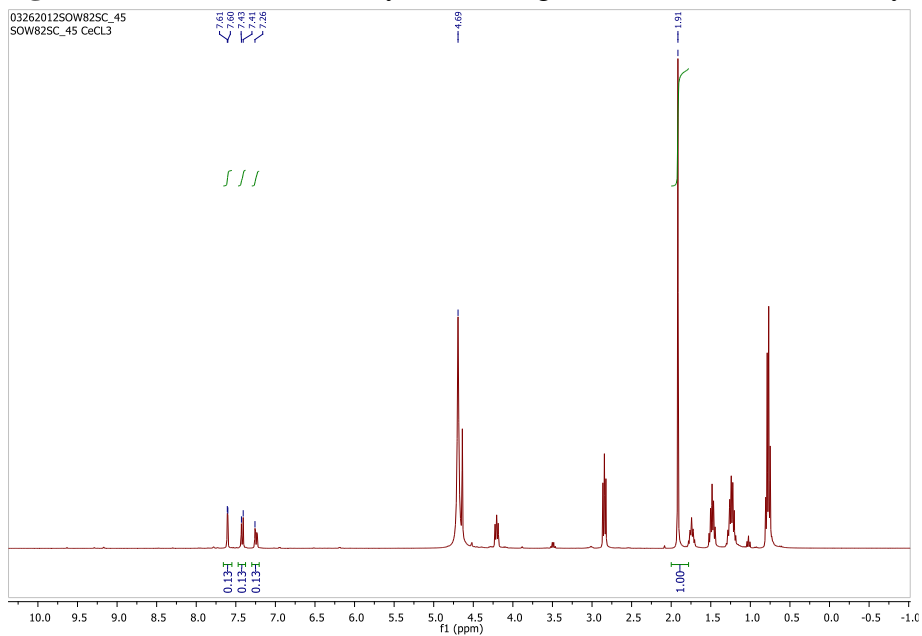


Fig S22: $^1\text{H NMR}_{(\text{D}_2\text{O})}$ of catalyst screening with $\text{CeCl}_3 \cdot 7\text{H}_2\text{O}$ as catalyst

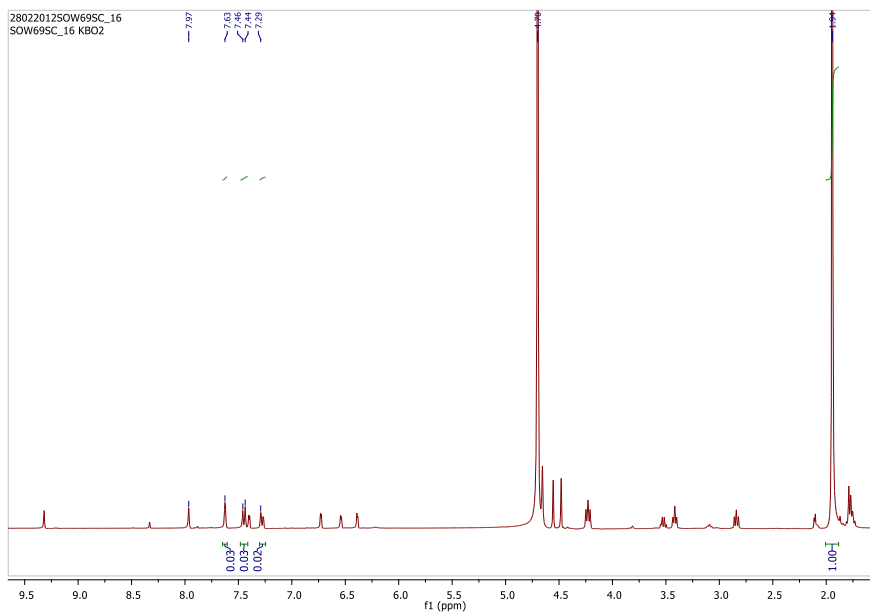


Fig S23: ^1H NMR(D_2O) of catalyst screening with $\text{KBO}_2 \cdot 2\text{H}_2\text{O}$ as catalyst

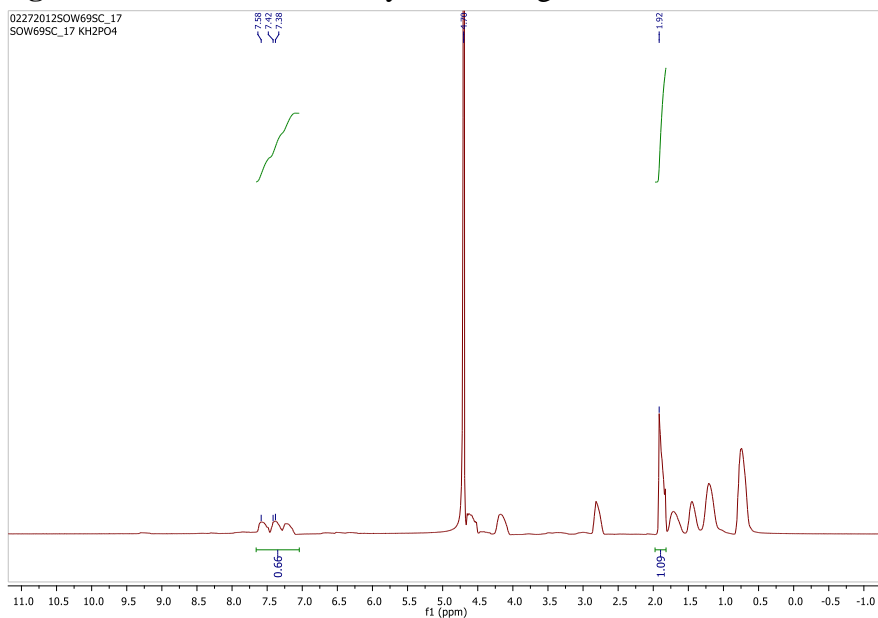


Fig S24: ^1H NMR(D_2O) of catalyst screening with KH_2PO_4 as catalyst

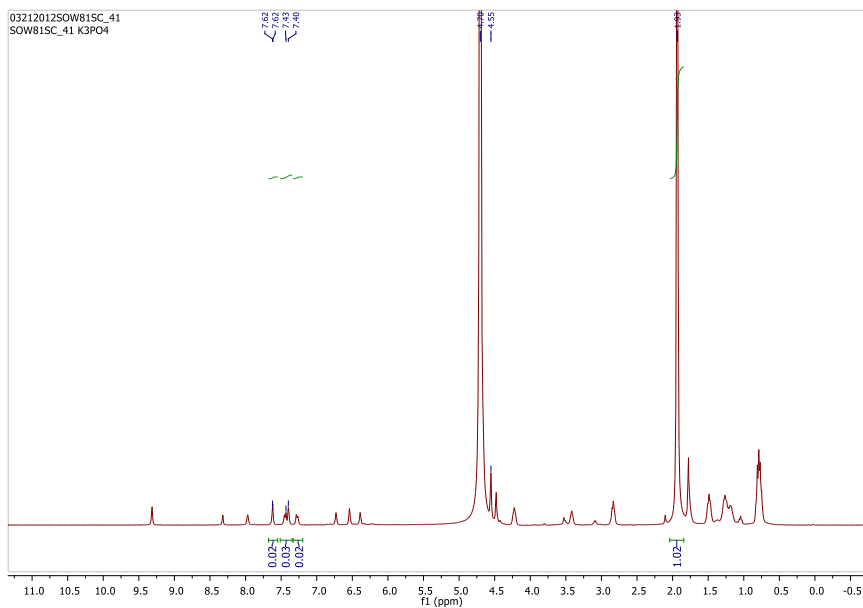


Fig S25: ¹H NMR(D₂O) of catalyst screening with K₃PO₄ as catalyst

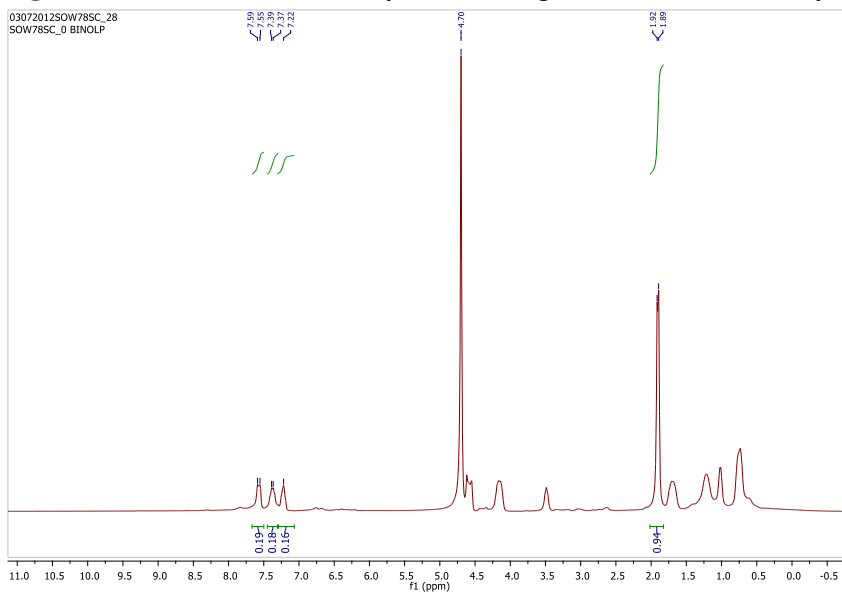


Fig S26: ¹H NMR(D₂O) of catalyst screening with BINAP as catalyst

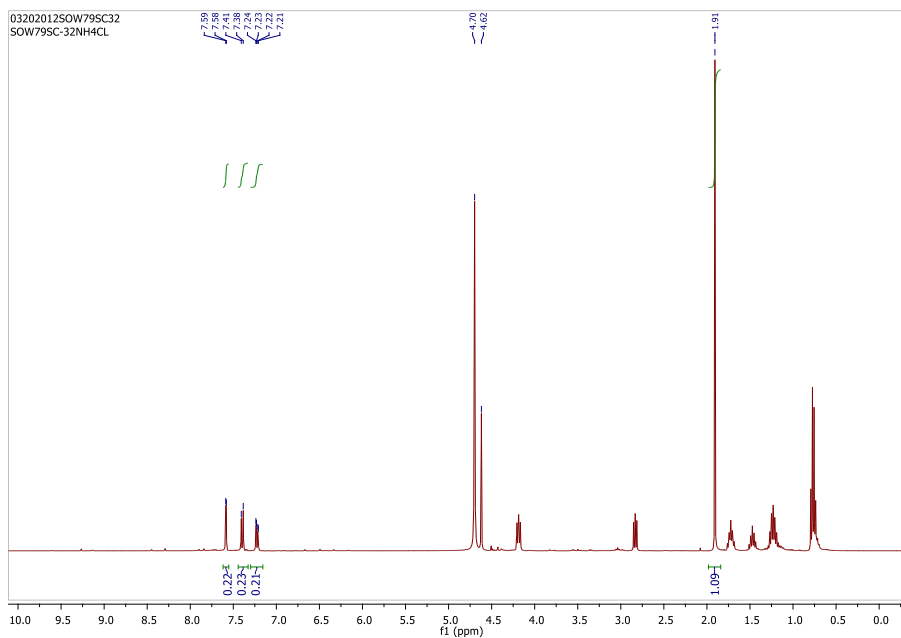


Fig S27: $^1\text{H NMR}_{(\text{D}_2\text{O})}$ of catalyst screening with NH_4Cl as catalyst

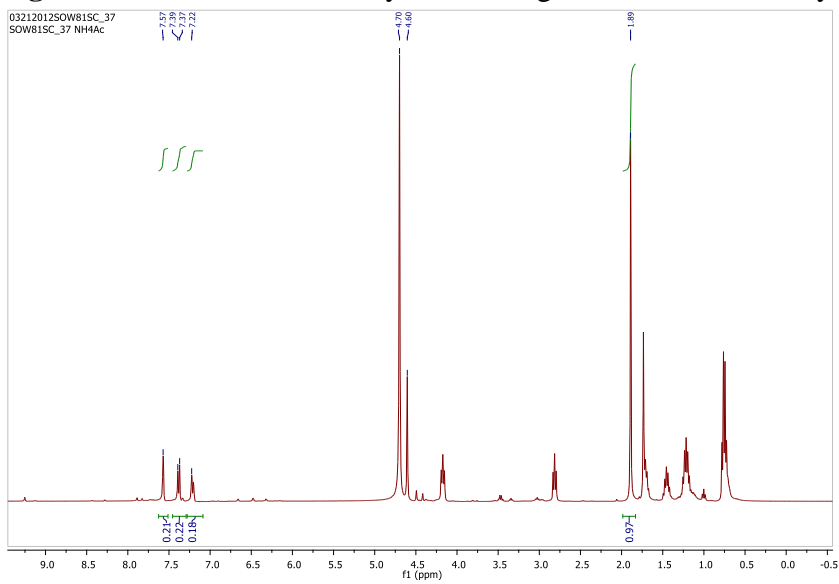


Fig S28: $^1\text{H NMR}_{(\text{D}_2\text{O})}$ of catalyst screening with NH_4Ac as catalyst

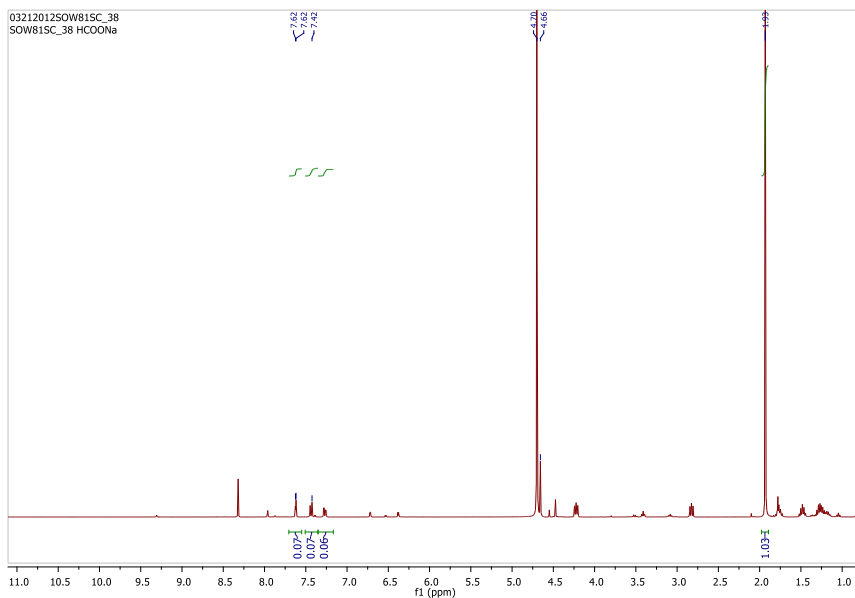


Fig S29: ^1H NMR(D_2O) of catalyst screening with HCOONa as catalyst

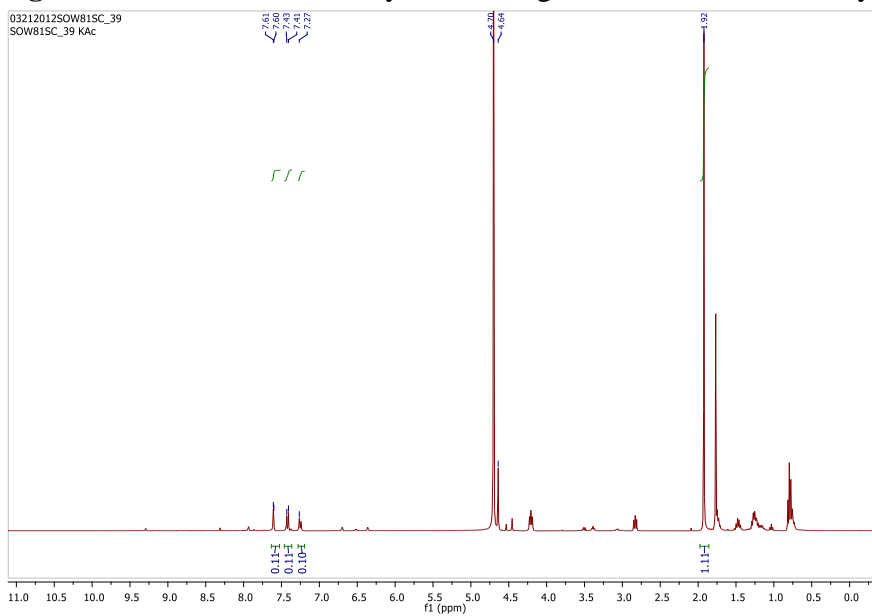


Fig S30: ^1H NMR(D_2O) of catalyst screening with KOAc as catalyst

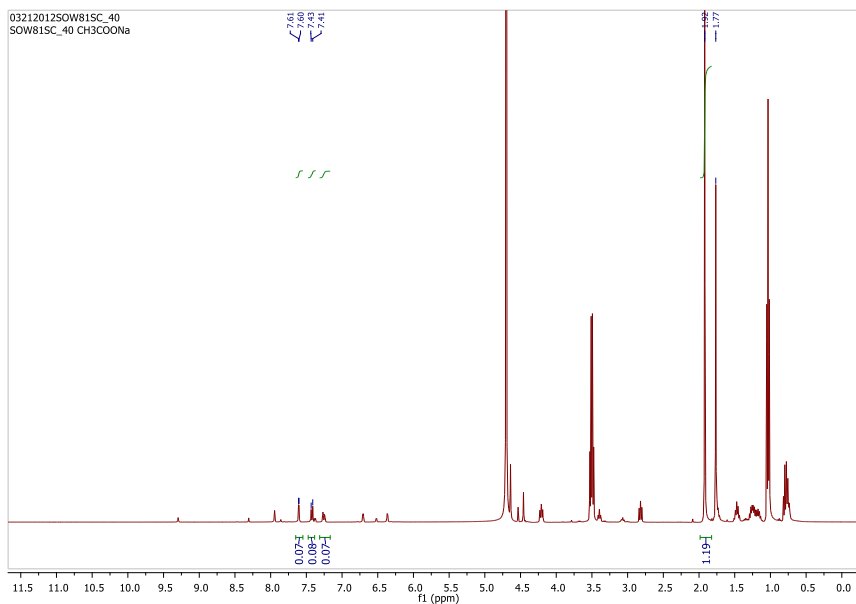


Fig S31: $^1\text{H NMR}_{(\text{D}_2\text{O})}$ of catalyst screening with NaOAc as catalyst

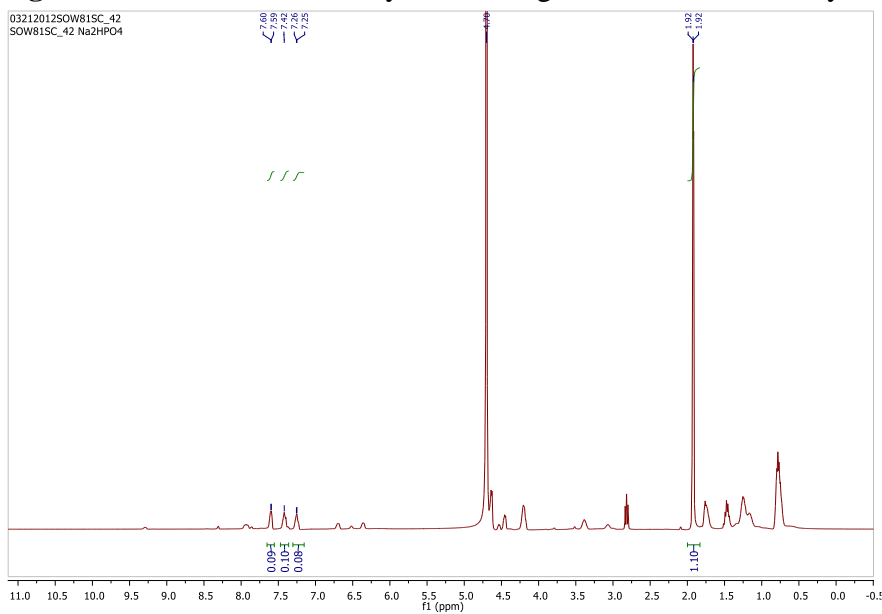


Fig S32: $^1\text{H NMR}_{(\text{D}_2\text{O})}$ of catalyst screening with Na_2HPO_4 as catalyst

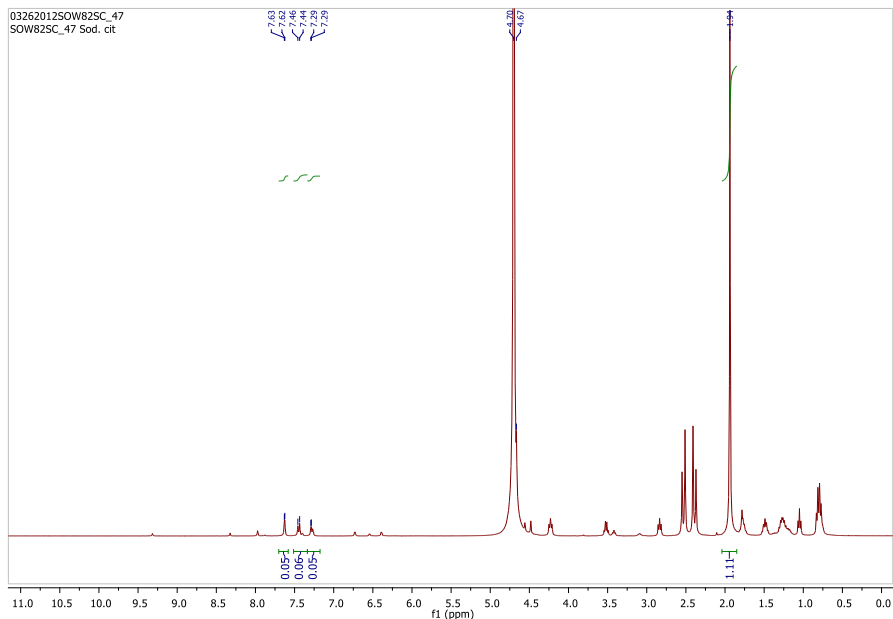


Fig S33: ^1H NMR(D_2O) of catalyst screening with Sodium Citrate as catalyst

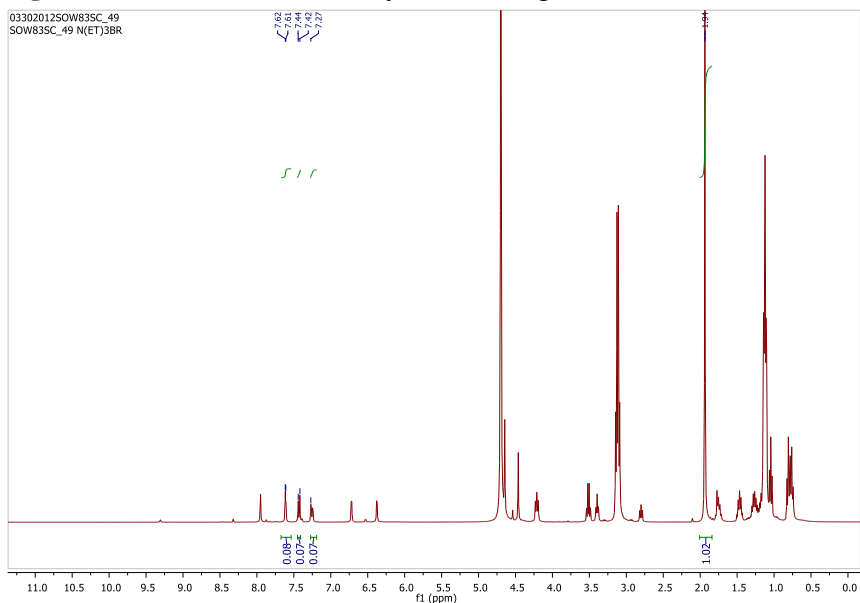


Fig S34: ^1H NMR(D_2O) of catalyst screening with $\text{N}(\text{Et})_3\text{Br}$ as catalyst

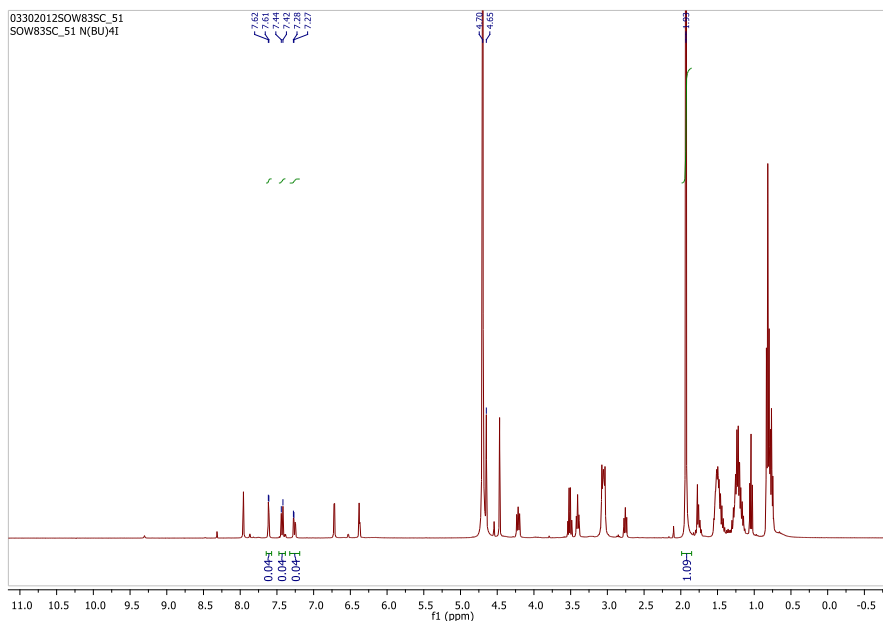


Fig S35: $^1\text{H NMR}_{(\text{D}_2\text{O})}$ of catalyst screening with $\text{N}(\text{Bu})_4\text{I}$ as catalyst

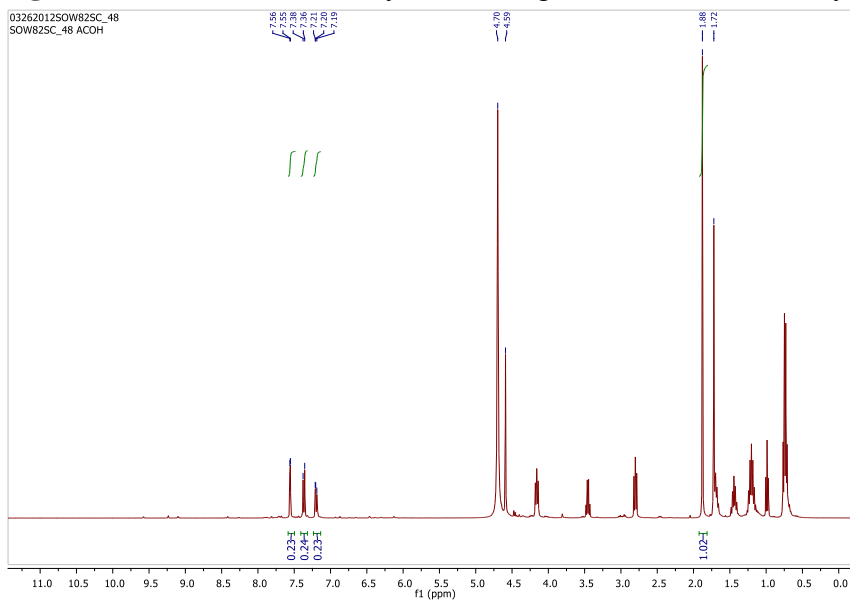


Fig S36: $^1\text{H NMR}_{(\text{D}_2\text{O})}$ of catalyst screening with AcOH as catalyst

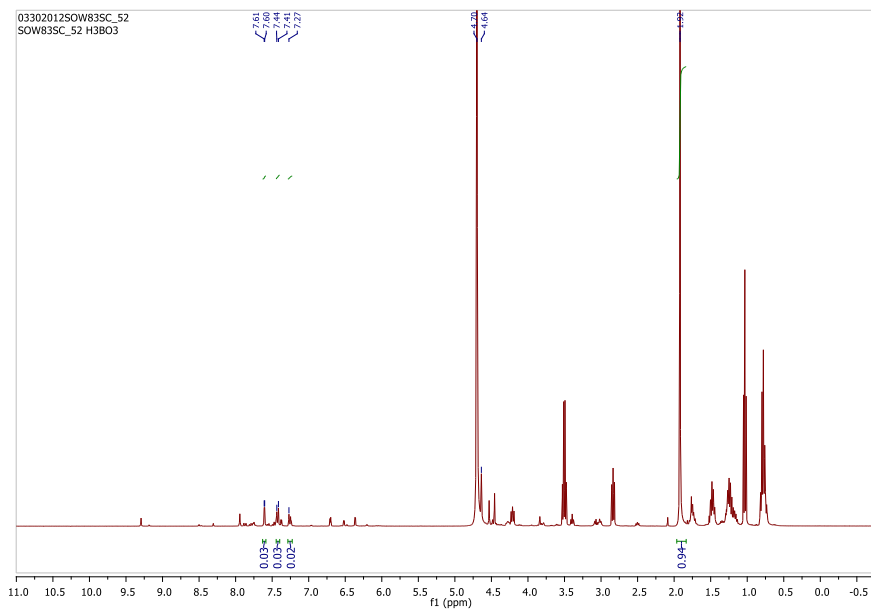


Fig S37: $^1\text{H NMR}_{(\text{D}_2\text{O})}$ of catalyst screening with H_3BO_3 as catalyst

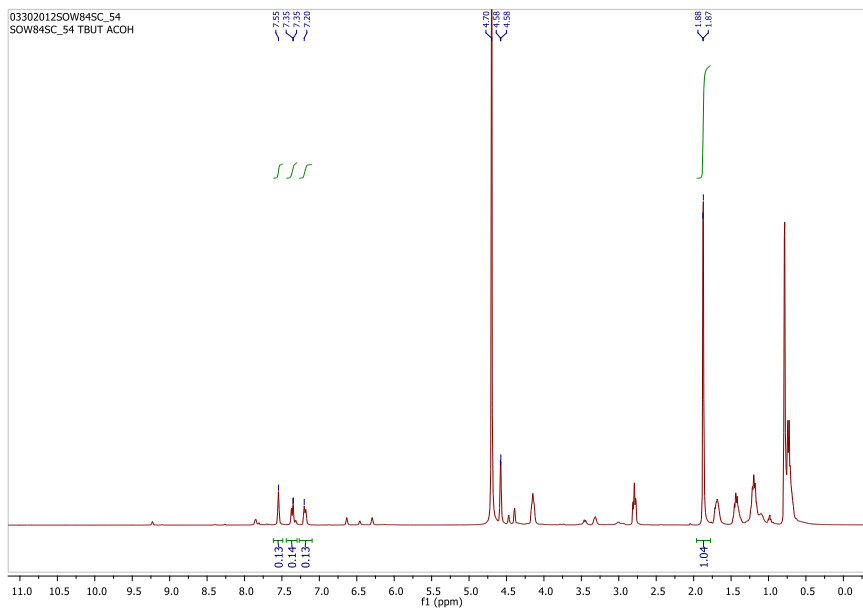


Fig S38: $^1\text{H NMR}_{(\text{D}_2\text{O})}$ of catalyst screening with t-butyl AcOH as catalyst

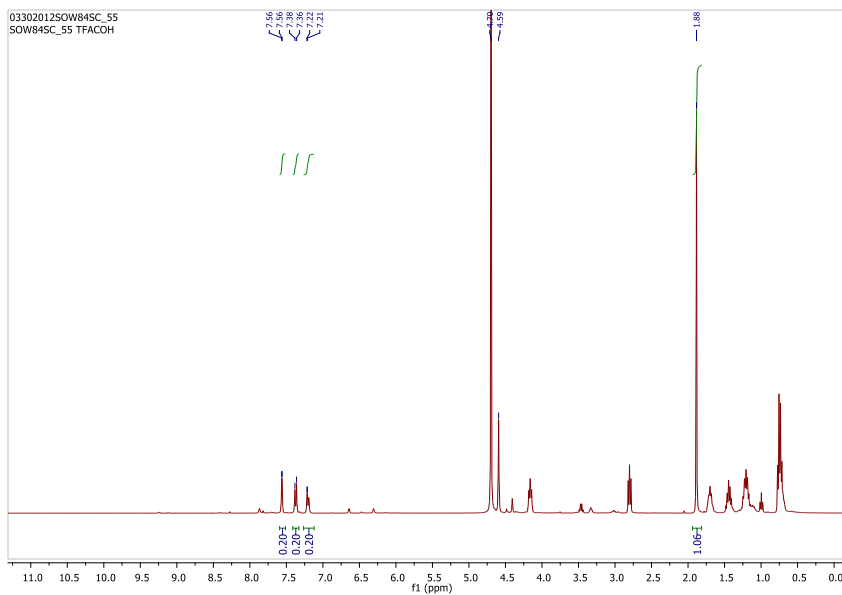


Fig S39: $^1\text{H NMR}_{(\text{D}_2\text{O})}$ of catalyst screening with TFA as catalyst

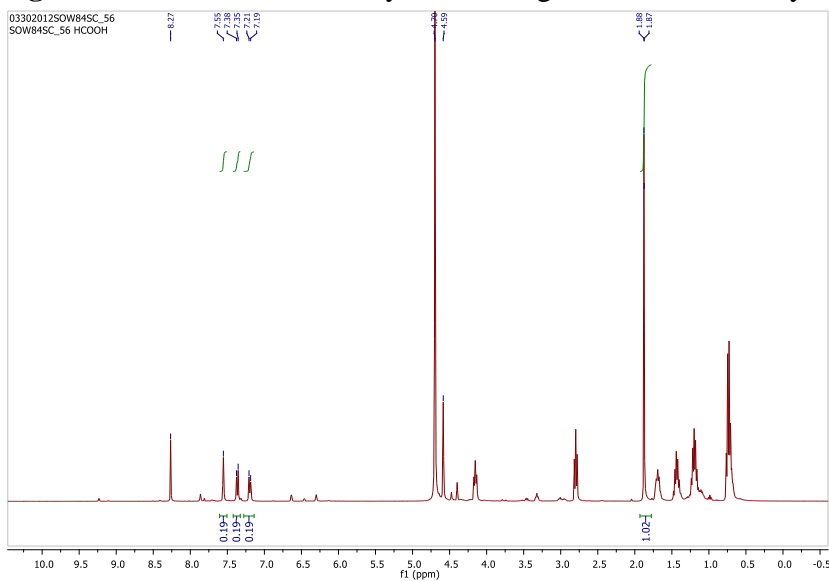


Fig S40: $^1\text{H NMR}_{(\text{D}_2\text{O})}$ of catalyst screening with Formic Acid as catalyst

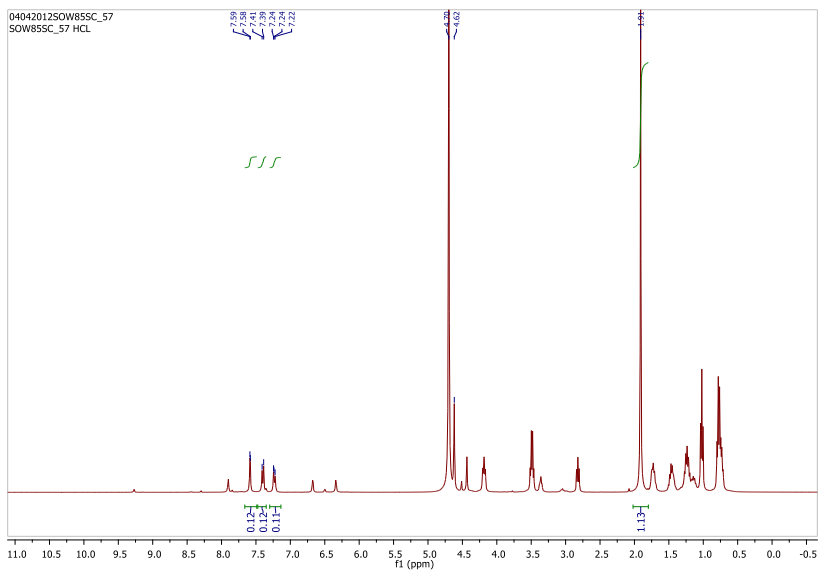


Fig S41: ^1H NMR(D_2O) of catalyst screening with HCl as catalyst

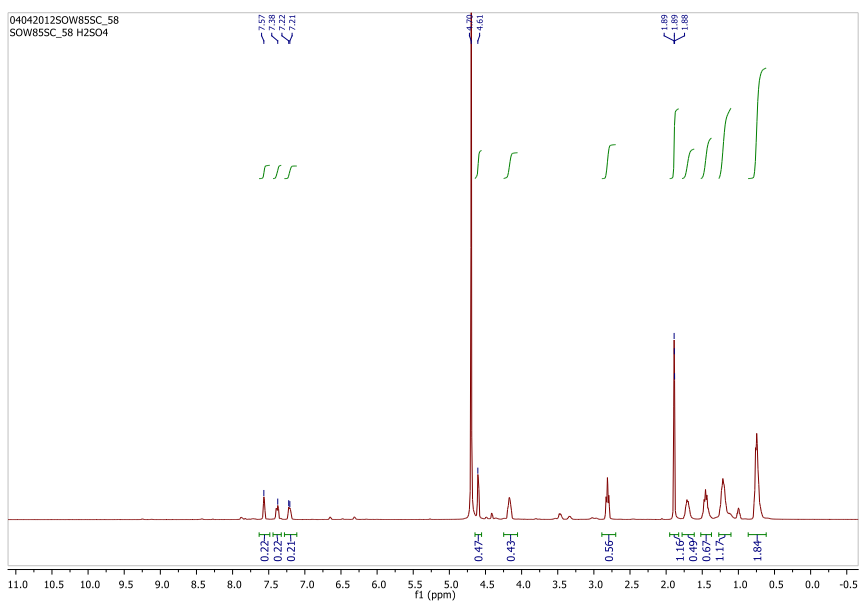


Fig S42: ^1H NMR(D_2O) of catalyst screening with H_2SO_4 as catalyst

Supporting details

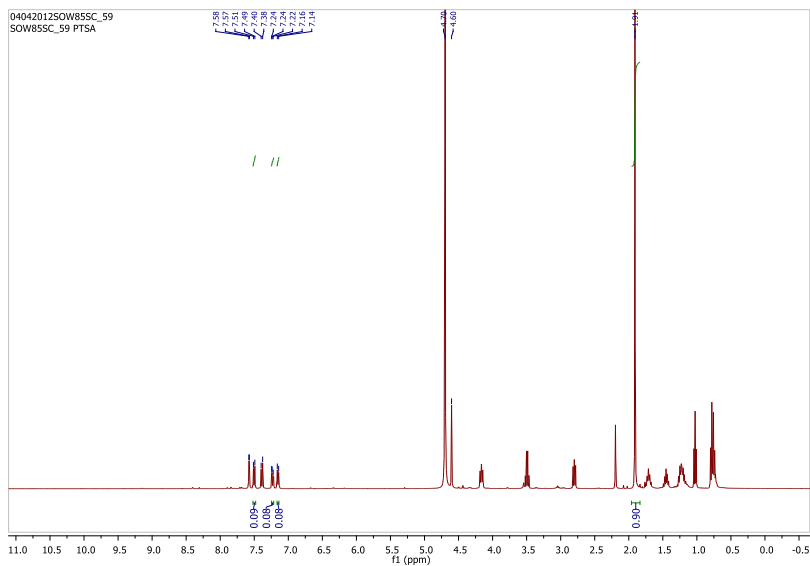


Fig S43: $^1\text{H NMR}_{(\text{D}_2\text{O})}$ of catalyst screening with PTSA as catalyst

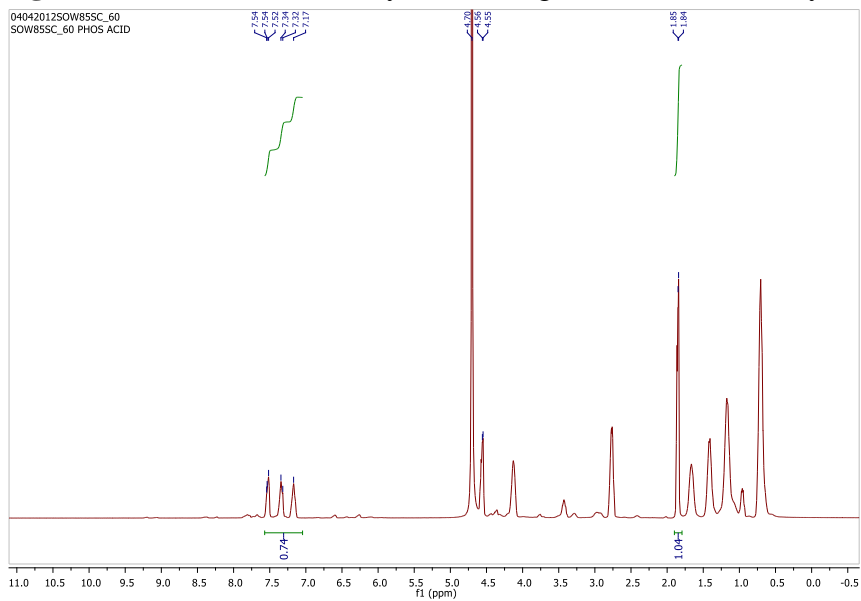


Fig S44: $^1\text{H NMR}_{(\text{D}_2\text{O})}$ of catalyst screening with Phosphoric acid as catalyst

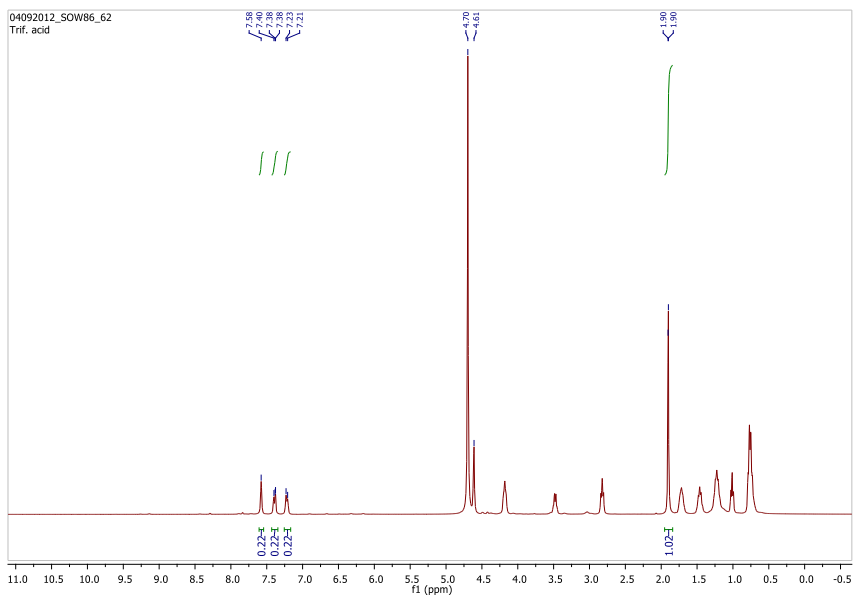


Fig S45: ^1H NMR(D_2O) of catalyst screening with Triflic acid as catalyst

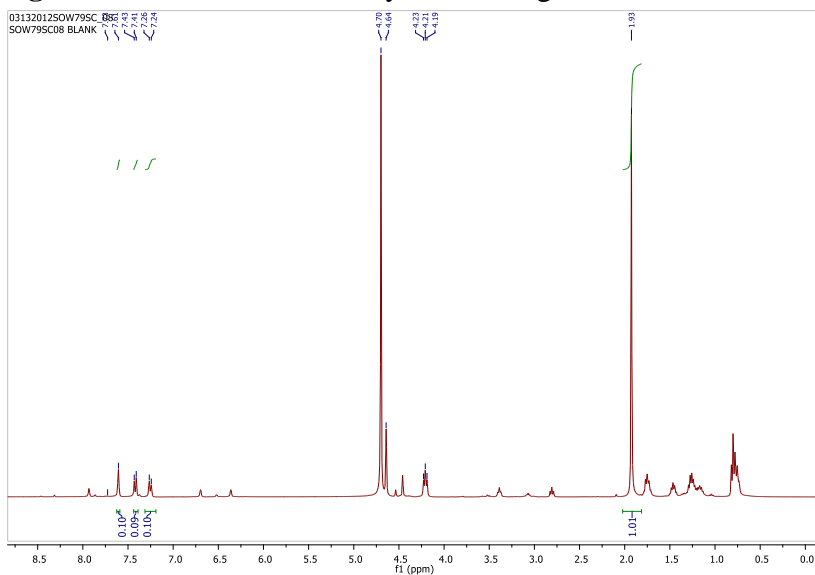


Fig S46: ^1H NMR(D_2O) of catalyst screening at 80 °C for 2 days without added catalyst

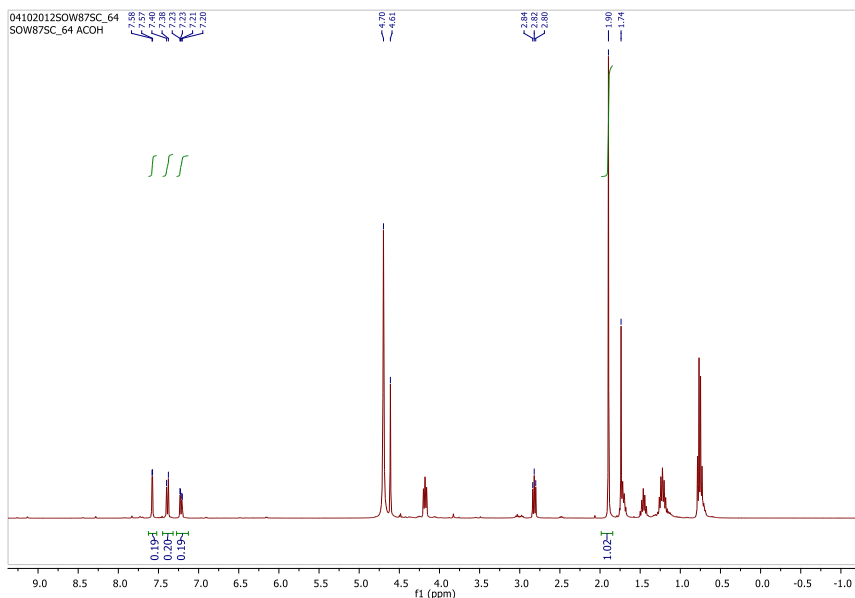


Fig S47: ^1H NMR(D_2O) of catalyst screening at 80 °C for 2days with Acetic acid as catalyst

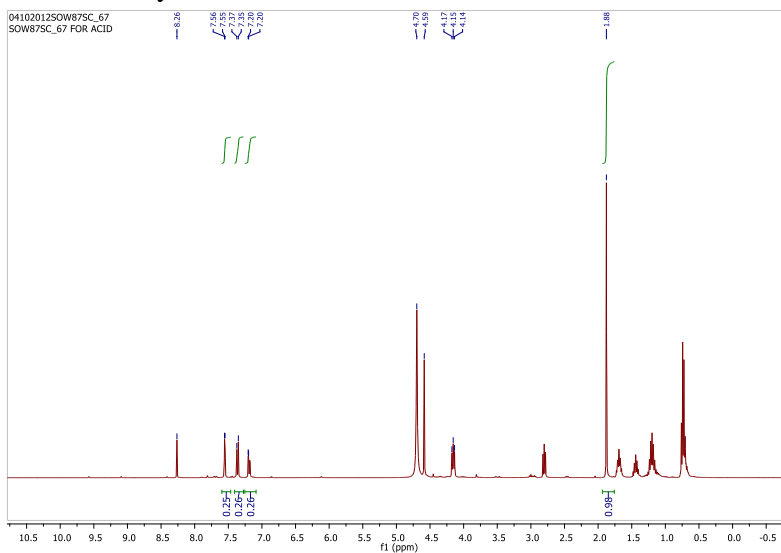


Fig S48: ^1H NMR(D_2O) of catalyst screening at 80 °C for 2days with Formic acid as catalyst

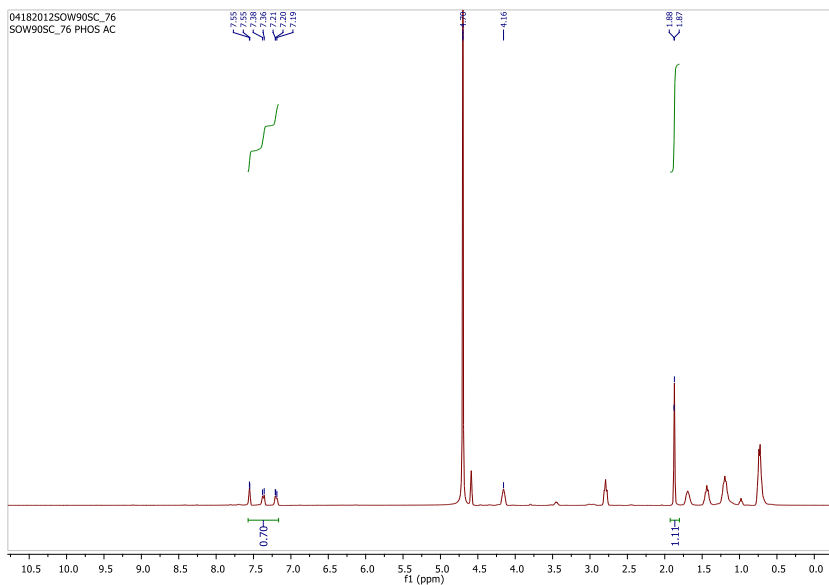


Fig S49: ^1H NMR(D_2O) of catalyst screening at 80°C for 2days with Phosphoric acid as catalyst

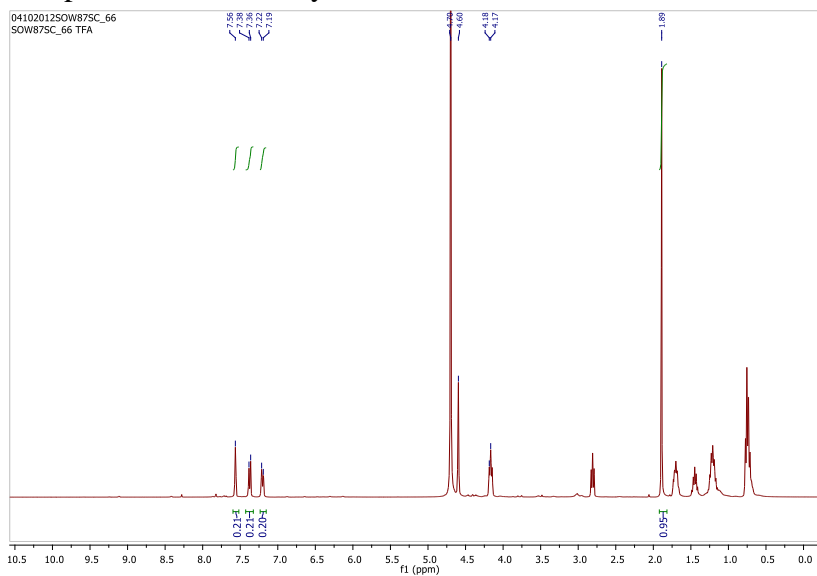


Fig S50: ^1H NMR(D_2O) of catalyst screening at 80°C for 2days with TFA as catalyst

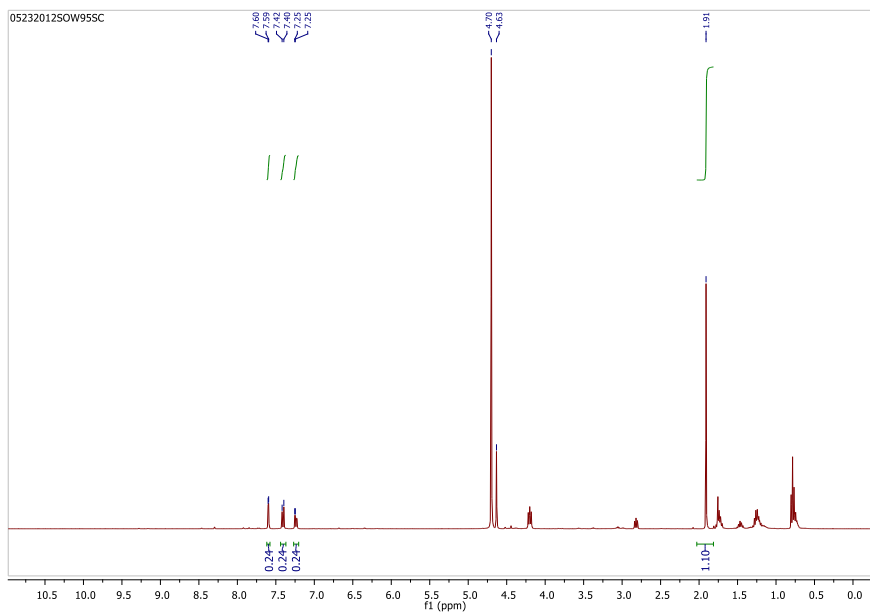


Fig S51: ^1H NMR(D_2O) of catalyst screening at 80°C for 2days with Triflic acid as catalyst

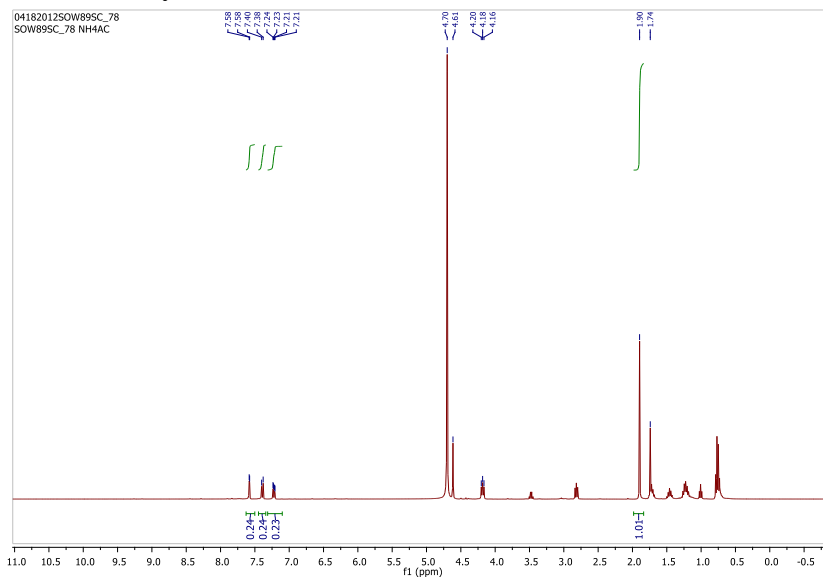


Fig S52: ^1H NMR(D_2O) of catalyst screening at 80°C for 2days with NH_4Ac as catalyst

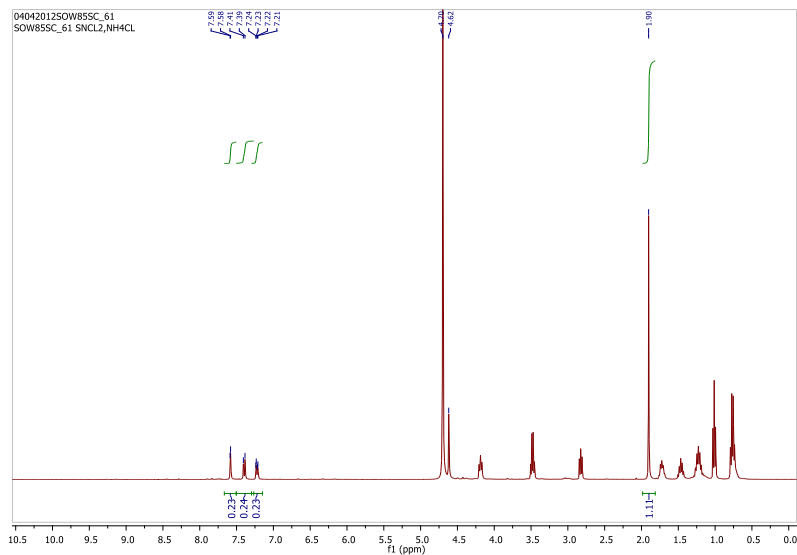


Fig S53: ^1H NMR(D_2O) of catalyst screening at 80°C for 2days with $\text{SnCl}_2 + \text{NH}_4\text{Cl}$ as catalyst

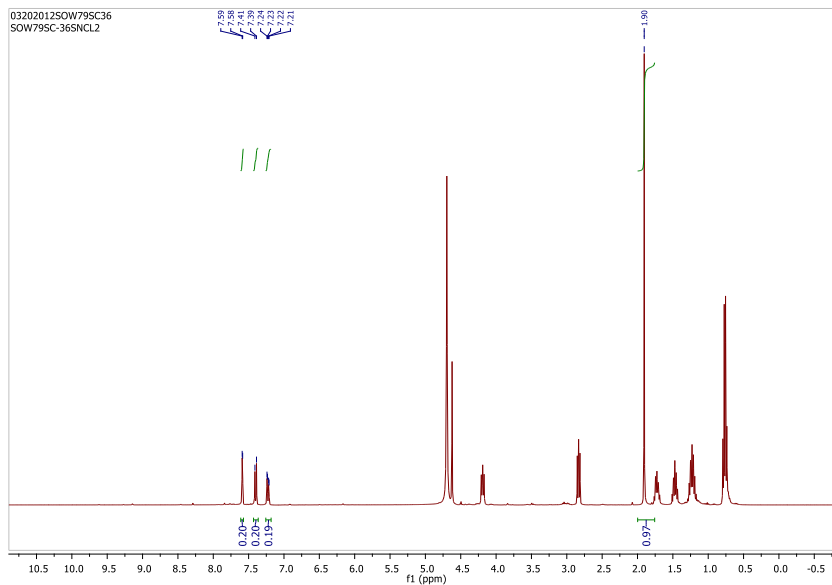


Fig S54: ^1H NMR(D_2O) of catalyst screening at 80°C for 2days with SnCl_2 as catalyst

Supporting details

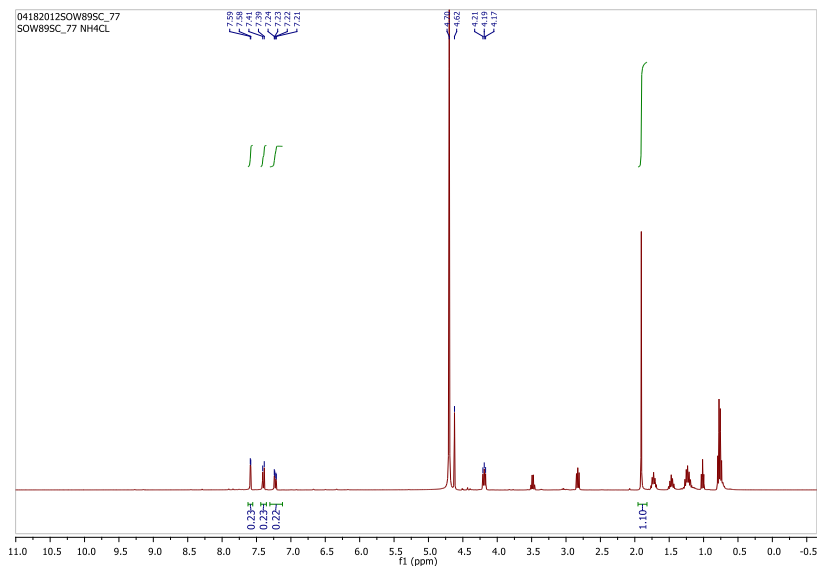


Fig S55: ^1H NMR(D_2O) of catalyst screening at 80 °C for 2days with NH_4Cl as catalyst

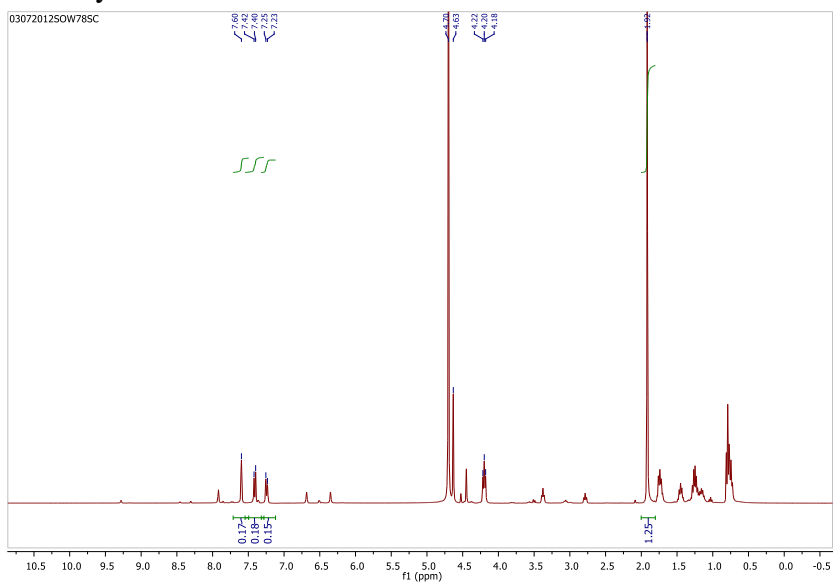


Fig S56: ^1H NMR(D_2O) of catalyst screening at 80 °C for 2days with H_2SO_4 as catalyst

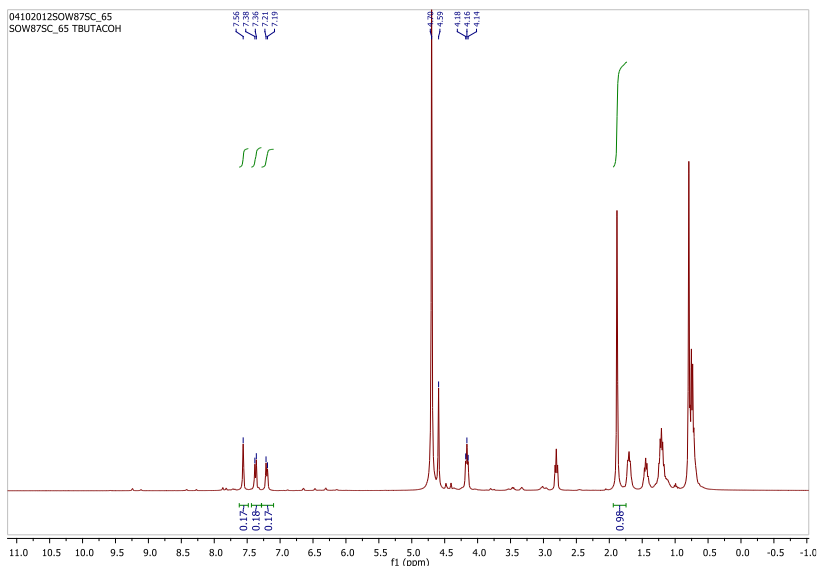


Fig S57: $^1\text{H NMR}_{(\text{D}_2\text{O})}$ of catalyst screening at $80\text{ }^\circ\text{C}$ for 2days with t-butyl AcOH as catalyst

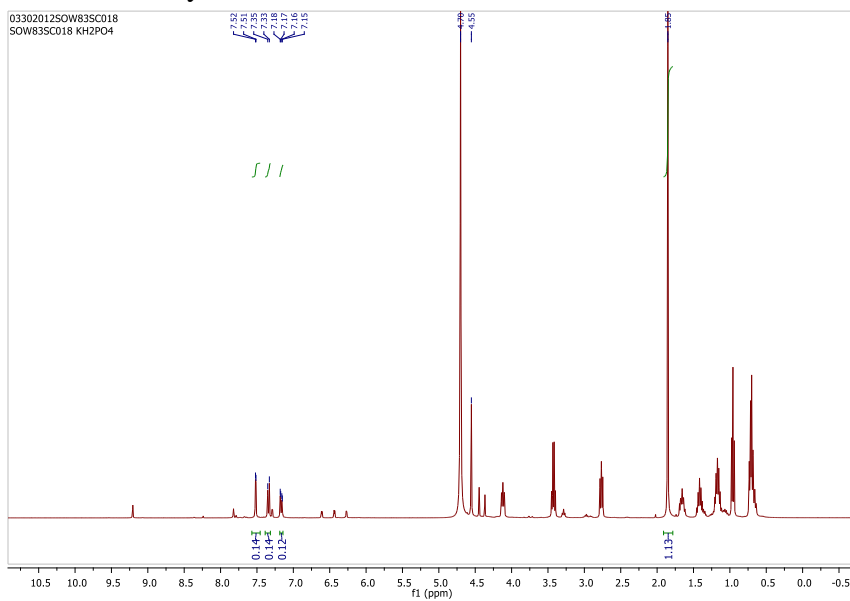


Fig S58: $^1\text{H NMR}_{(\text{D}_2\text{O})}$ of catalyst screening at $80\text{ }^\circ\text{C}$ for 2days with KH_2PO_4 as catalyst

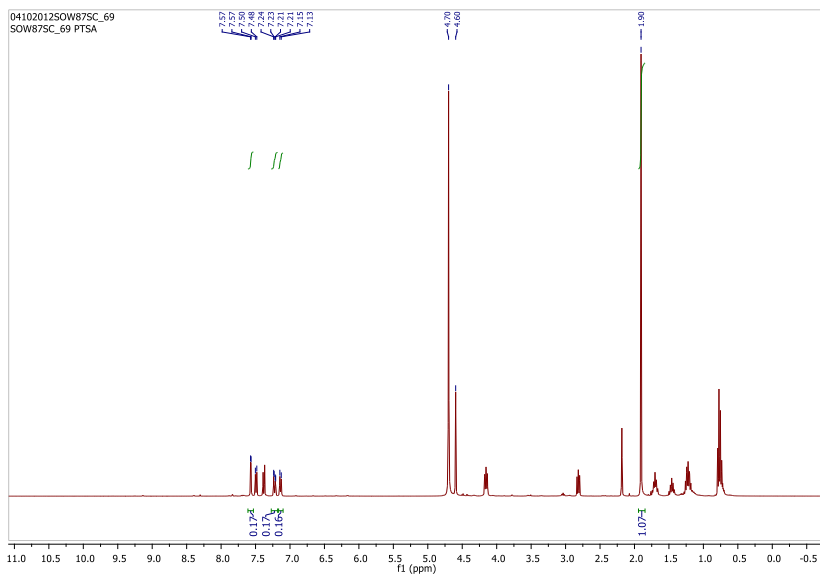


Fig S59: ^1H NMR(D_2O) of catalyst screening at 80°C for 2days with PTSA as catalyst

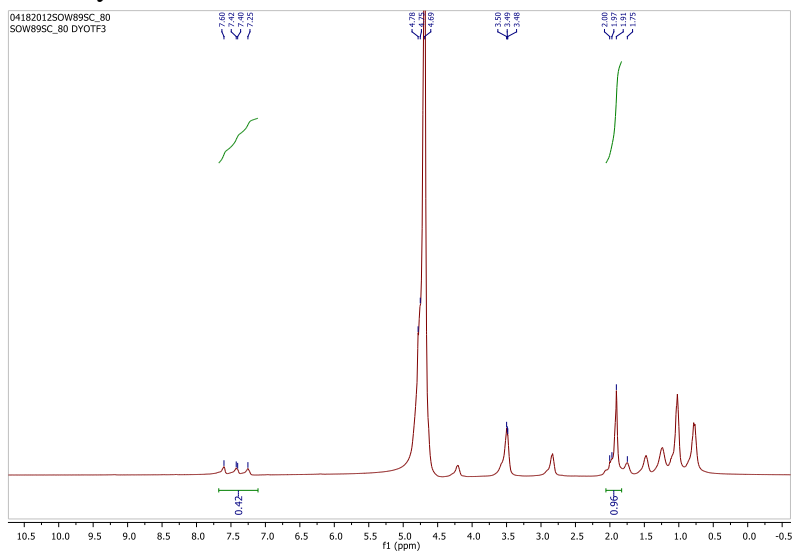


Fig S60: ^1H NMR(D_2O) of catalyst screening at 80°C for 2days with $\text{Dy}(\text{OTf})_3$ as catalyst

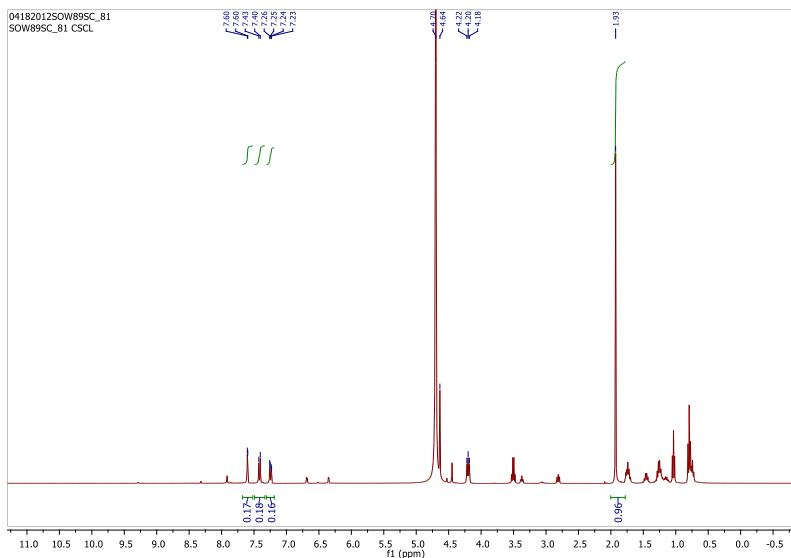


Fig S61: $^1\text{H NMR}_{(\text{D}_2\text{O})}$ of catalyst screening at 80 °C for 2 days with CsCl_2 as catalyst

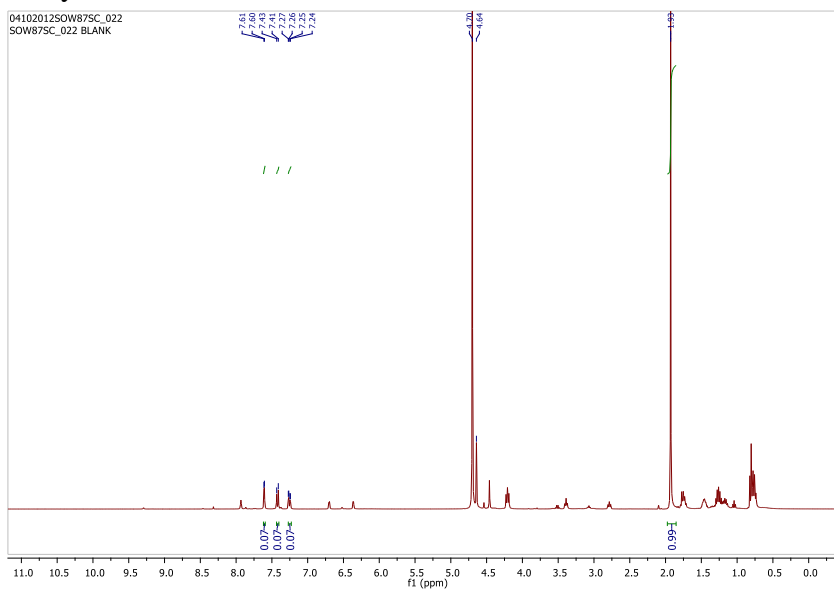


Fig S62: $^1\text{H NMR}_{(\text{D}_2\text{O})}$ of catalyst screening at 70 °C for 3 days without added catalyst

Supporting details

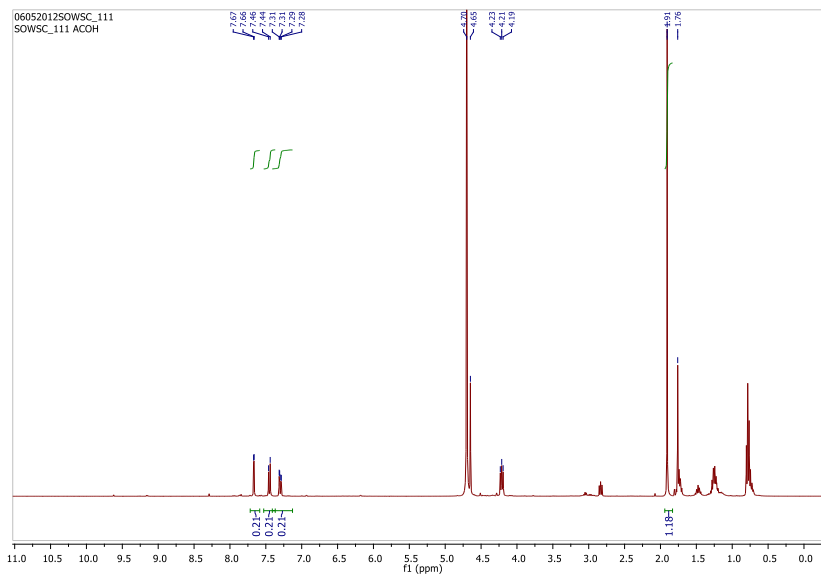


Fig S63: $^1\text{H NMR}_{(\text{D}_2\text{O})}$ of catalyst screening at 70 °C for 3days with Acetic acid as catalyst

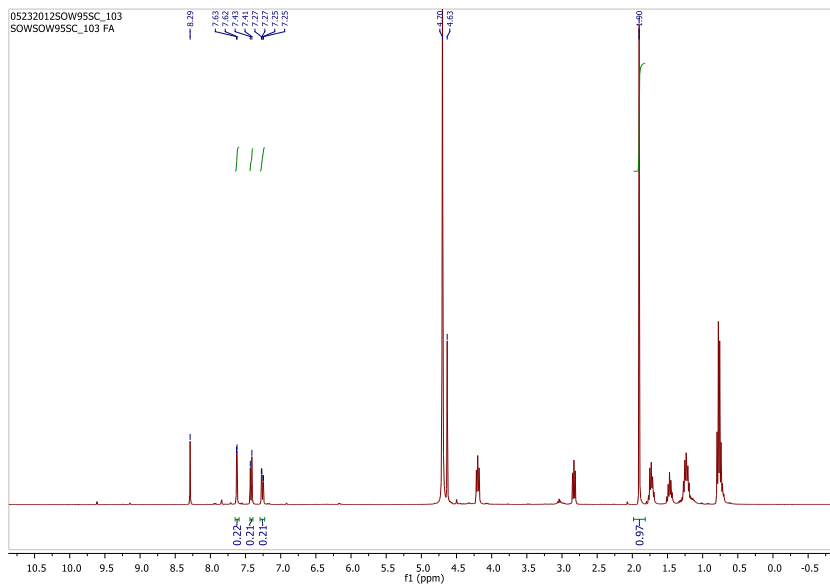


Fig S64: $^1\text{H NMR}_{(\text{D}_2\text{O})}$ of catalyst screening at 70 °C for 3days with Formic acid as catalyst

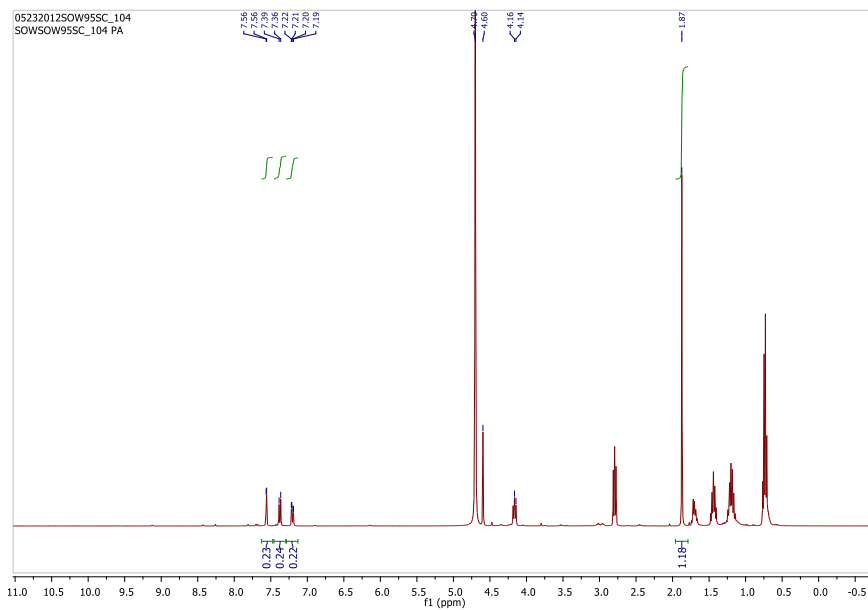


Fig S65: $^1\text{H NMR}_{(\text{D}_2\text{O})}$ of catalyst screening at 70 °C for 3days with Phosphoric acid as catalyst

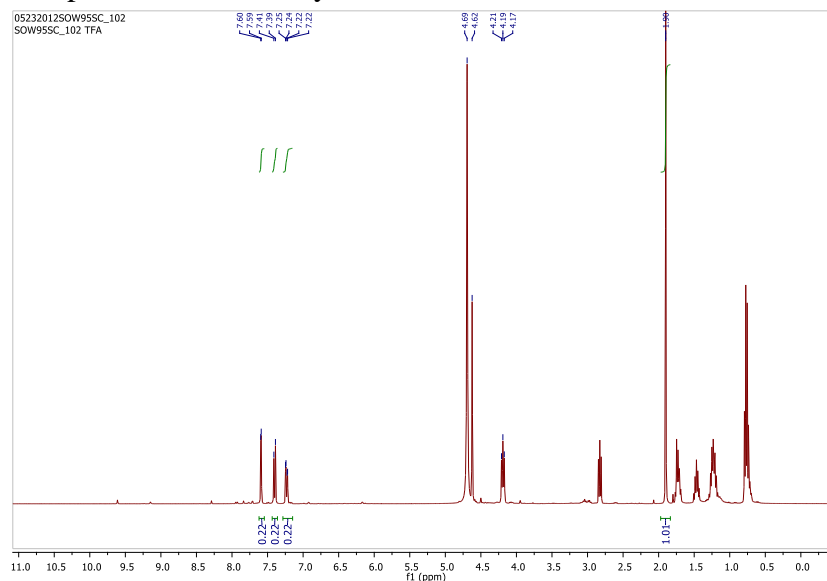


Fig S66: $^1\text{H NMR}_{(\text{D}_2\text{O})}$ of catalyst screening at 70 °C for 3days with TFA as catalyst

Supporting details

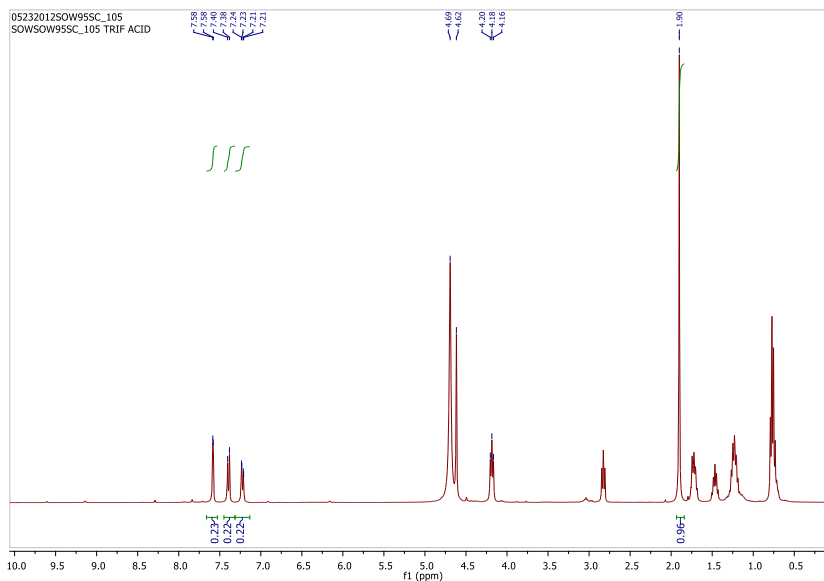


Fig S67: ¹H NMR(D₂O) of catalyst screening at 70 °C for 3days with Triflic acid as catalyst

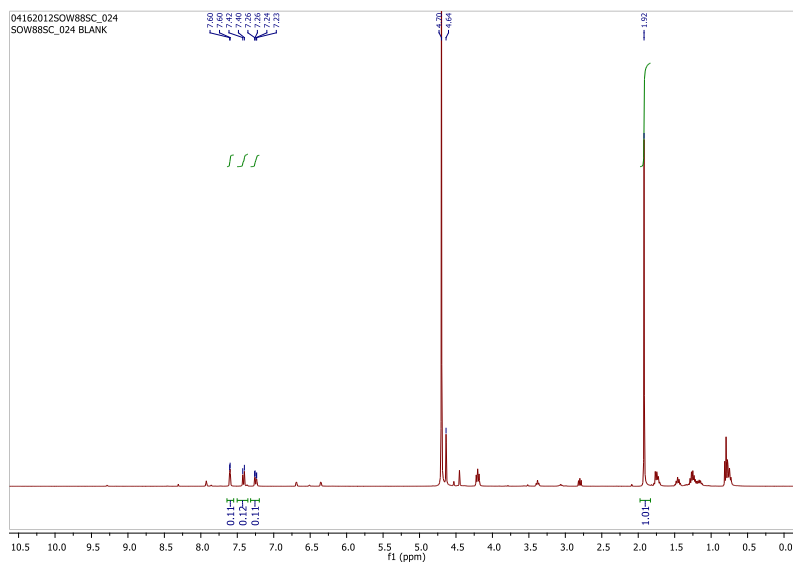


Fig S68: ¹H NMR(D₂O) of catalyst screening at 80 °C for 3days without added catalyst

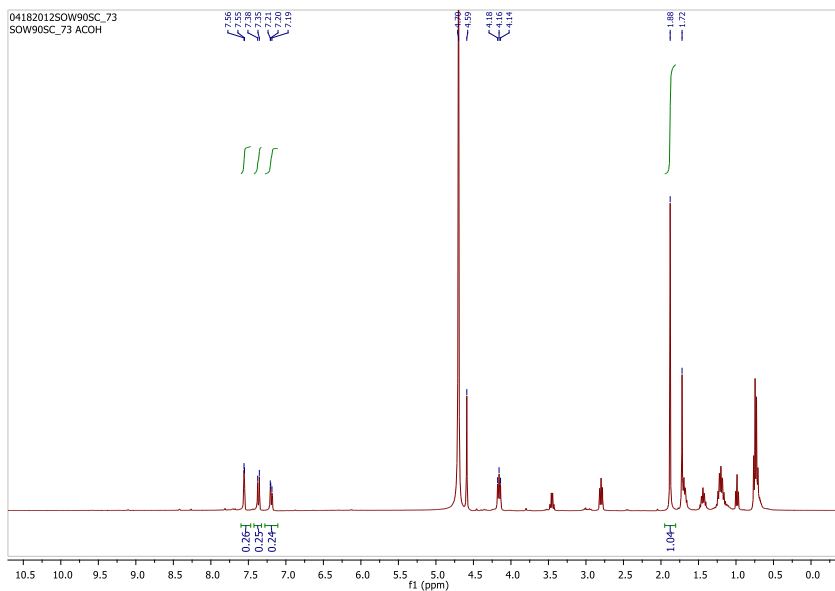


Fig S69: $^1\text{H NMR}$ (D_2O) of catalyst screening at 80°C for 3days with Acetic acid as catalyst

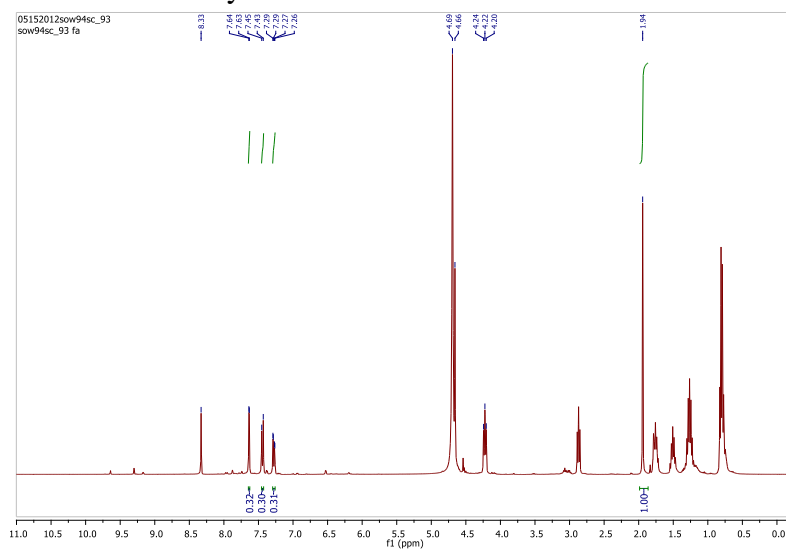


Fig S70: $^1\text{H NMR}$ (D_2O) of catalyst screening at 80°C for 3days with Formic acid as catalyst

Supporting details

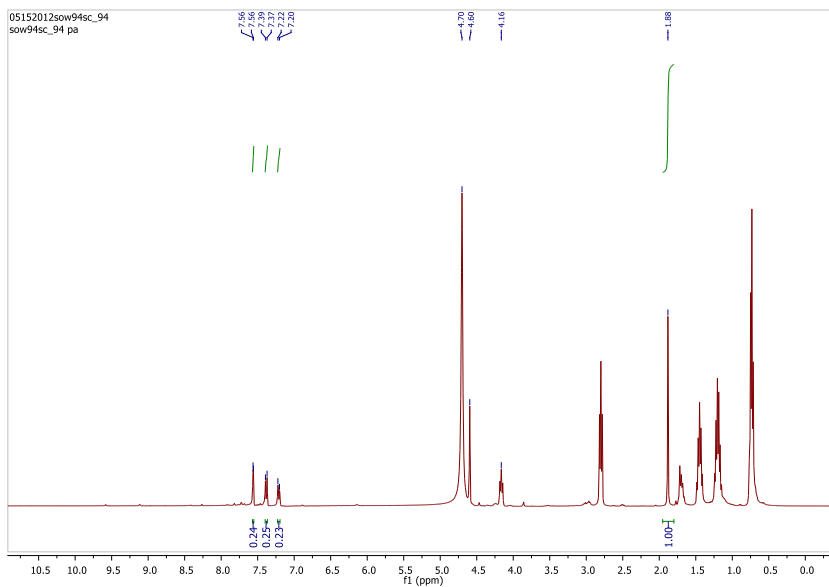


Fig S71: ^1H NMR(D_2O) of catalyst screening at 80 °C for 3days with Phosphoric acid as catalyst

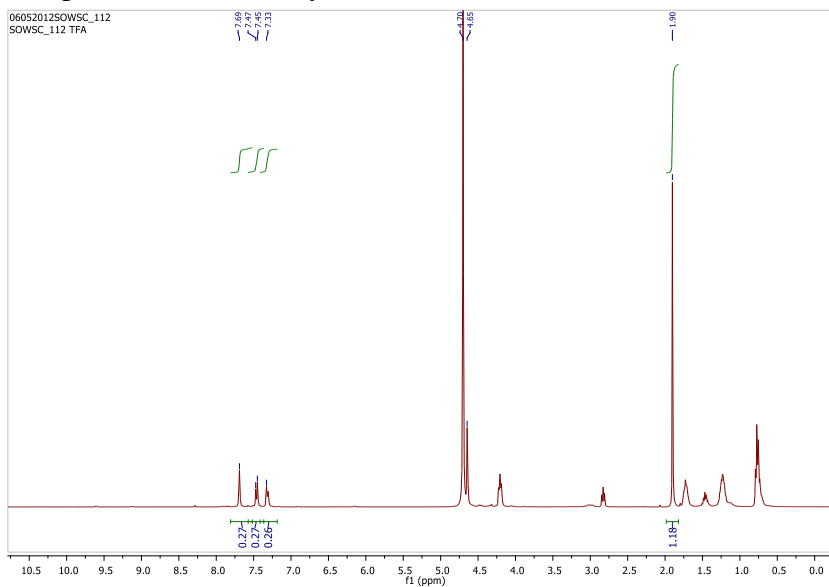


Fig S72: ^1H NMR(D_2O) of catalyst screening at 80 °C for 3days with TFA as catalyst

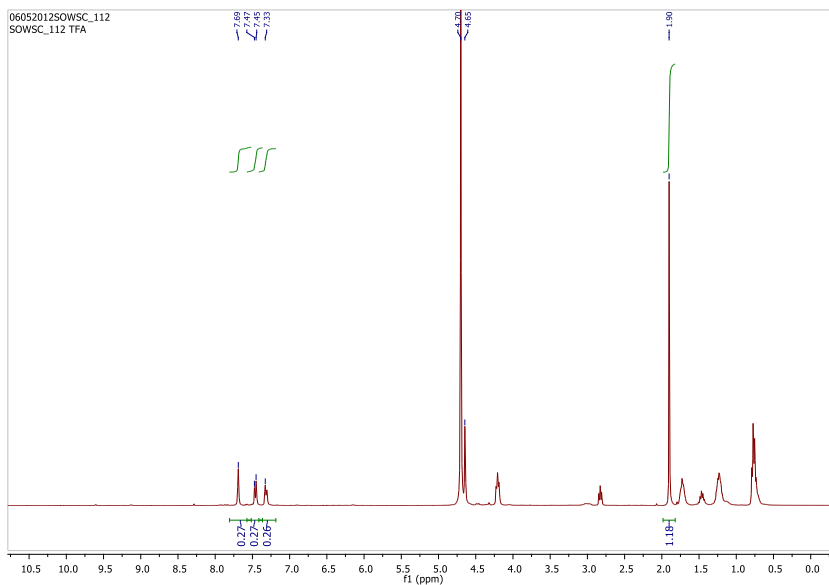


Fig S73: ^1H NMR(D_2O) of catalyst screening at 80 °C for 3days with Triflic acid as catalyst

Supporting details

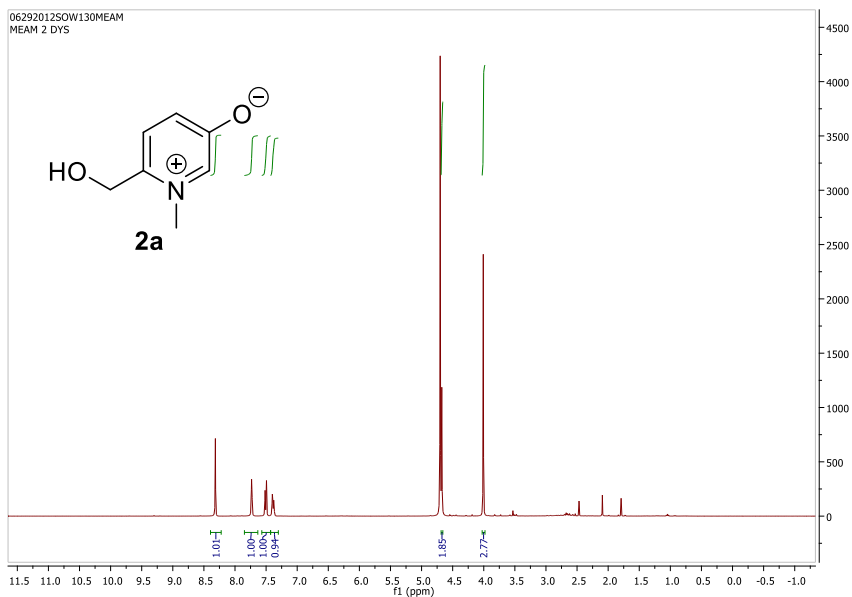


Fig S74: ^1H NMR(D_2O) of methylamine pyridinium salt.

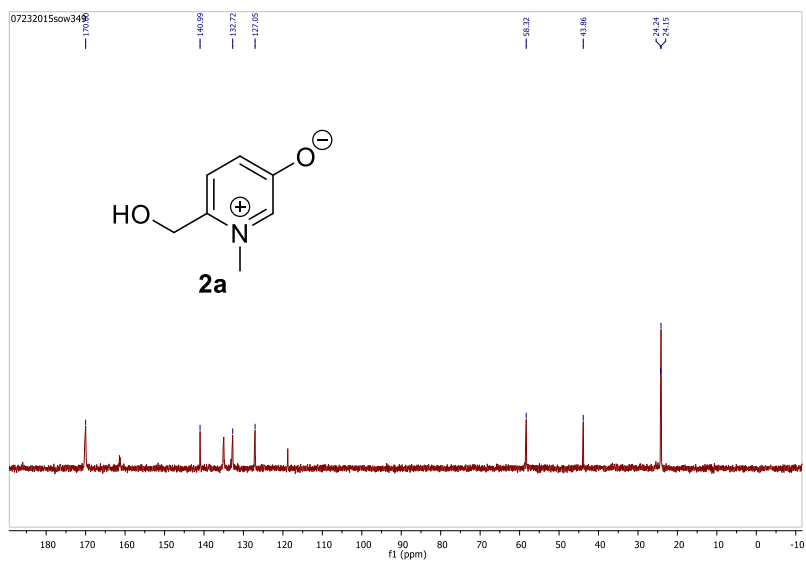


Fig S75: ^{13}C NMR(D_2O) of methylamine pyridinium salt.

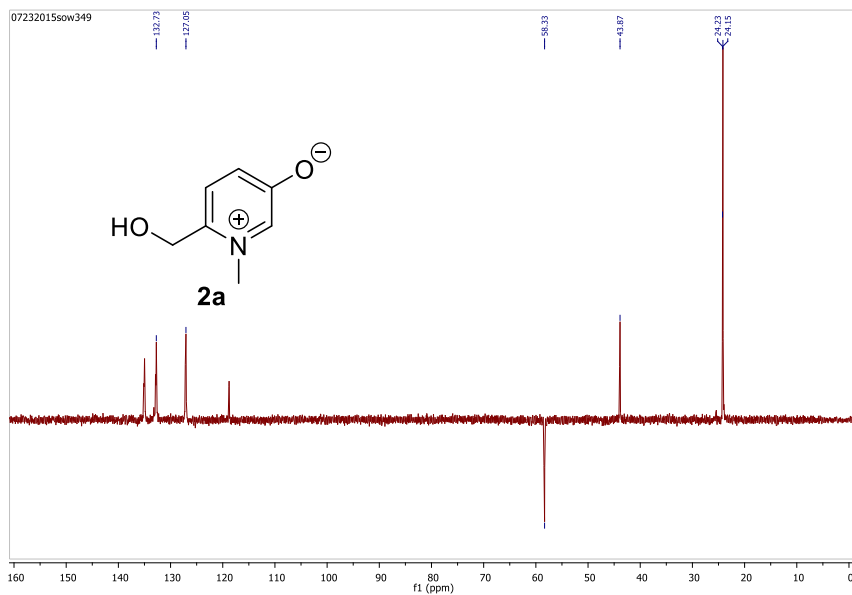


Fig S76: ^{13}C Dept NMR(D_2O) of methylamine pyridinium salt.

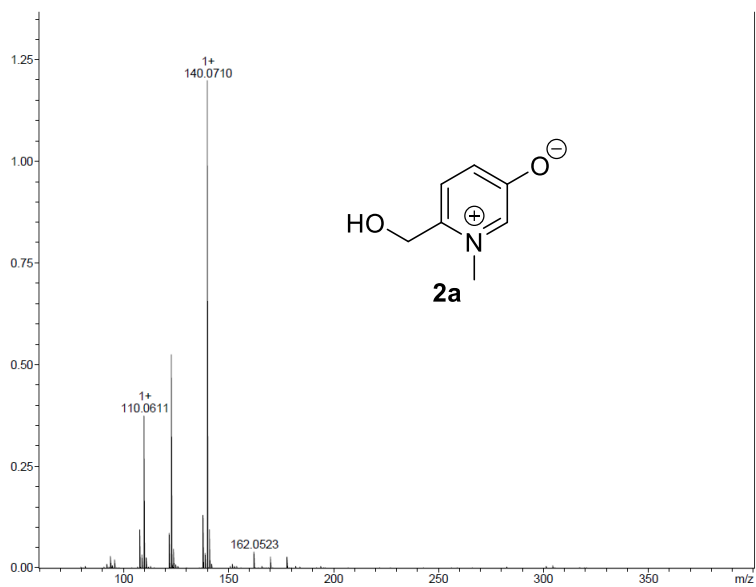


Fig S77: HRMS of methylamine pyridinium salt

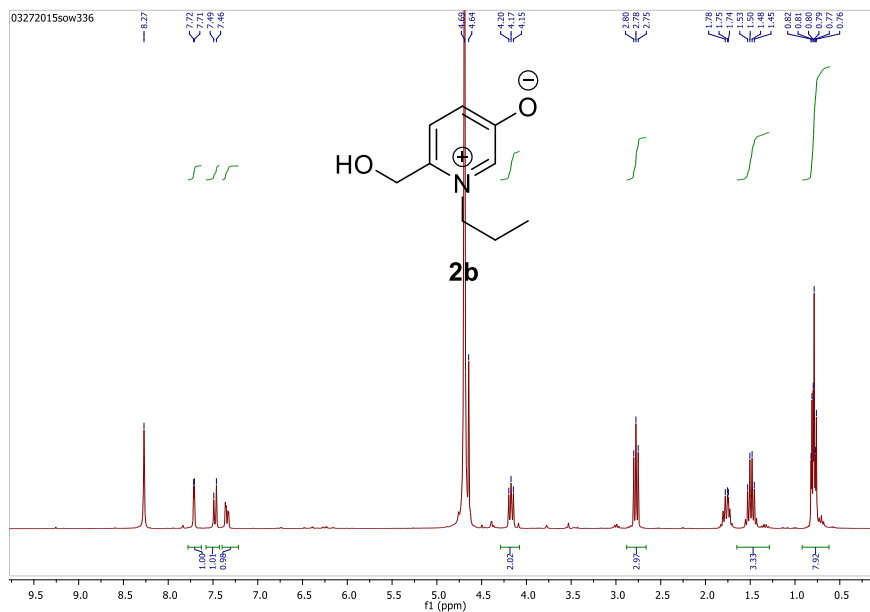


Fig S78: ¹H NMR(D₂O) of propylamine pyridinium salt.

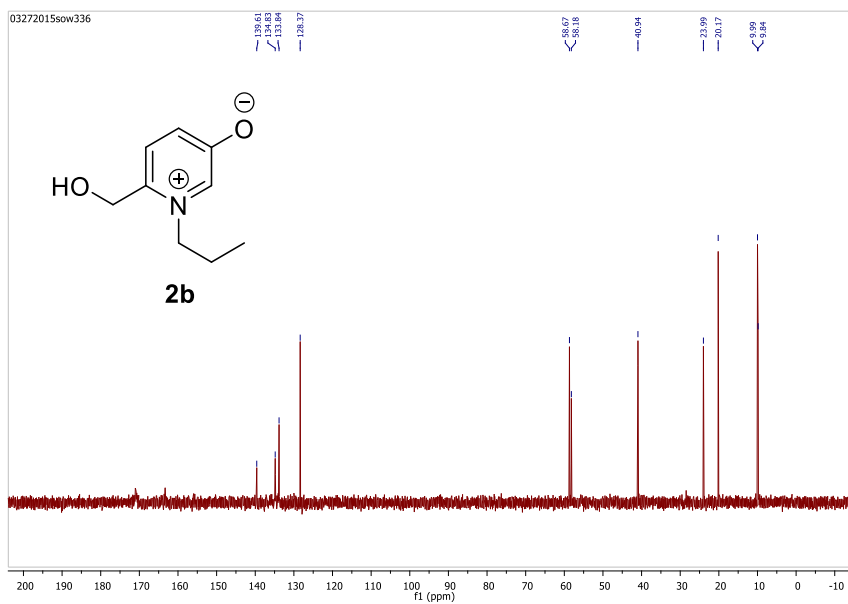


Fig S79: ¹³C NMR(D₂O) of propylamine pyridinium salt.

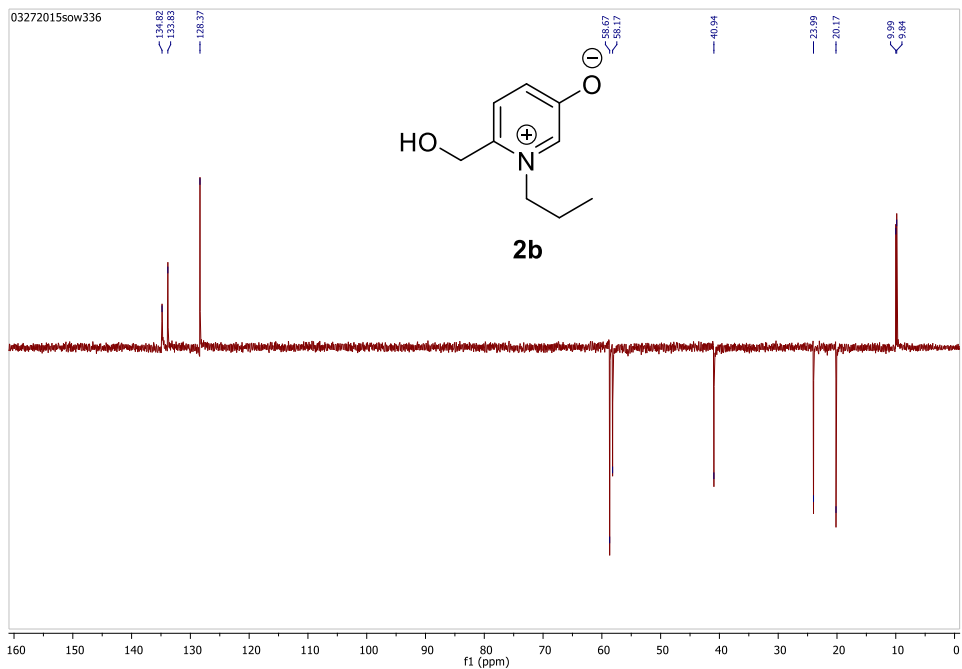


Fig S80: ^{13}C Dept NMR(D_2O) of propylamine pyridinium salt.

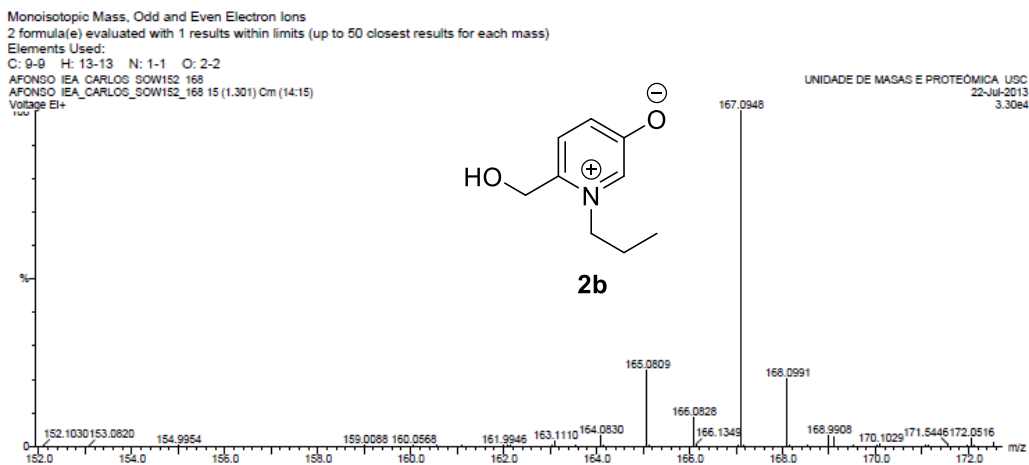


Fig S81: HRMS of propylamine pyridinium salt

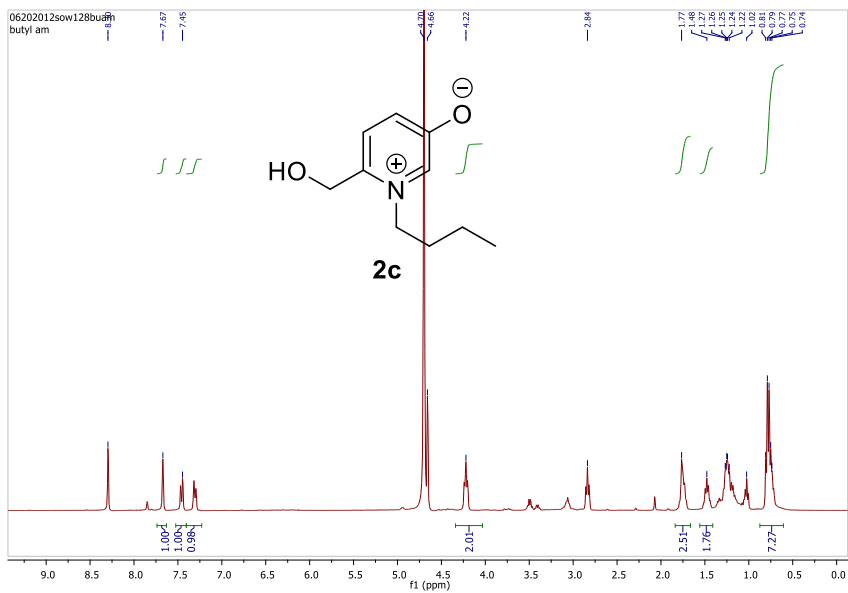


Fig S82: ¹H NMR(D₂O) of butylamine pyridinium salt.

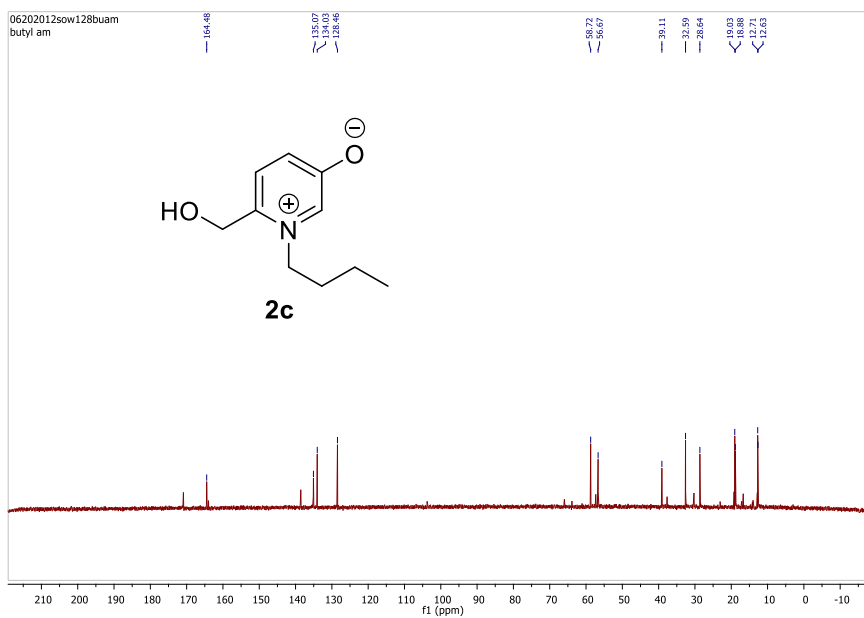


Fig S83: ¹³C NMR (D₂O) of butylamine pyridinium salt.

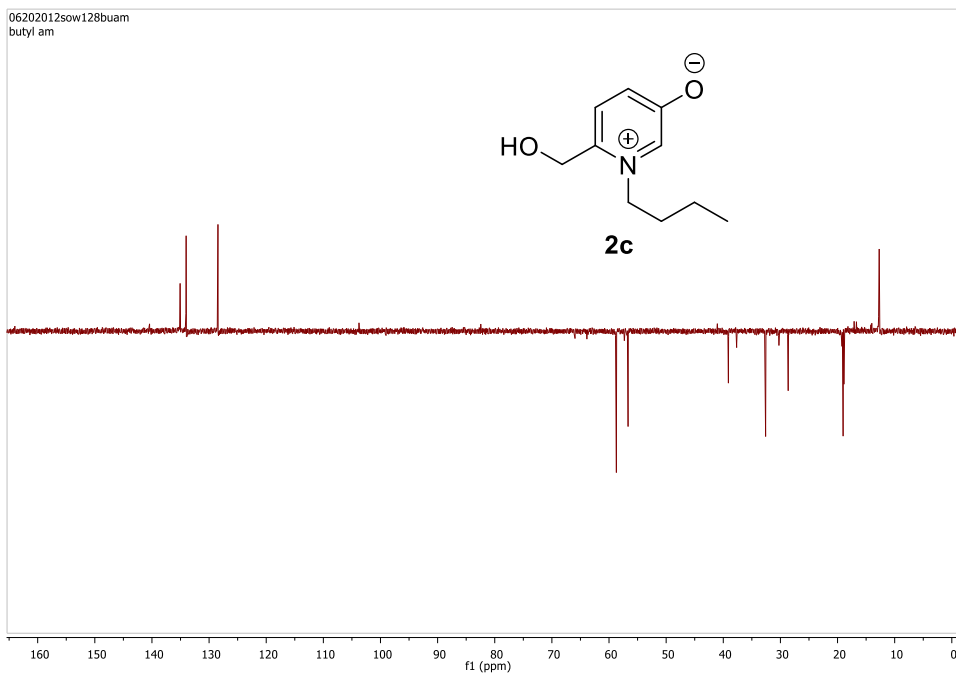


Fig S84: ^{13}C Dept NMR (D_2O) of butylamine pyridinium salt.

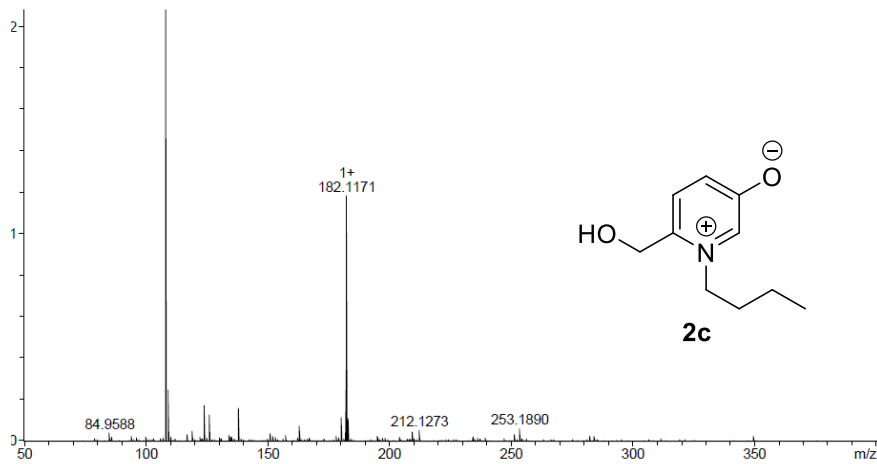


Fig S85: HRMS (D_2O) of butylamine pyridinium salt.

Supporting details

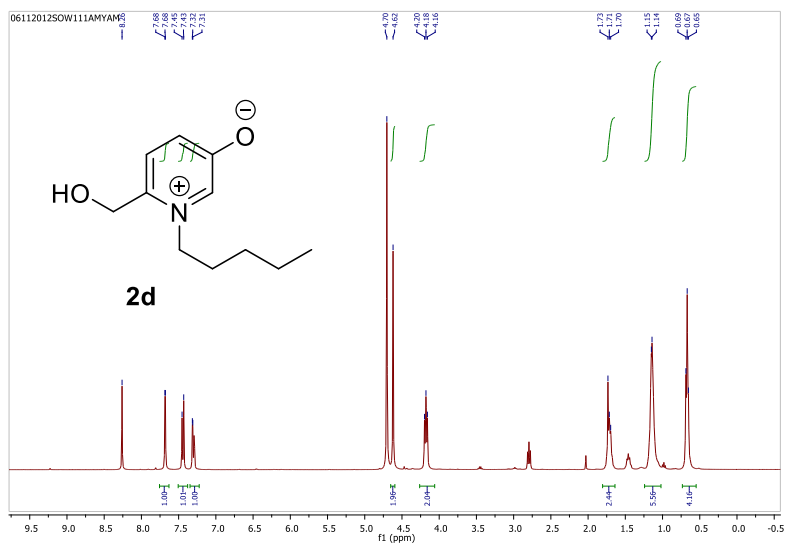


Fig S86: ¹H NMR(D₂O) of pentylamine pyridinium salt.

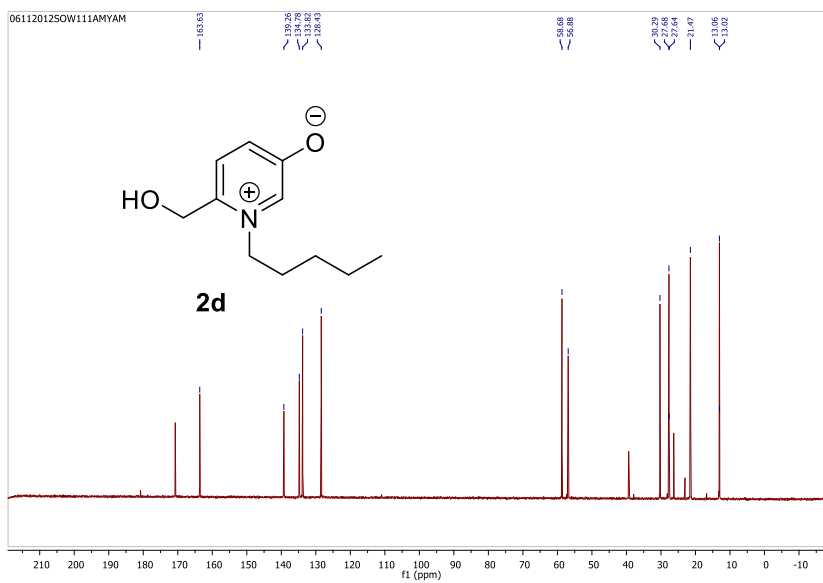


Fig S87: ¹³C NMR(D₂O) of pentylamine pyridinium salt.

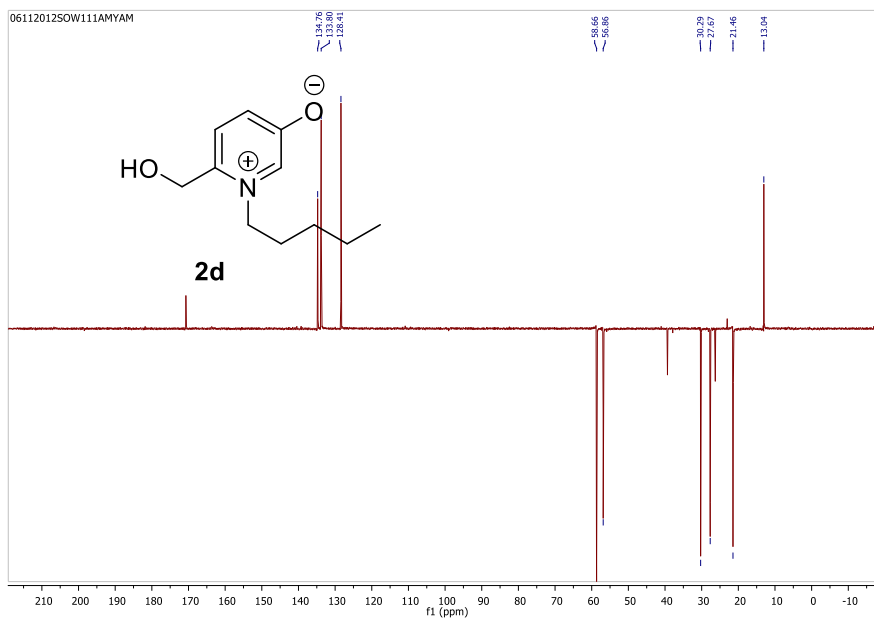


Fig S88: ^{13}C Dept NMR(D_2O) of pentylamine pyridinium salt.

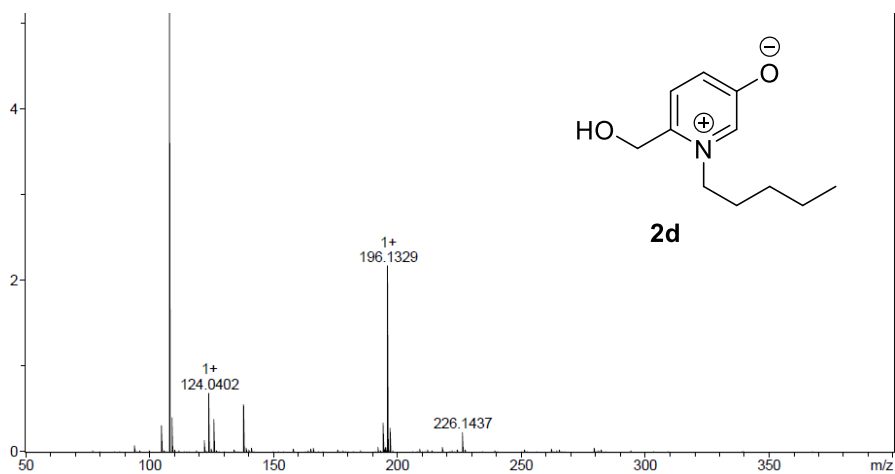


Fig S89: HRMS of pentylamine pyridinium salt

Supporting details

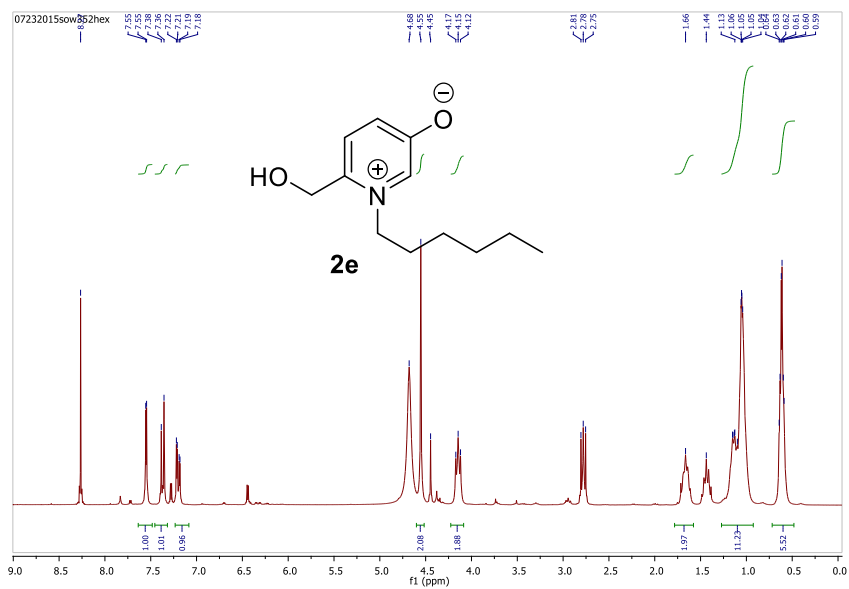


Fig S90: ¹H NMR(D₂O) of hexylamine pyridinium salt.

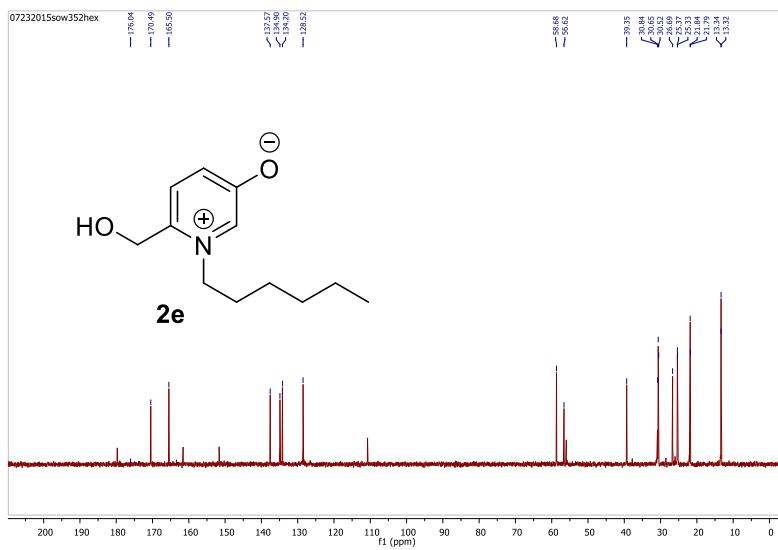


Fig S91: ¹³C NMR(D₂O) of hexylamine pyridinium salt.

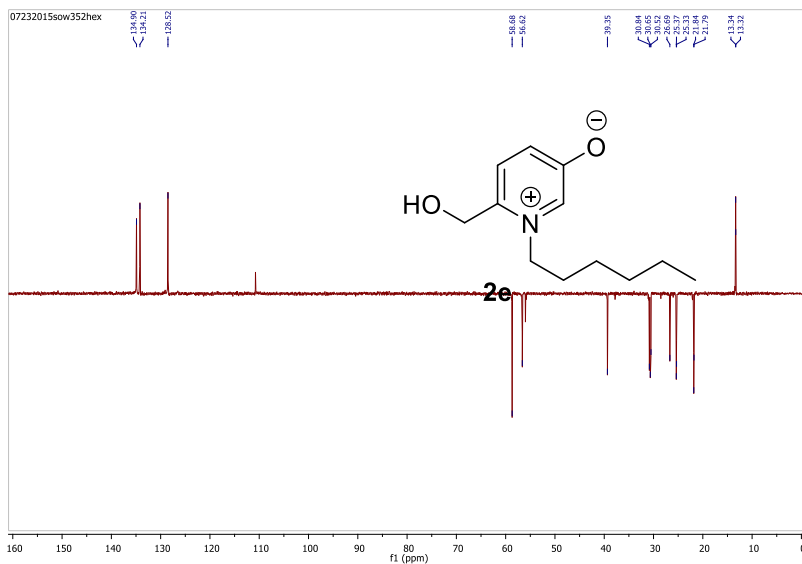


Fig S92: ^{13}C Dept NMR(D_2O) of hexylamine pyridinium salt.

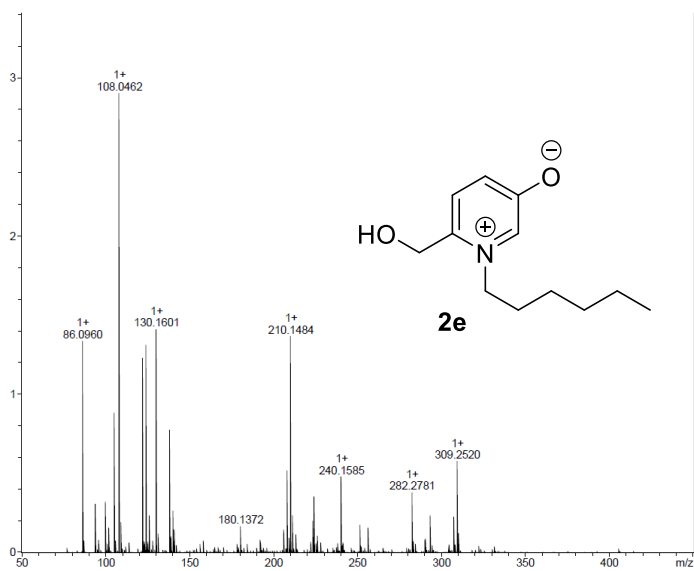


Fig S93: HRMS of hexylamine pyridinium salt

Supporting details

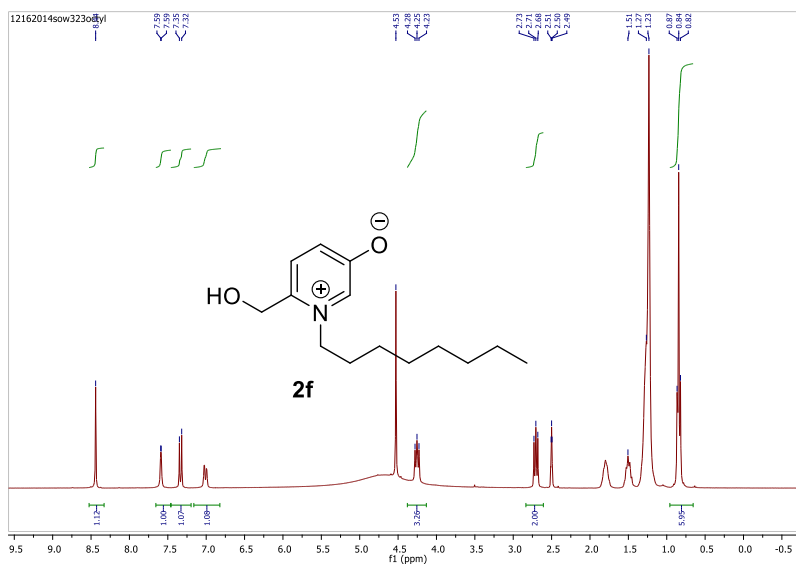


Fig S94: ^1H NMR(D_2O) of octylamine pyridinium salt.

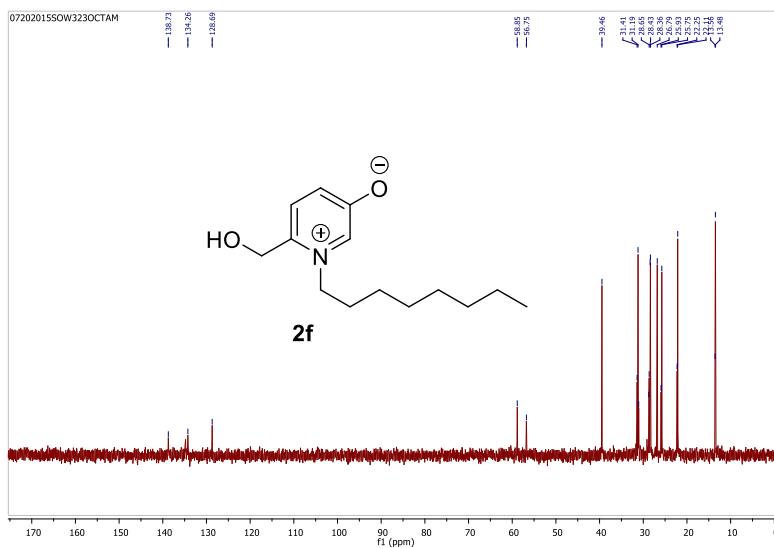


Fig S95: ^{13}C NMR(D_2O) of octylamine pyridinium salt.

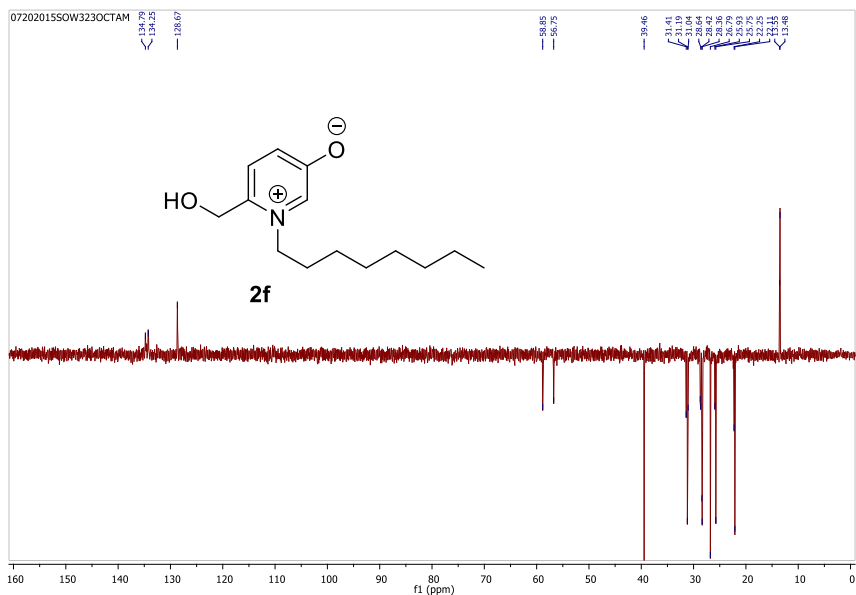


Fig S96: ^{13}C Dept NMR(D_2O) of octylamine pyridinium salt.

SOW-323 #8-12 RT: 0.20-0.31 AV: 5 NL: 2.08E8
F: FTMS + p ESI SIM ms [228.00-248.00]

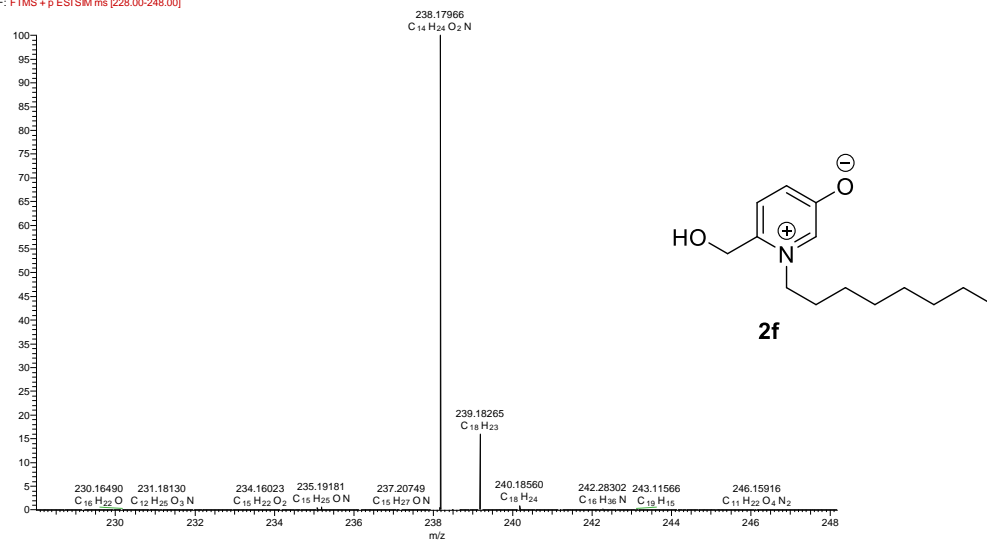


Fig S97: HRMS of octylamine pyridinium salt

Supporting details

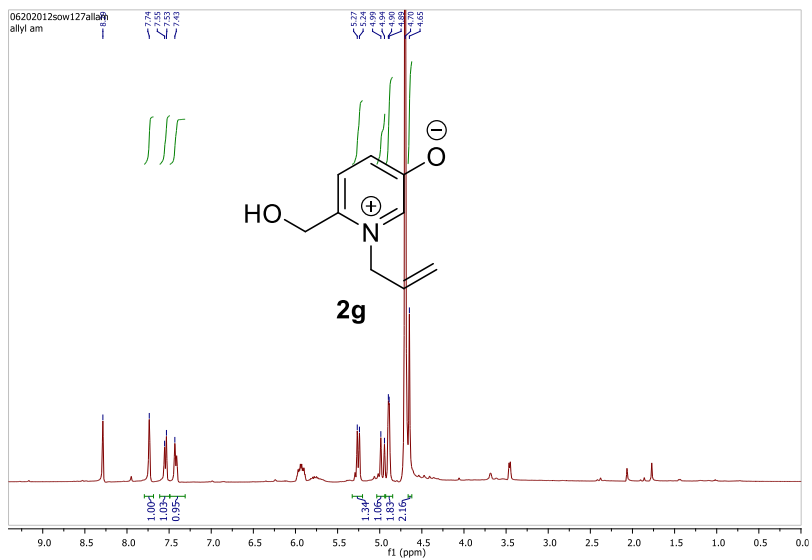


Fig S98: ^1H NMR(D₂O) of Allylamine pyridinium salt.

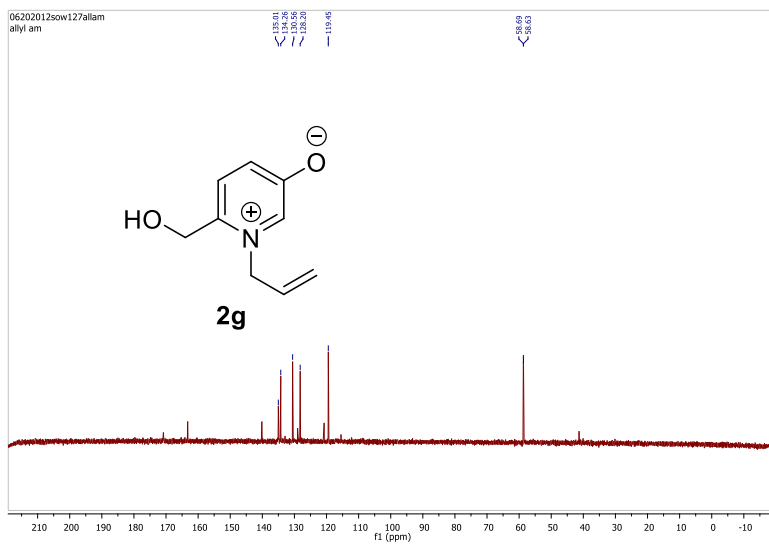


Fig S99: ^{13}C NMR(D₂O) of Allylamine pyridinium salt.

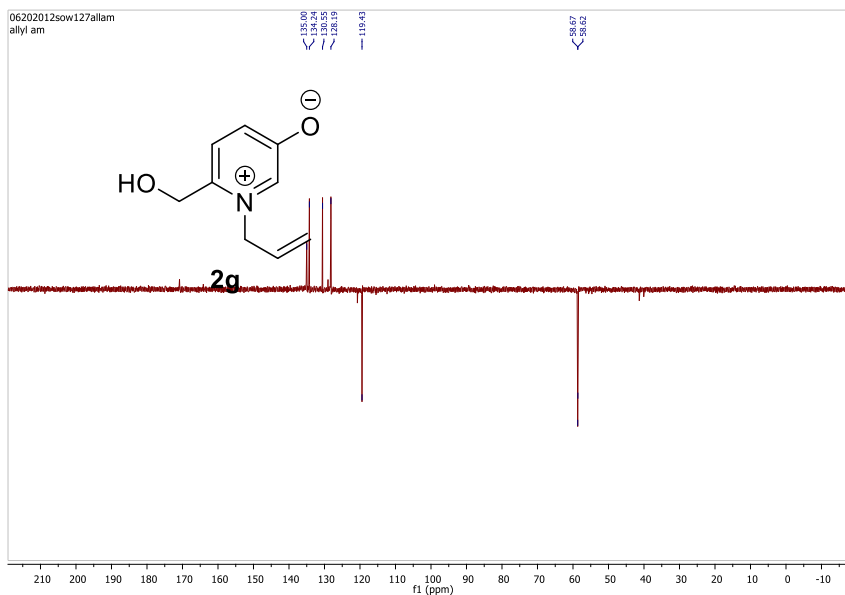


Fig S100: ^{13}C Dept NMR(D_2O) of Allylamine pyridinium salt.

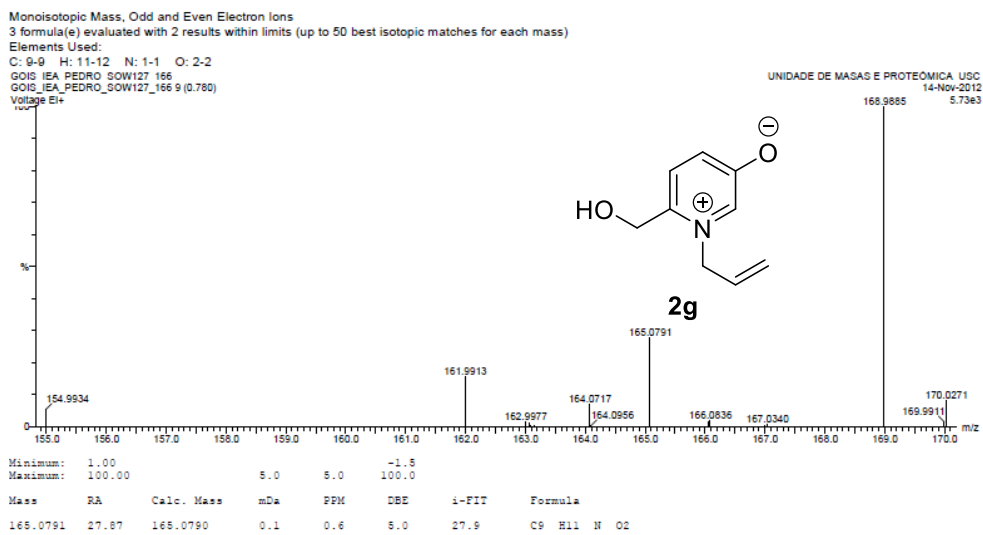


Fig S101: HRMS of Allylamine pyridinium salt

Supporting details

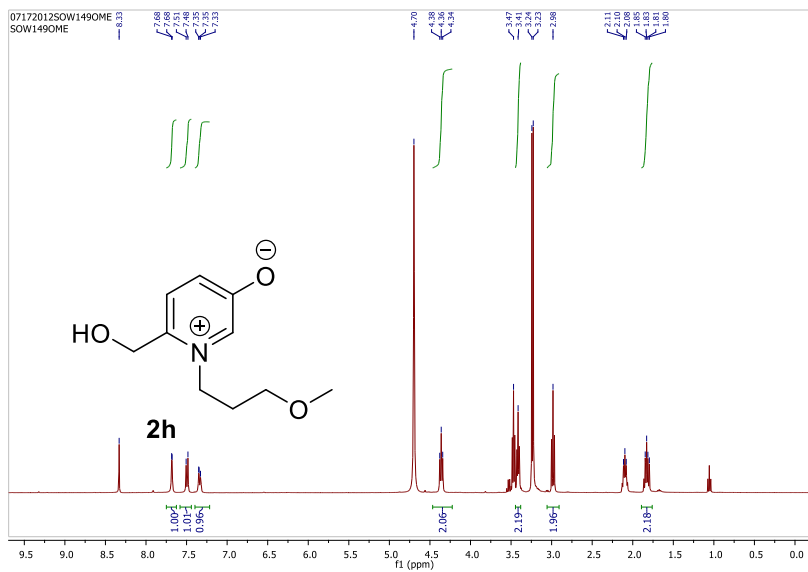


Fig S102: ^1H NMR(D_2O) of methoxypropylamine pyridinium salt.

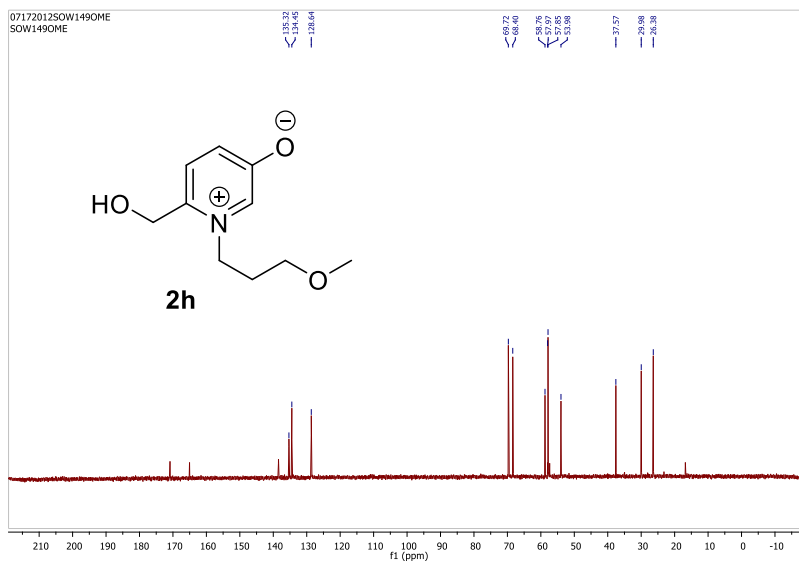


Fig S103: ^{13}C NMR(D_2O) of methoxypropylamine pyridinium salt.

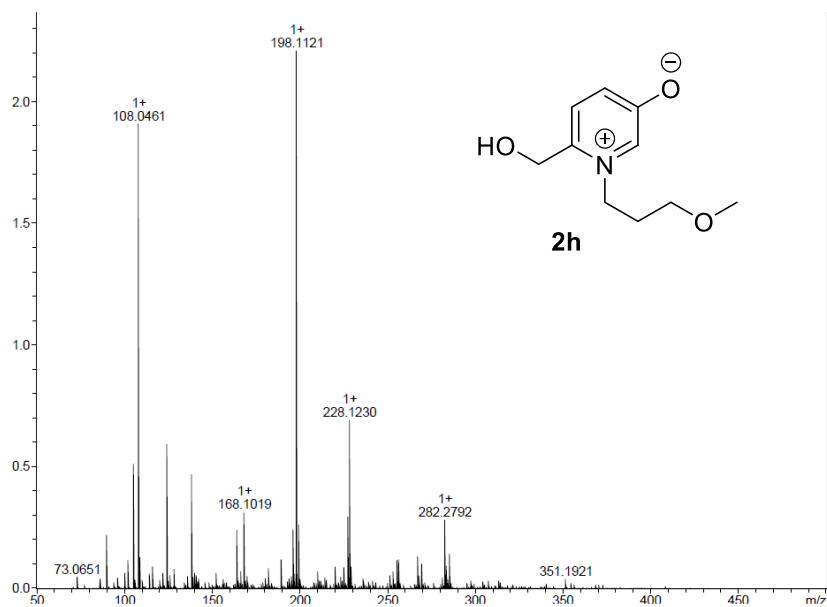


Fig S104: HRMS of methoxypropylamine pyridinium salt

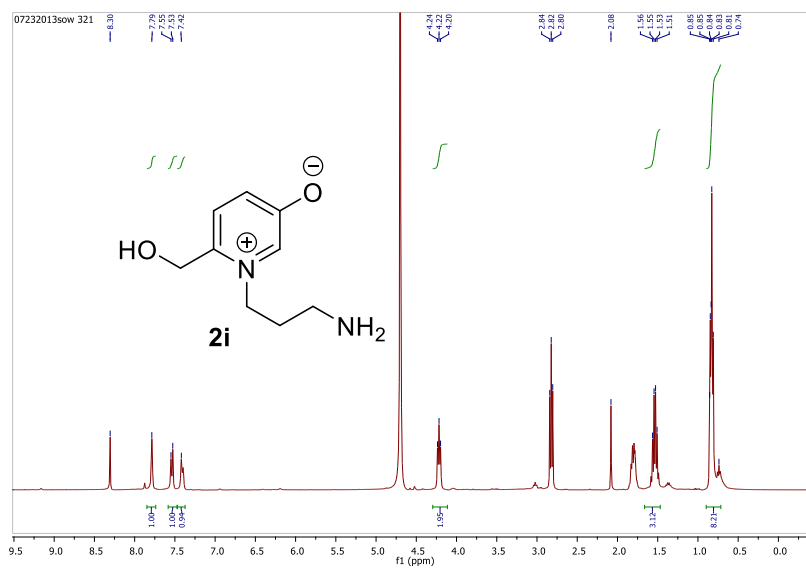


Fig S105: ^1H NMR(D_2O) of propyldiamine pyridinium salt.

Supporting details

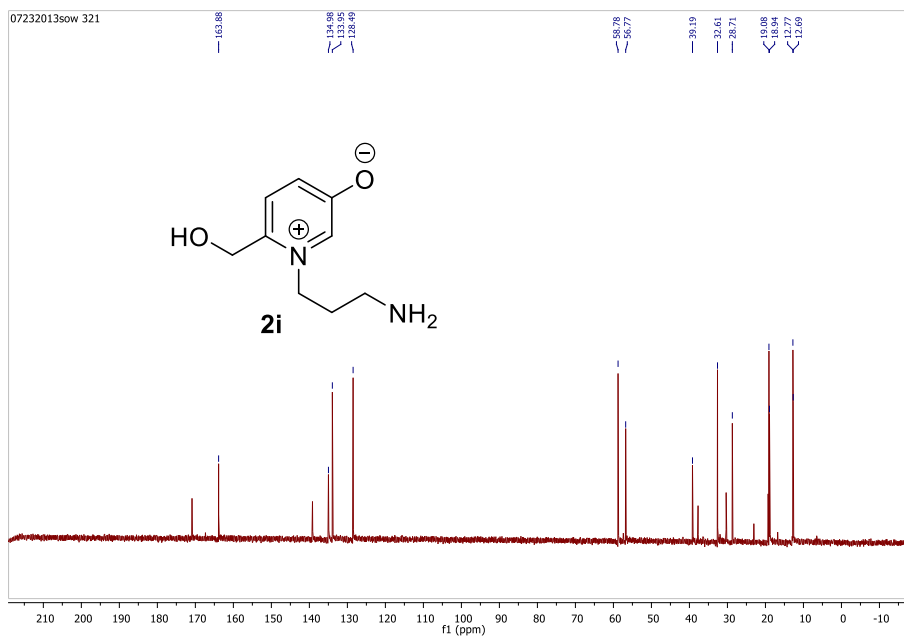


Fig S106: ^{13}C NMR(D_2O) of propyldiamine pyridinium salt.

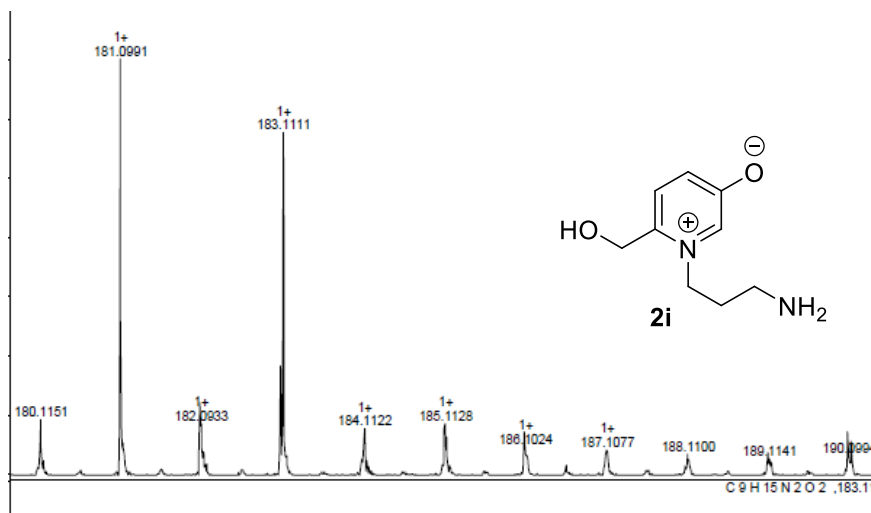


Fig S107: HRMS of propyldiamine pyridinium salt

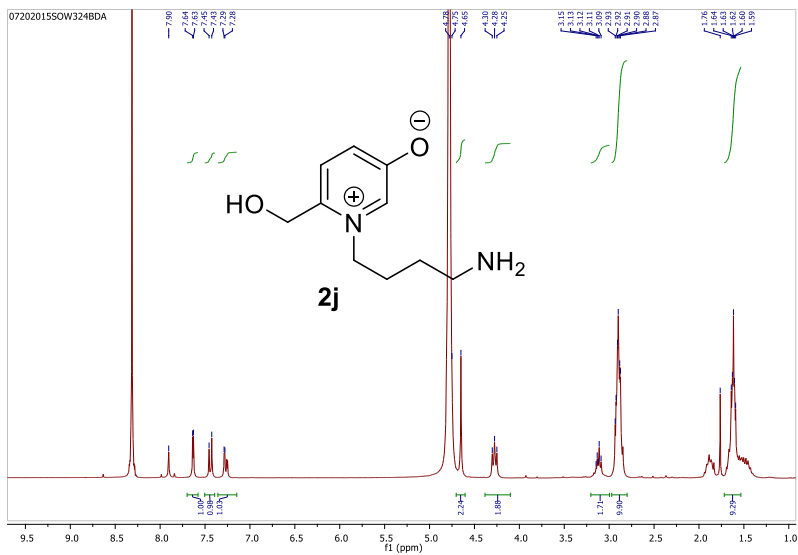


Fig S108: ¹H NMR(D₂O) of butyldiamine pyridinium salt.

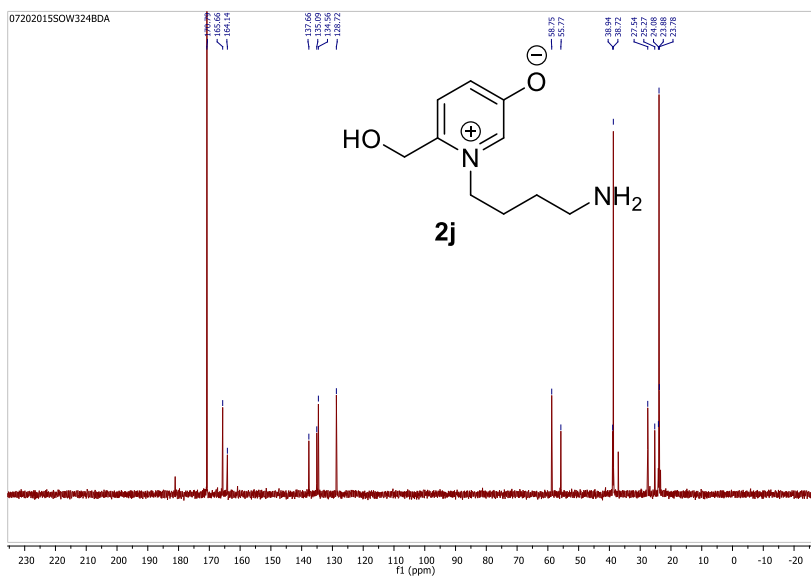


Fig S109: ¹³C NMR(D₂O) of butyldiamine pyridinium salt.

Supporting details

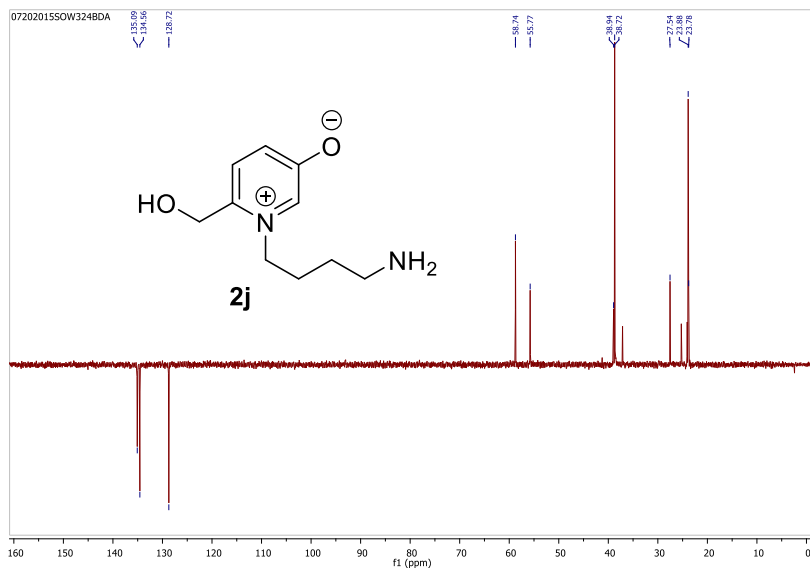


Fig S110: ^{13}C Dept NMR(D_2O) of butyldiamine pyridinium salt.

SOW-324 #12-16 RT: 0.33-0.43 AV: 5 NL: 2.57E7
F: FTMS + p ESI SIM ms [187.00-207.00]

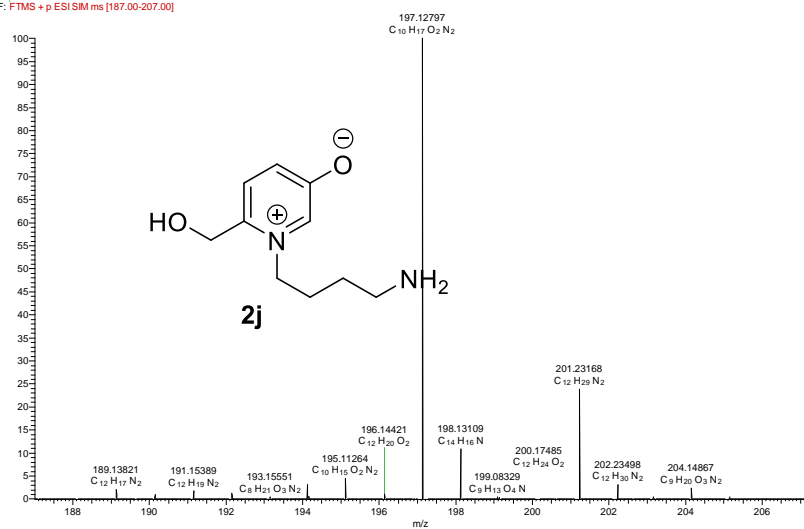


Fig S111: HRMS of butyldiamine pyridinium salt

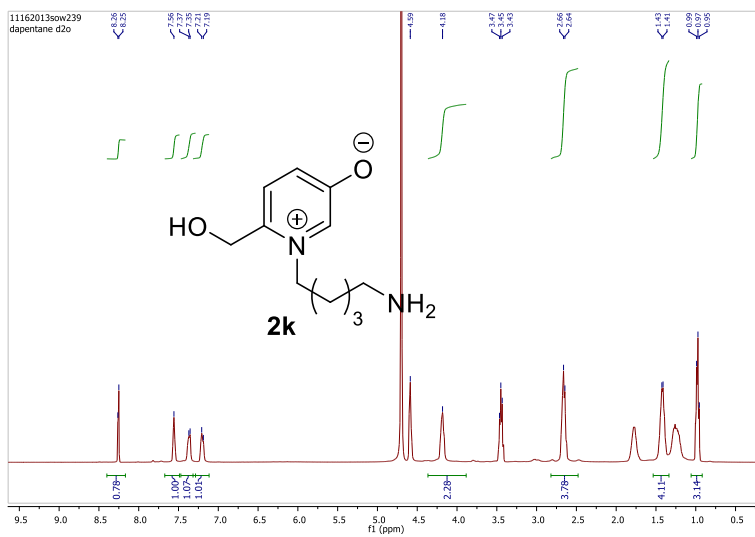


Fig S112: ^1H NMR(D_2O) of pentyldiamine pyridinium salt.

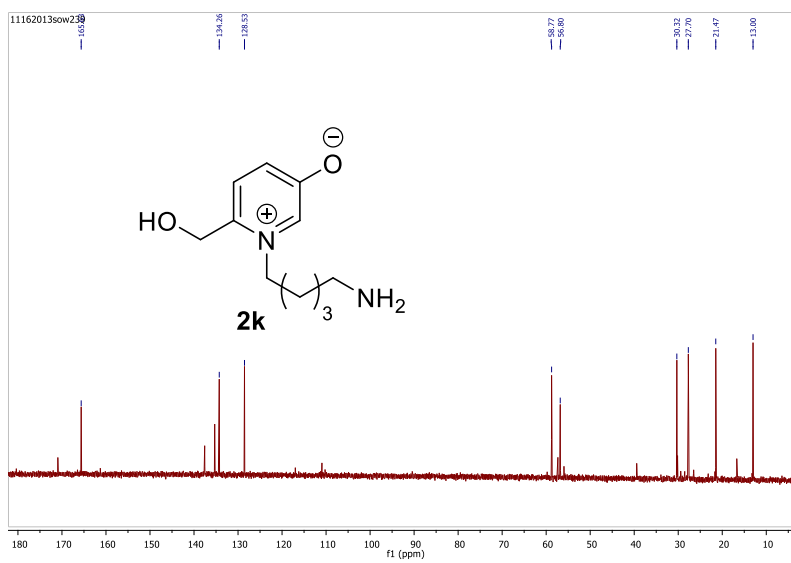


Fig S113: ^{13}C NMR(D_2O) of pentyldiamine pyridinium salt.

Supporting details

SOW-342 #11-13 RT: 0.28-0.34 AV: 3 NL: 3.46E7
 F: FTMS + p ESI SIM ms [202.00-220.00]

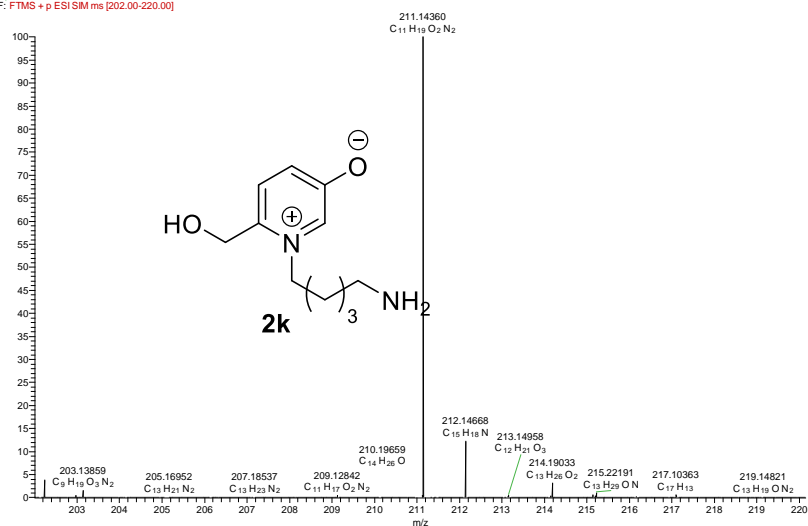


Fig S114: HRMS of pentyldiamine pyridinium salt

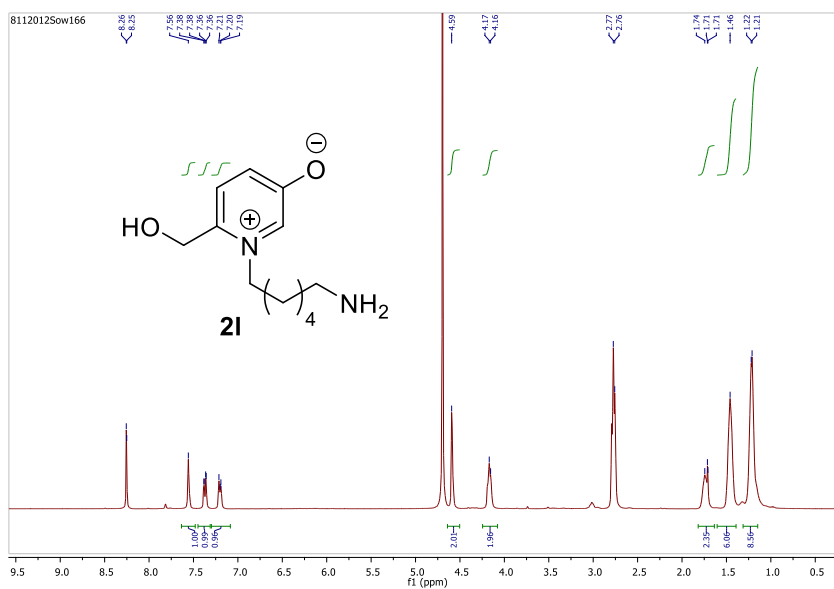


Fig S115: ¹H NMR(D₂O) of hexyldiamine pyridinium salt.

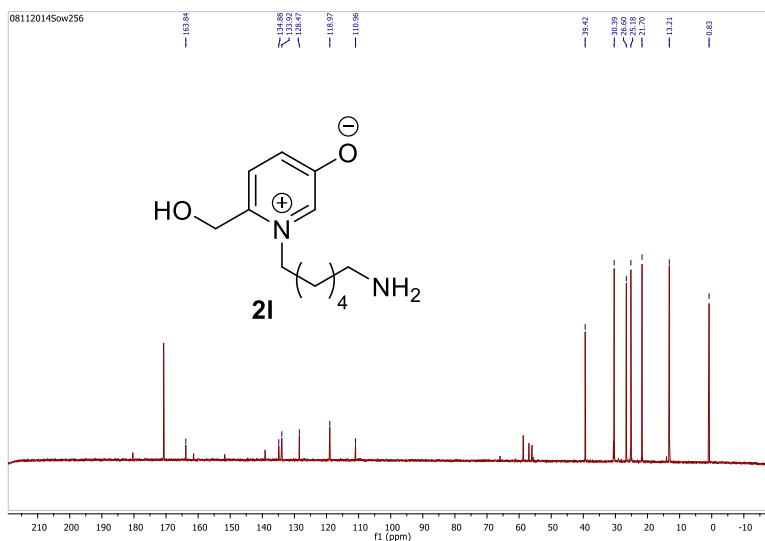


Fig S116: ^{13}C NMR(D_2O) of hexyldiamine pyridinium salt.

Monoisotopic Mass, Odd and Even Electron Ions

1 formula(e) evaluated with 1 results within limits (up to 50 closest results for each mass)

Elements Used:

C: 12-12 H: 21-21 N: 2-2 O: 2-2

AFONSO_JEA_CARLOS_SOW219_225

AFONSO_JEA_CARLOS_SOW219_225 17 (1.474)

Voltage E1+

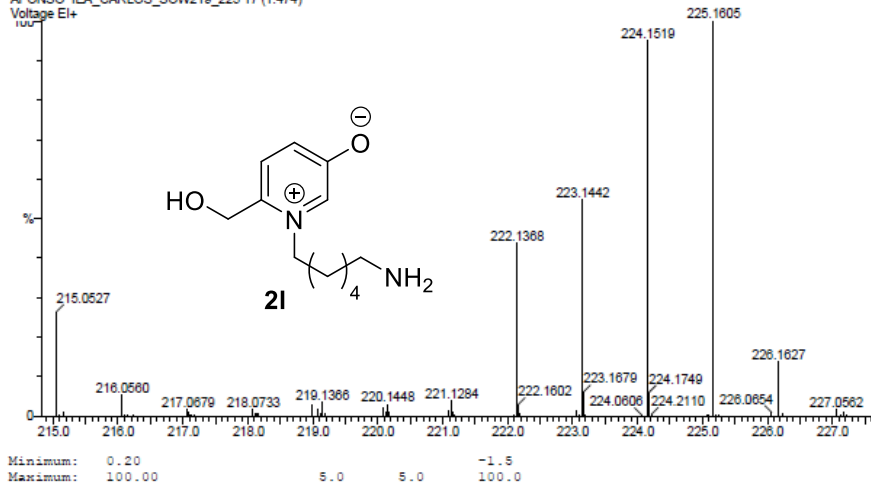


Fig S117: HRMS of hexyldiamine pyridinium salt

Supporting details

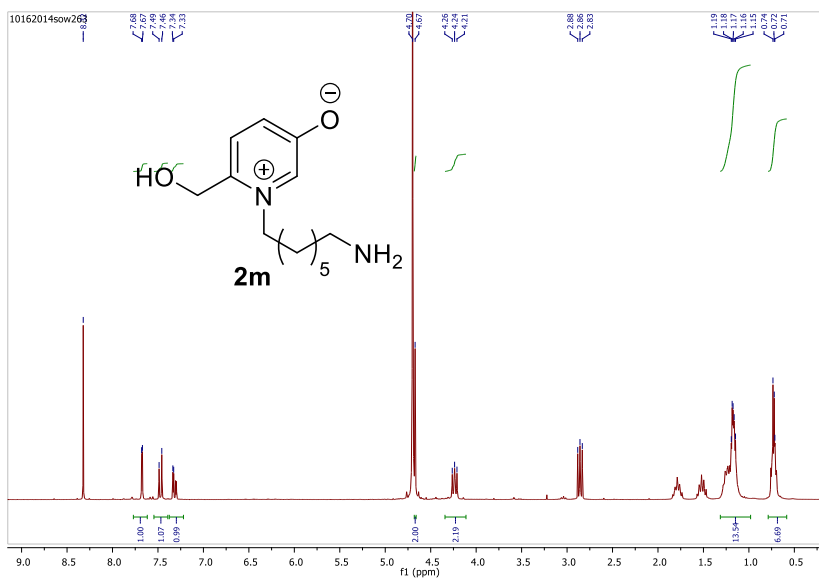


Fig S118: ¹H NMR(D₂O) of heptyldiamine pyridinium salt.

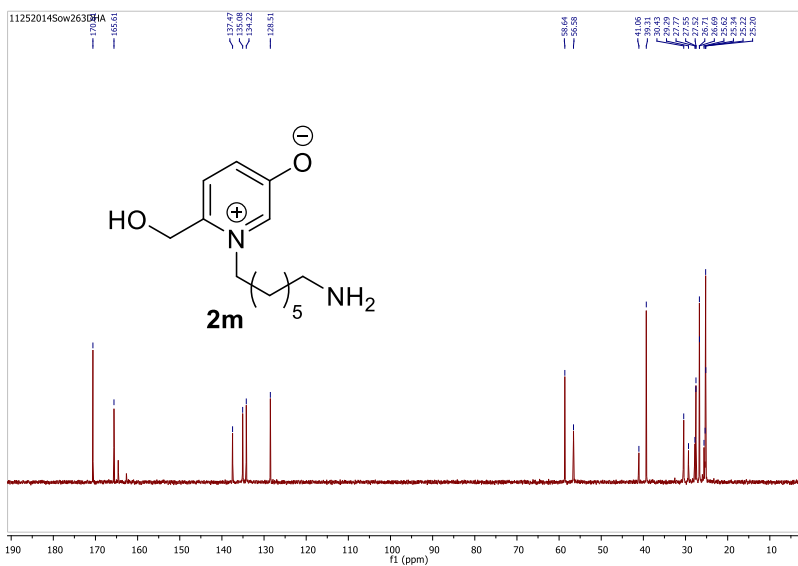


Fig S119: ¹³C NMR(D₂O) of heptyldiamine pyridinium salt.

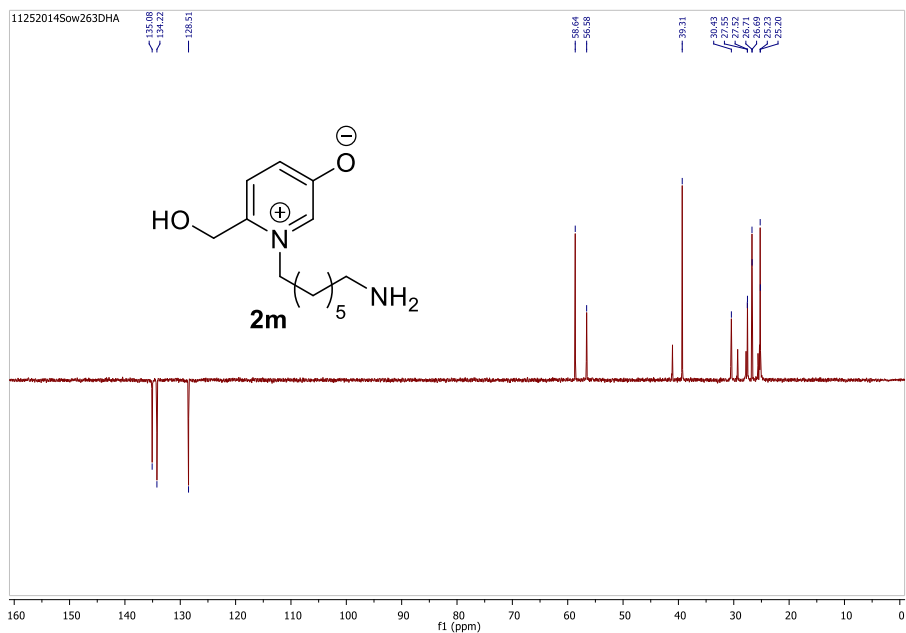


Fig S120: ^{13}C Dept NMR(D_2O) of heptyldiamine pyridinium salt.

SOW-263 #7-18 RT: 0.18-0.48 AV: 12 NL: 1.56E8
F: FTMS +p ESI SIM ms [229.00-249.00]

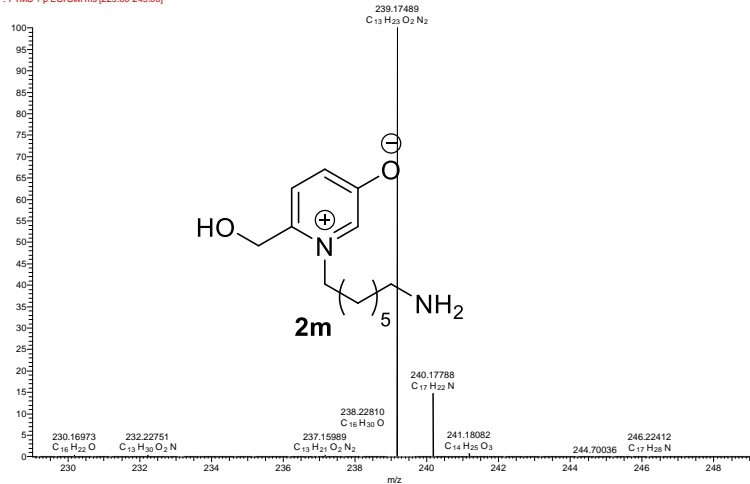


Fig S121: HRMS of heptyldiamine pyridinium salt

Supporting details

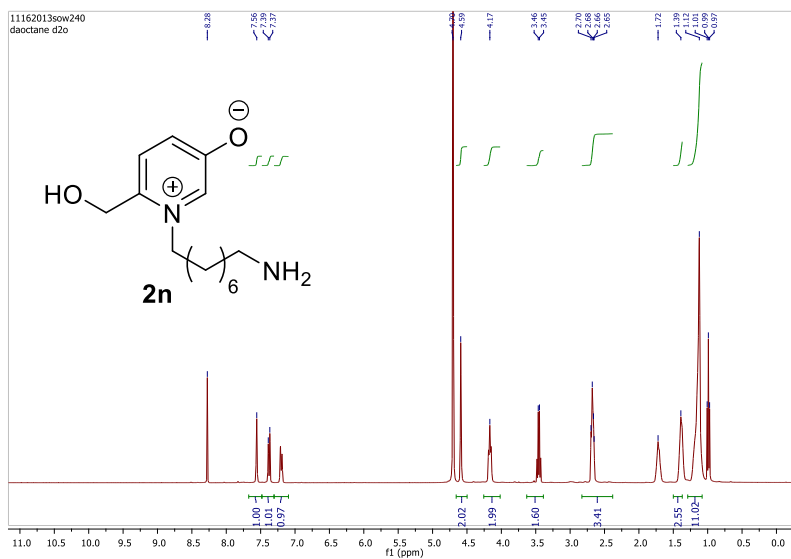


Fig S122: ^1H NMR(D_2O) of octyldiamine pyridinium salt.

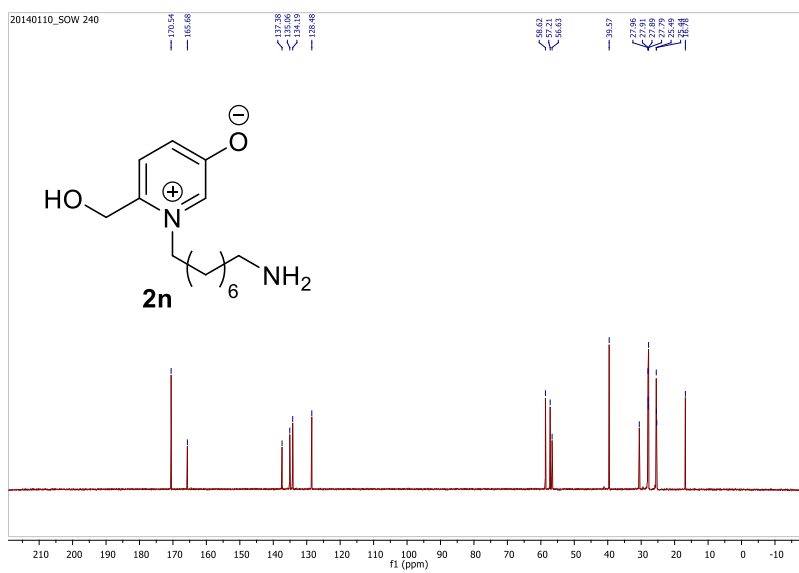


Fig S123: ^{13}C NMR(D_2O) of octyldiamine pyridinium salt.

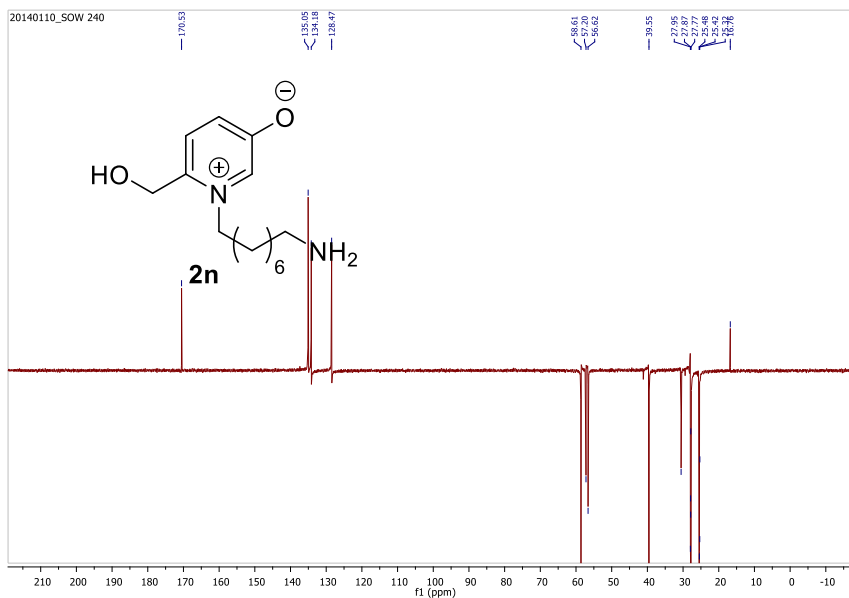


Fig S124: ¹³C Dept NMR(D₂O) of octyldiamine pyridinium salt.

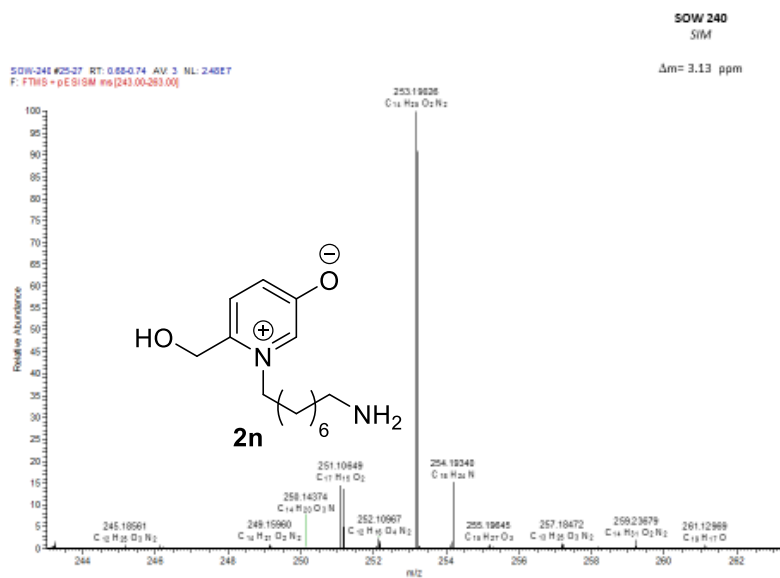


Fig S125: HRMS of octyldiamine pyridinium salt

Supporting details

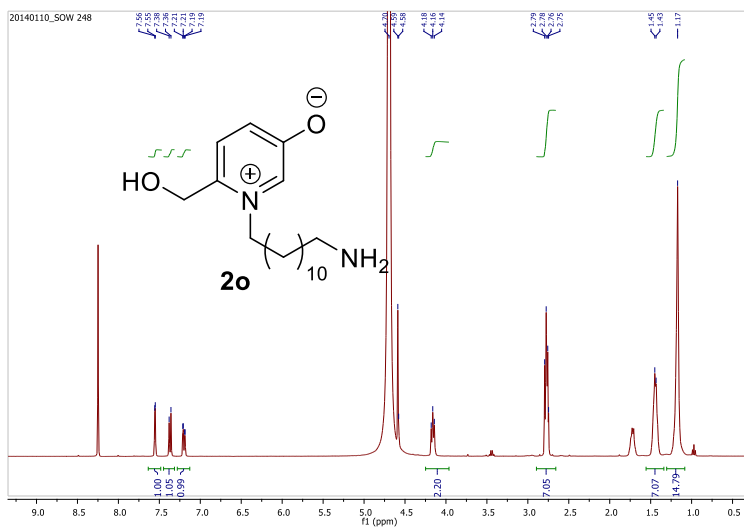


Fig S126: ¹H NMR(D₂O) of dodecylamine pyridinium salt.

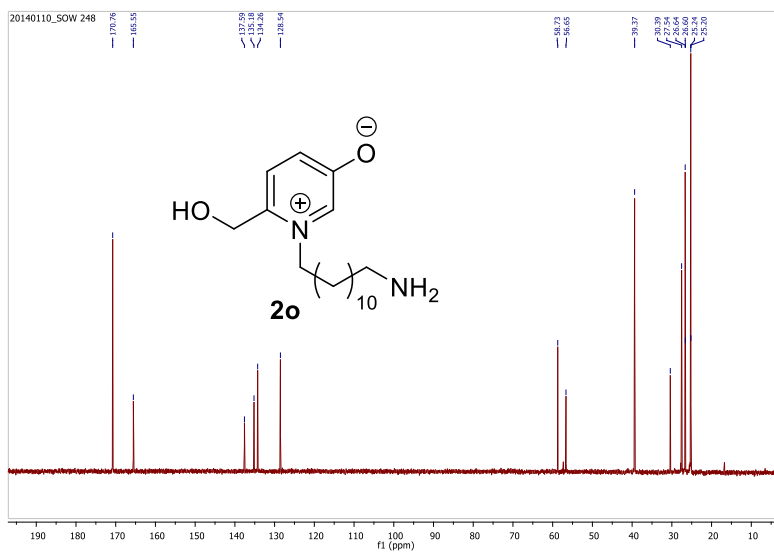


Fig S127: ¹³C NMR(D₂O) of dodecylamine pyridinium salt.

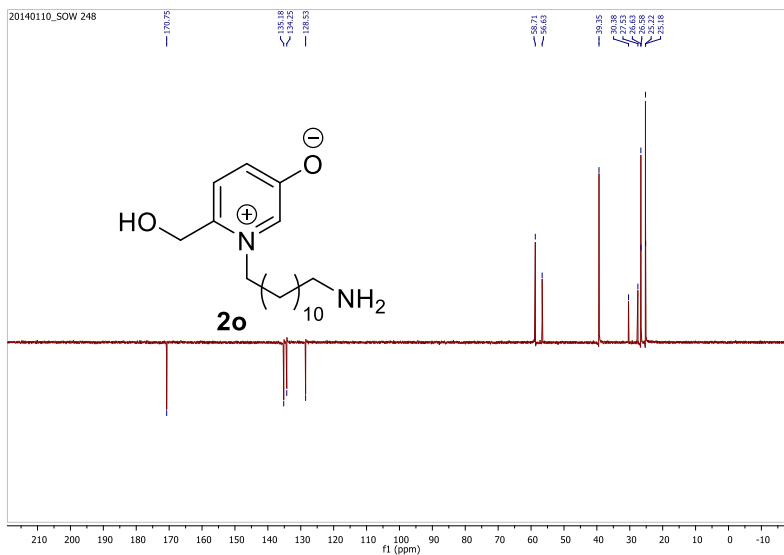


Fig S128: ¹³C Dept NMR(D₂O) of dodecylamine pyridinium salt.

SOW-343 #18-29 RT: 0.49-0.79 AV: 12 NL: 9.23E7
F: FTMS + p ESI/SM ms [299.00-319.00]

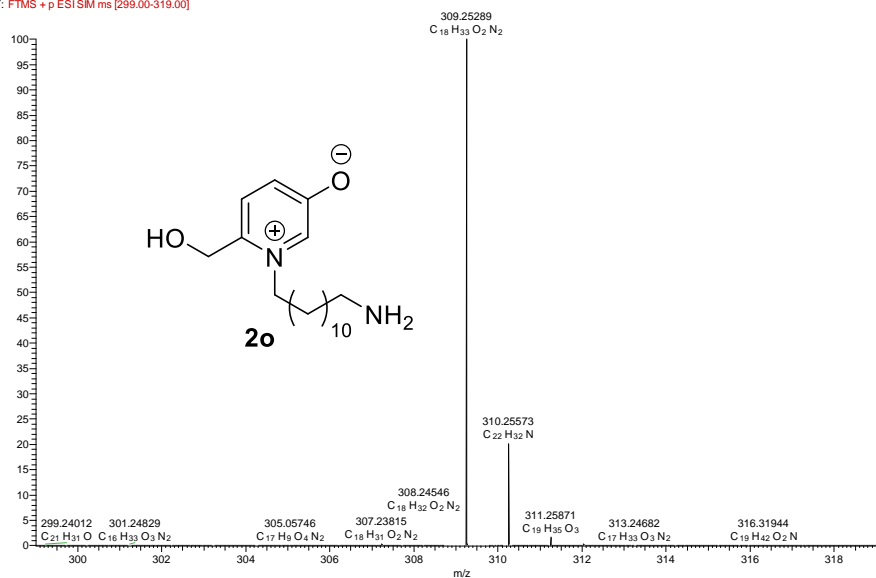


Fig S129: HRMS of dodecylamine pyridinium salt

Supporting details

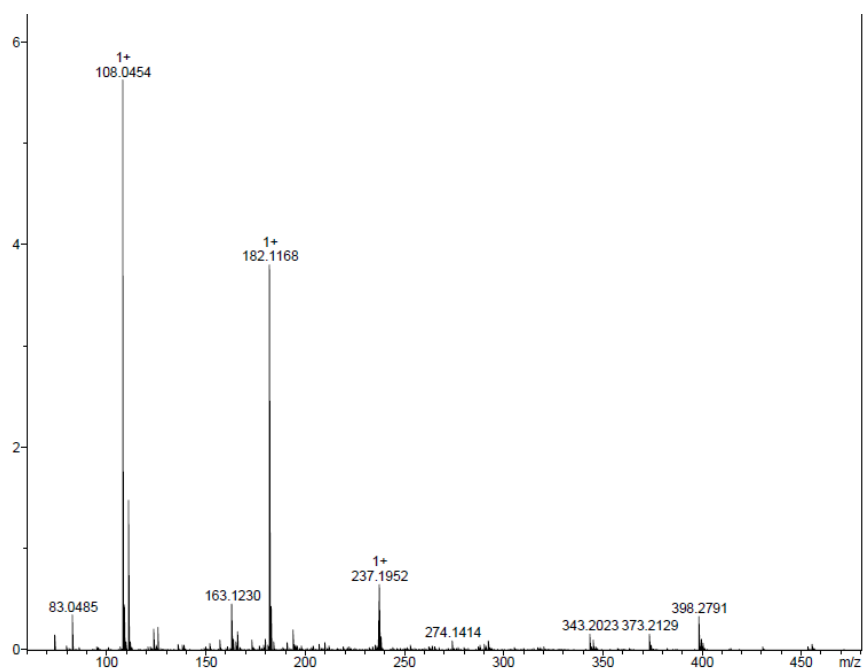


Fig S130: HRMS of isotope water experiment

DFT calculations – Results and Discussion

The mechanism proposed for the formation of the pyridinium salts was investigated by means of DFT calculations.[1] Two explicit water molecules (solvent) were considered in the computational model, in order to have a reasonable description for the solvent assistance on the various proton transfer steps along the mechanism. The complete energy profile obtained for the reaction is represented in Figures S131 and S132.

The reaction starts with the iminium ion resulting from the reaction of HMF with methylamine (**A**). The first step is a nucleophilic attack of one water molecule on the C5 atom of the furan ring with a subsequent proton loss, yielding intermediate **B**. This step is formally a OH^- addition, has a barrier of 27 kcal/mol ($\text{TS}_{\text{A} \rightarrow \text{B}}$) and is clearly endoenergetic ($\Delta E = 24$ kcal/mol) reflecting the loss of the furan ring. The extra water molecule close to the molecule receives the proton in the form of a H_3O^+ ion, in **B**.

The second step of the mechanism, from **B'** to **C**, corresponds to the opening of the furan ring. This is accomplished through a proton transfer from the recently added OH group to the original furan O-atom. This process is assisted by the two neighbor water molecules, presents a barrier of 24 kcal/mol and is essentially thermoneutral with intermediate **C** being only 4 kcal/mol less stable than **B'**.

From **C** to **C'** there is a rearrangement of the H-bond network involving the two water molecules. The last step in the profile of Figure S131, from **C'** to **D**, corresponds to a keto-enol tautomerism, transforming the enol moiety in intermediates **C** and **C'** into a ketone $\text{C}=\text{O}$ group in intermediate **D**. This species is the equivalent of intermediate **1** in Scheme 2, with $\text{R} = \text{Me}$. The

Supporting details

proton transfer associated with the tautomerism is assisted by the water molecules giving another indication of the active role played by the solvent has a proton shuttle, along the path. The barrier calculated for the tautomerism step is similar to the ones obtained for the previous steps ($\Delta E^\ddagger = 27$ kcal/mol) and the energy balance reveals a slightly exoenergetic step ($\Delta E = -2$ kcal/mol).

The second part of the mechanism, from intermediate **D** on, is represented in Figure S132.

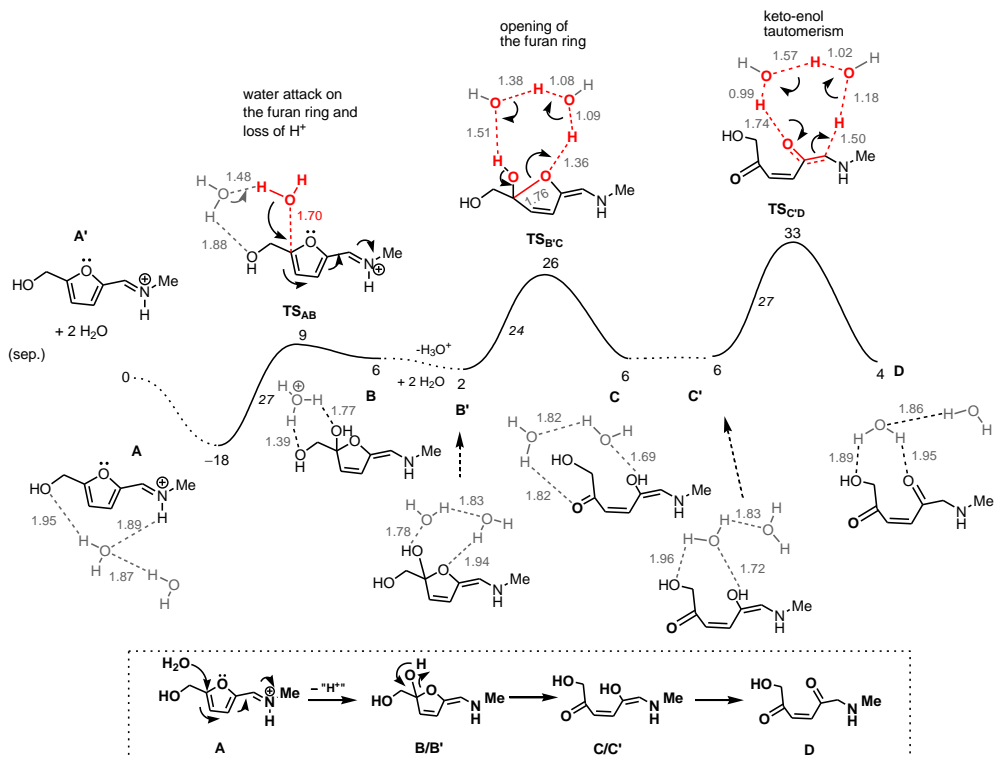


Figure S131. Energy profile calculated (M06-2X) for the formation of intermediate **1** (**D**) from the iminium cation (**A**). Energy values (kcal/mol) are referred to the separated reagents (**A** plus two water molecules) and the values in italics represent energy barriers. Relevant distances are indicated (Å).

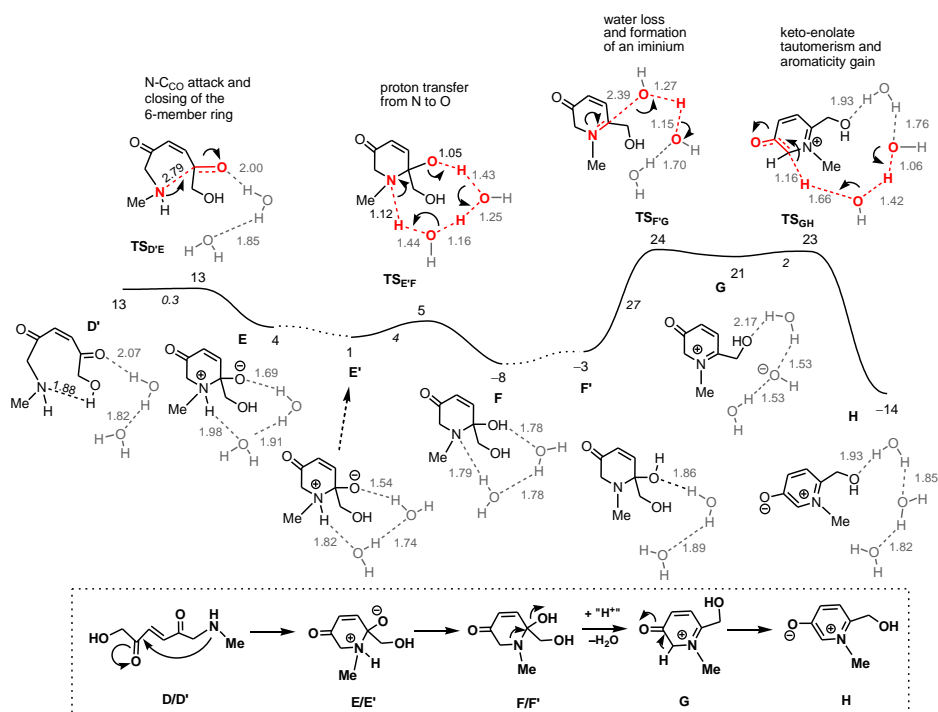


Figure S132. Energy profile calculated (M06-2X) for the mechanism of formation of pyridinium product (**H**) from intermediate **D**. Energy values (kcal/mol) are referred to the separated reagents (**A** plus two water molecules) and the values in italics represent energy barriers. Relevant distances are indicated (Å).

The mechanism proceeds from **D'** with N-nucleophilic attack on the carbonyl C-atom, resulting in 6-member ring, in **E**. This step is essentially barrierless from **D'** ($\Delta E^\ddagger = 0.3$ kcal/mol). However, the corresponding transition state (**TS_{D'E}**) is 9 kcal/mol above **D**, and, thus, this value represents better the barrier for the process. In fact, in **D'**, the molecule has a conformation that brings the N-atom and the carbonyl group to the orientation most favorable for the following bond formation step. The conformation of the intermediate and the H-bond network with the surrounding water molecules are considerably less stable in **D'** than in **D** (by 9 kcal/mol).

The following step is a simple proton transfer from N to O, changing a zwitterion (**E'**) into a neutral species (**F**). Again, participation of the water molecules is crucial, yielding a barrier of only 4 kcal/mol and a clearly exoenergetic process ($\Delta E = -7$ kcal/mol).

From **F** to **F'**, there is a re-organization of the H-bond network involving the intermediates and the two neighbor water molecules. From intermediate **F'** the path continues with loss of OH^- , following the establishment of N=C double bond (in **G**). Importantly, the hydroxide ion that leaves intermediate **F'** belonged to the initial water molecule that attacked the furan ring in the first step of the mechanism. Thus, although water participation is crucial to the reaction path, the corresponding O-atom that is added to the reagent in the beginning of the mechanism is lost further ahead in the path. This is in good accordance with the experimental observation indicating absence of ^{18}O in the reaction product when the reaction is carried on in H_2O^{18} . Formation of **G**, from **F'**, has a barrier of 27 kcal/mol and is an unfavorable

Supporting details

process, from the thermodynamic point of view ($\Delta E = 24$ kcal/mol). However, deprotonation of the methylene group in the ring by the recently formed hydroxide ion yields the final product (**H**) in the last step of the mechanism. This is a very easy and quite favorable process, with a negligible barrier of only 2 kcal/mol and $\Delta E = -35$ kcal/mol. The stability of product **H** reflects the aromaticity gain associated with the formation of the pyridinium ion.

The larger values obtained for the individual barriers along the path are 27 kcal/mol and the highest point in the profile (**TS_{C-D}**) is 33 kcal/mol above the initial reactants. This gives a rough indication of about 30 kcal/mol for the overall reaction barrier, a value in reasonable agreement with the experimental conditions of the reaction (two days at 80 °C). Nevertheless, it is important to notice that the accuracy of the energy values is somewhat limited by the modesty of the model used in the calculations, with only two explicit water molecules in a mechanism where that solvent plays a decisive part.

In conclusion, the mechanism proposed in Scheme 2 was reproduced by the DFT calculations. In the path obtained water plays a crucial role, not only as a proton carrier, assisting all the proton transfer steps, but also as an active participant in the reaction, being added to the furan ring of the initial iminium salt and lost in the final steps that lead to the pyridinium product.

DFT calculations – References

- 1 Parr, R. G. & Yang, W. in *Density Functional Theory of Atoms and Molecules*; Oxford University Press: New York, (1989).
- 2 Gaussian 09, Revision **A.01**, Frisch, M. J.; Trucks, G. W.; Schlegel, H. B.; Scuseria, G. E.; Robb, M. A.; Cheeseman, J. R.; Scalmani, G.; Barone, V.; Mennucci, B.; Petersson, G. A.; Nakatsuji, H.; Caricato, M.; Li, X.; Hratchian, H. P.; Izmaylov, A. F.; Bloino, J.; Zheng, G.; Sonnenberg, J. L.; Hada, M.; Ehara, M.; Toyota, K.; Fukuda, R.; Hasegawa, J.; Ishida, M.; Nakajima, T.; Honda, Y.; Kitao, O.; Nakai, H.; Vreven, T.; Montgomery, Jr., J. A.; Peralta, J. E.; Ogliaro, F.; Bearpark, M.; Heyd, J. J.; Brothers, E.; Kudin, K. N.; Staroverov, V. N.; Kobayashi, R.; Normand, J.; Raghavachari, K.; Rendell, A.; Burant, J. C.; Iyengar, S. S.; Tomasi, J.; Cossi, M.; Rega, N.; Millam, J. M.; Klene, M.; Knox, J. E.; Cross, J. B.; Bakken, V.; Adamo, C.; Jaramillo, J.; Gomperts, R.; Stratmann, R. E.; Yazyev, O.; Austin, A. J.; Cammi, R.; Pomelli, C.; Ochterski, J. W.; Martin, R. L.; Morokuma, K.; Zakrzewski, V. G.; Voth, G. A.; Salvador, P.; Dannenberg, J. J.; Dapprich, S.; Daniels, A. D.; Farkas, Ö.; Foresman, J. B.; Ortiz, J. V.; Cioslowski, J.; Fox, D. J. Gaussian, Inc., Wallingford CT, 2009.
- 3 (a) McClean, A. D.; Chandler, G. S. *J. Chem. Phys.* **1980**, *72*, 5639. (b) Krishnan, R.; Binkley, J. S.; Seeger, R. Pople, J. A. *J. Chem. Phys.* **1980**, *72*, 650. (c) Wachters, A. J. H. *J. Chem. Phys.* **1970**, *52*, 1033. (d) Hay, P. J. *J. Chem. Phys.* **1977**, *66*, 4377. (e) Raghavachari, K.; Trucks, G. W. *J. Chem. Phys.* **1989**, *91*, 1062. (f) Binning Jr., R. C.; Curtiss, L. A. *J. Comp. Chem.*, **1990**, *11*, 1206. (g) McGrath, M. P.; Radom, L. *J. Chem.*

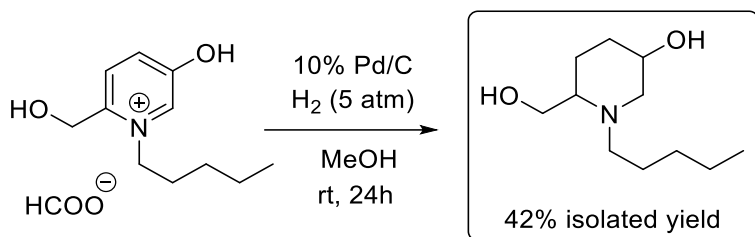
- Phys.* **1991**, *94*, 511. (h) Clark, T.; Chandrasekhar, J.; Spitznagel, G. W.; Schleyer, P. v. R. *J. Comp. Chem.* **1983**, *4*, 294. (i) Frisch, M. J.; Pople, J. A.; Binkley, J. S. *J. Chem. Phys.* **1984**, *80*, 3265.
- 4 Zhao, Y.; Truhlar, D.G. *Theor. Chem. Acc.*, **2008**, *120*, 215.
- 5 Zhao, Y.; Truhlar, D.G. *Acc. Chem. Res.*, **2008**, *41*, 157.
- 6 Zhao, Y.; Truhlar, D.G. *Chem. Phys. Lett.*, **2011**, *502*, 1.
- 7 (a) Peng, C.; Ayala, P.Y.; Schlegel, H.B.; Frisch, M.J. *J. Comp. Chem.*, **1996**, *17*, 49. (b) Peng, C.; Schlegel, H.B. *Israel J. Chem.*, **1994**, *33*, 449.
- 8 (a) Cancès, M. T.; Mennucci, B.; Tomasi, J. *J. Chem. Phys.* **1997**, *107*, 3032. (b) Cossi, M.; Barone, V.; Mennucci, B.; Tomasi, J. *Chem. Phys. Lett.* **1998**, *286*, 253. (c) Mennucci B.; Tomasi, J. *J. Chem. Phys.* **1997**, *106*, 5151. (d) Tomasi, J.; Mennucci, B.; Cammi, R. *Chem. Rev.* **2005**, *105*, 2999.
- 9 Marenich, A. V.; Cramer, C. J.; Truhlar, D. G. *J. Phys. Chem. B*, **2009**, *113*, 6378.

Chapter V

Supporting Information

**Studies on new biomass derived pyridinium
Salt**

5.1 Palladium catalyzed hydrogenation of *N*-Pentyl pyridinium salt



1-pentyl-5-hydroxy-2-(hydroxymethyl)pyridinium formate (120mg, 0.5 mmol) was dissolved in methanol (2mL) and added 10% Pd/C. Then the solution was stirred under 5 atm pressure of H₂ at room temperature for 24h. TLC analysis of the reaction mixture showed the presence of two distinct inseparable isomeric products. Methanol (10mL) was added to the reaction mixture and then filtered through celite. The solvent was evaporated and dried in vacuum to yield 42% of these isomeric products which were characterized by NMR. Due to the low yield and inseparable spots, the mixture of isomeric products were further treated with various protecting groups to be able to isolate them through column chromatography.

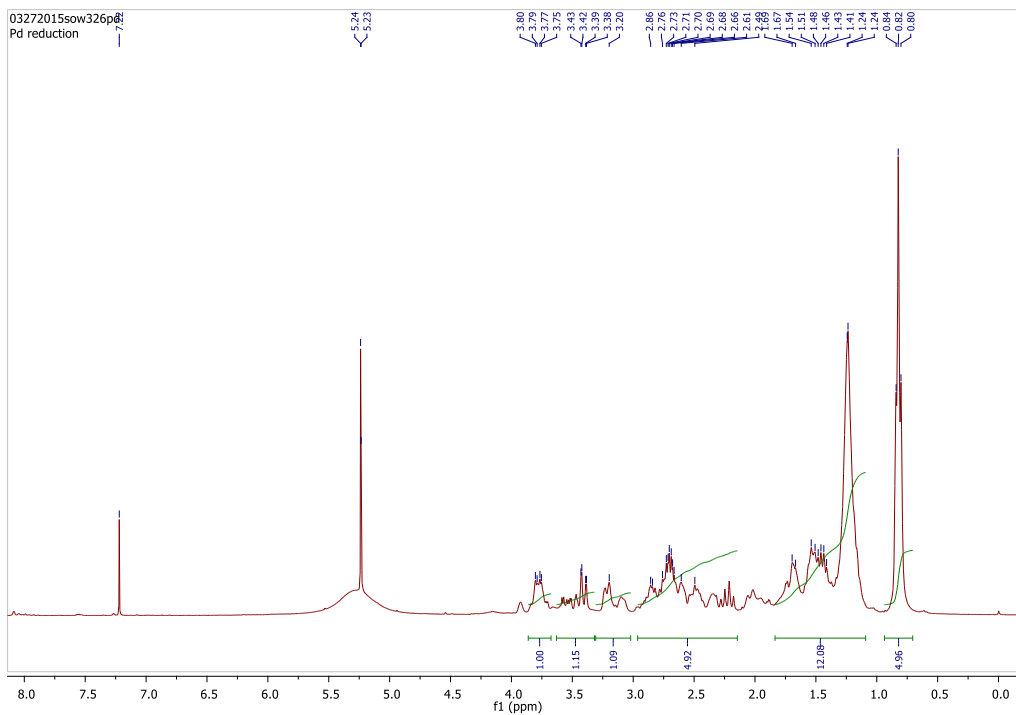
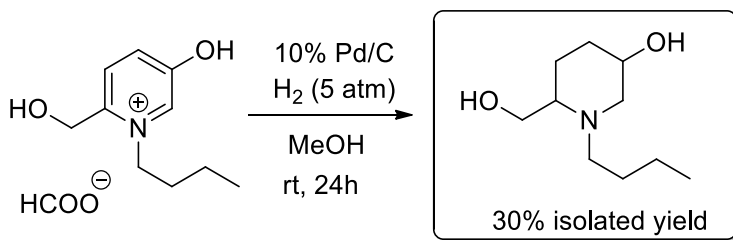


Fig SI 5.1: ^1H NMR reduction of *N*-Pentyl pyridinium salt

5.2 Palladium catalyzed hydrogenation of *N*-butyl pyridinium salt



Supporting details

1-butyl-5-hydroxy-2-(hydroxymethyl)pyridinium formate (114mg, 0.5 mmol) was dissolved in methanol (2mL) and added 10% Pd/C. Then the solution was subjected to 5 atm pressure of hydrogen and stirred at room temperature for 24h. When analysed by TLC, the reaction mixture showed two distinct inseparable spots, the presence of isomeric products. 10mL methanol was added to the reaction mixture and was then filtered through celite funnel. The solvent was evaporated and dried in vacuum to yield 30% of these isomeric products which were characterized by NMR. Due to the low yield and inseparable spots, the mixture of isomeric products were further treated with various protecting groups to be able to isolate them through column chromatography.

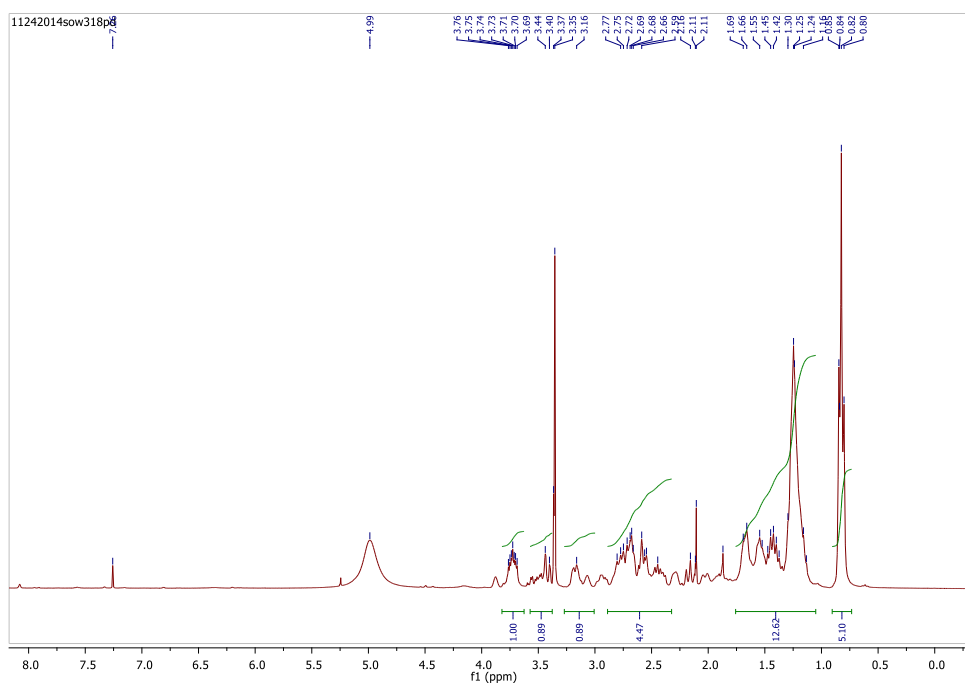
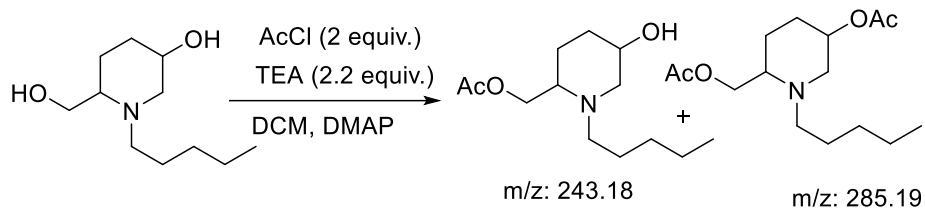


Fig SI 5.2: ^1H NMR reduction of *N*-butyl pyridinium salt

Acetyl protection of *N*-pentyl piperidine



To a solution of 6-(hydroxymethyl)-1-pentylpiperidin-3-ol (100 mg, 0.5 mmol) in dry DCM (5mL) was added 2.2 equivalent of Triethylamine base and stirred at 0 °C. To this mixture was added catalytic amount of DMAP and added 2 equivalent of acetyl chloride. The reaction mixture was stirred at 0 °C to room temperature for about 6 h. TLC analysis showed the reaction completion. To the reaction mixture in DCM added water and separated the organic layer followed by evaporation of the organic solvent, dried in vacuum and then analysed by ¹H NMR as shown below in Fig SI 5.3

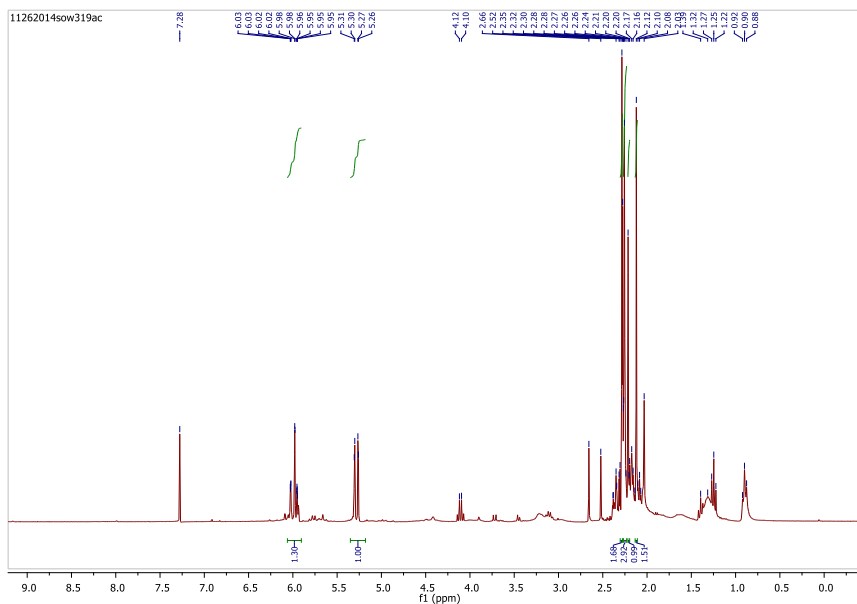


Fig SI 5.3: ^1H NMR of acetylation reaction with piperidine

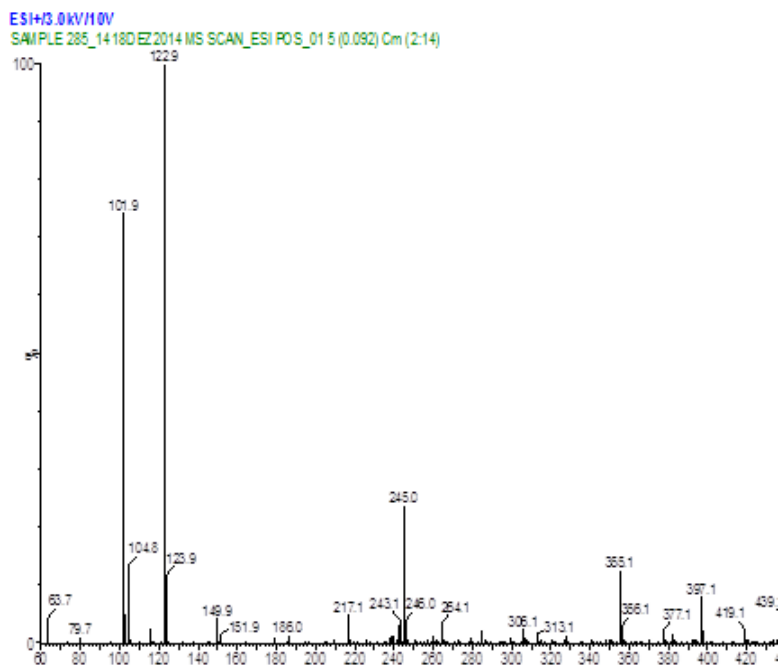
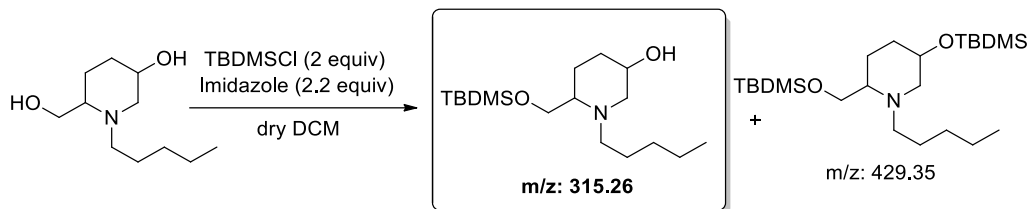


Fig SI 5.4: LCMS analysis of acetylation reaction with piperidine

TBDMS Protection of *N*-pentyl piperidine



To a solution of 6-(hydroxymethyl)-1-pentylpiperidin-3-ol (100 mg, 0.5 mmol) in dry DCM (5mL) was added imidazole (150 mg, 2.2 equiv) at 0 °C and stirred for 10 min. TBDMSCl (150 mg, 2 equiv) was dissolved in dry DCM (2 mL) and added to reaction mixture dropwise. Then the reaction mixture was slowly allowed to room temperature and further stirred for 6h. TLC analysis shows that complete consumption of starting material and presence of two new products which are separable by column chromatography. The two isomeric products were separated using EtOAc and Hexane (1:1) and analysed by ^1H NMR and LC-MS. The spectral analyses shows the presence of mono protected piperidine compound (Fig SI 5.5-5.7).

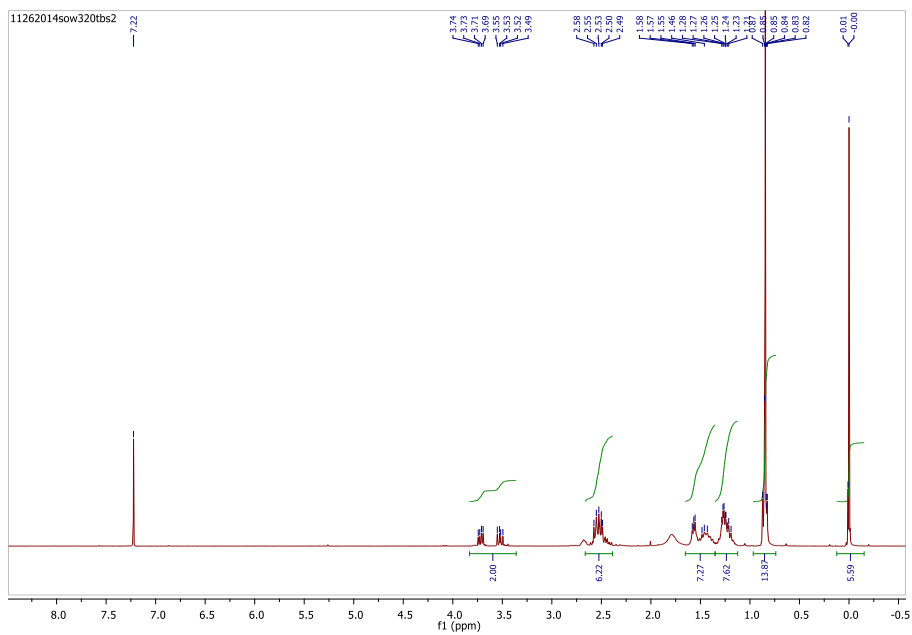


Fig SI 5.5: ^1H NMR of TBDMS Protection of pentyl piperidine 1st isomer

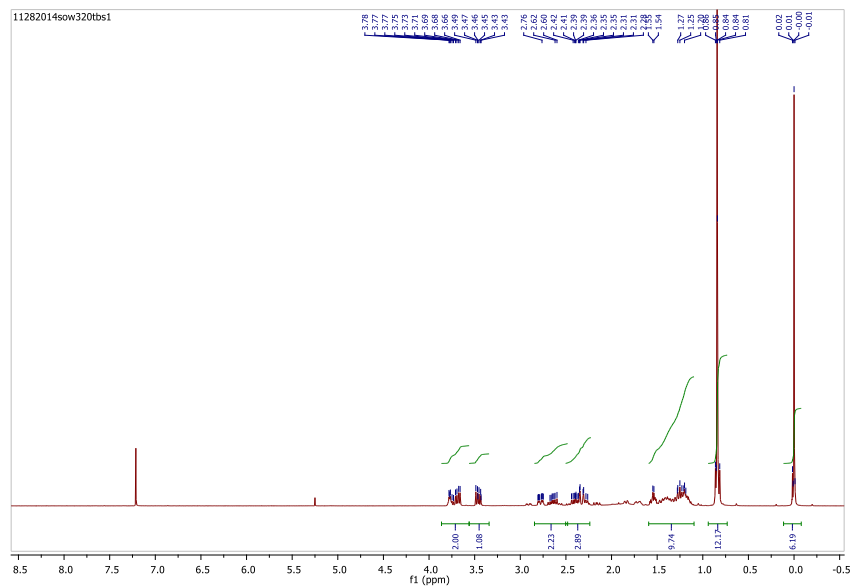


Fig SI 5.6: ^1H NMR of TBDMS Protection of pentyl piperidine 2nd isomer

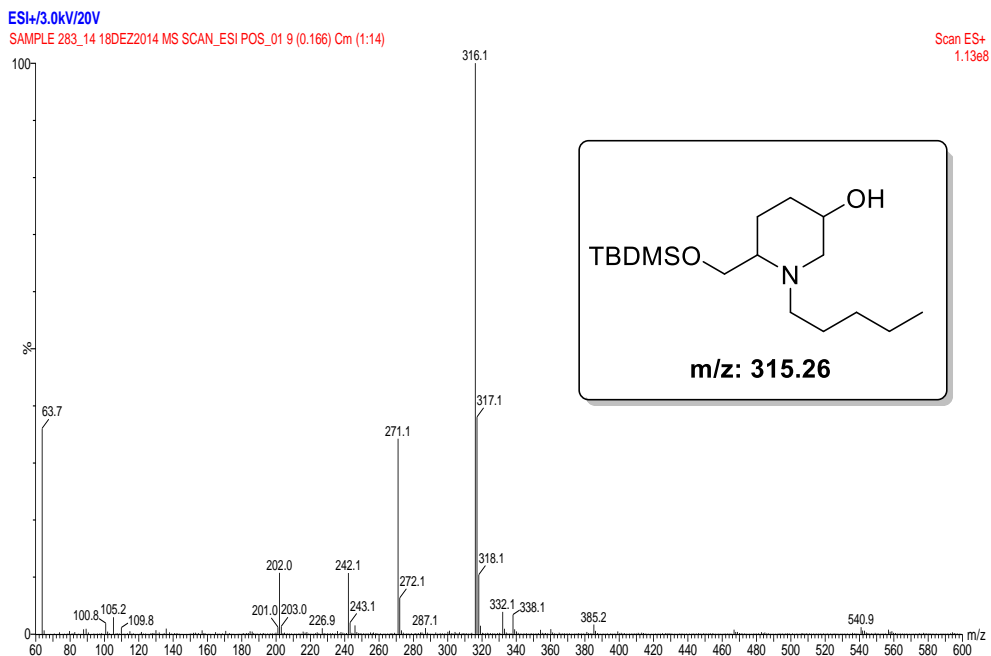
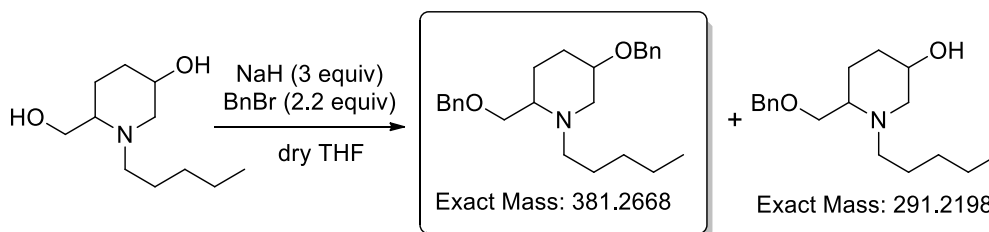


Figure 5.7 LCMS analysis of silylation reaction with piperidine

Benzyl protection of pentyl piperidine



To a solution of 60% NaH in mineral oil (36 mg, 3 equiv) in dry THF (5mL) was added 6-(hydroxymethyl)-1-pentylpiperidin-3-ol (100 mg, 0.5 mmol) at 0 °C and stirred for 10 min. Benzyl bromide (0.56 mL, 2.2 equiv) was added to reaction mixture dropwise. Then the reaction mixture was

slowly allowed to room temperature and further stirred for 12h. TLC analysis shows that complete consumption of starting material and presence of two new products which are inseparable by column chromatography. ^1H NMR analysis of reaction mixture indicates the benzylation of starting material 6-(hydroxymethyl)-1-pentylpiperidin-3-ol and peak at 382 in LC-MS analysis shows that the formation of dibenzylated product (Figure 5.9).

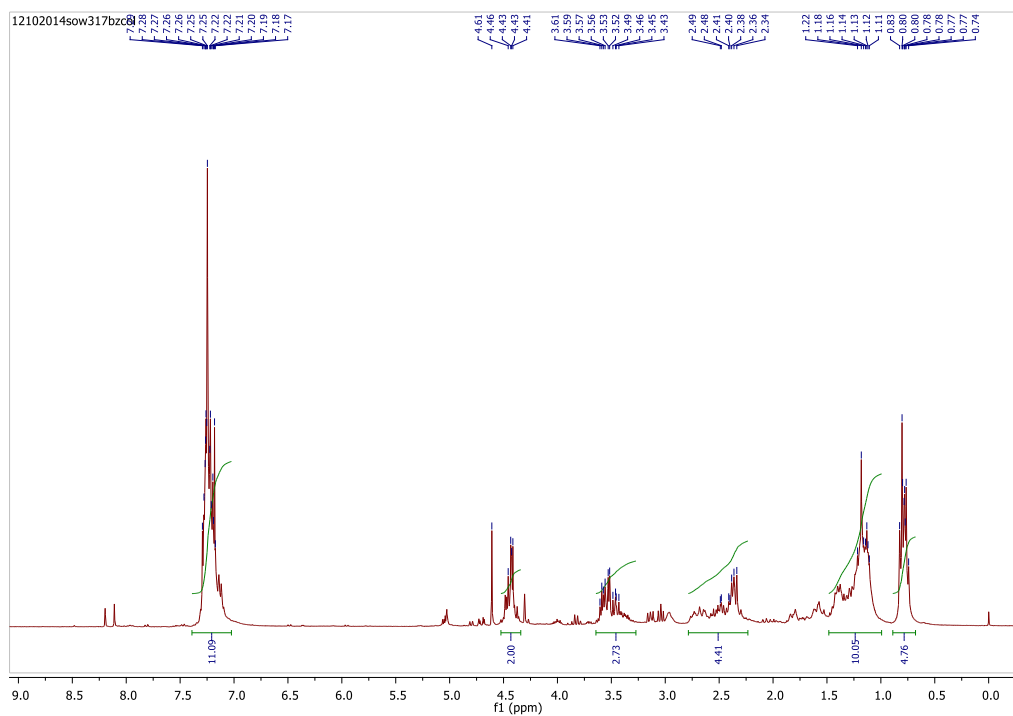


Figure 5.8: ^1H NMR of benzylation of *N*-pentyl piperidine

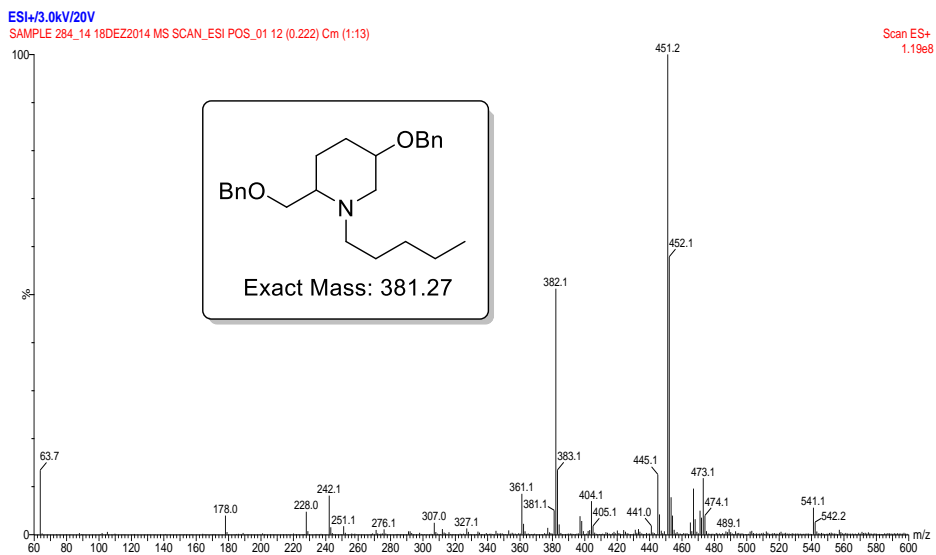


Figure 5.9 LCMS analysis of benzylation of *N*-pentyl piperidine

Supporting details

Oeiras, April, 2016

Synthetic approach towards biomass derived pyridinium salts

Subbiah Sowmiah



ITQB-UNL | Av. da República, 2780-157 Oeiras, Portugal
Tel (+351) 214 469 100 | Fax (+351) 214 411 277

www.itqb.unl.pt